

International Conference
Condensed Matter Research at the IBR-2

Dubna,
Russia

ABSTRACT

O

Functional and Nanostructured
Materials

O

Development of Neutron Scattering
Techniques and Instruments

K

Soft Condensed Matter

Carbon-based Materials

Dynamics of Materials

Magnetic Nanomaterials

Neutron Imaging

Materials under Extreme Conditions

Texture and Stress
Investigations of Materials

October 12-16,
2020

CMR @ IBR-2



Joint Institute for Nuclear Research

**CONDENSED MATTER RESEARCH
AT THE IBR-2**

International Conference

Dubna, October 12–16, 2020

Programme and Abstracts

УДК 538.9
ББК 22.386
С74

Organized by

the Frank Laboratory of Neutron Physics of the Joint Institute for Nuclear Research

Supported partially by

the RO-JINR Project No. 267/20.05.2020, item 16

**LOCAL ORGANIZING
COMMITTEE**

Prof. D. P. Kozlenko — Chairman
Mrs. V. Alfer'eva
Dr. M. V. Avdeev
Mrs. N. M. Belozerova
Dr. G. D. Bokuchava
Dr. M. Balasoju
Dr. D. M. Chudoba
Mrs. T. S. Donskova
Dr. Yu. E. Gorshkova
Dr. T. I. Ivankina — Scientific Secretary
Mr. S. V. Kozenkov
Dr. B. N. Savenko
Dr. T. V. Tropin

PROGRAMME COMMITTEE

Prof. V. L. Aksenov (Russia)
Prof. P. A. Alekseev (Russia)
Prof. A. M. Balagurov (Russia)
Prof. P. Balgavý (Slovak Republic)
Prof. A. V. Belushkin (Russia)
Prof. E. Burzo (Romania)
Dr. V. T. Em (Russia)
Dr. A. Ivanov (France)
Dr. E. A. Kenzhin (Kazakhstan)
Prof. P. Kopčanský (Slovak Republic)
Prof. D. Nagy (Hungary)
Prof. W. Nawrocik (Poland)
Prof. P. Petrov (Bulgaria)
Prof. D. Sangaa (Mongolia)
Dr. A. Senyshyn (Germany)
Prof. J. Wąsicki (Poland)

Editor T. I. Ivankina

The contributions are reproduced directly from the originals
presented by the Organizing Committee.

Condensed Matter Research at the IBR-2: Programme and Abstracts of the
C74 International Conference (Dubna, Oct. 12–16, 2020). — Dubna: JINR, 2020. — 243 p.
ISBN 978-5-9530-0540-1

Исследования конденсированных сред на реакторе ИБР-2: Программа и анно-
тации докладов международной конференции (Дубна, 12–16 окт. 2020 г.). — Дуб-
на: ОИЯИ, 2020. — 243 с.

ISBN 978-5-9530-0540-1

ISBN 978-5-9530-0540-1

© Joint Institute for Nuclear
Research, 2020

Preface

The International Conference “Condensed Matter Research at the IBR-2” (CMR@IBR2-2020) takes place in Dubna, Moscow Region, Russian Federation on October 12–16, 2020. The Conference is organized by the Frank Laboratory of Neutron Physics of the Joint Institute for Nuclear Research.

After modernization completed in 2011, the IBR-2 high-flux pulsed reactor renewed a regular operation and realization of the User Programme. Neutron scattering research at the IBR-2 reactor covers different fields of condensed matter physics, materials science, chemistry, biophysical, geophysical and engineering sciences. At present, more than 200 experiments per year are performed by scientists from more than 20 countries at IBR-2 instruments in the framework of the User Programme.

The aim of the Conference on Condensed Matter Research at the IBR-2 reactor, playing the role of the User Meeting, is to bring together the users of the neutron facility for discussion of recent experimental results, prospects of future research and development of IBR-2 instruments.

The previous Conferences held in 2014, 2015 and 2017 attracted participants from 18 countries: Azerbaijan, Belarus, Bulgaria, Czech Republic, Estonia, Germany, Italy, Kazakhstan, Latvia, Moldova, Mongolia, Poland, Romania, Russia, Serbia, Slovak Republic, Ukraine and Vietnam.

The topics of the Conference will highlight results of interdisciplinary research and development of neutron instruments and techniques, including:

- Functional and nanostructured materials;
- Magnetic colloid systems;
- Layered magnetic nanostructures;
- Carbon nanostructures;
- Materials under extreme conditions;
- Soft condensed matter (biological nanosystems, lipid membranes, polymers);
- Lattice and molecular dynamics of materials;
- Texture and properties of rocks, minerals and industrial materials;
- Residual stresses in materials and products;
- Neutron imaging;
- Cultural heritage and applied research;
- Development of IBR-2 instruments;
- Development of neutron scattering techniques and detectors.

Due to coronavirus outbreak, the Conference will be held online via Video conference.

We wish the CMR@IBR2-2020 Conference participants successful work and significant results!

Oral Programme

CMR@IBR2-2020 Scientific Programme

Due to coronavirus outbreak, the Conference will be held online via Video conference.

Monday, October 12, 2020

INTRODUCTORY SESSION

Chair: A. Belushkin

- | | |
|---------------|---|
| 10.00 – 10.20 | Opening and Welcome. |
| 10.20– 10.50 | Kozlenko D. (Frank Laboratory of Neutron Physics, Joint Institute for Nuclear Research, Dubna, Russia). Neutron scattering instrumentation of IBR-2 high flux pulsed reactor for Condensed Matter Research: recent developments. |
| 10.50 – 11.20 | Gordeliy V. (IBS Grenoble and ICS Forschungszentrum Jülich, Germany). Physics and Biology of Biomembranes. |
| 11.20 – 11.50 | Shvetsov V. (Frank Laboratory of Neutron Physics, Joint Institute for Nuclear Research, Dubna, Russia). Progress report on developing a concept for a new neutron source at FLNP. |
| 11.50 – 12.20 | Mezei F. (ESS, Lund, Sweden). The “LvB” compact neutron source project at Martonvásár (Hungary). |
| 12.20 - 12.40 | <i>Break</i> |

PLENARY SESSION 1: FUNCTIONAL AND NANOSTRUCTURED MATERIALS

Chair: A. Balagurov

- | | |
|---------------|--|
| 12.40 -13.10 | Fedotov S. (Skolkovo Institute of Science and Technology, Moscow, Russia). Defects structure in olivine-type cathode materials studied by neutron diffraction. |
| 13.10 – 13.40 | Golovin I. (National University of Science and Technology “MISIS”, Moscow, Russia). Study of first and second order transitions in Fe-Ga and Fe-Al alloys. |
| 13.40 – 14.00 | Mohamed A. (National University of Science and Technology “MISIS”, Moscow, Russia). Application of in situ neutron diffraction to study thermo-kinetic transitions in galfenols. |
| 14.00 – 15.00 | <i>Lunch</i> |

Chair: A. Ivanov

- | | |
|--------------|--|
| 15.00 –15.30 | Alekseev P. (NRC "Kurchatov Institute", Moscow, Russia). Inelastic neutron scattering in research on the physics of strongly correlated electron systems. |
|--------------|--|

15.30 – 15.50	Sun L. (National University of Science and Technology “MISIS”, Moscow, Russia). Influence of chemical composition on spinodal decomposition of austenite and thermo-elastic martensitic transition in low-Cu Mn-Cu alloys.
15.50 – 16.10	Krezov K, (Institute for Nuclear Research and Nuclear Energy BAS, Sofia, Bulgaria). Barium titanate from multicomponent oxide glass doped with iron oxide – crystallization effects.
16.10 – 16.30	Urusova N. (Institute of Solid State Chemistry Ural Branch RAS, Ekaterinburg, Russia). Features of magnetic phase transitions in the $\text{LiNi}_{1-x}\text{Co}_x\text{PO}_4$ magnetoelectrics.
16.30 – 16.50	Semkin M. (Institute of Metal Physics Ural Branch RAS, Ekaterinburg, Russia). Magnetic phase diagram $\text{LiNi}_{0.9}\text{Co}_{0.1}\text{PO}_4$.
16.50 – 17.00	<i>Break</i>

Chair: S. Fedotov

17.00 – 17.20	Lushnikov S. (Moscow State University, Moscow, Russia). Structure of RNi_3 (R-Dy, Ho)-based intermetallic hydrides at 5K and 293K temperature.
17.20 – 17.40	Savin A. (National Institute of R&D for Technical Physics, Iasi, Romania). Monitoring techniques of Yttria stabilized zirconia used as thermal barrier coating
17.40 – 18.00	D Souza A. (Manipal Academy of Higher Education, Manipal, India). Influencing structure property correlations in Bi doped $\text{La}_{0.7}\text{Sr}_{0.3}\text{MnO}_3$ manganites by Bi substitution.
18.00 – 18.20	Craus M.-L. (Frank Laboratory of Neutron Physics, Joint Institute for Nuclear Research, Dubna, Russia). Influence of low PB concentration on the structure and transport phenomena of LaMnO_3 manganites.

Tuesday , October 13, 2020

PLENARY SESSION 1: FUNCTIONAL AND NANOSTRUCTURED MATERIALS

Chair: M. Avdeev

10.00 -10.20	Zakharchenko T. (N.N. Semenov Federal Research Center for Chemical Physics, Moscow, Russia). Small-angle neutron scattering studies of pore filling in carbon electrodes: mechanisms limiting lithium-air battery capacity.
10.20 – 10.40	Ushakova E. (Moscow State University, Moscow, Russia). Monitoring of lithium plating by neutron reflectometry.
10.40 – 11.00	Valkov S. (Institute of Electronics Bulgarian AS, Sofia, Bulgaria). Hybrid techniques for manufacturing of aluminum composite layers with TiCN nanoparticles.

11.00 – 11.20	Belogorlov A. (A.V.Topchiev Institute of Petrochemical Synthesis RAS, Moscow, Russia). Application of the small-angle neutron scattering method to study dispersion of non-wetting liquids in nanoporous materials.
11.20 – 11.40	Korda D. (Petersburg Nuclear Physics Institute, NRC "Kurchatov Institute", Gatchina, Russia). Neutron reflectometry of carbon nanotubes layer deposited on conducting substrates.
11.40 – 12.00	Iftimie N. (National Institute of R&D for Technical Physics, Iasi, Romania). The possibility to use reconfigurable architecture structures as electromagnetic sensors array.
12.00 – 12.20	Larichev Yu. (Boreskov Institute of Catalysis Siberian Branch RAS, Novosibirsk, Russia). SANS and SAXS study of supported metal catalysts and nanocomposites
12.20 – 12.40	<i>Break</i>

PLENARY SESSION 2: DEVELOPMENT OF NEUTRON SCATTERING TECHNIQUES AND INSTRUMENTS

Chair: A. Ioffe

12.40 – 13.10	Ivanov A. (ILL, Grenoble, France). Magnetic interactions in single crystals studied with crystal spectrometers.
13.10 – 13.30	Chudoba D. (Frank Laboratory of Neutron Physics, Joint Institute for Nuclear Research, Dubna, Russia). Development of an inelastic neutron scattering spectrometer in inverse geometry at the IBR 2 reactor.
13.30 – 13.50	Kuklin A. (Frank Laboratory of Neutron Physics, Joint Institute for Nuclear Research, Dubna, Russia). Status and prospects of small-angle scattering at IBR2.
13.50 – 15.00	<i>Lunch</i>

Chair: E. Goremychkin

15.00 – 15.20	Kichanov S. (Frank Laboratory of Neutron Physics, Joint Institute for Nuclear Research, Dubna, Russia). The neutron radiography and tomography facility on the IBR-2 reactor: current state and recent results.
15.20 – 15.40	Zhaketov V. (Frank Laboratory of Neutron Physics, Joint Institute for Nuclear Research, Dubna, Russia). Polarized neutron reflectometry with secondary radiation registration.
15.40 – 16.00	Kozhevnikov S. (Frank Laboratory of Neutron Physics, Joint Institute for Nuclear Research, Dubna, Russia). Divergence of a neutron microbeam from planar waveguides.
16.00 – 16.20	Frank A. (Frank Laboratory of Neutron Physics, Joint Institute for Nuclear Research, Dubna, Russia). Intense UCN source at IBR2 reactor. The dream or opportunity?

16.20 – 16.40	Milkov V. (Frank Laboratory of Neutron Physics, Joint Institute for Nuclear Research, Dubna, Russia). Ring detector for small-angle scattering of thermal neutrons for real-time diffractometer (RTD).
16.40 – 17.00	Bodnarchuk V. (Frank Laboratory of Neutron Physics, Joint Institute for Nuclear Research, Dubna, Russia). The influence of delayed neutrons at the pulsed reactor IBR-2 on the signal/background ratio of low-resolution neutron instruments.
17.00 – 17.10	<i>Break</i>
17.10 – 19.00	<i>Poster Session 1</i>

Wednesday, October 14, 2020

PLENARY SESSION 3: MAGNETIC NANOMATERIALS

Chair: V. Bodnarchuk

10.00 – 10.30	Kravtsov E. (Institute of Metal Physics Ural Branch RAS, Ekaterinburg, Russia). Magnetism of rare-earth multilayers.
10.30 – 10.50	Devyaterikov D. (Institute of Metal Physics Ural Branch RAS, Ekaterinburg, Russia). Observation of helimagnetism in Dy and Ho thin films via neutron reflectivity measurements.
10.50 – 11.10	Shibaev A. (Moscow State University, Moscow, Russia). Synthesis of rod-like and spherical magnetite nanoparticles assisted by magnetic field.
11.10 – 11.30	Rajnak M. (Institute of Experimental Physics SAS, Košice, Slovakia). Structure and dielectric properties of low-polarity ferrofluids under an electric field.
11.30 – 11.50	Nagornyi A. (National Taras Shevchenko University, Kyiv, Ukraine / Frank Laboratory of Neutron Physics, Joint Institute for Nuclear Research, Dubna, Russia). Structural aspects of Fe ₃ O ₄ /CoFe ₂ O ₄ nanoparticles by X-Ray and neutron scattering: powders and stabilization in water.
11.50 – 12.10	<i>Break</i>

PLENARY SESSION 4: SOFT CONDENSED MATTER (BIOLOGICAL NANOSYSTEMS, LIPID MEMBRANES, POLYMERS)

Chairman: S. Grigoriev

12.10 – 12.40	Kucerka N. (Frank Laboratory of Neutron Physics, Joint Institute for Nuclear Research, Dubna, Russia). Advances in understanding the conformational diseases mimicking model membranes by neutron scattering.
---------------	--

12.40 – 13.00	Siposova K. (Institute of Experimental Physics, Slovak Academy of Sciences, Košice, Slovakia). Effect of nanomaterials on protein amyloid aggregation.
13.00 – 13.20	Molchanov V. (Moscow State University, Moscow, Russia). Living micelles-nanoparticles networks.
13.20 – 13.40	Hrubovcak P. (Frank Laboratory of Neutron Physics, Joint Institute for Nuclear Research, Dubna, Russia). Single lipid bilayer changes induced by cholesterol and melatonin.
13.40 – 15.00	<i>Lunch</i>

Chairman: N. Kucerka

15.00 – 15.30	Grigoriev S. (Petersburg Nuclear Physics Institute, NRC "Kurchatov Institute", Gatchina, Russia). Classification of fractal objects by SANS: case of logarithmic fractal.
15.30 – 16.00	Angelov B. (Institute of Physics Czech AS, Prague, Czech Republic). Multiphase and sponge lipid nanoparticles studied by SANS and time resolved SAXS.
16.00 – 16.20	Lebedev D. (Petersburg Nuclear Physics Institute, NRC "Kurchatov Institute", Gatchina, Russia). Effects of macromolecules and protein complexes on the interphase chromatin organization registered by SANS.
16.20 – 16.40	Kamynina A. (Moscow Institute of Physics and Technology, Moscow, Russia). Peptide (60-76) from RAGE and its analogue protect spatial memory in transgenic 5xFAD mice and induce calcium signaling in primary culture via activation of RAGE.
16.40 – 17.00	<i>Break</i>
17.00 – 19.00	<i>Poster Session 2</i>

Thursday, October 15, 2020

PLENARY SESSION 4: SOFT CONDENSED MATTER (BIOLOGICAL NANOSYSTEMS, LIPID MEMBRANES, POLYMERS)

Chair: B. Angelov

10.00 – 10.30	Baranchikov A. (Kurnakov Institute of General and Inorganic Chemistry RAS, Moscow, Russia). Small-angle neutron scattering for the structure of aerogel-based materials.
10.30 – 10.50	Artykulnyi O. (Frank Laboratory of Neutron Physics, Joint Institute for Nuclear Research, Dubna, Russia). Study of surfactant-polymer complexes structure by small-angle neutron scattering.

10.50 – 11.10	Lebedev V. (Petersburg Nuclear Physics Institute, NRC "Kurchatov Institute", Gatchina, Russia). Structure of diffusive polymer membranes for molecular and ionic transport.
11.10 – 11.30	Kwiatkowski A. (Moscow State University, Moscow, Russia). Small-angle neutron scattering study of polymer-containing (hybrid) wormlike micelles of ionic surfactant.
11.30 – 11.50	Safarik I. (Biology Centre, Ceske Budejovice, Czech Republic). Cotton textile/iron oxide nanozyme composites with peroxidase-like activity: Preparation and SANS/SAXS characterization.
11.50 – 12.10	<i>Break</i>

Chair: Yu. Gorshkova

12.10 – 12.30	Zajac W. (Institute of Nuclear Physics Polish Academy of Sciences, Krakow, Poland). Calamitic liquid crystal under nanometer spatial confinement – investigation by SANS and complementary methods.
12.30 – 12.50	Juszyńska-Gałązka E. (Institute of Nuclear Physics Polish Academy of Sciences, Poland). Vibrational dynamics of molecules phenyl substances with varying degrees of molecular ordering.
12.50 – 14.30	<i>Lunch</i>

PLENARY SESSION 5: TEXTURE AND STRESS INVESTIGATIONS OF MATERIALS

Chair: T. Ivankina

14.30 – 15.00	Froitzheim N. (Steimann Institute for Geology, Mineralogy and Paleontology, Uni Bonn, Germany). Time-of-flight neutron diffraction texture analysis of deformed rocks from shear zones related to continent collision in the Alps.
15.00 – 15.20	Zel I. (Frank Laboratory of Neutron Physics, Joint Institute for Nuclear Research, Dubna, Russia). Neutron tomography of anisotropic rocks: assessment of structural, magnetic and seismic anisotropy.
15.20 – 15.40	Pakhnevich A. (Borissiak Paleontological Institute RAS, Moscow, Russia). Crystallographic texture of freshwater bivalve molluscs of the Family Unionidae.
15.40 – 16.00	Duliu O. (University of Bucharest, Bucharest, Romania). Neutron diffraction and neutron computed tomography Investigation of Scleractinian Corals skeleton.
16.00 -16.10	<i>Break</i>

Chair: G. Bokuchava

16.10 – 16.40	Baczmarski A. (University of Science and Technology, Krakow, Poland). Deformation mechanisms and microstress evolution in polycrystalline materials studied using diffraction and modelling.
---------------	---

- 16.40 – 17.10 **Em V.** (NRC Kurchatov institute, Moscow, Russia). Neutron diffraction study of residual stresses at research reactor IR-8 of National Research Center “Kurchatov Institute”.
- 17.10 – 17.30 **Kot P.** (AGH University of Science and Technology, Krakow, Poland). Investigation of microstress evolution in Mg-alloy using TOF neutron diffraction.

Friday, October 16, 2020

PLENARY SESSION 6: NEUTRON IMAGING

Chair: S. Kichanov

- 10.00 – 10.30 **Saprykina I.** (Institute of Archaeology RAS, Moscow, Russia). The neutron tomography and diffraction as a routine research method for the non-ferrous metal archaeological objects.
- 10.30 – 10.50 **Abdurakhimov B.** (Frank Laboratory of Neutron Physics, Joint Institute for Nuclear Research, Dubna, Russia). The study of ancient Romanian pottery fragments by non-destructive techniques at the IBR-2 reactor.
- 10.50 – 11.10 **Kenessarın M.** (Frank Laboratory of Neutron Physics, Joint Institute for Nuclear Research, Dubna, Russia). Research of structure of cement materials for storage of radioactive graphite by neutron tomography.
- 11.10 – 11.30 *Break*

PLENARY SESSION 7: USER’S INFRASTRUCTURE

Chair: T. Tropin

- 11.30 – 11.50 **Chudoba D.** (Frank Laboratory of Neutron Physics, Joint Institute for Nuclear Research, Dubna, Russia). User Programme at FLNP JINR.
- 11.50 – 12.10 **Ivanshina O.** (Frank Laboratory of Neutron Physics, Joint Institute for Nuclear Research, Dubna, Russia). Synthesis of new materials and investigations using Raman spectroscopy and thermal analysis in FLNP JINR.
- 12.10 – 12.30 **Bobrikov I.** (Frank Laboratory of Neutron Physics, Joint Institute for Nuclear Research, Dubna, Russia). New equipment for sample preparation and study of functional materials.
- 12.30 – 12.50 **Gorshkova Yu.** (Frank Laboratory of Neutron Physics, Joint Institute for Nuclear Research, Dubna, Russia). Complementary methods in soft matter research in FLNP JINR: atomic-force microscopy and dynamic light scattering.
- 12.50 – 13.20 **Open discussion.** Kozlenko D.
- 13.20 – 13.30 **Workshop closing**

Poster Programme

1. **Abu Ghazal**, Surin V.I., Bokuchava G.D., Papushkin I.V. (Jordan Atomic Energy Commission, Amman, Jordan). Tracking martensitic transformation in AISI 321 stainless steel using scanning contact potentiometry and thermal neutron diffraction.
2. Azarova L.A., **Kopitsa G.P.**, Gorshkova Yu.E., Lermontov S.A., Malkova A. N., Volkov V.V., Baranchikov A.E. (Petersburg Nuclear Physics Institute NRC KI, Gatchina, Russia). Novel resorcinol-formaldehyde aerogels: synthesis, structure and fractal properties.
3. **Cornei N.**, Craus M.-L., Mita C. (University of Iasi, Faculty of Chemistry, Iasi, Romania). Spin-glass state influence on the low temperature transport phenomena in $\text{La}_{0.54}\text{Nd}_{0.11}\text{Sr}_{0.35}\text{Mn}_{1-x}\text{Co}_x\text{O}_3$ manganites.
4. **Fedoseev M.L.**, Petrov S.N., Mikhailov M.S., Islamov A.Kh., Drozdova N.F. (NRC "Kurchatov institute" – CRISM "Prometey", St. Petersburg). Research of structural transformation mechanism in high strength steel.
5. **Genov I.G.**, Rutkauskas A.V., Lukin E.V., Kozlenko D.P., Kichanov S.E., Raykova G.S., Vladikova D.E., Belozerova N.M., Turchenko V.A., Popov E.P., Krezhov K.A. (Frank Laboratory of Neutron Physics, Joint Institute for Nuclear Research, Dubna, Russia). Structural characterization of yttrium doped barium cerate $\text{BaCe}_{0.85}\text{Y}_{0.15}\text{O}_{3-\alpha}$ for application in solid oxide fuel cells.
6. **Ilinov D.V.**, Shabrin A.D., Sadilov V.V. (Orion R&P Association JSC, Moscow, Russia). Structural analysis of the ingaas/gaas heterostructures by high-resolution reciprocal space mapping and neutron scattering.
7. **Kalanda N.**, Yarmolich M., Petrov A., Bobrikov I., Demyanov S., Sobolev N. (Scientific-Practical Materials Research Centre of NAS of Belarus, Minsk, Belarus). Oxygen non-stoichiometry and superstructural ordering of Fe/Mo cations in the strontium ferromolybdate.
8. Kalanda N., Yarmolich M., **Petrov A.**, Kutuzau M., Blokhin, A., Tamulevicius S., Bobrikov I. (Scientific-Practical Materials Research Centre of NAS of Belarus, Minsk, Belarus). Thermodynamic, structural and magnetic characteristics of barium ferromolybdate compound.
9. **Krezhov K.**, Harizanova R., Lukin E., Beskrovny A., Popov E., Kozlenko D., Kichanov S., Mirzaev M. (Institute of Electronics and Institute for Nuclear Research and Nuclear Energy, Bulgarian Academy of Sciences). Barium titanate from multicomponent glass doped with iron oxide – low-temperature phase transitions of barium titanate.
10. **Lebedev V. T.**, Kulvelis Yu.V., Vul A.Ya, Kyzyma O.A., Tropin T.V. (Petersburg Nuclear Physics Institute -NRC KI, Gatchina, Russia). Ordering nanodiamonds in aqueous systems with active molecular additives.
11. Lychagina T., Nikolayev D., Dragolici C., **Balasoiu M.**, Sekretarev Z., Lizunov N., Ionascu L., Nicu M., Dragolici F. (Frank Laboratory of Neutron Physics, Joint Institute for Nuclear Research, Dubna, Russia). Neutron diffraction study of low pH cement-based materials used for aluminum radioactive waste conditioning: aging effects.

12. **Nabiyev A.A.**, Pawlukoic A., Islamov A.Kh., Soloviov D.V., Ivankov O.I., Ivanshina O.Yu., Kuklin A.I. (ANAS Institute of Radiation Problems, Baku, Azerbaijan/Joint Institute for Nuclear Research, Dubna, Russia). Fractal aggregate structure of HDPE/SiO₂ polymer nanocomposite films.
13. Racolta D., **Balasoiu M.**, Andronache C., Mihaly-Cosmuta L., Mata C., Belozerova N., Rogachev A., Orelovich O., Turchenko V., Balasoiu-Gaina A.-M., Sikolenko V. (Technical University of Cluj Napoca, North University Center of Baia Mare, Romania). Effects of iron and vanadium ions on lithium-phosphate glasses: morphological, structural and spectroscopic properties.
14. **Shahee A.**, Singh K., Suard E., Lalla N. P., Simon C. (UGC-DAE Consortium for Scientific Research, Indore, India). Room temperature charge orbital ordering and associated low-temperature spin ordering in SrMn_{0.85}Mo_{0.15}O₃ probed by neutron diffraction.
15. **Sikolenko V.V.**, Karpinsky D.V., Silibin M.V., Zhaludkevich D.V., Chobot A.N., Khomchenko V.A., Bobrikov I.A. (Frank Laboratory of Neutron Physics, Joint Institute for Nuclear Research, Dubna, Russia). Neutron diffraction studies of Ca/Ti doped Bi ferrites: HRFD results.
16. **Steigmann R.**, Savin A., Novy F., Craus M.L., Turchenko V. (National Institute of R&D for Technical Physics, Iasi, Romania). Influence of rare earth in magnesium calcium alloy used for medical implants.
17. **Thao L.T.P.**, Kozlenko D.P., Kichanov S.E., Rutkavkas A.V., Dang N.T., Khiem L.H. (University of Danang - University of Science and Education, Danang, Viet Nam). Complex behavior of BaYFeO₄ under magnetic fields.
18. **Tsvigun N.V.**, Golovkina D.A., Zhurishkina E.V., Yapryntsev A.D., Sokolov A.E., Kulminskaya A.A., Ivanova L.A., Baranchikov A.E., Gorshkova Yu.E., Volkov V.V., Kopitsa G.P. (FSRC "Crystallography and Photonics" RAS, Moscow, Russia). Mesostructure of calcium carbonate, obtained in the process of biomineralization.
19. **Yerdauletov M.** (Dubna State University, Russia). Effect of carbon additives on the structure of electrodes for high energy density Li-ion batteries by small-angle neutron scattering.
20. **Kulvelis Yu.V.**, Lebedev V.T., Shvidchenko A.V., Yudina E.B., Vul A.Ya., Yevlampieva N.P., Gelfond M.L. (Petersburg Nuclear Physics Institute NRC KI, Gatchina, Russia). Nanodiamond-poly(vinylpyrrolidone) complex as promising drug carrier and the agent enhancing photodynamic therapy.

Carbon-based materials

21. **Jargalan N.**, Tropin T.V., Avdeev M.V., Aksenov V.L., Sangaa D. (Institute of Physics and Technology, Mongolian Academy of Sciences, Ulaanbaatar, Mongolia). Dynamic light scattering investigations of the kinetics of cluster growth in fullerene C₆₀ solutions.
22. **Kulvelis Yu.V.**, Lebedev V.T., Kozlov V.S., Bogmut D.I., Vul A.Ya (Petersburg Nuclear Physics Institute NRC KI, Gatchina, Russia). Small angle neutron scattering and gamma resonance spectroscopy for metal-nanocarbon characterization.
23. **Kulvelis Yu.V.**, Rabchinskii M.K., Dideikin A.T., Shvidchenko A.V., Kirilenko D.A., Gudkov M.V. (Petersburg Nuclear Physics Institute NRC KI, Gatchina, Russia). Graphene-nanodiamond composites for biosensor and electronic applications.

24. **Nagorna T.V.**, Chudoba D. (Frank Laboratory of Neutron Physics, Joint Institute for Nuclear Research, Dubna, Russia). Specifics of fullerene C₆₀ and C₇₀ cluster formation in toluene /N-methyl-2-pyrrolidone solvent mixture.
25. **Tomchuk O.V.**, Kosiachkin Ye.N., Krasnikov D.V., Ilatovskii D.A., Nasibulin, A.G. (Frank Laboratory of Neutron Physics. Joint Institute for Nuclear Research, Dubna, Russia). On the impact of capillary forces on the morphology of thin films of single-walled carbon nanotubes by specular reflectometry.
26. **Tomchuk A.A.**, Avdeev M.V., Ivankov O.I., Shershakova N.N, Turetskii E.A., Andreev S.M. (Frank Laboratory of Neutron Physics, Joint Institute for Nuclear Research, Dubna, Russia). Structural study of aqueous solutions of C₆₀ amino derivatives for biomedical applications.

Development of neutron scattering techniques and instruments

27. **Diachkov M.V.**, Altynbayev E.V., Trunov D.N., Marin V.N., Solovey V.A. (Petersburg Nuclear Physics Institute NRC KI, Gatchina, Russia). SIPM and ZnS:Li6 based neutron scintillation detector.
28. **Glushkova T.I.**, Krivshich A.G., Solovei V.A., Kolkhidashvili M.R. (Petersburg Nuclear Physics Institute NRC KI, Gatchina, Russia). Development of a two-dimensional thermal-neutron detector with an entrance window of 600 × 600 mm.
29. **Klepachka M.** (Joint Institute for Nuclear Research, Dubna, Russia). Monte-Carlo simulation of inelastic neutron scattering spectrometer.
30. **Koryttseva A.K.**, Tinakov A.N., Beskrovnyy A.I. (N.I.Lobachevsky State University of Nizhniy Novgorod, Nizhniy Novgorod, Russia). Reaction cell for *in situ* neutron diffraction studies.
31. **Kosiachkin Y.** (Frank Laboratory of Neutron Physics, Joint Institute for Nuclear Research, Dubna, Russia). Electrochemical cells for neutron reflectometry.
32. **Lukin E.V.**, Kozlenko D.P., Kichanov S.E, Rutkauskas A.V., Savenko B.N. (Frank Laboratory of Neutron Physics, Joint Institute for Nuclear Research, Dubna, Russia). High-pressure neutron diffractometer DN-6: current state.
33. **Pavlova A.E.**, Konik P.I. (Saint Petersburg State University, Saint Petersburg, Russia). Diffractometer monopoly on compact neutron source DARIA.
34. **Sadilov V.** (Frank Laboratory of Neutron Physics, Joint Institute for Nuclear Research, Dubna, Russia).The influence of the delayed neutrons at the IBR-2 reactor on the instrumental resolution function.
35. **Sikolenko V.V.**, Müller B.I.R., Schilling F. (Frank Laboratory of Neutron Physics, Joint Institute for Nuclear Research, Dubna, Russia). EPSILON diffractometer: current status and perspectives.
36. **Soloviev A.G.**, Ivankov O.I., Rogachev A.V., Soloviev D.V., Kuklin A.I. (Frank Laboratory of Neutron Physics, Joint Institute for Nuclear Research, Dubna, Russia). Program package "SAS": status and new features.
37. **Subbotina V.V.**, Kovalenko N. A., Konik P. I., Pavlov K. A., Grigoryev S. V., Voronin V. V. (Petersburg Nuclear Physics Institute NRC KI, Gatchina, Russia). Design improvements of target-moderator-reflector assembly of compact neutron source DARIA.
38. **Teymurov E.S.**, Nezvanov A.Yu., Lychagin E.V. (Frank Laboratory of Neutron Physics, Joint Institute for Nuclear Research, Dubna, Russia). MCNP simulation of the background neutron radiation in the 11b experimental room of the IBR-2 reactor.

Dynamics of materials

39. **Hetmańczyk J.**, Hetmańczyk Ł. (Jagiellonian University, Krakow, Poland). Water dynamics in $[\text{Cu}(\text{H}_2\text{O})_4](\text{ReO}_4)_2$ studied by IR, RS and neutron scattering methods.
40. **Jóźwiak K.**, Goremychkin E., Jezierska A., Panek J., A. Filarowski. (Wrocław University, Poland). Proton dynamics in phthalic acid associates.

Magnetic nanomaterials

41. **Antropov N.O.**, Kravtsov E.A., Makarova M.V., Khaidukov Yu., Ustinov V.V. (Institute of Metal Physics, Ural Branch of the Russian Academy of Sciences, Ekaterinburg, Russia). Polarized neutron and x-ray study of FE/PD/GD multilayers.
42. **Astaf'eva S.**, Lysenko S., Balasoïu M., Yakusheva D., Kornilicina E., Kuklin A., Ivankov O., Soloviov D., Turchenko V., Balasoïu-Gaina A.-M. (Institute of Technical Chemistry, Perm Federal Research Center, Ural Branch, Russian Academy of Sciences, Perm, Russia). Small-angle neutron scattering investigation of several ferrofluids for magneto-optical applications.
43. **Yakunina E.M.**, Antropov N.O., Kravtsov E.A., Proglyado V.V. (Institute of Metal Physics, Ural Branch of the Russian Academy of Sciences, Ekaterinburg, Russia). Magnetic ordering in Fe/MgO/Cr/MgO/Fe heterostructures.
44. **Karpets M.**, Rajňák M., Paulovičová K., Parekh K., Upadhyay R. V., Gapon I., Kopčanský P., Timko M.. (Institute of Experimental Physics, Slovak Academy of Sciences, Kosice, Slovakia). Neutron reflectometry and dielectric spectroscopy study of transformer oil-based ferrofluids.
45. **Makarova M.V.**, Kravtsov E.A., Khaydukov Yu., Ustinov V.V. (Institute of Metal Physics, Ural Branch of the Russian Academy of Sciences, Ekaterinburg, Russia). Perpendicular magnetic anisotropy of layered heterostructure Dy/Co.
46. **Nikova E.S.**, Salamatov Yu. A., Kravtsov E. A., Ustinov V. V. (Institute of Metal Physics UB RAS, Russia, Ekaterinburg). Application of the GD reference layer approach for the study of magnetic metallic nanostructures.
47. Racuciu M., Barbu-Tudoran L., Morosanu C., Brinza F., **Creanga D.**, Balasoïu M. (Lucian Blaga University of Sibiu, Sibiu, Romania). Study on the granularity of magnetic nanoparticles in aqueous suspension: theoretical and experimental approach.

POSTER SESSION II (October 14, 2020)

Soft condensed matter (biological nanosystems, lipid membranes, polymers)

48. **Anghel L.L.**, Kuklin A.I., Bodnarchuk V.I., Erhan R.V. (Institute of Chemistry of Academy of Sciences of Moldova, Chisinau, Moldova). Pectin/beta-lactoglobulin interactions observed by small-angle scattering.
49. Anghel L., Kuklin A.I., Ivankov O., Bodnarchuk V.I., **Erhan R.** (Horia Hulubei National Institute for R&D in Physics and Nuclear Engineering, Bucharest - Magurele,

- Romania). Structural study of the beta-lactoglobulin - beta-glucan system using small-angle neutron scattering.
50. **Avdeev M.M.**, Kosiachkin Ye.N., Artykulnyi O.P., Gorshkova Yu.E., Shibaev A.V., Philippova O.E. (Moscow State University, Moscow, Russia). Study of immobilization of polyacrylamide on oxidized silicon surface by X-ray reflectometry and atomic force microscopy.
 51. **Bukhdruker S.S.**, Kavaleuski A., Ryzhykau Y.L., Varaksa T., Smolskaya S., Gilep A., Kuklin A.I., Strushkevich N., Borshchevskiy V.I. (Moscow Institute of Physics and Technology, Dolgoprudny, Russia). Crystallography and small-angle study of cytochrome P450 – redox partner electron-transfer complex.
 52. **Bocharov E.V.**, Pavlov K.V., Lesovoy D.M., Bocharova O.V., Urban A.S., Bershatsky Y.V., Volynsky P.E., Efremov R.G., Arseniev A.S. (Moscow Institute of Physics and Technology, Dolgoprudny, Russia). Molecular mechanisms of bitopic protein functioning revealed by structural-dynamic studies of transmembrane domain interactions.
 53. **Bondarev N.A.**, Okhrimenko I.S., Bazhenov S.V., Bulushova N.V., Kuklin A.I., Rizhikov Yu.L., Baranova A.V., Manukhov I.V. (Moscow Institute of Physics and Technology, Dolgoprudny, Moscow Region, Russia). The physical and chemical characteristics of fused protein methionine γ -lyase from *Clostridium Sporogenes* and S-3 domain of growth factor from vaccinia virus.
 54. **Gorshkova Yu.E.**, Barbinta-Patrascu M.E., Bokuchava G.D., Badea N., Ungureanu C., Lazea-Stoyanova A., Vlad A., Turchenko V.A., Zhigunov A., Juszyńska-Galazka E. (Frank Laboratory of Neutron Physics, Joint Institute for Nuclear Research, Dubna, Russia). Biohybrid complexes with phyto-generated entities from nettle & grapes and their potential application in the biomedical field.
 55. **Elnikova L.V.**, Ozerin A.N., Shevchenko V.G., Nedorezova P.M., Ponomarenko A. T., Skoi V.V., Kuklin A.I. (NRC “Kurchatov Institute” – Alikhanov Institute for Theoretical and Experimental Physics, Moscow, Russian Federation). Knotting of carbon nanotubes in isotactic polypropylene matrix due to the results of small-angle neutron scattering and lattice numerical modeling.
 56. **Egorov V.V.**, Gorshkova Y.E., Zabrodskaia Y.A. (Petersburg Nuclear Physics Institute NRC KI, Gatchina, Russia). Model system for immunosuppressive peptides interaction study.
 57. **Erhan R.V.**, Rada S., Suciú M., Macavei S., Dehelean A., Bodnarchuk V. (Horia Hulubei National Institute for R&D in Physics and Nuclear Engineering, Bucharest-Magurele, Romania). Manganese oxide doped lead-germanate glasses: Raman, EPR and SANS studies.
 58. **Erhan S.E.**, Kuklin A.I., Erhan R.V., Knudsen K.D., Roşioru C.L. (Horia Hulubei National Institute of Research and Development in Physics and Nuclear Engineering, Bucharest, Romania). Secondary osteoporosis in rats studied by small angle neutron scattering.
 59. **Ivanova L.A.**, Gorshkova Y.E., Verlov N.A., Burdakov V.S., Baranchikov A. E., Kopitsa G. P., Kulminskaya A.A. (Petersburg Nuclear Physics Institute NRC KI, Gatchina, Russia). Crystal and supra-molecular structure of bacterial cellulose hydrolyzed by cellobiohydrolase from *Scytalidium Candidum* 3c: a basis for development of biodegradable wound dressings.
 60. **Kondela T.**, Hrubovčák P., Dushanov E., Kholmurodov K., Ivankov O., Murugova T., Kuklin A., Kučerka N. (Frank Laboratory of Neutron Physics, Joint Institute for

- Nuclear Research, Dubna, Russia). Investigation into the effect of cholesterol and melatonin on the amyloid embedded model membrane through neutron scattering.
61. **Kuzmenko M.O.**, Gapon I.V., Avdeev M.V., Gorshkova Yu.Ye., Maslova V.A., Dmytrenko O.P. (Frank Laboratory of Neutron Physics, Joint Institute for Nuclear Research, Dubna, Russia). Support silicon oxide nanolayer for neutron reflectometry solid-liquid cell for studying biological solutions.
 62. **Makhaldiani N.** (Joint Institute for Nuclear Research, Dubna, Russia). Unified theory of dynamical systems with applications including biological systems.
 63. **Osipov S.D.**, Vlasov A.V., Ryzhykau Yu.L., Kuklin A.I., Gordeliy V.I. (Moscow Institute of Physics and Technology, Dolgoprudny, Russia). Structural parameters of thylakoid membrane: lipid and protein parts.
 64. **Okhrimenko I.S.**, Zagryadskaya Y.A., Ryzhykau Y.L., Kuklin A.I., Dencher N.A., Gordeliy V.I. (Moscow Institute of Physics and Technology, Dolgoprudny, Russia). Preparation of liposomes from native cell membrane for SAXS/SANS studies.
 65. **Ospennikov A.S.**, Artykulnyi O.P., Shibaev A.V., Kuklin A.I., Philippova O.E. (Moscow State University, Moscow, Russia). Effect of water-soluble monomer on wormlike micelles of surfactant studied by small-angle neutron scattering.
 66. **Ospennikov A.S.**, Kuklin A.I., Shibaev A.V., Philippova O.E. (Moscow State University, Moscow, Russia). Investigation of hydrogels based on cross-linked polymer and wormlike surfactant micelles by small-angle neutron scattering.
 67. **Pavlova A.A.**, Bugrov A.N., Smyslov R.Yu., Gorshkova Yu.E., Kopitsa G.P. (Petersburg Nuclear Physics Institute NRC KI, Gatchina, Russia). Investigation of the domain structure of segmented polyurethane ureas by small angle neutron scattering.
 68. **Ryzhykau Yu.L.**, Orekhov P.S., Rulev M.I., Vlasov A.V., Zabelskii D.V., Rogachev A.V., Murugova T.N., Vlasova A.D., Gordeliy V.I., Kuklin A.I. (Moscow Institute of Physics and Technology, Dolgoprudny, Russia). SANS investigation of membrane protein oligomerization: the case of the TCS photoreceptor complex NpSR11/NpHtrII.
 69. **Skoï V.V.**, Soloviev D.V., Rogachev A.V., Chupin V.V., Kuklin A.I., Gordeliy V.I. (Frank Laboratory of Neutron Physics, Joint Institute for Nuclear Research, Dubna, Russia). Complex effect of AgNO₃ and KNO₃ on DPPC bilayer: SANS and densitometry study.
 70. Shibaev A.V., **Aleshina A.L.**, Kuklin A.I., Iliopoulos I., Philippova O.E. (Moscow State University, Moscow, Russia). PH-triggered structural transformations in the mixtures of an ionic surfactant and a hydrophilic polymer.
 71. **Sudarev V.V.**, Vlasov A.V., Osipov S.D., Ryzhykau Y.L., Vlasova A.D., Skoy V.V., Murugova T.N., Rogachev A.V., Bukhalovich S.M., Dolotova S.M., Kuskov A.S., Gordeliy V.I., Kuklin A.I. (Moscow Institute of Physics and Technology, Dolgoprudny, Russia). Stability of ferritin protein complex at various pH.
 72. **Vlasov A.V.**, Ryzhykau Yu.L., Osipov S.D., Vlasova A.D., Dencher N.A., Kuklin A.I., Gordeliy V.I. (Moscow Institute of Physics and Technology, Dolgoprudny, Russia). The possibility of dimerization of atp synthase from spinach chloroplasts.
 73. **Żyła A.**, Jurczak P., Szymańska A., Wolak J., Taube M., Zhukov I., Kuklin A.I., Koza M. (Adam Mickiewicz University, Poznań, Poland). Structural investigation interaction between amyloid-beta peptides and associated proteins — the human serum albumin and human cystatin C.

Materials under extreme conditions

74. **Lis O.N.**, Kichanov S.E., Belozerova N.M., Lukin E.V, Savenko, B.N., Balakumar S. (Frank Laboratory of Neutron Physics, Joint Institute for Nuclear Research, Dubna, Russia). The neutron diffraction study of crystal and magnetic structures of multiferroic $\text{Bi}_{2-x}\text{Fe}_x\text{WO}_6$.
75. **Rutkauskas A.V.**, Kozlenko D.P., Kichanov S.E., Savenko B.N. (Frank Laboratory of Neutron Physics, Joint Institute for Nuclear Research, Dubna, Russia). The effect of doping of Sr^{2+} ions on the crystal and magnetic structure of barium hexaferrites $\text{Ba}_{1-x}\text{Sr}_x\text{Fe}_{12}\text{O}_{19}$.
76. Kozlenko D.P., **Zel I.Yu.**, Dang T.N., Le T.P.T. (Frank Laboratory of Neutron Physics, Joint Institute for Nuclear Research, Dubna, Russia). High pressure induced structural and magnetic phase transformations in BaYFeO_4 .

Texture and stress investigation of materials

77. **Badmaarag A.**, Sangaa D., Sikolenko V., Scheffzuk Ch, Enkhtur L., Duinkherjav Y., Otgobayar P. (Institute of Physics and Technology, Ulaanbaatar, Mongolia). Tensional residual strain investigation by force direction of the rebar steel sample using time-of-flight neutron diffraction at the strain/stress diffractometer EPSILON.
78. **Carro-Sevillano G.**, Fernández Serrano R., Bokuchava G., Millán L., González-Doncel G. (CENIM-CSIC, Madrid, Spain). Residual stress distribution after a quenching treatment obtained by neutron diffraction experiments and fem simulation.
79. **Kirillov A.K.**, Vasilenko T.A., Islamov A. Kh. (Institute for Physics of Mining Processes NAS Ukraine, Dnipro, Ukraine). Features of the structure of the Chelyabinsk meteorite according to neutron SAS.
80. **Kucerakova M.**, Rohlicek J., Nikoayev D., Lychagina T. (Institute of Physics CAS CZ, Prague, Czech Republic). Texture study of Sinanodonta Woodiana shells by X-ray diffraction.
81. **Millán L.**, Bokuchava G., Hidalgo J.I., Fernández R., Kronberger G., Haldova P., Sáez A., Papushkin I., Garnica O., Lanchares J., González-Doncel G. (Centro Nacional de Investigaciones Metalúrgicas CENIM-CSIC, Madrid, Spain). Study of residual stresses in an extruded aluminium alloys after thermal treatments.
82. **Oponowicz A.**, Marciszko-Wiąckowska M., Baczmanski A., Klaus M., Genzel Ch., Wroński S., Wróbel M. (AGH-University of Science and Technology, Kraków, Poland). Synchrotron energy dispersive method and grazing incident X – ray diffraction used to measure stresses in surface layers of polycrystalline materials.
83. **Silva P.N.**, Erhan R.V., Scheffzuk Ch., Gomes J.A.C.P. (COPPE - Federal University of Rio de Janeiro, Rio de Janeiro, Brazil). Preliminary study of residual stress distribution in high strength steel wires at EPSILON neutron diffractometer.
84. Wróbel M., Nikolayev D., Lychagina T., Kopyściański M., **Dymek S.**, Węglowski M.S., Sekretarev Z., Baczmanski A. (AGH University of Science and Technology, Kraków, Poland). Comparison of local and global texture in friction stir processed aluminum alloys.

**Abstracts:
Introductory
Session**

NEUTRON SCATTERING INSTRUMENTATION OF IBR-2 HIGH FLUX PULSED REACTOR FOR CONDENSED MATTER RESEARCH: RECENT DEVELOPMENTS

D.P. Kozlenko¹

¹*Frank Laboratory of Neutron Physics, Joint Institute for Nuclear Research, 141980 Dubna, Moscow Reg., Russia*

E-mail: denk@nf.jinr.ru

Since the re-start of the regular operation of the IBR-2 high flux pulsed reactor after full-scale modernization in 2012, the complex of neutron scattering instruments installed at the reactor was substantially upgraded. Now it contains in total 15 instruments, including diffractometers, small angle scattering spectrometer, reflectometers, inelastic neutron scattering spectrometers.

The isotope identifying reflectometry method at the REMUR reflectometer has been realized. The parabolic neutron focusing device ($m = 5$) at the NERA spectrometer has been installed. The new mirror neutron guide ($m = 2$) has been installed at the FSS diffractometer at the 13 beamline of IBR-2. The modernization of the electrochemical cells for neutron reflectometry experiments at the GRAINS reflectometer has been realized. The upgrade of the neutron splitting system at the 10 channel of IBR-2 has been made. The development of the new small angle neutron scattering and imaging spectrometer to be installed at the 10A beamline is in progress. The plans for future developments of the IBR-2 instruments are discussed.

PROGRESS REPORT ON DEVELOPING A CONCEPT FOR A NEW NEUTRON SOURCE AT FLNP

V.N. Shvetsov¹, V.L.Aksenov¹, S.A.Kulikov¹, E.P.Shabalina¹, A.V.Vinogradov¹,
A.V.Lopatkin², I.T.Tretyakov², A.V.Goryachikh²

¹FLNP, JINR

²NIKIET

E-mail: shv@nf.jinr.ru

Systematic shortage of the neutron beam time in Europe and in the world raises demand in construction of new neutron sources. We propose to build a new advanced neutron source, DNS-IV (Dubna Neutron Source IV-th generation), at JINR. To be constructed in the combination with modern moderators, neutron guides and neutron scattering instruments (DNS-IV) promises to become one of the best neutron sources in the world and will open unprecedented possibilities for scientists from JINR member states and worldwide for research in condensed matter physics, fundamental physics, chemistry, material and life science.

DNS-IV will provide shorter neutron pulses, however containing the same number of neutrons as at European Spallation Source (ESS, to be operational in 2024). Indeed, it will be as good as ESS for low-resolution experiments and significantly outperform it for high-resolution experiments.

Two alternative concepts of DNS-IV were considered: the pulsed neutron reactor IBR-3 with Np-237 core and the accelerator-driven spallation neutron source with PuO₂ core providing neutron multiplication factor of about 20-50. Both options have been under the feasibility study in N.A. Dollezhal Research and Development Institute of Power Engineering (NIKIET, Moscow). The final recommendation is based on such criteria as achievable neutron characteristics, nuclear safety, engineering complexity, timeline and expected costs. It was found that the engineering complexity of 2nd option makes its realization rather uncertain, both in time and costs. Therefore, the pulsed neutron reactor IBR-3 with NpN fuel currently became the working project with the planned start of the DNS-IV operation is 2036-2037.

First meetings with the specialists from A. A. Bochvar All-Russian Scientific Research Institute for Inorganic Materials (VNIINM) starts JINR-VNIINM cooperation aimed to the development of the roadmap for NpN reactor fuel fabrication detailed Roadmap of the DNS-IV implementation will be presented.

THE “LvB” COMPACT NEUTRON SOURCE PROJECT AT MARTONVÁSÁR

F. Mezei¹, Cs.Pétermann¹, P. Sipos¹ and Á. Horváth²

¹*Mirrotron Ltd, 1121 Budapest, Konkoly Thege u. 29-33, Hungary*

²*Centre for Energy Research, 1121 Budapest, Konkoly Thege u. 29-33, Hungary*

E-mail: mezei.ferenc@mirrotron.hu

The “LvB” compact neutron source project is under construction at the dedicated site operated by Mirrotron Ltd at the town of Martonvásár, 30 min train ride from the closest metro station in Budapest. The project is a collaborative effort between Mirrotron Ltd, the Centre for Energy Research of the Eötvös Loránd Research Network and Varius Ltd., Budapest. Funding is secured by a 3.5 million Eur regional development grant (structural funds) and 1.5 million Eur own capital from Mirrotron Ltd and Varius Ltd. The project started in November 2017, the construction of the new facility building was completed by December 2019. The public tender for the construction of the 20 mA peak current, 2.5 MeV pulsed RFQ accelerator has been accomplished by March 2020 and its construction has started. The construction project for the first neutron scattering instrument, a reflectometer for testing neutron supermirrors, amongst others, started in July 2019 and is due to be operational by early 2022. The first pieces of hardware for this instrument have been delivered in July 2020. The official deadline for completion and start of test operation for neutron production is December 2021, after 3 months extension (by now) for delays due to the Covid pandemic. At a second stage, an afterburner will be added in order to reach 5 MeV final proton beam energy for the generation of 3×10^{12} neutrons/s at 5 kW proton beam time average power at 5 % duty factor pulsed operation. The facility will be alternatively used for delivering 2.5 MeV proton beam for epithermal neutron production for irradiation purposes, and for 5 MeV proton beam for moderated bi-spectral cold-thermal neutron beam and fast neutron beam production in beam bundles of different directions around a dedicated target-moderator-reflector assembly. The primary industrial goal of the LvB compact neutron source is to test components, primarily neutron supermirrors both for product development and production quality assurance as part of the manufacturing activities at Mirrotron Ltd. Following the successful example of RANS at Riken, Tokyo in serving a broad industrial community, LvB will provide neutron beams of different parameters for various industrial applications, beyond the in-house needs of Mirrotron Ltd. It is envisaged for this purpose – in addition to contractual studies – to provide beam-time on a number of neutron instruments and on un-instrumented beam lines, e.g. for development of compact neutron source technology. The cold and thermal neutron beams will be available for neutron radiography and tomography, neutron reflectometry, small angle scattering, prompt gamma activation analyses and neutron diffraction for phase analysis, texture studies and strain scanning. At all of these instruments, the scope is to study the high intensity features of the scattered neutron spectra, often with good resolution (for example shifts of Bragg peaks for strain studies). High-resolution capability will here be achieved by superposing a fast, random beam modulation on the basic pulsed time structure of the long pulse neutron generation, and observing the correlations between fluctuations of the detector counting rate in time and the random beam modulation. With the help of this doubly time modulated neutron beam delivery pattern, low and high time resolution information will be simultaneously delivered by the instruments. Using the most advanced moderator and neutron instrumentation technology, LvB will offer neutron research capabilities for applied research purposes that would have required a quarter of a century ago orders of magnitude more expensive conventional, much larger neutron sources, such as reactors of a few MW power.

**Abstracts:
Oral
Presentations**

DEFECTS STRUCTURE IN OLIVINE-TYPE CATHODE MATERIALS STUDIED BY NEUTRON DIFFRACTION

I.A. Trussov¹, D.A. Aksyonov¹, A.A. Savina¹, A. Senyshyn², A.M. Abakumov¹,
E.V. Antipov^{1,3}, S.S. Fedotov¹

¹ Skoltech Center for Energy Science and Technology, Skolkovo Institute of Science and Technology, 121205, Moscow, Russia

² Forschungsneutronenquelle Heinz Maier-Leibnitz (FRM II), 85747, Garching, Germany

³ Chemistry Department, Lomonosov Moscow State University, 119991, Moscow, Russia

E-mail: s.fedotov@skoltech.ru

LiFePO₄ is a commercialized cathode material ensuring wide applications of Li-ion battery technology for stationary energy storage and renewable energy sources. Regardless of the obvious simplicity of its crystal structure and chemical composition, LiFePO₄ holds astonishing defects chemistry arising from the rearrangement of cations and vacancies within tetrahedral and octahedral sites, variations in the their occupancies and iron oxidation state. It was shown that so-called Li-rich phases might form with the Li excess at the Fe sites reaching up to 10% [1]. At the same time the polyanion sublattice was rarely considered defective. It was taken for granted that the PO₄ group is highly durable, with no defects being possible at the P site [2].

In this talk, we will concentrate upon various defects peculiarities in LiFePO₄ and its Li-rich counterpart studied by combined X-ray and neutron diffraction methods coupled with high-throughput DFT and MD calculations. The recently discovered cations arrangements and off-stoichiometry in LiFePO₄ due to a partial replacement of Fe with Li atoms or PO₄ with hydroxyl groups for hydrothermally prepared samples at different synthesis conditions will be discussed. Such off-stoichiometries can reach over 10% yielding Li_{1+x}Fe_{1-x}PO₄ ($x \leq 0.1$) and Li_{1-x}Fe_{1+x}(PO₄)_{1-y}(OH)_{4y} ($x \leq 0.05$, $y \leq 0.1$) solid solutions respectively. Both Li and OH-substitutions trigger essential changes in the crystal structure and properties, increasing the migration barriers for Li ions and affect the electrochemical performance. We demonstrated that the off-stoichiometry significantly depends on the precursors and reducing agents concentrations and the order of mixing thereof, rendering them critical parameters that control the defects formation of the hydrothermally synthesized LiFePO₄-based cathode materials.

More data on the crystal structure and properties of Li-rich LiFePO₄ and OH-substituted LiFePO₄ as well as the interconnection between “new” and “old” defects in synthetic phosphates and natural olivine-type minerals will be presented and analyzed.

Acknowledgements: This research was supported by Russian Foundation for Basic Research (grant 18-29-12097)

[1] O.A. Drozhzhin et al (2019) Exploring the Origin of the Superior Electrochemical Performance of Hydrothermally Prepared Li-Rich Lithium Iron Phosphate Li_{1+δ}Fe_{1-δ}PO₄. J. Phys. Chem. C 124, 126-134.

[2] V.D. Sumanov et al (2019) Hydrotriphylites Li_{1-x}Fe_{1+x}(PO₄)_{1-y}(OH)_{4y} as Cathode Materials for Li-ion Batteries. Chem. Mater. 31, 5035-5046

STUDY OF FIRST AND SECOND ORDER TRANSITIONS IN Fe-Ga AND Fe-Al ALLOYS

I.S. Golovin¹ and A.M. Balagurov²

¹ National University of Science and Technology “MISIS”, Moscow, Russia

² Frank Laboratory of Neutron Physics, Joint Institute for Nuclear Research, Dubna, Russia

E-mail: i.golovin@misis.ru

In this talk we present the results of cooperation between research groups of National University of Science and Technology “MISIS” and Frank Laboratory of Neutron Physics, Joint Institute for Nuclear Research. Overview of first and second order phase transitions in Fe-Ga and Fe-Al alloys includes analysis of transitions at heating, cooling and isothermal annealing, construction of TTT diagrams, cluster-like structures and properties of the alloys. Key role in these studies belongs to *in situ* neutron diffraction.

APPLICATION OF IN SITU NEUTRON DIFFRACTION TO STUDY THERMO-KINETIC TRANSITIONS IN GALFENOLS

A.K. Mohamed¹, V.V. Palacheva¹, I.S. Golovin¹, I.A. Bobrikov², A.M. Balagurov^{2,3}

¹ National University of Science and Technology "MISIS", Moscow, Russia

² Frank Laboratory of Neutron Physics, Joint Institute for Nuclear Research, Dubna, Russia

³ Lomonosov Moscow State University, Moscow, Russia

E-mail: abdelkarim.abdelkarim@feng.bu.edu.eg

The development of a new class of structural magnetostrictive materials makes them promise for use in a host of applications. Fe–Ga alloys (Galfenol) exhibit moderate magnetostriction (~350 ppm) under very low magnetic fields 100 Oe (8000 A.m⁻¹), have very low hysteresis, and demonstrate high tensile strength (500 MPa) and limited variation in magnetomechanical properties for temperatures between 20 and 80°C [1]. Besides, they have a high Curie temperature [1], biodegradable and corrosion resistant [2,3].

In situ neutron diffraction along with several other methods were used to study structure and phase transitions at cooling and isothermal annealing of two Fe-Ga alloys with the chemical composition close to the two maxima magnetostriction curves [4]. They are Fe-19at.%Ga and Fe-27at.%Ga. XRD is used to investigate the structure of the isothermally annealed samples for different times that reaches to 300 h. The time-temperature-transformation (TTT) diagrams were built, and critical cooling rates were determined [5]. The TTT diagrams for Fe-19at.%Ga and Fe-27at.%Ga alloys are useful to control the structure in the alloy which greatly affects their functional property.

[1] R.A. Kellogg (2003). Development and modeling of iron–gallium alloys, PhD Thesis Engineering Mechanics, Iowa State University, Ames, Iowa.

[2] H. Wang, Y. Zheng, J. Liu, C. Jiang, Y. Li (2017). In vitro corrosion properties and cytocompatibility of Fe-Ga alloys as potential biodegradable metallic materials, Mater. Sci. Eng. C. 71, 60–66.

[3] T.V. Jayaraman, N. Srisukhumbowornchai, S. Guruswamy, M.L. Free (2007). Corrosion studies of single crystals of iron–gallium alloys in aqueous environments, Corros. Sci. 49, 4015–4027.

[4] Q. Xing, Y. Du, R.J. McQueeney, T.A. Lograsso, Structural investigations of Fe–Ga alloys: Phase relations and magnetostrictive behavior, Acta.Mater. 56 (2008) 4536-4546.

[5] I.S. Golovin, A.K. Mohamed, I.A. Bobrikov, A.M. Balagurov, Time-Temperature-Transformation from metastable to equilibrium structure in Fe-Ga, Materials Letters, 263 (2020) 127257

The work was carried out with support from the RNF project no. 19-72-20080.

INELASTIC NEUTRON SCATTERING IN RESEARCH ON THE PHYSICS OF STRONGLY CORRELATED ELECTRON SYSTEMS

P.A. Alekseev^{1,2}, P.S. Savchenkov^{1,2}, V.N. Lazukov¹

¹National Research Centre «Kurchatov Institute», Moscow, 123182, Russian Federation

²National Research Nuclear University MEPhI, 115409, Moscow, Russian Federation

E-mail: pavel_alekseev-r@mail.ru

The unique set of the physical properties of strongly correlated electron systems (SCES) results from the combination and competition of the three main factors: hybridization between *f*-electrons and band electrons near Fermi-level, exchange interaction between rare earth (RE) ions with local magnetic moments specific for the unfilled *f*-electron shell and the crystal electric field (CEF) splitting of the ground state multiplet of the *f*-electron shell. All three type of interaction can be effectively studied by the inelastic thermal neutron scattering – the neutron spectroscopy. .

The particular series of the magnetic neutron spectroscopy studies of the CEF effects for SCES allow to establish the characteristic *f*-electron spectral features for systems with well-defined local moments, heavy fermion systems, systems with *f*-electron instability (i.e. intermediate valence systems) and co-called Kondo insulators.

One another interesting phenomenon of the “induced magnetic ordering” for the local magnetic moments with singlet ground state formed by CEF splitting in a periodical RE lattice is recently studied in details for the prototype intermetallic rare-earth compound PrNi ordered ferromagnetically at temperature $T_c = 21\text{K}$. Magnetic phase transition takes place due to “soft magnetic mode” behavior near T_c fixed by neutron spectroscopy of the single crystal.

We studied the influence of La (nonmagnetic) and Ce (intermediate valence) impurities on the magnetic ordering temperature T_c of compounds $\text{RE}_{1-x}(\text{La,Ce})_x\text{Ni}$ (RE=Pr, Gd) [1,2]. The Gd-based system is considered as the classical local magnetic moment system with long range magnetic order driven by RKKY exchange interaction. The introduction of a spin-fluctuating intermediate valence impurity in the Pr sublattice of PrNi leads to the dramatic increase in the area of the ordered state on the phase diagram as function of *x*, due to an increase in T_c , compared to the impact of La-impurity over the entire concentration range.

The modification of the CEF splitting by the Ce intermediate valence impurity appears to be the decisive factor affecting T_c wherein the intermediate valence Ce ions carry zero static magnetic moments similar to the La case. The latter explains the identical dependencies of the ordering temperature on the La- and Ce-impurity concentration observed in systems with a long-range order of local magnetic moments $\text{Gd}_{1-x}\text{La}_x\text{Ni}$ and $\text{Gd}_{1-x}\text{Ce}_x\text{Ni}$, contrary to the case of Pr-based systems.

[1] P.S. Savchenkov, E.S. Clementyev, P.A. Alekseev, V.N. Lazukov (2019) Induced magnetism and “magnetic hole” in singlet ground state system PrNi. Journal of Magnetism and Magnetic Materials 489 165413

[2] P.S. Savchenkov, E.S.Clementyev, V.N. Lazukov, P.A. Alekseev (2020) Dramatic impact of intermediate-valence impurity on Induced magnetism in singlet ground state system PrNi. Journal of Magnetism and Magnetic Materials (2020)

INFLUENCE OF CHEMICAL COMPOSITION ON SPINODAL DECOMPOSITION OF AUSTENITE AND THERMO-ELASTIC MARTENSITIC TRANSITION IN LOW-Cu Mn-Cu ALLOYS

Liying Sun^{1*}, I.S. Golovin¹, A.Kh. Islamov², R.N. Vasin², I.A. Bobrikov², V. Sumnikov², A.M. Balagurov^{2,3}, W.C. Cheng⁴, A.V. Shuitcev⁵

¹ National University of Science and Technology "MISIS", Leninsky Ave. 4, 119049, Moscow, Russia

² Frank Laboratory of Neutron Physics, Joint Institute for Nuclear Research, 141980, Dubna, Russia

³ Department of Mechanical Engineering, NTUST, Taipei, Taiwan, ROC

⁴ Lomonosov Moscow State University, 119991 Moscow, Russia

⁵ Institute of Materials Processing and Intelligent Manufacturing, College of Materials Science and Chemical Engineering, Harbin Engineering University, Harbin 150001, China

E-mail: liying.sun@mail.ru

Mn-Cu alloys are extensively used in the industry with good mechanical properties, high damping capacity, and shape memory effect. Functional properties are based on the face-centered tetragonal (f.c.t.) martensite \leftrightarrow face-centered cubic (f.c.c.) austenite phase transition that occurs by the mechanism of thermo-elastic martensitic transition (MT). Influence of Cr addition on spinodal decomposition of f.c.c.-phase in Mn-13Cu and Mn-10Cu-4Cr (at.%) alloys is investigated after different ageing regimes using small-angle neutron scattering (SANS), *in situ* neutron and X-ray diffraction, TEM, heat flow (DSC) and tensile test tests. An increase in ageing temperature from 400 °C to 520 °C for 8 hrs and time up to 120 hrs at 440 °C phase transition temperatures for both direct and reverse MT increase in both alloys. The thermal hysteresis between direct and reverse MT is independent on the ageing treatments in the both alloys. According to SANS data, ageing treatment leads to formation of Mn-rich matrix, Cu-rich nanoclusters and α -Mn phase due to the spinodal decomposition. An increase in Mn content in the Mn-rich matrix and in overage volume of the nanoclusters without an increase in their volume fraction is recorded with ageing temperature and time. This explains changes in the MT temperatures, yield strength, and hardness of both alloys subjected to different ageing treatments. The *in situ* ND results reveal that direct and reverse MT complete instantaneously in both alloys, and the volume effect for both direct and reverse MT is small during the phase transition, indicating that the lattice distortions are also small. The structural and magnetic transitions take place at the same temperature upon heating and cooling. Addition of Cr to Mn-Cu alloy enhances degree of tetragonality of martensite and leads to formation of the α -Mn phase. In addition, Cr retards decomposition of the f.c.c.-austenite during ageing, owing to formation of numerous α -Mn precipitations, and therefore the Mn concentration in Mn-rich matrix decreases.

BARIUM TITANATE FROM MULTICOMPONENT GLASS DOPED WITH IRON OXIDE – CRYSTALLIZATION EFFECTS

K. Krezhov¹, R. Harizanova², I. Gugov², I. Mihailova², A. Beskrovny³, E. Popov^{1,3}, E. Lukin³

¹*Institute of Electronics and Institute for Nuclear Research and Nuclear Energy, Bulgarian Academy of Sciences, Sofia, Bulgaria*

²*University of Chemical Technology and Metallurgy, Sofia, Bulgaria*

³*Joint Institute for Nuclear Research, Dubna, Russia*

E-mail: kiril.krezhov@gmail.com

The crystallization of oxide glasses with high concentrations of Ba and Ti oxides can lead to preparation of glass-ceramics containing barium titanate (BaTiO₃) with tuneable crystallite sizes and high volume fraction which can be used as cheap materials with relatively large dielectric constants and application in electronics and sensor technology [1, 2]. The addition of Fe₂O₃ can result, after heat treatment, into precipitation of BaTiO₃ crystals with inclusions of Fe or core-shell particles of BaTiO₃-Fe₃O₄ with application in spintronics [3, 4]. One approach to obtaining the aforementioned crystals is to synthesize a specific glass that is phase separated. Usually, one of the phases will contain the crystallizing elements, i.e. Ba and Ti, possibly also Fe. A suitable system for such purpose is Na₂O/BaO/TiO₂/SiO₂/B₂O₃/Al₂O₃/Fe₂O₃, in which the phase separation is to be expected [5] and has already been observed [6].

We report neutron diffraction (ND) experiments on selected glasses from the system Na₂O/Al₂O₃/BaO/TiO₂/B₂O₃/SiO₂/Fe₂O₃ prepared using conventional melt-quenching technique and on barium titanate containing glass-ceramics obtained from them. Actually, samples (23.1-x)Na₂O/23.1BaO/23TiO₂/17.4SiO₂/7.6B₂O₃/xAl₂O₃/5.8Fe₂O₃, x = 0, 3, 7, 11 and 15 mol%, were subjected to thermal treatment above the glass-transition temperature which leads to the crystallization of BaTiO₃ as confirmed by evidence from other experimental techniques (XPS, XRD, EM, and IR spectroscopy).

The electron microscopy (EM) results show that the microstructures of all annealed samples are similar and consist of globular interconnected particles in which nanosized formations grow randomly. The mean size of these formations increases with the increasing annealing time from 200 to 600 nm. The EM provides evidence for phase separation into two phases – one enriched in Ba and Ti from which subsequently BaTiO₃ crystallizes (Fig.1) and the matrix containing all other composition constituents. X-ray diffraction reveals changes of peak positions and intensities compared to that of stoichiometric BaTiO₃ which suggests that the occurrence of defect cubic barium titanate crystals or even modified crystals from the type BaTi_{1-x}Fe_xO_{3-δ} is possible [6]. Temperature-dependent impedance measurements show that relaxor type phase transitions are observed in the glass-ceramics below room temperature [7]. The in-situ temperature dependent ND investigations on the studied systems confirmed the possibility to crystallize barium titanate at temperatures close to those predicted from the differential thermal analysis (DTA) which revealed that the crystallisation temperatures T_c are 550, 560, 620, 650 and 660°C for x = 0, 3, 7, 11 and 15 mol.%, respectively. The ND results indicate for the first time that the crystallization of tetragonal BaTiO₃ is possible in the studied glass series and Fig. 2 illustrates the specific case of formation of compounds adopting a polar structure with tetragonal symmetry with space group P4mm. One should bear in mind that iron doping could result in reduced temperature of the transition of the tetragonal ferroelectric phase of BaTiO₃ into the cubic paraelectric phase with space group Pm-3̄m as

observed in [8] for an iron concentration of $x = 0.01$ where the phase transition ferro-paraelectric occurs at 390 K while for pure BaTiO₃ it is approximately 410 K [8].

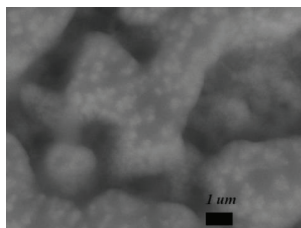


Figure 1. SEM (BSE) of an annealed specimen with 3 mol% alumina [6]

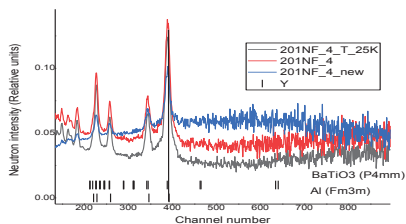


Figure 2 TOF patterns of a powder sample from the studied system taken on the instrument DN 12 at room temperature and 25 K. The ND patterns are processed by the Rietveld method. The vertical marks show the calculated position of allowed Bragg reflections. The lowest row of marks is arising from the aluminium container.

- [1] M. M. Vijatović, J. D. Bobić, B. D. Stojanović, History and Challenges of Barium Titanate: Part I, (2008) *Science of Sintering*, 40,(2), 155-165
- [2] J.F. Capsal, E Dantras, L Laffont, J Dandurand, C Lacabanne., Nanotexture influence of BaTiO₃ particles on piezoelectric behaviour of PA11/BaTiO₃ nanocomposites, (2010) *J. Non-Cryst. Sol.*, 356, 629-634.
- [3] R.P. Maiti, S. Basu, S. Bhattacharya, Multiferroic behavior in silicate glass nanocomposite having a core-shell microstructure, (2009) *J. Non-Cryst. Sol.*, 355, 2254–2259.
- [4] G. Du, Z. Hu, Q. Han et al, Effects of niobium donor doping on the phase structures and magnetic properties of Fe-doped BaTiO₃ ceramics, (2010) *J. Alloys Comp.*, 492, L79-L81.
- [5] W. Vogel, (1985) *Glass chemistry*, Springer-Verlag, 2nd edition.
- [6] R. Harizanova, M. Abrashev, I. Avramova, L. Vladislavova, C. Bocker, G. Tsutsumanova, G. Avdeev, C. Rüssel, Phase composition identification and microstructure of BaTiO₃ containing sodium-aluminoborosilicate glass-ceramics (2016) *Solid State Sciences*, 52, 49-56.
- [7] R. Harizanova, S. Slavov, L. Vladislavova, L. C. Costa, G. Avdeev, C. Bocker, C. Rüssel, Barium titanate containing glass-ceramics - The effect of phase composition and microstructure on dielectric properties, (2020) *Ceramics International*, doi.org/10.1016/j.ceramint.2020.06.247
- [8] D.P. Kozlenko, N.T. Dang, S.E. Kichanov, et al., Neutron-diffraction study of the crystal structure of BaTiO₃ ferroelectric doped with iron, (2016) *Journal of Surface Investigation. X-ray, Synchrotron and Neutron Techniques*, 10(2) 370–374.

FEATURES OF MAGNETIC PHASE TRANSITIONS IN THE $\text{LiNi}_{1-x}\text{Co}_x\text{PO}_4$ MAGNETOELECTRICS

N.V. Urusova^{1,2}, M.A. Semkin^{2,3} and A.N. Pirogov^{2,3}

¹*Institute of Solid State Chemistry, Ural Branch, Russian Academy of Sciences, Ekaterinburg, Russian Federation*

²*Institute of Natural Sciences and Mathematics, Ural Federal University, Ekaterinburg, Russian Federation*

³*M.N. Miheev Institute of Metal Physics, Ural Branch, Russian Academy of Sciences, Ekaterinburg, Russian Federation*

E-mail: natalia.urusova@urfu.ru

Magnetolectrics (ME) are the materials, where such coexisting order parameters couple ferroelectricity with magnetization under external magnetic field. An incommensurate (IC) – commensurate (C) antiferromagnetic (AFM) transition has been found in the LiNiPO_4 magnetolectric. The IC phase occurs over a narrow range of intermediate temperatures (20.8–21.8) K between the C magnetic structure and a paramagnetic phase [1]. The transition to the paramagnetic state for LiCoPO_4 occurs without the IC phase [2]. The aim of our work is to study the effect of particular replacement of nickel ions by cobalt ions on the features of magnetic phase transitions in the $\text{LiNi}_{1-x}\text{Co}_x\text{PO}_4$ magnetolectrics.

We present the magnetic properties of $\text{LiNi}_{1-x}\text{Co}_x\text{PO}_4$ $x = (0-0.4)$. The magnetic phase transition temperatures were determined from an analysis features on the dependence of the first derivative of magnetisation vs. temperature – $dM/dT(T)$. For example, fig. 1 presents $dM/dT(T)$ of the $\text{LiNi}_{0.8}\text{Co}_{0.2}\text{PO}_4$. For all samples the temperatures of C–IC antiferromagnetic phase transitions (T_{C-IC}) and Néel points (T_N) are distinctly observed. Here, the T_{max} is the temperature, at which the magnetization reaches maximum. All the T_{C-IC} , T_N , and T_{max} temperatures decrease with increasing the cobalt concentration. Such the behavior of the magnetic phase transitions is explained by a magnetic ordering competition. In the compounds with $x = 0$ and 1.0 the spins are oriented along the c - and b -axis, respectively. The partial doping of $\text{LiNi}_{1-x}\text{Co}_x\text{PO}_4$ by cobalt ions leads to a narrowing of the temperature interval where the IC phase is established. The difference between temperatures T_N and T_{max} originates probably due to a disappearance of both long-range magnetic order above T_N and the short-range magnetic order above T_{max} .

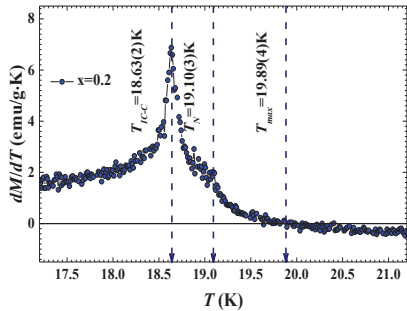


Fig. 1. The temperature dependence of the first derivative of the magnetisation of the $\text{LiNi}_{0.8}\text{Co}_{0.2}\text{PO}_4$.

The reported study was funded by RFBR (project No. 19-32-60011).

[1] R. Toft-Petersen, J. Jensen, et al. (2011). High-field magnetic phase transitions and spin excitations in magnetolectric LiNiPO_4 . Phys. Rev. B. 84, 054408-10.

[2] E. Fogh, R. Toft-Petersen, et al. (2017). Magnetic order, hysteresis, and phase coexistence in magnetolectric LiCoPO_4 . Phys. Rev. B 96, 104420-10.

MAGNETIC PHASE DIAGRAM $\text{LiNi}_{0.9}\text{Co}_{0.1}\text{PO}_4$

M.A. Semkin^{1,2}, N.V. Urusova^{2,3}, A.I. Beskrovnyi⁴, and A.N. Pirogov^{1,2}

¹*M.N. Miheev Institute of Metal Physics, Ural Branch, Russian Academy of Sciences, Ekaterinburg, Russian Federation*

²*Institute of Natural Sciences and Mathematics, Ural Federal University, Ekaterinburg, Russian Federation*

³*Institute of Solid State Chemistry, Ural Branch, Russian Academy of Sciences, Ekaterinburg, Russian Federation*

⁴*Frank Laboratory of Neutron Physics, Joint Institute for Nuclear Research, Dubna, Russian Federation*

E-mail: semkin@imp.uran.ru

The lithium orthophosphates LiMPO_4 , where $M = (\text{Ni}, \text{Co}, \text{Fe}, \text{and Mn})$ have high potential as magnetoelectric materials [1]. An incommensurate (IC) – commensurate (C) antiferromagnetic (AFM) transition has been found in the LiNiPO_4 single crystal. The IC phase occurs over a narrow range of intermediate temperatures (20.8–21.8) K between the C magnetic structure and a paramagnetic phase. The transition to the paramagnetic state for LiCoPO_4 occurs without the IC phase [2]. The aim of our work is to study the effect of 10 % replacement of nickel ions by cobalt ions on the magnetic phase transitions. We present results of neutron scattering of $\text{LiNi}_{0.9}\text{Co}_{0.1}\text{PO}_4$ single crystal.

The single crystals $\text{LiNi}_{0.9}\text{Co}_{0.1}\text{PO}_4$ has been synthesized by a conventional solution growth in a LiCl flux. Neutron experiments performed at the IBR-2 reactor of JINR with a DN-2 diffractometer [3] using cryostat on the basis of closed-cycle helium refrigerator. We have carried out neutron scans along $(0k0)$ direction for each single crystals from 10 K up to 25 K with temperature steps 1 K and 0.2 K.

$\text{LiNi}_{0.9}\text{Co}_{0.1}\text{PO}_4$ crystallize in the orthorhombic olivine crystal structure, with the space group $Pnma$, at which the $4a$ position are occupied by Li-ions; the Ni/Co-ions are located at the $4c$ site; and the O-ions are found at the $4c$ and $8d$ positions.

$\text{LiNi}_{0.9}\text{Co}_{0.1}\text{PO}_4$ possesses three magnetic structures states: C AFM, IC AFM and paramagnetic states. Magnetic moment in the C AFM structure is oriented along the c -axis and disappears at 21.0 K. The IC state is characterized by neutron scans, showing magnetic satellites $(0, 1 \pm \tau, 0)$ described with the propagation vector $\mathbf{k} = (0, \tau, 0)$, $\tau = 0.098$ r.l.u. (at 20.2(1) K). The long-range ordering IC structure described as a transfer spin wave, prolonging along the b -axis. Magnetic satellites of $\text{LiNi}_{0.9}\text{Co}_{0.1}\text{PO}_4$ exist over temperature range (20.2–21.0) K. The module of the propagation vector increases with a heating of the sample from 0.098 up to 0.118 r.l.u. The 10 % doping by cobalt ions decreases the transition temperature and the temperature range of the IC phase narrows.

The reported study was funded by RFBR (project No. 19-32-60011).

[1] E.Bousquet, N.A.Spaldin, and K.T.Delaney (2011). Unexpectedly large electronic contribution to linear magnetoelectricity. *Phys. Rev. Lett.* 106, 107202-4.

[2] D.Vaknin, J.L.Zarestky, and et.al (2004). Commensurate-incommensurate magnetic phase transition in magnetoelectric single crystal LiNiPO_4 . *Phys. Rev. Lett.* 92(20), 207201-4.

[3] A.M.Balagurov, A.I.Beskrovnyy, and et.al (2016). Neutron diffractometer for real-time studies of transient processes at the IBR-2 pulsed reactor. *J. Surface Investig.* 10(3), 467-479.

STRUCTURE OF THE RNi₃ (R-Dy, Ho)-BASED INTERMETALLIC HYDRIDES AT 5K AND 293K TEMPERATURE

S.A. Lushnikov¹, T.V. Filippova¹ and I.A. Bobrikov²

¹*Chemistry Department of Lomonosov Moscow State University, Moscow, Russia*

²*Joint Institute for Nuclear Research, Dubna, Moscow oblast, Russia*

E-mail: steplushnikov@yandex.ru

Intermetallic compounds (IMC) with RNi₃ (R-Dy, Ho) composition are able to absorb reversibly a large amount of hydrogen and are perspective materials for hydrogen energy [1]. Most of these compounds have PuNi₃ (space group *R-3m*, no 166) structure type and consists of structural fragments with RT₂ (MgZn₂ structure type) and RT₅ (CaCu₅ structure type) composition, arranging in the direction perpendicular of the *z* crystallographic axis. For the duration of the hydride formation atoms of hydrogen occupy different sites in the crystal lattice of intermetallic compounds. With points of the view of crystallographic positions all these sites form several hydrogen sublattices in the structure hydride [2]. After increasing of the hydrogen concentration in metal matrix, hydrogen atoms take up different types of the hydrogen sublattices and after that take place formation of the new hydride phases. Also at low temperature in hydrides can appear different hydride phases due to the hydrogen atoms redistribution inside of hydrogen sublattices. This redistribution at low temperature was first observed in the hydrides of *d*-metals [3]. For RNi₃ (R-Dy, Ho)-based hydrides with complex lattices also is possible to observe formation of the new hydride phases at low temperature. At the same time the samples of these hydrides have different stability and can be partly amorphous. It's possible to suggest that different stability and amorphisation of the hydride samples also take place due to the hydrogen redistribution at low temperature. At low temperature in hydrogen sublattices of hydride occurs ordering of the hydrogen atoms and this initial hydride decomposed for several hydride phases. These phases can be ordered or disordered and have different hydrogen concentration. For the study of hydride structure and hydrogen atoms distribution in the crystal lattice usually apply of the neutron diffraction method. In our case for neutron study were used DyNi₃ and HoNi₃-based samples containing deuterium with low concentration (about 1.0 D/IMC). Using deuterium in the samples allows decreasing of the non-coherent neutron scattering and obtains diffraction patterns with good quality. Small hydrogen concentration in samples, near of the solid solution of hydrogen permits to decrease the number of the phase transitions, which can be appears at low temperature. Hydride with high hydrogen concentration at low temperature can decompose for several hydride phases and this leads to more difficult interpretation of the diffraction spectra. At fig. 1 presented HoNi₃-based hydride sample, obtained after cooling up to 5K and following heating up to room temperature. Neutron diffraction analyses shown that this sample doesn't contain hydrogen atoms. This indicates that after fast quenching at low temperature the sample became unstable and desorbed all hydrogen.

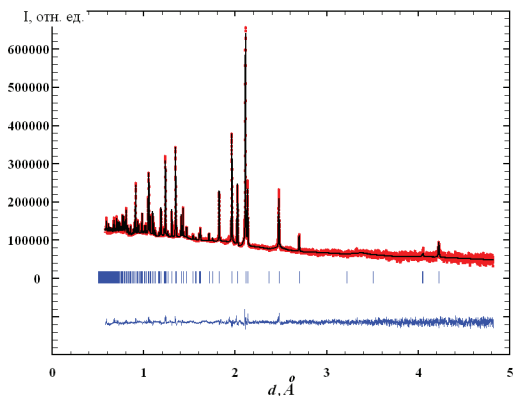


Fig. 1. Diffraction pattern of HoNi₃-based hydride measured on HRFD neutron diffractometer and processed by the Rietveld method. Experimental (points) and calculation (upper line) profiles are shown, the difference between them (lower line). The row of lines corresponds to the Bragg's positions.

The neutron spectra of the HoNi₃-based hydride with amount of hydrogen close to 1.0 H/IMC measured at 5K shown that the intensity of several lines suddenly increased strongly. This behavior indicates that is possible changing of the sample morphology and appearing of the texture of powder. Also is possible that at low temperature take place substantial dislocation of the metallic atoms in their positions due to the ordering of the hydrogen atoms. At the same time obtained data shown that the structure of the hydride sample was unchanged. Therefore it's necessary to continue of the study of hydride samples with small amount of hydrogen at low temperature. This can to lead for understanding of influences of hydrogen atoms redistribution on the structure of the hydride samples.

- [1]. M. Latroche, A. Percheron-Guegan (2003). Structural and thermodynamic studies of some RM₃-compounds (R=lanthanide, M=transition metal). *J. Alloys Compd.* 356-357, 461-468.
- [2] V.A. Yartys (1992). New aspects of the structural chemistry of intermetallic hydrides: «isotropic» and «anisotropic» structures. *Koord. Khim.* 18, 4, 401-408.
- [3] V.A. Somenkov (1972). Structure of hydrides. *Ber. Bunsen-Ges. Phys. Chem.* 76, 724-728.

MONITORING TECHNIQUES OF YTTRIA STABILIZED ZIRCONIA USED AS THERMAL BARRIER COATING

A.Savin¹, R.Steigmann¹, M.Soare², V. Turchenko³, M.-L. Craus^{1,3}

¹National Institute of R&D for Technical Physics, Iasi, Romania

²Nuclear NDT Research and Service, Bucharest, Romania

³Joint Institute for Nuclear Research, Dubna, Russia

E-mail: asavin@phys-iasi.ro, craus@phys-iasi.ro

Thermal barrier coating (TBC) is used as thermal protective layer dedicated to metallic components in high temperature regions. Thermal protection of metals used in construction of gas-turbine engines and internal combustion parts in order to increase their power, use the experience gained over the years in the study of protective coatings against corrosion, wear and erosion. Hundreds of coatings types are used nowadays and works about development of TBC applicable to gas-turbine engines are known since 1950 [1]. It is well known that three polymorphic forms of pure ZrO_2 can be found: the monoclinic state, $P2_1/c$, stable at temperatures below 1170 °C; the tetragonal phase, $P4_2/nmc$ stable in the temperature range between 1170 and 2370 °C; and the cubic, $Fm-3m$ phase, appearing at a temperature above 2370 °C [2]. The properties of tetragonal and cubic ZrO_2 are preferred instead of monoclinic. ZrO_2 tetragonal is important due to its active surface and relatively small grains [3]. However, polycrystalline $t-ZrO_2$ slowly converts to $m-ZrO_2$ in a narrow but important temperature range, usually between room temperature and about 400 °C, depending on the stabilizer, its concentration, the presence of moisture and the size of the ceramic grains. The transformation $t \rightarrow m$ during cooling is accompanied by an increase in volume (approximately 4%) and a shear distortion, enough to cause failure. At the nanoscale, the main method of stabilizing the tetragonal phase is the introduction of a stabilizing component, such as Ce or Y. In particular, pure yttrium oxide (yttria) is a very stable compound with a high melting point; it is chemically inert and has an excellent electrical insulation (volume resistivity and dielectric breakdown strength). The weakest part of TBCs is the substrate-ceramic interface, where fractures can occur under the action of thermal shock and the effect of $t \rightarrow m$ transformation. Using Yttria Stabilized Zirconia (YSZ) ceramics, the quality of the coating applied to the metal surface of the substrate increases. For a good quality coating, it is necessary to ensure the optimization of the substrate surface in order to achieve a reasonable balance between the induced stresses and the deposition of the ceramic layer. The laminar structures of YSZ TB layers deposited on stainless steels are usually porous, the pore size and character depending on the process parameters.

Figure 1 presents the influence of yttria concentration over adherent support for specimen with 0.2 mm thick monolithic coating ZrO_2 with addition of 20 % Y_2O_3 .

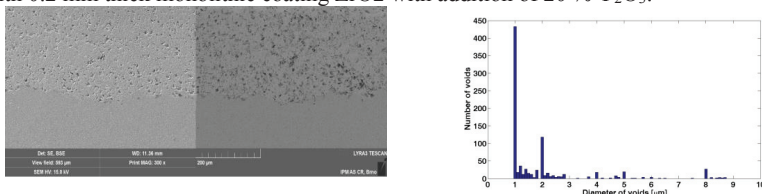


Figure 1. The influence of yttria concentration over adherent support for specimen with 0.2 mm thick monolithic coating ZrO_2 with addition of 20 % Y_2O_3 : a) SEM images; b) voids counting

Therefore, it is very important to evaluate the quality of coverage. The paper presents an analysis method based on the use of an electromagnetic sensor with metamaterials (MM) lenses[4] and the results obtained in evaluating the quality of the zirconium oxide layer deposited on an austenitic steel AISI 316L. Figure 2 shows the diffractograms observed and calculated for austenitic steel on which a layer of ZrO_2 was deposited. Complementary methods and results of the layer analysis are presented, such as scanning electron microscopy (SEM), X-ray diffraction and metallography.

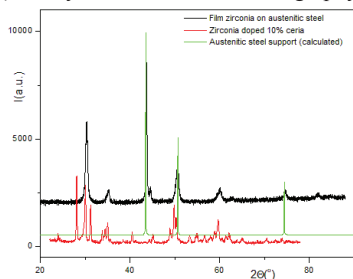


Figure 2a The X-ray diffractograms of film ZrO_2 on austenitic steel (observed - black), of $ZrO_2+10\%CeO_2$ (observed - red) and austenitic steel (calculated - green)

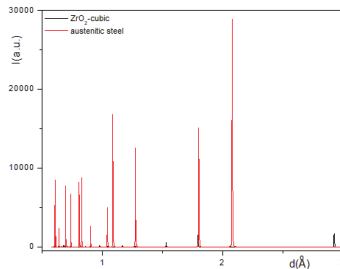


Figure 2b The calculated neutron diffractograms of film ZrO_2 (black) and of austenitic steel (red); d - interplanar distances

We determined using X-ray diffraction the structure of thin film of zirconia deposited on austenitic steel, the structure of zirconia doped with ceria and calculated the diffractogram of the austenitic steel with PowderCell software (Fig. 2a). The separate calculated neutronograms of a mixture between zirconia and austenitic steel was performed (Fig.2b). We will present some results obtained about thin films and bulk state of zirconia doped with Y_2O_3/CeO_2 , including phase composition, microstructural characteristics and mechanical properties.

- [1] C.H.Liebert and R.A.Miller (1984). Ceramic thermal barrier coatings. Industrial & engineering chemistry product research and development, 23(3), 344-349.
- [2] R.H.French, S.J.Glass, F.S.Ohuchi, Y-N. Xu, W.Y. Ching (1994) Experimental and theoretical determination of the electronic structure and optical properties of three phases of ZrO_2 . Phys. Rev. B, 49, 5133
- [3] E. Ryshkewitz , D. W. Richardson (1985). Oxide Ceramics: Physical Chemistry and Technology, American Ceramic Society Inc.
- [4] A.Savin, A. Bruma, R. Steigmann, N. Iftimie, D. Faktorova, (2015). Enhancement of spatial resolution using a metamaterial sensor in nondestructive evaluation. Applied Sciences, 5(4), 1412-1430.

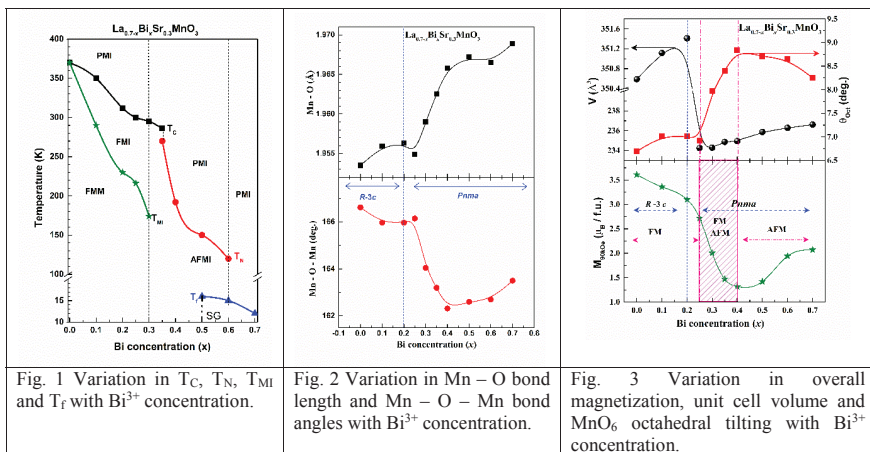
INFLUENCING STRUCTURE-PROPERTY CORRELATIONS IN $\text{La}_{0.7}\text{Sr}_{0.3}\text{MnO}_3$ MANGANITES BY BI SUBSTITUTION

Anita D. Souza¹, Sudhindra Rayaprol², Mamatha Daivajna¹

¹Department of Physics, Manipal Institute of Technology, MAHE, Manipal-576104, INDIA
²UGC-DAE Consortium for Scientific Research, Mumbai Centre, BARC Campus, Trombay, Mumbai-400085, INDIA

E-mail: anitasurathkal@gmail.com

Bi^{3+} substitution for La^{3+} induces pronounced effects on the structural, electrical, and magnetic properties of polycrystalline $\text{La}_{0.7-x}\text{Bi}_x\text{Sr}_{0.3}\text{MnO}_3$ ($0 \leq x \leq 0.4$) manganites. The structural analysis carried using Rietveld refinement method on the powder X-ray diffractograms and neutron diffractograms show that with increase of Bi^{3+} content, the structure changes from rhombohedral, (space group $R-3c$, SP Group #167) for $x \leq 0.2$ to orthorhombic, (space group $Pnma$, SP Group #62) for $x \geq 0.3$. It is interesting to note that along with changes in the crystallographic structure, a cross over from ferromagnetic (for $x = 0.0$, $T_C = 370$ K) to antiferromagnetic ground state ($x \geq 0.4$) is also observed. Electrical resistivity measurements shows metallic character observed (for $x = 0.0$, $T_{MI} = 370$ K) changes to insulating with increase in Bi^{3+} ($x \geq 0.35$) concentration. With the changes in the magnetic and electrical properties, we also find that as Bi^{3+} content increases, T_C and T_{MI} , and T_N decreases. For ($x \geq 0.5$), spin cluster glass like freezing has been observed at T_f , which decreases with increase in Bi^{3+} content (Fig. 1). The variation in the overall magnetization with Bi^{3+} content could be correlated with the changes in $\text{Mn}-\text{O}-\text{Mn}$ bond angles, $\text{Mn}-\text{O}$ bond length (Fig. 2) and tilting of MnO_6 octahedra (Fig. 3). The observed changes in the structural and physical properties could be attributed to the $6s$ lone pair character of Bi^{3+} ions [1,2]. Details of structural analysis, magnetization and resistivity measurements will be presented and discussed.



References:

- [1] Z. X. Cheng, T. M. Silver, A. H. Li, X. L. Wang, H. Kimura., J Magn. Magn. Mater. 283, (2004) 143.
- [2] R. Seshadri, Nicola A. Hill., Chem. Mater 13, (2001) 2892.

INFLUENCE OF LOW PB CONCENTRATION ON THE STRUCTURE AND TRANSPORT PHENOMENA OF LAMNO₃ MANGANITES

M.-L.Craus^{1,2}, C. Mita³, V. Dobrea¹ and N. Cornei³

¹National Institute for Technical Physics, Iasi, Romania

²FLNP-Joint Institute for Nuclear Research, Dubna, Russia

³"A.I.Cuza"University, Iasi, Romania

E-mail: kraus@nf.jinr.ru

The partial substitution of La³⁺ with Alk=Sr²⁺, Ca²⁺, Pb²⁺ etc, with corresponding ionic radii, in LaMnO₃ (ABO₃) induces a variation of mixed valence state Mn³⁺/Mn⁴⁺, distorts the original cubic structure, led to an increase of chemical disorder degree with a change of the Curie temperature and the metal-insulator transition temperature. A change of the A-O distances and B-O-B angles led to a change magnetic and transport properties. For the possible technological applications, good magnetotransport properties are required at temperatures close to room temperature. Pb doped manganites exhibit a relatively high Curie temperature and resistivity, both being strongly dependent by difference between ionic radius of A site cations. The La_{1-x}Pb_xMnO₃ manganites (x=0.03; 0.10; 0.15; 0.20) were obtained by sol-gel methods and treated in air at maximum 1250°C. The phase composition and microstructural parameters (lattice constants, cations and anions positions, average size of crystalline blocks, microstrains) were determined by powder X-ray Diffraction (XRD) using a DRON 2.0 diffractometer with CoK α ₁₂ radiation, at room temperature.

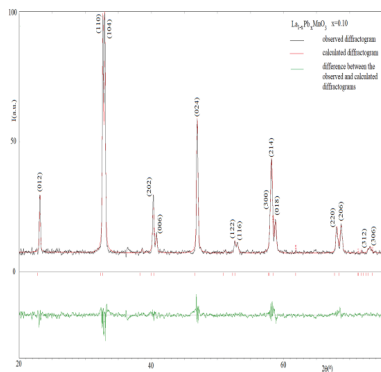


Figure 1 The observed (black) and calculated (red) diffractograms of La_{0.9}Pb_{0.1}MnO₃.

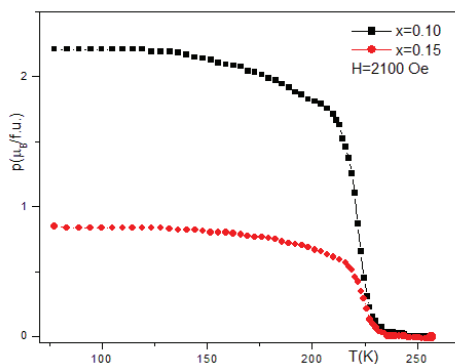


Figure 2 The molar magnetization of La_{1-x}Pb_xMnO₃ vs temperature at low magnetic field.

The lattice constants, unit cell volume, average size of mosaic blocks and microstrains were determined by using Fullprof or PowderCell codes (s. Fig. 1 and Table 1). Variation of molecular magnetization with temperature and magnetic field intensities were determined with a Foner type magnetometer between 77 and 500 K (s. Fig. 2 and Table 2). Resistance measurements with temperature and magnetic field intensities were performed by using a

closed cycle refrigerator and an electromagnet. The magnetic and electric measuring systems were previewed with data acquisition systems.

Table 1. Variation of lattice constants (a, b, c), unit cell volume (V), average size of crystalline blocks (D), microstrains (ϵ) for with Pb concentrations (x) in $\text{La}_{1-x}\text{Pb}_x\text{MnO}_{3\pm\delta}$ manganites (treated samples)

x	a=b(Å)	c(Å)	V(Å ³)	D(Å)	ϵ
0.03	5.5115	13.3285	352.053	452	0.00068
0.10	5.5320	13.3779	354.554	720	0.00121
0.15	5.5178	13.3427	351.808	635	0.00020

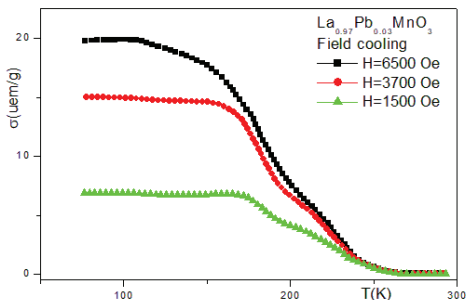


Figure 3 Variation of the specific magnetization with intensity of magnetic field

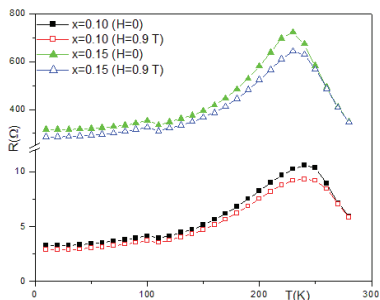


Figure 4 variation of the resistance with temperature and intensity of the magnetic field for $\text{La}_{1-x}\text{Pb}_x\text{MnO}_3$ for $x=0.10$ and 0.15

The molar magnetization change with the the intensity of applied magnetic field. All magnetization curves have a common characteristic, for the samples cooled in magnetic field. A transition from a spin glass to ferromagnetic state takes place, transition temperature decreasing with the decrease of the magnetic cooling field intensity (s. Fig. 3).

Table 2 Variation of specific magnetization (σ), the Curie temperature (T_C), the transition temperature from spin glass to ferromagnetic state ($T_{\text{sg-M}}$; $H=6500$ Oe) and the transition from metallic to insulator state (T_{tr}) with the Pb concentration (x)

Code	x	$\sigma(\text{uem/g})$	$T_C(\text{K})$	$T_{\text{sg-M}}(\text{K})$	$T_{\text{tr}}(\text{K})$
GXVIII	0.03	19.5	225	107	
GXVII3	0.10	58.5	225	108	240
GXVII4	0.15	68.1	265	107	230

The decrease of spin-glass state concentration with the increase of the temperature contributes to an increase of the resistance of the manganites. The increase of the intensity of magnetic field lead to an increase of the metallic-ferromagnetic electronic phase concentration and a decrease of the resistance (s. fig. 4). At the transition from metallic to insulator state takes place the maximum of the resistance and of the magnetoresistance (s. Fig. 4).

SMALL-ANGLE NEUTRON SCATTERING STUDIES OF PORE FILLING IN CARBON ELECTRODES: MECHANISMS LIMITING LITHIUM-AIR BATTERY CAPACITY

T.K. Zakharchenko^{1,2}, M.V. Avdeev³, A.V. Sergeev^{1,2}, V.V. Isaev^{1,2}, V. I. Petrenko³, O.I. Ivankov³, L.V. Yashina^{1,2}, D.M. Itkis^{1,2}

¹*N.N. Semenov Federal Research Center for Chemical Physics, Moscow, Russia*

²*Lomonosov Moscow State University, Moscow, Russia*

³*Frank Laboratory of Neutron Physics, Joint Institute for Nuclear Research, Dubna, Russia*

E-mail: t.zakharchenko@chph.ras.ru

The development of lithium-air batteries (LAB) today faces a number of fundamental problems restricting the system rechargeability. Nevertheless, its promise of achieving of 1 kWh/kg at cell according to some estimations [1] drives an active interest to the lithium-oxygen electrochemical system. The possibility of achieving such specific energy, however, is also still under question as a number of processes can limit the battery capacity. They include oxygen transport limitations, pore clogging and electrode passivation by insulating discharge product – lithium peroxide [2]. Its deposition is a multistep process, which is rather complex in both underlying chemistry and in the crystallization pathway diversity. Discharge of the lithium-air battery (LAB) with aprotic electrolyte is accompanied by single-electron oxygen reduction resulting in superoxide anion (O_2^-). This intermediate can further associate with Li^+ , receive the second electron and form lithium peroxide (Li_2O_2) or undergo disproportionation reaction yielding the same final insulating solid product, Li_2O_2 , which precipitates inside the porous cathode [3]. Rate of disproportionation is primarily governed by solvent, more precisely, by its solvation ability towards both for Li^+ and superoxide anion. Here, we uncover the mechanisms limiting $\text{Li}-\text{O}_2$ porous carbon electrode capacity by analysis of the cathode pore filling in highly and poorly solvating media, DMSO and MeCN correspondingly. We employ electron microscopy coupled with small-angle neutron scattering (SANS) for *ex situ* analysis of the electrodes discharged to various depths at a number of current densities. Also, we performed *in situ* SANS measurements in DMSO-based electrolyte.

We found that the main factor that trigger mechanisms responsible for death of lithium-oxygen cells with carbon black electrode is the oxygen transport blockage inside the carbon black agglomerates. It is caused by clogging of either pores inside the agglomerate or its surface by the discharge products. Mechanism of blockage and, consequently, discharge capacity of LAB strongly depends on electrolyte solvation ability. For poorly solvating media, such as MeCN where the discharge intermediate LiO_2 is unstable and disproportionate fast, discharge capacity is rather small and finally fraction of the pores filled by discharge products scales inversely with discharge current density. It reaches 85% at low currents that is also consistent with theoretical calculations. For DMSO-based electrolyte, where superoxide has notable lifetime and Li_2O_2 is formed in solution bulk enabling higher capacity, the fraction of filled pores in fully discharged electrodes does not depend on current density since most of Li_2O_2 is precipitated in the form of mesocrystals with ca. 3.3 nm periodic stacking of the individual lithium peroxide plates.

[1] J. Christensen, P. Albertus, R.S. Sanchez-Carrera, et al., (2012) A Critical Review of Li/Air Batteries, *J. Electrochem. Soc.* 159, R1.

[2] P. Albertus, G. Girishkumar, B. McCloskey, et al., (2011) Identifying Capacity

Limitations in the Li/Oxygen Battery Using Experiments and Modeling, *J. Electrochem. Soc.* 158, A343.

[3] L. Johnson, C. Li, Z. Liu, Y. Chen, et al., (2014) The role of LiO_2 solubility in O_2 reduction in aprotic solvents and its consequences for Li- O_2 batteries, *Nature Chemistry*. 6, 1091–1099.

MONITORING OF LITHIUM PLATING BY NEUTRON REFLECTOMETRY

E.E. Ushakova^{1,2,3}, A.A. Rulev^{1,2}, M.V. Avdeev³, E.N. Kosiachkin^{3,5}, V.I. Petrenko^{3,5}, I.V. Gapon^{3,6}, E.Yu. Kataev⁷, V.A. Matveev⁸, L.V. Yashina^{1,2}, D.M. Itkis^{1,2}

¹ *Lomonosov Moscow State University, Moscow, Russia*

² *Semenov Institute of Chemical Physics, Russian Academy of Sciences, Moscow, Russia*

³ *Frank Laboratory of Neutron Physics, Joint Institute for Nuclear Research, Dubna, Moscow Region, Russia*

⁴ *Dubna University, Dubna, Moscow Region, Russia*

⁵ *Kyiv Taras Shevchenko National University, Kyiv, Ukraine*

⁶ *Institute for Safety Problems of Nuclear Power Plants, NAS Ukraine, Chornobyl, Ukraine*

⁷ *Chair of Physical Chemistry II, Friedrich-Alexander-University of Erlangen-Nürnberg, Germany*

⁸ *St.Petersburg Nuclear Physics Institute named by B.P. Konstantinov of National Research Centre 'Kurchatov Institute', Gatchina, Leningradskaya oblast, Russia*

E-mail: ushelen1171@gmail.com

Main reason preventing successful deployment of high-energy and high-power rechargeable lithium metal batteries is connected with non-uniform lithium plating during charge.

The process of lithium precipitation is rather complicated and can't be studied with only electrochemical techniques. Hence, in order to monitor the deposits formation and evolution from standard LiClO₄ in propylene carbonate solution with and without additive (TBA+) we suggest using neutron reflectometry (NR)[1],[2]. Being intrinsically interface-sensitive, neutron reflectometry provides surface-averaged information on the spatial distribution of the components at electrified interfaces in contrast to microscopy tools, which are also suitable for probing electrochemical interfaces.

NR measurements of operating electrochemical cells have been performed in originally designed three electrode electrochemical cell at GRAINS reflectometer with horizontal sample plane (IBR-2 reactor, Dubna). The sensitivity of the method of specular neutron reflectometry was studied with respect to the nanoscale structure of planar electrochemical interfaces in which a metal anode (copper) was in contact with an aprotic liquid lithium ion electrolyte. The structure of the lithium enriched layers formed on the working electrode including solid electrolyte interphase (SEI) and next depositions was analysed in terms of the scattering length density (SLD) depth profiles obtained from the modelling of the reflectivity curves [1],[2].

The preferable choice of fully deuterated electrolyte for better analysis of the structural features of such layers was experimentally proven. From the comparison of the profiles obtained for interfaces with fully deuterated and fully protonated electrolytes the porosity of the deposited layer was estimated [1]. The analysis of the SLD has also demonstrated that the deposition of nm-thin Li layers above initially formed solid-electrolyte interphase (SEI) layer can be detected and their roughness, which is a characterising parameter of electrodeposition nonuniformity, can be estimated. A principal change in the interface profile evolution was observed when non-electroactive additive (TBA+) is present in the electrolyte (see Figure 1) [2].

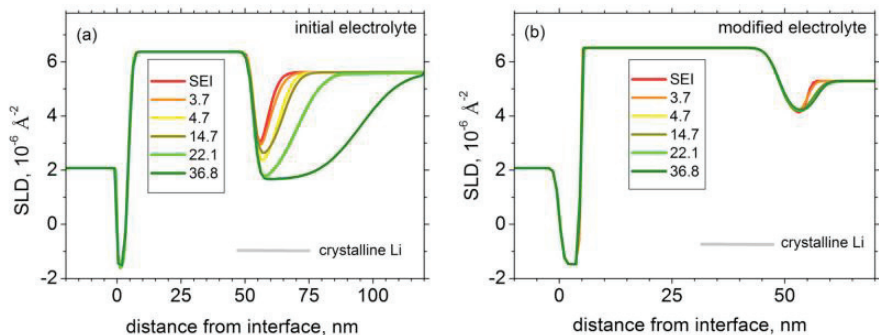


Figure 1. SLD profiles derived from experimental NR curves in Fig. 4 for the ‘initial electrolyte’ (a) and ‘modified electrolyte’ (b). The total charge passed through the cell (mC cm^{-2}) is indicated in the legends. The crystalline lithium SLD is shown for comparison.

- [1] M.V. Avdeev, A.A. Rulev, E.E. Ushakova, D.M. Itkis. (2017) Monitoring of lithium plating by neutron reflectometry. *Applied Surface Science*, 424, 378–382
- [2] M.V. Avdeev, A.A. Rulev, E.E. Ushakova, D.M. Itkis. (2019) On nanoscale structure of planar electrochemical interfaces metal/liquid lithium ion electrolyte by neutron reflectometry, *Applied Surface Science*, 486, 287–291.

HYBRID TECHNIQUES FOR MANUFACTURING OF ALUMINUM COMPOSITE LAYERS WITH TiCN NANOPARTICLES

S. Valkov¹, G. Bokuchava², Yu. Gorshkova², P. Petrov¹

¹ Institute of Electronics, Bulgarian Academy of Sciences, 72 Tsarigradsko Chaussee Blvd., 1784 Sofia, Bulgaria

² Frank Laboratory of Neutron Physics, Joint Institute for Nuclear Research, 6 Joliot-Curie Str., 141980 Dubna, Moscow Region, Russia

E-mail: stsvalkov@gmail.com

The aluminum and its alloys are widely used in the field of the modern aerospace and automotive industries, aircraft manufacturing, railway cars, light ships, etc., due to their attractive mechanical properties and light weight. However, the applications of the discussed materials are still limited due to their low hardness and wear resistance. It is known that the mentioned limitations depend mostly on the surface properties of the materials and, therefore, the application of appropriate technology for surface manufacturing can overcome these drawbacks.

In this work, aluminum nanocomposites containing 2 at.%, 5 at.%, 10 at.% and 15 at.% TiCN nanoparticles were produced as rods with 12 mm diameter by means of preliminary cold volume compression and succeeding hot pressing. The structure of the obtained composites was studied by neutron diffraction method. The experiments were realized under different loads. The experimentally obtained diffraction patterns are presented in Fig. 1.

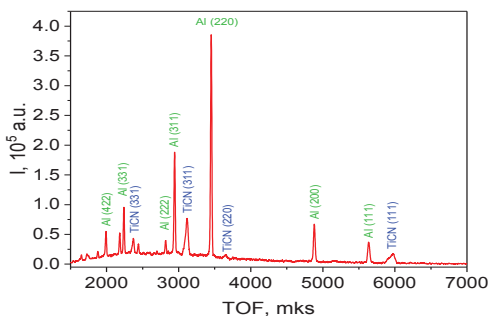


Fig. 1. Neutron diffraction pattern of Al/TiCN nanocomposite containing 10 at. % nanoparticles.

The results revealed that the Al composite with 10% TiCN exhibited the highest Young's modulus and Poisson coefficient. Therefore, this specimen was electron-beam treated (EBT) in order to form a surface layer with enhanced functional properties. The EBT was carried out by continuously scanning electron beam using different technological conditions, namely low input energy density TC1 and high input energy density TC2. The following parameters were used in this work: accelerating voltage $U=52$ kV; electron beam scanning frequency $f=1$ kHz; electron beam current $I=20$ mA; amplitude $A=20$ mm; speed of the specimen motion $V1=5$ cm/sec for TC1, and $V2=2$ cm/sec for TC2. Scanning electron microscopy (SEM) and energy-dispersive X-ray spectroscopy (EDX) were used for characterizing the microstructure. The

phase composition of the obtained specimens was studied by means of X-ray diffraction (XRD). The microhardness was discussed with respect to the applied technological conditions of the EBT and corresponding microstructure and crystallographic structure of the formed layers.

APPLICATION OF THE SMALL-ANGLE NEUTRON SCATTERING METHOD TO STUDY DISPERSION OF NON-WETTING LIQUIDS IN NANOPOROUS MATERIALS

A.A. Belogorlov^{1,2}, Yu.E. Gorshkova³, G.P. Kopitsa^{4,5}, A.I. Kuklin³, D.V. Lvov^{2,6}, P.G. Mingalev⁷ and A.N. Tyulyusov^{2,6}

¹*A.V.Topchiev Institute of Petrochemical Synthesis, RAS, Moscow, Russian Federation*

²*National Research Nuclear University MEPhI, Moscow, Russian Federation*

³*Joint Institute for Nuclear Research, Dubna, Russian Federation*

⁴*Petersburg Nuclear Physics Institute named by B.P.Konstantinov of NRC «Kurchatov Institute», Gatchina, Russian Federation*

⁵*Institute of Silicate Chemistry, RAS, Saint-Petersburg, Russian Federation*

⁶*Institute for Theoretical and Experimental Physics, National Research Center Kurchatov Institute, Moscow, Russian Federation*

⁷*Faculty of Chemistry, Lomonosov Moscow State University, Moscow, Russian Federation*

E-mail: aabelogorlov@ips.ac.ru

The study of systems "nanoporous material - non-wetting liquid" has a long history, but so far there is no uniform model for describing the processes of intrusion and extrusion of liquids. The existence of a hysteresis of intrusion and extrusion pressures and the phenomenon of non-outflow liquids from pores, depending on the conditions, make these systems interesting for many applications. For example, the pressure hysteresis can be used to develop mechanical energy absorption systems and the non-outflow phenomenon can be used to develop drug delivery systems. Therefore, studying the dispersion of liquids in material space is an important task for understanding the physics of observed phenomena.

In classical methods of study of the processes of intrusion and extrusion of liquids, the data of the system volume changes under the applied pressure cannot provide information about the distribution of liquid inside the porous material. One of possible methods for realization of the task can be the small-angle neutron scattering method. The method is widely used to study porous materials [1], but it has not been previously used to study the process of non-wetting liquids intrusion in nanoporous materials.

In the present work we studied the process of intrusion of hydrophobic mesostructured material based on SiO₂ MCM-41-C1 with ordered structure of cylindrical pores with two water concentrations: heavy water (100%) and mixture of heavy water (64%) and light water (36%), which corresponds to "zero contrast" between SiO₂ matrix and mixture in neutron experiment. Previously, for this material the phenomenon of hysteresis of intrusion and extrusion pressures as well as the phenomenon of non-outflow of non-wetting liquids were observed on light water [2]. The studies were carried out on the YuMO spectrometer [3] of the IBR-2 reactor (JINR, Dubna). For this purpose the bench and high pressure cell were designed and manufactured, which allow to make measurements by the small-angle neutron scattering (SANS) method in the pressure range of 1 - 1000 atm. The main purpose of the experiment was to study the process of intrusion of the liquid into pores at different pressures. The scheme of the experiment is presented on Fig. 1. The experimental bench is similar to the one described in [4]. The upper and lower bases are fixed with stands. An automatic rhombic screw jack was mounted on the upper base, and a force transducer was mounted on the lower base. On the force transducer was installed an experimental cell with the rod inserted into the plug through the gaskets (Fig. 1 does not show the cover, fixing the plug in the cell chamber). The movement of the rod through gaskets by the screw jack leads to pressure increase inside the cell. When the intrusion pressure was reached, the non-wetting liquid filled the pores. The

change in neutron intensity at different pressures corresponding to different pores fill level is shown on Fig. 2.

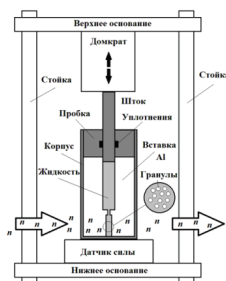


Fig. 1. Scheme of experiment, bench and cell.

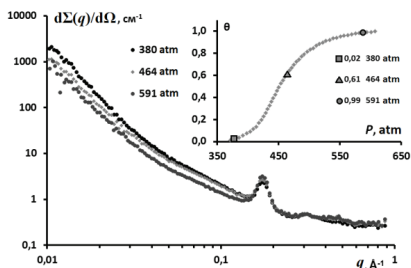


Fig. 2. Influence of pressure in the system MCM-41-C1 – D₂O on the intensity of the transmitted beam and the dependence of the filling level (θ) of the volume of pores on the pressure.

It can be seen from Fig. 2 that the increase of the fraction of the filled volume of pores leads to a decrease in the intensity of the past beam, which can be associated with changes in the structure of the scattering layer in the track of the beam.

Thus, the developed bench and cell to study the interaction of nanoporous materials and liquids at pressures up to 1000 atm by the SANS allow to study the dispersion of non-wetting liquid in nanoporous materials.

This work was supported by the Russian Science Foundation (project no. 18-13-00398).

[1] N.N.Gubanova et al (2014). Structure of zirconium dioxide based porous glasses. Journal of Surface Investigation. X-ray, Synchrotron and Neutron Techniques, 8(5), 967-975.

[2] A.A.Belogorlov et al (2017). Study of hydrophobized mesostructured material MCM-41-C1 by gas adsorption and liquid porometry methods. Journal of Surface Investigation: X-ray, Synchrotron and Neutron Techniques, 11(2), 425-428.

[3] A.I.Kuklin et al (2011). New opportunities provided by modernized small-angle neutron scattering two-detector system instrument (YuMO). In Journal of Physics: Conference Series, 291(1), p. 012013)

[4] V.D.Borman et al (2005). The percolation transition in filling a nanoporous body by a nonwetting liquid. Journal of Experimental and Theoretical Physics, 100(2), 385-397.

NEUTRON REFLECTOMETRY OF CARBON NANOTUBES LAYER DEPOSITED ON CONDUCTING SUBSTRATES

N.V. Kamanina¹, D.V.Korda², A.V. Tomchuk³, Yu.V.Kulvelis², V.T. Lebedev²

¹*S.I.Vavilov State Optical Institute, Saint-Petersburg, Russia*

²*Petersburg Nuclear Physics Institute named by B.P. Konstantinov, NRC "Kurchatov Institute", Gatchina, Leningrad distr., Russia*

³*Joint Institute for Nuclear Research, Dubna, Moscow distr., Russia*

E-mail: korda-dmitrii@mail.ru

Coating conducting substrates by single wall carbon nanotubes (CNT) promises prospects in the design of advanced materials using laser ablation since there are various opportunities to apply such structures as active optical films and base components of cold emitters for electronics[1]. The knowledge of the structure of CNT-layers as defined by the technological approaches may serve for their improvement. Neutron reflectometry application for the studies of packages of CNT on metal (metal-oxide) substrates is needed for fundamental and practical purposes and especially for the development of modern technologies using laser ablation and electromagnetic treatment of the surfaces formed by CNT embedded into substrate border. We report the results of experiments of specular reflection of neutrons from the samples prepared when electric field was applied to provide more smooth relief of CNT by deposition on the surface of thin films of Indium Tin Oxide (ITO) and following polishing the border by laser beam. The measurements on the reflectometer GRAIN at IBR-2 reactor have demonstrated really a significant influence of the conditions of electromagnetic treatment onto the structure and quality of CNT layers (Fig.1,2). The reflectivity profile $R(q)$ for substrate covered by ITO demonstrates the oscillations with the period defined by the thickness of conducting film $d \sim 150$ nm (Fig.1). The preparation of hybrid structures when the tubes are stuck into the surface creates really dense continuous carbon layer on the ITO surface since the reflection pattern did not change qualitatively while the period of oscillations became shorter (Fig.1).

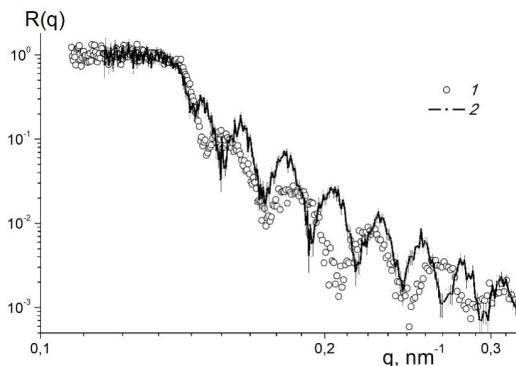


Fig.1. Reflectivity data for the samples of ITO film on the glass (1) and this one after sample coating by CNT in electric field (600 V/cm).

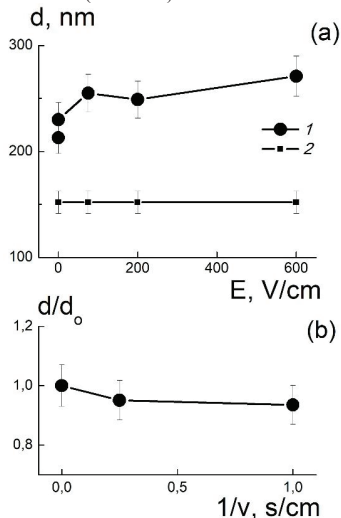


Fig.2. Effective thickness $d(E)$ (a) of the total layer (1) and original ITO film (2) on substrate vs. electric field strength applied during the process of deposition. The normalized thickness d/d_0 of composite film vs. reciprocal velocity of beam scanning over the carbon surface (b).

This indicated the increased thickness of film on substrate up to the magnitudes $d \sim 200-270$ nm (Fig.2a). The application of electric field of higher strength during coating makes the effective thickness greater. It means better packing CNT on the ITO surface due to field action. Comparatively to this, the laser beam showed only small leveling effect as dependent on the time of carbon surface treatment (Fig.2b).

As we found the structure of CNT layers depends on the modes of surface treatment and their optimization will enable to provide more smooth and perfect border being continuous. The performed experiments allowed highlight general regularities in the formation of CNT layers on conducting substrates which can be varied, e.g. by using advanced materials such as graphenes and diamonds being very promising for electronics.

The work was supported by the Russian Fund for Basic Research (project 18-29-19008).

[1] N.V. Kamanina (2014). Features of Optical Materials Modified with Effective Nanoobjects: Bulk Properties and Interface”, New York, Physics Research and Technology, Nova Science Publishers, Inc., New York, ISBN: 978-1-62948-033-6

THE POSSIBILITY TO USE RECONFIGURABLE ARCHITECTURE STRUCTURES AS ELECTROMAGNETIC SENSORS ARRAY

N. Iftimie¹, R. Steigmann¹

¹National Institute of R&D for Technical Physics, Iasi, Romania

E-mail: niftimie@phys-iasi.ro, steigmann@phys-iasi.ro

According to [1] a sensor array is a *group of sensors, usually deployed in a certain pattern used for collecting and processing electromagnetic or acoustic signals*. To determine the direction of wave field travel, a set of sensors are deployed in space to monitor the radiating energy. The localization of the object in a given image frame can be derived from knowledge of the sensor position in relation to the target pursued. The technique using eddy current sensors array to recognize the inspected zone [2] it has been intensively studied since 1986 [3]. The signals processing starts from classical direction of arrival [4] which indicate the direction from where the wave is propagating, arrive in the localization point of the sensors set. In nondestructive testing method using electromagnetic (EM) field, at a C-scan obtained from an eddy current sensors array, the identification of the flaw boundary is difficult to estimate.

To overcome the problem, using conventional eddy current techniques (which extract only temporal characteristics), the characteristics are complemented by spatial location (the location of the area in the electromagnetic image can be derived from knowing the position of the sensor relative to the target). Along with all these benefits, the advantage of these sensor array also includes the simplified procedure of reducing the inspection time of complex parts. Eddy current sensor array implies the necessity for uniformity of each element, the tendency to miniaturize the array must not compromise its sensitivity to defect and the signal-to-noise ratio.

Reconfigurable periodic structures are constructed using areas of dielectric and magnetic materials, with periodic spacing close to the operational wavelength of radiation, intended to cause the target element. The periodic microstructures incorporating EM materials use the concept of propagation behavior to generate EM structures that have the desired functions. Reconfigurable EM structures are widely used in electrical devices and can be adapted to exploit the specific properties of materials, especially EM properties that are not usually observed in nature, through the appropriate reconfiguration of metasurfaces.

A reconfigurable architecture structures has been studied in order to be used as sensors array in electromagnetic nondestructive evaluation. A set of constituent elements (CE) based on periodic unit cells (UCs) is based on an anisotropic response, but in the used wavelength range, the response of the material is approximately isotropic due to the spatial arrangement.

The sensors array is constituted by the emission part E_m and reception part E_r , thus, we denoted with X_i the amplitude of in phase component and Y_i , in phase quadrature, measured at the output, the electromotive force is $a_i = \sqrt{X_i^2 + Y_i^2}$ and $\psi_i = \text{atan}\left(\frac{Y_i}{X_i}\right)$.

In the field of radar application [5] the resolution of eddy current array can be significantly improved by detecting the direction of propagation. The signals received from the sensor array can be written as a vector $x_j = a_j e^{j\psi_j}$ where M is the number of receivers, $a_1 \dots a_M$ the amplitude and respectively $\psi_1 \dots \psi_M$ the phase of the induced electromotive force for each element, and j is the unit imaginary number.

The maximum sensitivity of a sensor array appears in the center of the array, meanwhile on the border is minimum, as seen in the simulation carried out using Finite Difference Time Domain (FDTD) method, Figure 1.

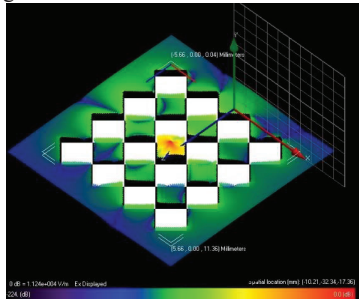


Figure 1. The electric field along x-axis for a RAS

The sensitivity in the center of the array depends on the amplitude and phase of the excitation current in a region without discontinuities. For placing the sensor in the XY plane, the EM wave will propagate in the radial direction and perpendicular to the plane of the sensor array, so that only the EM wave component in the direction of the Oz axis is considered.

This type of electromagnetic sensors array, whose construction and simulation are based on a reconfigurable architecture, is using Metal -Dielectric-Metal type material. The model was designed in SolidWorks in CAD-*STL format and imported in XFDTD 6.3 REMCOM and its behavior has been simulated. The CAD/CAM models of reconfigurable architecture were designed in the multiple UC structure considering that the kinematics of a structure with CEs is function of the angle in the XY horizontal plane.

Once the UC is designed, its function is fixed, for example, an absorber works at a certain frequency where the input impedance is matched to the free space. Thus, if change the working frequency or even the functionality, reconfigurable architectures are made due to the structural nature of the UC. In fact, the properties of the metasurfaces can be adjusted by adding tuning capability in the UCs.

The real challenge in order to apply the eddy current sensors array method appears when two discontinuities are closer than the spatial resolution of the UC.

When the distance between discontinuities is large enough, the position of the local maximum of the normalized response as a function of position is distinct [6], so two maxima of the discontinuity location curves appear. When the distance between the discontinuities is small, the corresponding peaks will overlap, the signal increases in intensity and a single peak will appear [7]. The modification of the architecture, could vary this distance so that the spatial resolution between two flaws shall be acceptable. In order to be able to locate multiple closer flaws, the solution is applying the super resolution method based on maximum likelihood and performing multiple simulations.

[1] https://en.wikipedia.org/wiki/Sensor_array

[2] G.Lafontaine (2000). Eddy current array probes for faster, better and cheaper inspections. e-Journal NDT.

[3] B.A.Auld, J. Kenney, and T.Lookabaugh (1986). Electromagnetic sensor arrays— Theoretical studies. Review of progress in QNDE. Volume 5A New York, Plenum Press, 681-690.

[4] C.Zhou, Y. Gu, Y.D. Zhang, Z. Shi, T. Jin, and X.Wu (2017). Compressive sensing-based coprime array direction-of-arrival estimation. IET Communications, 11(11), 1719-1724.

- [5] V.S.Luong, M. Le, K.D.Nguyen, D.K. Le, and J.Lee (2020). Electromagnetic Testing of Moisture Separation Reheater Tube based on Multivariate Singular Spectral Analysis. *Applied Sciences*, 10(11), p.3954.
- [6] S.V. Schell, and W.A.Gardner (1993). 18 High-resolution direction finding. *Handbook of statistics*, 10, 755-817.
- [7] R.Grimberg, A.Savin, R.Steigmann, B.Serghiac, A.Bruma, (2011) Electromagnetic nondestructive evaluation using metamaterials, *INSIGHT*, 53, 3, 132-137.

SANS AND SAXS STUDY OF SUPPORTED METAL CATALYSTS AND NANOCOMPOSITES

Yu.V. Larichev^{1,2}, O.I. Ivankov^{3,4}

¹*Boreskov Institute of Catalysis, Novosibirsk, Russia*

²*Novosibirsk State University, Novosibirsk, Russia*

³*Joint Institute for Nuclear Research, Dubna, Russia*

⁴*Institute for Safety Problems of Nuclear Power Plants NAS of Ukraine, Kyiv, Ukraine*

E-mail: ylarichev@gmail.com

The quantitative determination of the particle sizes is one of the keystone tasks for catalysis and material science because a lot of properties of applied materials strongly depend from the particle sizes. Typical methods for particle sizes determination such as TEM and XRD have different limitations. For example, scanty information about amorphous or paste-like samples, local information about particle sizes from TEM study, mean values of particle sizes instead of particle sizes distribution from XRD study. Therefore scattering techniques (SAXS and SANS) nominally have a greater advantages comparing to TEM and XRD. Nevertheless the main reason of low popularity SAXS and SANS for the study of supported catalysts and nanocomposites is the problem of distinguishing a weak scattering signal originating from the active component from the strong background scattering signal of matrix or porous support. In our work has been discussed the application of high dense liquid sets for SAXS and D₂O/H₂O sets for SANS for the selective determination scattering signal from an active component in poly-phase samples. After sample impregnation of such liquid sets, residual scattering signal should correspond to an active component only. The SAXS and SANS contrast matching techniques have been tested on a set of supported metal catalysts with different types of supports and natural nanocomposites. It has been shown a good agreement between SAXS and SANS with contrast matching techniques on the one side and reference data TEM and XRD to the other side. Depending on the material types SAXS and SANS methods are complementary to each other. For SAXS with masking liquids are more preferable supports and matrix with low density (less than 2.5 g/cm³). At the same time, such materials are difficult to mask by D₂O for SANS analysis. Application SANS with D₂O/H₂O contrast matching is very effective for analyzing catalysts with high density. While SAXS with masking liquids for such samples is not effective due to the big difference between support and masking liquid density values.

This work was supported by Ministry of Science and Higher Education of the Russian Federation (project AAAA-A17-117041710079-8).

Yu.V.L. acknowledge resource center “VTAN” (Novosibirsk State University) for the access to experimental equipment.

**PLENARY SESSION 2: DEVELOPMENT OF NEUTRON SCATTERING
TECHNIQUES AND INSTRUMENTS**

**DEVELOPMENT OF AN INELASTIC NEUTRON SCATTERING
SPECTROMETER IN INVERSE GEOMETRY AT THE IBR-2 REACTOR**

Dorota Chudoba^{1,2}, Goremychkin Evgeny², Alexander Belushkin²

¹*Faculty of Physics, Adam Mickiewicz University, Poznan, Poland*

²*Frank Laboratory of Neutron Physics, Joint Institute for Nuclear Research, Dubna, Russia*

E-mail: dmn@amu.edu.pl

The status of Inelastic Neutron Scattering Spectroscopy at FLNP has been under concern of both the user community and the Laboratory Management, instigating discussions within both parties. It became clear that the two spectrometers available at the moment, once competitive to European class instruments, have lost the race years ago, and they no longer satisfy the needs of the user community in the Eastern Europe region. It is therefore of the utmost importance to advance INS Spectroscopy in the direction set historically, and to support the maintaining the world renown scientific position of the FLNP JINR. In order to regain competitiveness with the instrumentation of European neutron scattering facilities, it is necessary to build new INS spectrometers that would make use of up to date neutron optics and design solutions in order to deliver high resolution results, of excellent signal-to-background ratio over a broad range of energy transfer, from as small samples as possible in a time-wise highly efficient way. The first instrument to build will be an inverted geometry versatile spectrometer. The brightness of the IBR-2 source will be made use of to the maximum, and a very large surface or the reflecting energy analysers will assure the highest luminosity (largest acceptance) design.

The progress of works towards opening a new project of the new INS spectrometer will be outlined.

STATUS AND PROSPECTS OF SMALL-ANGLE SCATTERING AT IBR-2

A.I.Kuklin¹, D.V.Soloviov^{1,2}, O.I.Ivankov^{1,2}, A.V.Rogachev^{1,2}, V.V.Skoy^{1,2}, A.Kh.Islamov¹, Yu.S.Kovalev¹, A.G.Soloviov¹, A.V.Vlasov^{1,2,3}, Yu.L. Rizhikau^{1,2}, A.A.Nabiyev¹, M.I.Rulev^{1,4,5,7}, V.I.Gordeliy^{1,2,4,5,6}

¹ *Joint Institute for Nuclear Research, Dubna, Russia*

² *Research Center for Mechanisms of Aging and Age-Related Diseases, Moscow Institute of Physics and Technology, Dolgoprudny, 141700, Russian Federation*

³ *Institute of Crystallography, University of Aachen (RWTH), Aachen, 52056, Germany*

⁴ *Institute of Biological Information Processing (IBI-7: Structural Biochemistry), Forschungszentrum Jülich, Jülich, 52425, Germany*

⁵ *JuStruct: Jülich Center for Structural Biology, Forschungszentrum Jülich, Jülich, 52425, Germany*

⁶ *Institut de Biologie Structurale Jean-Pierre Ebel, Université Grenoble Alpes–Commissariat à l’Energie Atomique et aux Energies Alternatives–CNRS, Grenoble, F-38027, France*

⁷ *Structural biology group, European Synchrotron Radiation Facility, 71 Avenue des Martyrs, Grenoble, 38000, France*

E-mail: kuklin@nf.jinr.ru

Small angle neutron scattering method is very useful for supramolecular structural studies of condensed matter. Neutronographic investigations of supramolecular structures on the upgraded small-angle spectrometer YuMO (Dubna, JINR, IBR-2) is also demonstrated [1]. Here, the key parameters of small-angle spectrometers are considered. It is shown that the key parameter of the spectrometer based on pulsed sources is the fluxes on the sample, which, along with the multi-detector system, allow expanding the dynamic range (and q-range) in terms of the magnitude of the scattering vector. The results of experimental and computer modeling investigations of neutron spectra and fluxes obtained with cold and thermal moderators at the IBR2 reactor (Joint Institute for Nuclear Research (JINR), Dubna) are presented. These studies are related to the YuMO small-angle neutron scattering (SANS) spectrometer (IBR2 beamline 4). The neutron spectra have been measured using two methane cold moderators and the standard configuration of the SANS instrument. The data from both moderators under different -operation conditions are compared [2].

The problems concerning specific features of experiment realization on the small angle neutron scattering spectrometer located at the 4-th beamline of IBR-2 are discussed [3-5]. The scheme and mathematical background of the experiment are described. The possibility of two ways of measuring the transmission, background conditions of the experiment as well as another standard for normalization are considered. The advantages of the existing spectrometer configuration are shown. The time range for experiments was from several minutes up to 12 hours. It was shown that two-detector system [6,7] shortens more than twice the time of the measurement. While making structural investigations using advanced software the two-detector system allows treating the data at a qualitatively new level.

The prospects of SANS methodic and, in particular, the YuMO spectrometer development, are considered.

- [1] Kuklin, A. I., et al. "Neutronographic investigations of supramolecular structures on upgraded small-angle spectrometer YuMO." *J. Phys. Conf. Ser.* Vol. 848. 2017.
- [2] Kuklin, A. I., et al. "Analysis of neutron spectra and fluxes obtained with cold and thermal moderators at IBR-2 reactor: Experimental and computer-modeling studies." *Physics of Particles and Nuclei Letters* 8.2 (2011): 119.
- [3] Kuklin, A. I., et al. "New opportunities provided by modernized small-angle neutron scattering two-detector system instrument (YuMO)." *Journal of Physics: Conference Series*. Vol. 291. No. 1. IOP Publishing, 2011.
- [4] Nyam-Osor, M., et al. "Silver behenate and silver stearate powders for calibration of SAS instruments." *Journal of Physics: Conference Series*. Vol. 351. No. 1. IOP Publishing, 2012.
- [5] Soloviev, A. G., et al. "SAS program for two-detector system: seamless curve from both detectors." *J. Phys. Conf. Ser.* Vol. 848. No. 1. 2017.
- [6] Kuklin, A. I., A. Kh Islamov, and V. I. Gordeliy. "Scientific reviews: Two-detector system for small-angle neutron scattering instrument." *Neutron News* 16.3 (2005): 16-18.
- [7] Kuklin, A. I., et al. "Optimization two-detector system small-angle neutron spectrometer YuMO for nanoobject investigation." *Journal of Surface Investigation: X-ray, Synchrotron and Neutron Techniques* 6 (2006): 74-83.

THE NEUTRON RADIOGRAPHY AND TOMOGRAPHY FACILITY ON THE IBR-2 REACTOR: CURRENT STATE AND RECENT RESULTS

S.E. Kichanov¹, D.P. Kozlenko¹, E.V. Lukin¹, B.N. Savenko¹, and I.A. Saprykina²

¹*FLNP, Joint Institute for Nuclear Research, 141980, Dubna, Russia*

²*Institute of Archeology RAS, 117036 Moscow, Russia*

E-mail: ekich@nf.jinr.ru

The neutron based methods are characterized by exceptional penetration into a massive matter. One of the corresponding neutron methods is the neutron radiography and tomography. This method belongs to the family of non-destructive testing methods and analysis, which plays an important part in industrial and scientific research. The fundamental difference in the nature of neutron interaction with matter compared to X-rays provides additional benefits to neutron methods, including sensitivity to light elements and high penetration ability. All these features make neutron tomography an attractive tool with a growing range of applications in industry, archeology and geophysics, where provides structural information on the spatial distribution of internal components inside the large objects.

The special research facility located at the beamline 14 of the high-flux pulsed IBR-2 reactor provides possibilities for studies by means of neutron radiography and neutron tomography methods. A specially designed detector module with two mirrors scheme for reduction of radiation damage effects is used for data collection. The camera based on Hamamatsu CCD chip with 2048×2048 pixels and precision remote control digital system of confocal coated lens provide the ability to vary the field-of-view of detector from 20×20 cm to 5×5 cm and clip of imaging data depending on the experimental requirements.

The neutron radiography and tomography methods are currently used in a wide range of research including engineering sciences, cultural heritage, paleontology and materials studies. In the talk, the recently obtained results are overviewed. The cement samples with selected compositions as prospective construction materials for radioactive graphite stores were studied. The spatial distribution of composition components and the geometric arrangement of graphite grains inside cement matrixes have been obtained. The mica distribution inside several granite samples was reconstructed. The internal organization of cultural heritage objects from collections of the Institute of Archeology RAS (Russia) and Museum of National History and Archaeology (Romania) was also studied.

POLARIZED NEUTRON REFLECTOMETRY WITH SECONDARY RADIATION REGISTRATION

V.D. Zhaketov¹, A.V. Petrenko¹, Yu.M. Gledenov¹, Yu.N. Kopatch¹, N.A. Gundorin¹,
Yu.V. Nikitenko¹, V.L. Aksenov^{1,2,3}

¹*Joint Institute for Nuclear Research, Dubna, Russia*

²*National Research Center "Kurchatov Institute", Russia*

³*Lomonosov Moscow State University, Moscow, Russia*

E-mail: zhaketov@nf.jinr.ru

One of the most actual problem at the physics of low-dimensional superconducting/ferromagnetic heterostructures is determination of the correlation between magnetic spatial profile and the spatial profiles of the elements at the interface between layers. Standard neutron reflectometry can't be used to measure neutron interaction with separate element, in particular, magnetic field induction. A new method allows one to determine the elemental and magnetic profiles. The reflected neutron beam and secondary radiation are simultaneously recorded in this method. Charged particles and gamma-quanta can be secondary radiation because of neutron capture reaction. Also scattered neutrons and spin-flip neutrons can be secondary radiation.

At the REMUR reflectometer at the IBR-2 reactor, channels for secondary radiation registration were realized: spin flip neutrons, charged particles and gamma-quanta. Currently, a sufficiently large number of element isotopes are available for measurements. At measuring time $t=1$ day, resolution by the wave vector $\delta k/k=0.1$, $\lambda=1.5$ Å, cross section of the beam at a sample of 0.1 cm², layer thickness 5 nm and neutron flux density at the sample of $2 \cdot 10^{14}$ cm⁻²s⁻¹ it's: a) for the charged particles registration channel, the minimum value of the cross section is $\sigma_{\min}=0.025$ barn, the cross section $\sigma>\sigma_{\min}$ has 22 isotopes; b) for the gamma-quanta registration channel, $\sigma_{\min}=0.3$ barn, more than 100 isotopes have a cross section $\sigma>0.3$ barn; c) for the polarized neutrons registration channel, the minimum, perpendicular to the neutron polarization, component is 1 G.

Further progress is possible. The first is increasing of neutron intensity to 5–10 times. The second is the reduction of the fast neutrons and gamma-quanta background from the reactor core by 5-10 times. Third is increasing of the solid angle visible to gamma-ray detector by 4 times or increasing of the detectors number to 4. Realization of these improvements at the REMUR reflectometer make available cross section 1 mbarn for an absorbing layer 5 nm or cross section 50 mbarn for 1 Å layer. The spatial resolution can reach 1 Å by using super-mirror neutron reflector at the structure. In the case of studying periodic structures, high spatial resolution can be achieved by reducing the period of the structure. At nowadays technological level, structures with period 1 nm are available, which gives a value of 1-2 Å for resolution.

DIVERGENCE OF A NEUTRON MICROBEAM FROM PLANAR WAVEGUIDES

S.V. Kozhevnikov¹, V.D. Zhaketov² and F. Radu²

¹*Frank Laboratory of Neutron Physics, JINR, Dubna, Russia*

²*Helmholtz-Zentrum Berlin für Materialien und Energie, Berlin, Germany*

E-mail: kozhevn@nf.jinr.ru

Neutron planar waveguides are tri-layer structures which transform a conventional neutron beam into a narrow but slightly divergent neutron microbeam used for the investigations of local microstructures with high spatial resolution 1 – 10 μm . At fixed geometry, the final microbeam width depends on its divergence. Fraunhofer diffraction on a narrow slit which is the middle layer (or channel) gives the main contribution into the microbeam divergence as $\delta\alpha \sim \lambda/d$, where λ is neutron wavelength and d is the channel width.

In our previous measurements [1], the system of neutron microbeams from the planar waveguide $\text{Ni}_{0.67}\text{Cu}_{0.33}(20\text{ nm})/\text{Cu}(150)/\text{Ni}_{0.67}\text{Cu}_{0.33}(50)/\text{Si}$ was observed at the time-of-flight reflectometer REMUR at the pulsed reactor IBR-2 in Dubna. It is measured experimentally that the angular divergence of the microbeam depends on the neutron wavelength as $\delta\alpha \sim \lambda$.

In this communication [2] we investigated the microbeam divergence as a function of the channel width d using the waveguides $\text{Ni}_{0.67}\text{Cu}_{0.33}(20\text{ nm})/\text{Cu}(d)/\text{Ni}_{0.67}\text{Cu}_{0.33}(50)/\text{Al}_2\text{O}_3$ where $d = 80, 100, 120$ and 180 nm . The time-of-flight neutron reflectometer REMUR was used. The experimental results confirm the Fraunhofer diffraction contribution as $\delta\alpha \sim 1/d$. The same result was obtained later [3] at the reflectometer NREX (MLZ, Garching, Germany) with fixed neutron wavelength.

This work was partially supported by JINR-Romania scientific project № 268/20.05.2020, item 47.

- [1] S.V. Kozhevnikov et al. (2015). System of neutron microbeams from a planar waveguide. JETP Letters. 102, 1-6.
- [2] S.V. Kozhevnikov et al. (2018). Neutron microbeam from a planar waveguide. JETP. 127, 593-607.
- [3] S.V. Kozhevnikov et al. (2019). Divergence of neutron microbeams from planar waveguides. Nuclear Instruments and Methods in Physics Research. A 975, 54-64.

INTENSE UCN SOURCE AT IBR2 REACTOR. THE DREAM OR OPPORTUNITY?

A.I. Frank¹, N.V. Rebrova¹ and G.V.Kulin¹

¹Frank Laboratory of Neutron Physics, JINR, Dubna, Russia

E-mail: frank@nf.jinr.ru

The possibility of focusing in time of very slow neutrons generated by a pulsed source was discussed for the first time in [1]. It was noted that it can be very attractive in connection with the idea of F. L. Shapiro [2] on the accumulation of UCNs generated by a pulsed source. In [2], it was noted that "if UCNs are introduced into a neutron trap at the moment of a pulsed reactor burst, and the trap is isolated at the end of the burst, then in the ideal case of absence of losses, the UCN density in the trap will correspond to the peak neutron density, which may be several orders of magnitude higher than the time-averaged density."

The complexity of implementing Shapiro's proposal is largely related to the need to place biological shield between the UCN generation zone and the corresponding experimental facility, to which the UCN is transported using a neutron guide. The length of the latter is usually several meters. When the shutter is placed next to the converter, the neutron guide is included in the storage volume, which reduces the lifetime of neutrons in the installation. Placing the shutter close to the trap is useful only for sources with a very low repetition rate, because of the large spread in the UCN time of flight through the neutron guide.

Time focusing removes this difficulty by forming a time image of the source directly near the trap. In this case, the duration of the time image pulse is of the same order as the duration of the true flux pulse of the UCNs in the source (see fig.1).

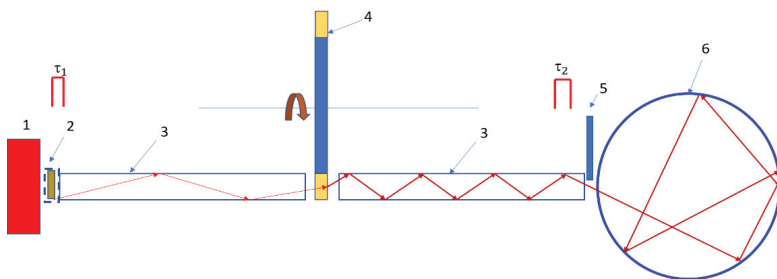


Fig. 1. Source schematic diagram. 1 – main moderator, 2- moderator-converter, 3 – neutron guide, 4- time lens with diffraction gratings, 5 – fast shutter, 6 – UCN trap

As for the principle of the lens operation, as an attractive, but somewhat extravagant possibility, in the Ref. [1] it was proposed to turn to quantum non-stationary effects. Two possibilities were considered: the phase modulation of a neutron wave by the moving the phase diffraction grating across the direction of neutrons and the resonant neutron spin flip in a magnetic field.

The principal possibility of neutron time focusing was soon confirmed in experiments with a moving grating [3], and later with a resonant spin-flipper [4]. Despite a fairly successful demonstration of the principle of time focusing based on non-stationary diffraction, no practical steps have been taken to design a source based on this idea. This was probably due to the fact that in order to increase the energy transmitted to the neutron, it is

necessary to increase the frequency of neutron wave modulation, which is equal to the ratio of the grating speed and its spatial period, and this leads to a decrease in the diffraction efficiency of the so-called π - gratings which were usually used.

Relatively recently, two important factors have been realized that have significantly influenced the assessment of the prospects for this idea. It was realized that by rejecting the idea of a π -grating, it is possible to significantly increase the diffraction efficiency of the grating at grazing incidence of the wave by varying the depth of the grating profile [5]. Besides, a very significant advantage of using a time lens not only for time focusing, but also for neutron deceleration was realized, although this idea was briefly discussed in [1].

The idea of time focusing with deceleration is shown in figure 2. Its advantages are due to two circumstances. First, due to the non-stationary nature of diffraction by a moving grating, the intensity of diffracted waves is determined by the value $|A_n|^2 = |a_n|^2 (k_0/k_n)$

[6], where a_n is the amplitude of the diffracted wave of the order n in the rest frame of the grating, and k_0 and k_n are the wave numbers of initial and diffracted waves correspondently. In the case under consideration $k_0/k_n > 1$. Second, and more important, an increase in the velocity of neutrons incident on the grating V_0

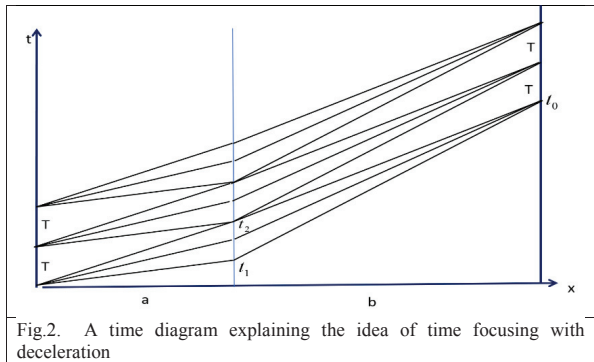


Fig.2. A time diagram explaining the idea of time focusing with deceleration

, substantially increases the phase volume of the focused neutrons, leading to an increase in the momentum density of neutrons entering the system in proportion to the ratio $K = (V_0/V_{UCN})^4$, where V_{UCN} - maximum UCNs velocity.

We have made preliminary calculations of the UCN source based on the time focusing and deceleration of neutrons. A set of diffraction gratings moving at a uniform speed across the direction of neutron propagation is used as a time lens. The grating parameters were optimized for the velocity of neutrons incident on the lens at each moment of time.

Such a source can, in principle, be built at the IBR2 reactor or at the future DNS IV reactor. The density of UCNs accumulated in the trap of such a source is at the level of the best modern sources or even exceed it.

[1] A. Frank and R. Gaehler, in Proceedings of IV International Seminar on Interaction of Neutrons with Nuclei, ISINN-4, JINR, Dubna (1996), JINR E3-96-336, p. 308; A. I. Frank and R. Gaehler, Phys. At. Nucl. **63**, 545 (2000)

[2] F. L. Shapiro, Neutron Research (Nauka, Moscow, 1976), p. 229 (in Russian)

[3] S.N. Balashov, I.V. Bondarenko, A.I. Frank, P. Geltenbort, P. Høghøj, G.V. Kulin, S.V. Masalovich, V.G. Nosov, A.N. Strepetov. Physica B, **350** 246 (2004)

[4] Y. Arimoto, P. Gertenbort, S. Imajo, Y. Iwashita, M. Kitaguchi, Y. Seki, H. M. Shimizu, T. Yoshioka. Phys. Rev. A **86**, 023843 (2012)

[5] G. V. Kulin, A. I. Frank, M. A. Zakharov, S. V. Goryunov, V. A. Bushuev, A. Panzarella, P. Geltenbort, and M. Jentschel. JETP, **129**, 806 (2019)

[6] V.A. Bushuev, A.I. Frank, G.V. Kulin, JETP, **122**, 32 (2016)

RING DETECTOR FOR SMALL-ANGLE SCATTERING OF THERMAL NEUTRONS FOR REAL-TIME DIFFRACTOMETER (RTD)

V.M.Milkov¹, A.A.Bogdzel¹, A.P.Buzdavin¹, S.A. Kutuzov¹, A.I.Beskrovnyi¹, E.P.Popov^{1,2,3}, M.Balasoiu^{1,4}, A.I.Zhuravlev¹, Ts.Ts.Pantelev¹.

¹*Joint Institute for Nuclear Research (JINR), Joliot-Curie 6, 141980 Dubna, Moscow region, Russia*

²*Institute for Nuclear Research and Nuclear Energy, Bulgarian Academy of Sciences, Sofia 1784, Bulgaria*

³*Acad. E. Budevski Institute of Electrochemistry and Energy Systems, Bulgarian Academy of Sciences, 10 Acad. G. Bonchev St., Sofia 1113, Bulgaria*

⁴*Horia Hulubei National Institute of Physics and Nuclear Engineering, Magurele, Romania*

E-mail: milkov@nf.jinr.ru

The development of the detector is based on the design and experience of working with a one-dimensional coordinate-sensitive ring thermal neutron detector [1, 2], which allows measurements of the spatial distribution of thermal neutrons scattering from samples in 8 discrete coaxial rings.

The detector is designed to measure small-angle scattering of thermal neutrons at the IBR-2 reactor, Real-Time Neutron Diffractometer (RTD) (channel No. 6a). Structurally the detector is divided into 9 independent equidistant coaxial rings. The cathodes of each of the rings are divided into 16 independent sectors, the same for each ring. The cathodes are located with inner side of rings and have a rectangular shape, their length being a function of the radius of the corresponding ring. Thus, each separate cathode segment takes position $\sim 1/16$ of the total angle 2π of any ring counter.

This innovation made it possible to introduce a new coordinate as a measurement parameter.

Due to its feature in design, the detector is a suitable tool for any researches in which angular or axial anisotropy of the scattering of slow neutrons can be observed.

To check the azimuthally sensitivity of the detector were made measured of small-angle scattering with magnetic fluid from particles of CrFe₂O₄ by application of an external magnetic field at different orientations.

dimensions.

[1] Б. Н. Ананьев, и др. (1978). Кольцевой многонитевой детектор медленных нейтронов с гелием-3, Препринт ОИЯИ, № 3-11502, Дубна.

[2] Б. Н. Ананьев, Ю. М. Останевич и Е. Я. Пикельнер, (Опубликовано 30.11.80, № 44). Описание изобретения № 690959, – Нитяной детектор медленных нейтронов Государственный комитет СССР по делам изобретений и открытий.

THE INFLUENCE OF DELAYED NEUTRONS AT THE PULSED REACTOR IBR-2 ON THE SIGNAL/BACKGROUND RATIO OF LOW-RESOLUTION NEUTRON INSTRUMENTS

V.I. Bodnarchuk¹, V.V. Sadirov¹ and A. Ioffe²

¹*Frank Laboratory of Neutron Physics, Joint Institute for Nuclear Research, Dubna, Russia*

²*Juelich Centre for Neutron Science at Heinz Maier-Leibnitz Centre (JCNS@MLZ), Forschungszentrum Jülich GmbH, Garching, Germany*

E-mail: bodnarch@nf.jinr.ru

Time-of-flight neutron scattering instruments at pulsed reactors of the IBR-2 type encounter the problem of the background of delayed neutrons that are emitted by the fission fragments of the reactor fuel within the time interval of up to several tens of seconds from the moment of fission. Because the time of flight of neutrons with wavelengths of $(0.1 \div 2)$ nm for any neutron scattering instrument is significantly less than this time interval, then the entire instrument wavelength band will be populated by such background neutrons, that are time uncorrelated with the neutron pulse generated by the pulsed reactor. This background will limit the minimal detected signal and, indeed, seriously influence the performance of neutron instruments.

In this work, we analyze the influence of the delayed neutron background on low resolution momentum transfer measurements using a neutron reflectometer at the IBR-2 as an example. The analysis is based upon the experimentally measured time dependence of the IBR-2 reactor power [1], that allows us to determine the background level of delayed neutrons with respect to the main power pulse.

By Monte-Carlo simulations (with the VITESS software package) we have demonstrated that the admixture of delayed neutrons to the neutron beam incident on a sample doesn't limit the minimal measurable neutron reflectivity even for measurements with a large, up to 0.2 nm^{-1} , momentum transfer.

[1] V.D. Ananiev et al., JINR Preprint P13-2004-156.

MAGNETISM OF RARE-EARTH MULTILAYERS

N.O. Antropov^{1,2}, D.I. Devyaterikov¹, M.V. Makarova^{1,2}, E.S. Nikova¹, Yu.A. Salamatov¹, and E.A. Kravtsov^{1,2}

¹*Institute of Metal Physics, Ekaterinburg, Russia*

²*Ural Federal University, Ekaterinburg, Russia*

E-mail: karavtsov@imp.uran.ru

Heavy rare-earth metals (from Gd to Tm) are well known to display rich magnetic phase diagrams depending on temperature and magnetic field. These include temperature-dependent magnetic anisotropy in Gd, helicoidal magnetic ordering in Dy and Ho, etc. When rare-earth metals are used as constituents of planar multilayered nanostructures, complex magnetic structures never observed in bulk systems may appear due to dimensional effects, proximity effects from neighboring layers, interfacial effects, epitaxial strains, long range exchange coupling, and others.

Here we report on our recent results on magnetic multilayers composed of 4f, 3d, and 5d metals received by complementary application of polarized neutron reflectometry and x-ray scattering. In particular, we consider antiferromagnetic exchange ordering in Fe/Gd superlattices and its modification with introducing antiferromagnetic (Cr) and paramagnetic (Pd) spacers between Fe and Gd. We discuss the role of dimensional effects, atomic and magnetic microstructure in formation of perpendicular magnetic anisotropy in Co/Dy multilayers.

We show that in magnetic multilayers composed of alternating rare-earth metals Dy/Gd and Dy/Ho there appears coherent magnetic structure propagating throughout all the multilayer. In Dy/Gd superlattices, magnetic moments in ferromagnetically ordered Gd layers are oriented out-of-plane, while Dy magnetic moments form a fan structure propagating coherently throughout all the Dy layers. This complex interlayer and intralayer magnetic ordering causes to additional Bragg peak detected with polarized neutron reflectometry in limited temperature region.

In Dy/Ho superlattices, we observed different magnetic helicoidal structures in Dy and Ho layers alternating coherently in all the structure. The magnetic helix periods are different in Dy and Ho, the magnetic phase transition observed in bulk Dy and Ho at low temperatures does not occur in Dy/Ho multilayers, so helicoidal ordering exists down to very low temperatures.

The research was partly supported by RFBR (projects Nos. 20-42-660024, 19-32-90007, 19-02-00674).

OBSERVATION OF HELIMAGNETISM IN DY AND HO THIN FILMS VIA NEUTRON REFLECTIVITY MEASUREMENTS

V. D. Zhaketov¹, Yu.V. Nikitenko¹, V.L. Aksenov¹, E.A. Kravtsov², D.I. Devyaterikov², V.V. Proglyado²

¹Frank Laboratory of Neutron Physics, Joint Institute for Nuclear Research, Dubna, Russia

²Institute of Metal Physics UB RAS, Ekaterinburg, Russia

E-mail: devidor@yandex.ru

Rare earth gelimagnetics, such as Dy, Ho, Tb, etc., grown in the form of epitaxial films, are characterized by a complex magnetic structure and are extremely sensitive to deformation of the crystal lattice. For example, in bulk Dy, a helicoidal magnetic ordering is formed below the Neil temperature of 178 K, and below the Curie temperature of 85 K, it passes into a ferromagnetic state. Bulk Ho goes into the helimagnetic state at 133 K, and below 20 K it forms a conical spiral. It was shown [1],[2] that minor changes in the lattice parameter Dy lead to a significant modification of the phase diagram- suppression of the transition to the ferromagnetic phase when the lattice expands and an increase in the Curie temperature during compression. Epitaxial stresses in Ho films lead to suppression of the transition to the conical phase, a significant change in the period of the helicoid, and modification of its temperature dependence [3].

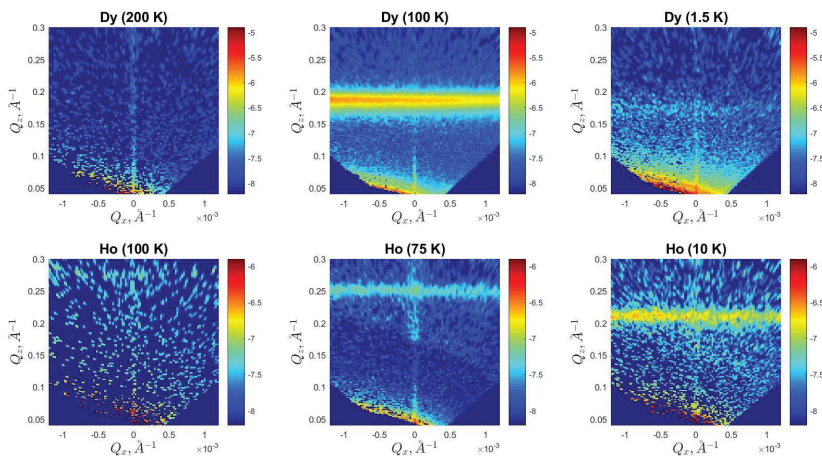


Figure 1: Experimental data on the offspecular neutron scattering from the Dy film (upper layer) and Ho film (lower layer) in different temperatures. Bragg sheet is a horizontal sheet of varying brightness on the four patterns on the right.

Neutron reflectometry (NR) is a powerful method for studying magnetic properties of rare-earth metals both in volume and thin films due to its ability to detect helicoidal magnetic ordering, which gives rise to the magnetic bragg sheet. We have performed two series of NR measurements (Fig.1) on the following samples

- 1) Al₂O₃(a-plane)/Nb (400 Å)/Dy (2000 Å)/V (150 Å)
- 2) Al₂O₃(r-plane)/Nb (400 Å)/Ho (2000 Å)/V (150 Å)

on the REMUR station in JINR, Dubna. The crystal structure of the samples along surface normal was tested via X-ray diffraction (XRD) on PANalitical diffractometer in IMP UB RAS. It appears, that most of rare-earth layer has its HCP cell c-axis directed perpendicularly to the surface, which corresponds to (0002) peak on diffraction pattern. The wave vector of the magnetic helix in such parts of the layer is expected to coincide with surface normal. During the NR measurements, temperature dependent bragg sheet was observed in the temperature range of at least 150 K- 1.5 K for Dy film and 75-1.5 K for Ho film. This leads to a conclusion, that magnetic properties of the samples are somewhat different from the properties of the volume materials, with the most impressive difference in the form of suppression of AFM-FM phase transition, which occurs at about 80 K for volume Dy and at 20-21 K for volume Ho. Period of helicoid in the samples was also calculated and it appears to be relatively close to the one in the volume[4],[5] (Fig.2). All NR data was transformed into Qx-Qz coordinates by means of Överlåtaren software created by Franz Aldmann [6].

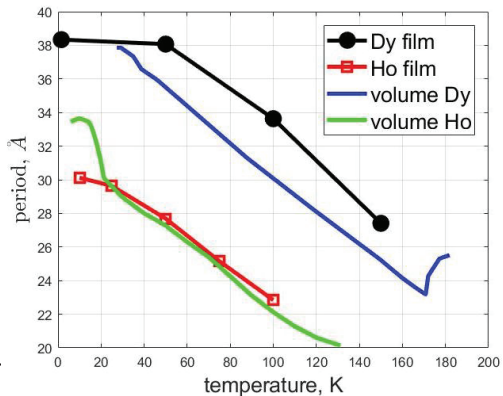


Figure 2: temperature dependence of period of magnetic helicoid in thin Dy and Ho films compared to volume materials

This study is supported by RFBR project № 19-32-90007.

- [1] F. Tsui, C. P. Flynn(1993). Magnetic phase diagram of epitaxial dysprosium. Phys. Rev. Lett. 71, 1462-1465.
- [2] C. Dufour, K. Dumesnil, P. H. Mangin (2006). Strain-induced modification of magnetic structure and new magnetic phases in rare-earth epitaxial films. Pramana 67, 173-190.
- [3] A. D. F. Herring, W. J. Nuttall, M. F. Thomas, J. P. Goff, A. Stunault, R. C. C. Ward, M. R. Wells, W. G. Stirling (2005). Thickness effects on the magnetism of Ho thin films Journal of Physics: Condensed Matter 17, 2543-2552.
- [4] J. Yu, P. R. LeClair, G. J. Mankey, J. L. Robertson, M. L. Crow, W. Tian (2015). Exploring the magnetic phase diagram of dysprosium with neutron diffraction. Phys. Rev. B 91, 014404.
- [5] M. J. Pechan, C. Stassis (1984). Magnetic structure of holmium. Journal of Applied Physics 55, 1900-1902.
- [6] F. A. Adlmann, G. K. Pálsson, J. C. Bilheux, J. F. Ankner, P. Gutfreund, M. Kawecki, M. Wolff (2016). Överlåtaren: a fast way to transfer and orthogonalize two-dimensional off-specular reflectivity data. J. of Applied Crystallography 49, 2091-2099

SYNTHESIS OF ROD-LIKE AND SPHERICAL MAGNETITE NANOPARTICLES ASSISTED BY MAGNETIC FIELD

A.V. Shibaev¹, D.E. Kessel¹, P.V. Shvets², S.S. Abramchuk¹, A.R. Khokhlov³ and O.E. Philippova¹

¹ *Physics Department, Lomonosov Moscow State University, Moscow, Russia*

² *REC “Functional Nanomaterials”, Immanuel Kant Baltic Federal University, Kaliningrad, Russia*

³ *Institute of Advanced Energy Related Nanomaterials, Ulm University, Ulm, Germany*

E-mail: shibaev@polly.phys.msu.ru

In this work, we study the effect of pH on the synthesis of magnetite (Fe₃O₄) nanorods assisted by external magnetic field. We use reverse co-precipitation of Fe³⁺ and Fe²⁺ ions to obtain magnetic nanoparticles. Synthesis of the magnetite phase is confirmed by electron diffraction and Raman spectroscopy. The morphology of the synthesized nanoparticles strongly depends on the pH of the reaction medium, e.g on the amount of OH⁻ ions in the reaction mixture. As shown by TEM, magnetite nanorods are synthesized at the comparable amounts of iron ions and hydroxyl ions, whereas spherical nanoparticles are obtained at the excess of OH⁻ ions. Magnetite nanorods are single crystals, and they are presumably formed by the magnetic assembly of building blocks – small hexagonal faceted magnetite nanocrystals, which are formed at the first step of the reaction.

The study offers a prospective way towards a facile, green and controllable method of anisotropic magnetic nanoparticles production in the absence of a stabilizer (like surfactant or polymers), which is important for modification of their surface or incorporation into polymer nanocomposites.

Acknowledgement

The work is financially supported by the Russian Foundation for Basic Research (project № 18-53-76007 ERA_a).

[1] A.V. Shibaev, P.V. Shvets, D.E. Kessel, R.A. Kamyshinsky, A.S. Orekhov, S.S. Abramchuk, A.R. Khokhlov, O.E. Philippova (2020). Magnetic field-assisted synthesis of anisotropic iron oxide nanoparticles: Effect of pH. *Beilstein J. Nanotechnol.*, in press.

STRUCTURE AND DIELECTRIC PROPERTIES OF LOW-POLARITY FERROFLUIDS UNDER AN ELECTRIC FIELD

M. Rajnak^{1,2}, V. I. Petrenko³, M. V. Avdeev³, A. Feoktystov⁴, J. Kurimsky², R. Cimbala², B. Dolnik², M. Karpets^{1,2}, K. Paulovicova¹, P. Kopcansky¹ and M. Timko¹

¹*Institute of Experimental Physics SAS, Watsonova 47, 04001 Kosice, Slovakia*

²*Faculty of Electrical Engineering and Informatics, Technical University of Košice, Letná 9, 04200 Košice, Slovakia*

³*Joint Institute for Nuclear Research, Joliot-Curie 6, 141980 Dubna, Moscow region, Russia*

⁴*Forschungszentrum Jülich GmbH, Jülich Centre for Neutron Science (JCNS) at Heinz Maier-Leibnitz Zentrum (MLZ), Garching, Germany*

E-mail: rajnak@saske.sk

Magnetic field-induced structural changes in ferrofluids are well-known and intensively studied phenomena [1,2]. The ferrofluids based on low-polarity liquids then exhibit the intuitive magneto-dielectric anisotropy. However, recently it was demonstrated that structural changes in transformer oil-based ferrofluids may be induced even by an external electric field [3,4]. This paper aims to summarize recent findings on structural behavior of ferrofluids based on transformer oil and iron oxide nanoparticles under the action of electric fields. *In situ* small-angle neutron scattering (SANS) study of ferrofluids under various AC (alternating current) and DC (direct current) electric field intensities will be presented. Based on the obtained scattering profiles, one can conclude that depending on the field intensity, the anisotropic aggregates with a tendency to align in the electric field direction are formed. On a macroscopic scale, the electric field induced structural changes are observed visually as bulk patterns. Subsequently, we present the influence of the induced aggregates on dielectric properties of the ferrofluid. It is clear that dielectric spectra (1 mHz–1 MHz) obtained at various temperatures exhibit a remarkable dependence on the DC electric field intensity. We demonstrate that the applied DC bias voltage results in a permittivity sign switching at low frequencies. Taking into account the confirmed structural changes, the directed nanoparticle assembly and conductive percolative paths formation are considered as key mechanisms leading to the transition from capacitive to inductive reactance. Thus, it is believed that electric field-controllable dielectric response of ferrofluids may complement the controllable effects in ferrofluids by external forces and may open a new avenue of research and applications of ferrofluids.

[1] F. L. de O. Paula, *Condens. Matter*, 4, 2, p. 55, 2019

[2] V. Socoliuc and R. Turcu, *J. Magn. Magn. Mater.*, 500, p. 166348, 2020

[3] M. Rajnak et al., *Appl. Phys. Lett.* 107, 073108 (2015).

[4] P. A. Selyshchev et al., *J. Mol. Liq.*, 278, pp. 491–495, 2019.

STRUCTURAL ASPECTS OF Fe₃O₄/CoFe₂O₄ NANOPARTICLES BY X-RAY AND NEUTRON SCATTERING: POWDERS AND STABILIZATION IN WATER

A.V. Nagornyi^{1,2,*}, L.A. Bulavin², Yu.Yu Shlapa³, M.V. Avdeev¹, S.O. Solopan³, O.I. Ivankov^{1,4}, A. Shulenina⁵, A.G. Belous³

¹ Joint Institute for Nuclear Research, Dubna, Russia

² Taras Shevchenko National University of Kyiv, Kyiv, Ukraine

³ Vernadsky Institute of General and Inorganic Chemistry, Kiev, Ukraine

⁴ Institute for Safety Problems of Nuclear Power Plants, Chornobyl, Ukraine

⁵ National Research Center «Kurchatov Institute», Moscow, Russia

E-mail: avnagorny@jinr.ru

Synthesis of magnetic nanoparticles (MNPs), such as Fe₃O₄, CoFe₂O₃ etc., are of great interest because of the possibility of their wide using in technology and science, especially in medicine [1-4]. For medical applications MNPs have to be nanosized, monodispersed, nontoxic and have stability to aggregation.

The structural aspects of powders Fe₃O₄/CoFe₂O₄ magnetic nanoparticles with the anticipated “core–shell” structure are analyzed by comparison with individual Fe₃O₄ and CoFe₂O₄ particles using X-ray powder diffraction, small-angle neutron and X-ray (synchrotron) scattering. It is shown that MNPs in the powders are strongly polydisperse and form complex aggregates [5]. The characteristic sizes of the crystallites, as well as the ratio between magnetite and cobalt ferrite in the composition of the Fe₃O₄/CoFe₂O₄ particles are estimated based on analysis of the diffraction peaks. Analyzing the small-angle scattering data, the characteristics particles’ size and aggregates are obtained. The fractal dimensions of the aggregates are determined. A significant difference between scattering at Fe₃O₄/CoFe₂O₄ particles and the total scattering derived from the partial contributions of scattering events at powders of separate magnetite and cobalt ferrite particles is observed, which suggests the formation of a “core–shell” structure.

To distinguish the form-factor and to avoid scattering on large aggregates, magnetic nanoparticles were dispersed into a water. To prevent agglomeration in aqueous media the MNPs were covered by molecules of Polysorbate-80 (Tween-80). The DLS treatment shows the presents of single-particle fraction in a volume against of agglomeration. The structures of water-based ferrofluids with a low concentration of MNPs were analyzed in a framework of the SAXS and SANS data. The contrast variation approach within the SANS was applied to resolve core-shell structure of MNPs.

[1] O.V.Yelenich et al. (2013) Polyol synthesis and properties of AFe₂O₄ nanoparticles (A = Mn, Fe, Co, Ni, Zn) with spinel structure. *Solid State Phenomena*. 200, 149–155.

[2] O.V.Yelenich et al. (2013) Synthesis and Properties of AFe₂O₄ (A = Mn, Fe, Co, Ni, Zn) Nanoparticles produced by deposition from diethylene glycol solution. *Russ. J. of Inorg. Chem.* 58 (8), 901–905.

[3] L.Vekas, D.Bica, M.V.Avdeev (2007) Magnetic nanoparticles and concentrated magnetic nanofluids: Synthesis, properties and some applications. *China Particology*. 5, 43–49.

[4] A.Belous et al. (2014) Synthesis and Properties of Ferromagnetic Nanoparticles for Potential Biomedical Application. *IEEE ELNANO: Kyiv*, 245–249.

[5] A.V. Nagornyi, M.V. Avdeev, O.V. Yelenich, et al. Structural Aspects of Fe₃O₄/CoFe₂O₄ Magnetic Nanoparticles According to X-Ray and Neutron Scattering. *Journal of Surface Investigation*. 12(4) (2018) 737-743. <http://dx.doi.org/10.1134/S102745101804033X>

**ADVANCES IN UNDERSTANDING THE CONFORMATIONAL DISEASES
MIMICKING MODEL MEMBRANES BY NEUTRON SCATTERING**

Ivankov O.^{1,2}, Ermakova E.¹, Murugova T.^{1,2}, Badreeva D.¹, Dushanov E.^{1,3},
Kondela T.^{1,4}, Kholmurodov Kh.^{1,3}, Kuklin A.^{1,2}, Kučerka N.^{1,4}

¹*Joint Institute for Nuclear Research, Dubna, Russia*

²*Moscow Institute of Physics and Technology, Dolgoprudny, Russia*

³*Dubna State University, Dubna, Russia*

⁴*Comenius University in Bratislava, Bratislava, Slovakia*

E-mail: kucerka@nf.jinr.ru

The Alzheimer's disease (AD) is a conformational disease caused by the formation of senile plaques, consisting primarily of Amyloid-beta peptides. The crucial role in this process at its pre-clinical stage is likely imparted by peptide-membrane interactions. The experimental data suggest several intriguing structural properties of biomimetic membranes that modulate such interactions. First, it is their sensitivity to the charge present in the surrounding environment. The structure of membranes changes for example with increasing concentration of ions, which appears to be an effect born by peculiar properties of ions and lipid themselves. Interestingly, the differences in lipid interactions with ions have been linked to the hydration properties of the ions. A plausible mechanism of action in the case of many membrane additives seems to be in shifting the water encroachment the way that bilayers absorb more or less water molecules. The hydration interactions appear to determine also the location of membrane constituents, such as cholesterol, melatonin, and amyloid-beta peptides. Moreover, cholesterol increases the order of lipid hydrocarbon chains while increasing the stiffness of membrane, in the contrary to the fluidizing effect of melatonin.

The observations discussed (based on the neutron scattering experiments and MD simulations) may prove to be important for studies on amyloid toxicity, as they may lend some insight into understanding the molecular mechanism of melatonin's protection in AD. For example, melatonin levels in the body have been shown to decrease with age. As AD is more prevalent later in life, the effects of melatonin and cholesterol on lipid membrane become increasingly important as their amounts in membranes also change with age. The conclusions of various investigations can thus provide an understanding for the possible structural changes taking place within biological membranes. Since the AD seems to be correlated with peptides aggregating outside the membrane, capability of membrane to retain peptides within its interior could also be understood as a preventive mechanism to the disease onset.

Acknowledgement: This work has been supported by the Russian Science Foundation under grant 19-72-20186.

[1] Ivankov O., Ermakova E., Murugova T., Badreeva D., Dushanov E., Kondela T., Kholmurodov Kh., Kuklin A., Kučerka N.: Interactions in the model membranes mimicking preclinical conformational diseases in *Advances in Biomembranes and Lipid Self-Assembly*, Elsevier (2020).

EFFECT OF NANOMATERIALS ON PROTEIN AMYLOID AGGREGATION

K. Sipošova¹, A. Musatov¹

¹*Department of Biophysics, Institute of Experimental Physics SAS, Watsonova 47, 04001 Kosice, Slovakia*

E-mail: sipošova@saske.sk

Both natural and synthetic nanoparticles (NPs) have practical applications in a variety of areas, ranging from environmental remediation to an emerging multidisciplinary field that combines chemistry, engineering, physics, biology, and medicine. Additionally, over the last decades, there has been increased interest in the studies of *in vitro* and *in vivo* applications of NPs in radiation, photodynamic and thermal therapies. Proteins are important biological macromolecules that are fundamental to the proper functioning of cells and organisms; therefore, the impact of nanoparticles in living organisms at the protein level is a critical issue that is attracting increasing attention from researchers. Moreover, nanoparticles are being explored for their role in diagnosing, preventing, treating or even causing amyloid diseases. Amyloid-related diseases are characterized by unusual protein-protein interactions of normally soluble proteins that have undergone structural transitions and result in the formation of intracellular and extracellular amyloid aggregates. The pathogenesis of these and other neurodegenerative diseases remains unclear, and effective treatments are currently lacking. It was demonstrated that nanoparticles can significantly influence the process of protein amyloid fibrillization.

Within our long-term aim of study, we have examined the physical properties of the bio-nanocomposites, particularly those, which contain within themselves magnetic (Fe₃O₄-based) NPs [1], [2], [3], [4]. The Fe₃O₄-based NPs possess a unique property of superparamagnetism that confers advantages such as the generation of heat when influenced by alternating magnetic fields and the ability to be guided to a specific tissue or organ by an external magnetic field. Prerequisite for successful application is the proper surface functionalization of such nanocomposites, which determines their interaction with the environment, stabilizes them against precipitation, and ensures their biocompatibility and low cytotoxicity. To address this, the surface functionalization of nanocomposites with different ligands and natural biomolecules has been tested extensively. The results demonstrated that magnetic component of magnetic fluids was important for their anti-amyloid activity, however, the physico-chemical properties of NPs such as type of coating layer, charge, concentration, etc. determined the extent of inhibition/depolymerization activity [1], [2], [3], [4]. Moreover, application of irradiation enhanced the destruction of fibrils particularly in the presence of NPs. Other potential anti-amyloidogenic agents are the fullerenes, which due to their unique spherical structure are known for their antioxidant, neuroprotective, cytoprotective and antitumor properties [5], [6]. Moreover, they might be used as carriers of contrast agents, radiopharmaceuticals or drugs, and thus serve as promising tools with applications in medical diagnostics and therapy. Biomedical applications require a dispersal of C60 fullerene in a solvent, with aqueous dispersions being preferred because of biocompatibility, safety, or environmental concerns. Another promising material for biomedicine and pharmaceuticals due to their non-toxicity, thermal stability, expanded surface area, and exceptional ability to adsorb various atoms, organic molecules, photodynamic agents, and nanoparticles into micro- and mesopores are natural zeolite particles, especially clinoptilolite zeolites (CZ). We have found that CZ affect amyloid aggregation of proteins, namely insulin and lysozyme in dose-dependent manner. In addition, anti-amyloid activity of CZ was enhanced after incorporation

of magnetic (Fe_3O_4 -based) nanoparticles into pores of CZ particles and by co-application of external magnetic field and induction of hyperthermia or co-application of radiation. It is important to be noted that a synthetic zeolite (Zeolite Y) did not affect amyloid aggregation. One currently accepted theory is that oxidative stress initiates accumulation of amyloid fibrils which can lead to neurodegenerative diseases. Therefore, knowledge of interplay between oxidative stress and amyloidogenesis, is crucial for understanding of both, aging and age-related neurodegenerative diseases. CeO_2 -NPs are used increasingly in nanotechnology and particularly in bioresearch. In bioscience the great attention is paid to CeO_2 -NPs because of their antioxidant properties, i.e. CeO_2 -NPs possess ability for multi-enzymatic scavenging of reactive oxygen species, exhibit superoxide dismutase and catalase enzymes mimetic activities in a redox-state dependent manner [7]. Recently, we have demonstrated anti-amyloidogenic effect of “naked” CeO_2 -NP [8]. However, although the interaction of CeO_2 -NPs with insulin was strong enough to reduce the fibrillation process, the addition of nanoparticles to mature fibrils seems to be incapable of significant fibril disaggregation. We concluded, that our results will allow us to gain deep insights into the mechanisms of amyloid fibril formation, inhibition and disaggregation of protein aggregates. We also concluded that using NPs in combination with the thermal, photon and radiation can significantly enhance the effect of NPs.

Acknowledgement

This work was supported by grants: VEGA 2/0009/17, APVV 15-453, 19-324, SAS-MOST JRP 2017/6, NATO Science for Peace and Security Programme #G5683 and EuroNanoMed Magbbris.

- [1] A.Bellova, A., E.Bystrenova, M.Koneracka, et al. (2010) Effect of Fe_3O_4 magnetic nanoparticles on lysozyme amyloid aggregation. *Nanotechnology*, 21(6), 065103.
- [2] K.Siposova, M.Kubovcikova, Z.Bednarikova, et al. (2012) Depolymerization of insulin amyloid fibrils by albumin-modified magnetic fluid. *Nanotechnology*, 23(5), 055101.
- [3] P.Kopcansky, K.Siposova, L.Melnikova, et al. (2015) Destroying activity of magnetoferritin on lysozyme amyloid fibrils. *J. Magn. Magn. Mater.*, 377, 267-271.
- [4] K.Siposova, K.Pospiskova, Z.Bednarikova, et al. (2017) The molecular mass of dextran used to modify magnetite nanoparticles affects insulin amyloid aggregation. *J. Magn. Magn. Mater.*, 427, 48-53.
- [5] S.Goodarzi, T.Da Ros, J.Conde, et al. (2017) Fullerene: biomedical engineers get to revisit an old friend. *Materials Today*, 20, 460-480.
- [6] V.K.Torres, B. Srdjenovic, B. (2011) Biomedical Application of Fullerenes. In: *Handbook on Fullerene: Synthesis, Properties and Applications*. Nova Science Publishers, Inc., 199-239.
- [7] S. Das, J.M.Dowding, K.E.Klump, et al. (2013) Cerium oxide nanoparticles: applications and prospects in nanomedicine. *Nanomedicine*, 8 (9), 1483-1508.
- [8] K.Siposova, V.Huntosova, Y.Shlapa, et al. (2019) Advances in the Study of Cerium Oxide Nanoparticles: New Insights into Anti-amyloidogenic Activity. *ACS Appl. Bio. Mater.*, 2, 5, 1884-1896.

LIVING MICELLES-NANOPARTICLES NETWORKS

Molchanov V.S.¹, Efremova M.A.¹, Orekhov A.S.^{2,3}, Arkharova N.A.⁴, Rogachev A.V.^{3,5},
Kuklin A.I.^{3,5}, Philippova O.E.¹

¹*Lomonosov Moscow State University, Moscow, Russia*

²*National Research Centre "Kurchatov Institute", Moscow, Russia*

³*Moscow Institute of Physics and Technology, Dolgoprudny, Russia*

⁴*A.V. Shubnikov Institute of Crystallography FSRC "Crystallography and Photonics" RAS, Moscow, Russia*

⁵*Joint Institute for Nuclear Research, Dubna, Russia*

E-mail: molchan@polly.phys.msu.ru

Soft nanocomposite nanomaterials can be based either on polymer network or on self-assembled network of wormlike surfactant micelles (WLMs). To provide additional functionality to the matrix the nanomaterial can contain delivery vehicle components, for instance, nanoclay tactoids, which make them very promising for drug delivery and tissue engineering applications. Injectable systems represent an evergrowing class of nanomaterials possessing a unique combination of physical and chemical properties. Such materials, for instance, hydrogels can be used as control delivery systems, since they can be delivered in a minimally invasive manner, because their final form and shape are defined by the space, into which they are injected. The influence of organoclay on the mechanical properties of mixed WLMs of surfactants was studied. The present study is devoted to soft nanocomposite based on network of WLMs composed of biocompatible zwitterionic and anionic surfactants with embedded plate-like bentonite nanoclay particles. It is shown that nanoparticles significantly enhance the rheological properties of WLM hydrogel acting as physical cross-links between micellar chains [1]. It was explained by the formation of micelle-nanoparticle junctions as a result of binding of the WLMs end-caps to the layer of surfactant adsorbed on the particle surface [2,3]. The studied network possesses gel-like properties. Its rheological properties demonstrated plateau modulus, low values of loss factor. At the same time, under high deformation, the micellar chains were disrupted, which induced a much more pronounced drop of viscosity than the disruption of physical cross-links in polymer gels. The disrupted micellar chains were completely recovered due to restoration of non-covalent bonds between surfactant molecules within the micelle. It was demonstrated that the prepared nanocomposite hydrogels possess promising properties for injection applications.

Acknowledgements: the financial support of Russian Science Foundation (project №17-13-01535).

[1] V.S. Molchanov, M.A. Efremova, A.S. Orekhov, N.A. Arkharova, A.V. Rogachev, and O.E. Philippova (2020) Soft nanocomposites based on nanoclay particles and mixed wormlike micelles of surfactants. *Journal of Molecular Liquids*. 315, 113684.

[2] O. Philippova and V. Molchanov (2019) Enhanced rheological properties and performance of viscoelastic surfactant fluids with embedded nanoparticles. *Current Opinion in Colloid and Interface Science*. 43, 52–62.

[3] V.S. Molchanov, M.A. Efremova, T.Y. Kiseleva, and O.E. Philippova (2019) Injectable ultra-soft hydrogel with natural nanoclay. *Nanosystems: Physics, Chemistry, Mathematics*. 10, 76–85.

SINGLE LIPID BILAYER CHANGES INDUCED BY CHOLESTEROL AND MELATONIN

P. Hrubovčák^{1,2}, E. Dushanov³, T. Kondela^{1,4}, O. Tomchuk¹, K. Kholmurodov^{1,5}
and N. Kučerka^{1,4}

¹*Frank Laboratory of Neutron Physics, Joint Institute for Nuclear Research, Dubna, Russia*

²*Department of Condensed Matter Physics, University of P. J. Šafárik, Košice, Slovakia*

³*Laboratory of Radiation Biology, Joint Institute for Nuclear Research, Dubna, Russia*

⁴*Department of Physical Chemistry of Drugs, Faculty of Pharmacy, Comenius University in Bratislava, Bratislava, Slovakia*

⁵*Department of Chemistry, New Technologies and Materials, Dubna State University, Dubna, Russia*

E-mail: hrubovcak.pavol@gmail.com

Biological importance of lipid membrane as a primary barrier separating internal environment of each living cell from the ambient is tremendous. There is an ample evidence on the modification of its various functions upon the structure, composition or pressure changes. Cell membrane is also a place of action of serious diseases, among which Alzheimer's disease (AD) is currently becoming one of the most relevant. The incidence of AD is accompanied by the presence of peptide plaques on the surface of the brain tissue that are anchored to the cell membrane. It is believed that the relative concentration of cholesterol and melatonin in the cells might be connected to the AD development. Due to this, their interaction with cell structures are studied extensively employing a range of methods.

In this study, the influence of cholesterol and/or melatonin on the single lipid bilayer have been investigated by means of neutron reflectometry for the first time. The two compounds are known to affect the structure of lipid membrane that results in the significant changes of its overall thickness. Reflectometry, unlike the other methods, examines single planar model membrane. This allows for eradication of the effects induced by the interaction of adjacent membranes or bilayer curvature when characterizing. Our findings are corroborated by the results from molecular dynamics (MD) simulations of examined systems. Owing to the MD, a plausible interpretation of observed membrane changes has been facilitated.

This work is being supported by the Russian Science Foundation under grant 19-72-20186.

CLASSIFICATION OF FRACTAL OBJECTS BY SANS: CASE OF LOGARITHMIC FRACTAL

S.V. Grigoriev^{1,2}, E.G. Yashina¹, P.M. Pustovoit¹, K.A. Pshenichnyi^{1,2}

¹*Petersburg Nuclear Physics Institute of NRC "Kurchatov Institute, 188300, Gatchina, Russia*

²*Saint Petersburg State University, Saint Petersburg, Russia*

E-mail: grigoryev_sv@pnpi.nrcki.ru

The classification of fractal objects on nanometer scale in the three-dimensional space is well developed on the base of small-angle neutron and X-ray scattering. Using the power law of the scattering intensity vs momentum transfer ($I \propto q^{-\Delta}$) one can distinguish between the surface fractals ($3 < \Delta < 4$) and mass fractals ($2 < \Delta < 3$) as well as the logarithmic fractals ($\Delta = 3$) [1, 2]. The exponent Δ close to 3 was until recently interpreted as an intermediate case of the transition from mass to surface fractal. We showed that the cubic dependence in the SANS cross-section corresponds to the pair correlation function $\gamma(r) \propto \ln(\xi/r)$ in the limit $r/\xi \ll 1$, where ξ is the size of the scattering object [2]. It has the specific scaling property $\gamma(r/a) = \gamma(r) + \ln(a)$, when the scaling down by a gives an additive constant to the correlation function, in contrast to the mass fractal, which is characterized by multiplicative constant. We found that the logarithmic correlation function is not a rare case for the structural organization of the life forms. In nature the structures are often-times generated by multiple repetition of the same morphogenetic mechanism, for example the branching. Tree is the most illustrative example of its realization. It grows in a way that on each next level of branching, the sum of squares of radii of the branches equals the square of the radius of the branch that was divided: the property which was noticed long ago by Leonardo da Vinci [3].

[1] Martin J.E., Hurd A.J., J. Appl. Cryst. 20 (1987) 61; J. Teixeira, J. Appl. Cryst. 21 (1988) 781.

[2] E.G. Yashina, S.V. Grigoriev, Journal of Surface Investigation: X-ray, Synchrotron and Neutron Techniques 11, No. 5, (2017) 897–907.

[3] J.O. Indekeu, G. Fleerackers, Physica A 261 (1998) 294–308; C. Eloy, Phys.Rev.Lett. 107 (2011) 258101

MULTIPHASE AND SPONGE LIPID NANOPARTICLES STUDIED BY SAXS AND SANS

B. Angelov¹, A. Angelova², M. Drechsler³, and Y.E. Gorshkova⁴

¹*Institute of Physics, ELI Beamlines, Academy of Sciences of the Czech Republic, Na Slovance 2/1888, CZ-18221 Prague, Czech Republic*

²*Institut Galien Paris-Saclay, CNRS UMR 8612, Université Paris-Saclay, F-92296 Châtenay-Malabry, France*

³*Keylab "Electron and Optical Microscopy", Bavarian Polymerinstitute (BPI), University of Bayreuth, 95440 Bayreuth, Germany*

⁴*Frank Laboratory of Neutron Physics, Joint Institute for Nuclear Research, Joliot-Curie Str. 6, 141980 Dubna, Russia*

E-mail: borislav.angelov@eli-beams.eu

Lipid cubic phases (LCP) have attracted tremendous scientific attention in the past two decades. The main applications behind this strong interest are related to protein crystallization in LCP and LCP-derived nanoparticles for drug delivery, called cubosomes. The mechanisms of protein loading and release from drug delivery vehicles and/or protein loading and nucleation in a LCP matrix for crystallization are still not understood. There are several models, which are partly complete and do not cover all of the aspects of these complex kinetics processes. The main structural methods include cryo-transmission electron microscopy (CryoTEM), time resolved X-ray scattering (TR-SAXS) and neutron scattering (SANS). Here we present results from a monoolein-based model LCP system loaded with therapeutic proteins (BDNF or hemoglobin) and stabilizing agents such as vitamin E and PEG polymers. The performed TR-SAXS investigation on a millisecond time scale (ID02, ESRF, Grenoble, France) showed a cubic multiphase coexistence in single cubosome nanoparticles triggered by the loading of the protein BDNF. Concentration series of hemoglobin loading in cubosomes were studied by SANS (IBR-2 Pulsed Reactor, Dubna, Russia). The obtained results contribute to the elucidation of the mechanism of phase transformations of LCP and their stability upon interaction with proteins.

Acknowledgement: B.A. is supported by the projects "Structural dynamics of biomolecular systems" (ELIBIO) (CZ.02.1.01/0.0/0.0/15_003/0000447), "Advanced research using high-intensity laser produced photons and particles" (CZ.02.1.01/0.0/0.0/16_019/0000789) from the European Regional Development Fund, and a cooperation with JINR (3+3 project). M.D. is supported by the SFB840 collaborative research centre of DFG.

[1] B. Angelov, A. Angelova, S. K. Filippov, M. Drechsler, P. Štěpánek, and S. Lesieur, Multicompartment Lipid Cubic Nanoparticles with High Protein Upload: Millisecond Dynamics of Formation, *ACS Nano* 2014, 8, 5, 5216–5226.

[2] A. Zou, Y. Li, Y. Chen, A. Angelova, V.M. Garamus, N. Li, M. Drechsler, B. Angelov, Y. Gong, Self-assembled stable sponge-type nanocarriers for *Brucea javanica* oil delivery, *Colloids and Surfaces B: Biointerfaces* 2017, 153, 310-319.

[3] A. Angelova, B. Angelov, V.M. Garamus, M. Drechsler, A vesicle-to-sponge transition via the proliferation of membrane-linking pores in omega-3 polyunsaturated fatty acid-containing lipid assemblies, *Journal of Molecular Liquids* 2019, 279, 518-523.

EFFECTS OF MACROMOLECULES AND PROTEIN COMPLEXES ON THE INTERPHASE CHROMATIN ORGANIZATION REGISTERED BY SANS

D.V. Lebedev^{1,2}, Ya. A. Zabolotskaya^{1,2,3,4}, A. V. Shvetsov^{1,2,3}, V. Pipich⁵, A. I. Kuklin⁶, V. V. Egorov^{1,2,7} and V. V. Isaev-Ivanov¹

¹*Petersburg Nuclear Physics Institute of NRC “Kurchatov Institute”, Gatchina, Russia*

²*National Research Centre Kurchatov Institute, Moscow, Russia*

³*Peter the Great St. Petersburg Polytechnic University, St. Petersburg, Russia*

⁴*Smorodintsev Research Institute of Influenza, St. Petersburg, Russia*

⁵*Jülich Centre for Neutron Science at Heinz Maier-Leibnitz Zentrum, Munich, Germany*

⁶*Joint Institute for Nuclear Research, Dubna, Russia*

⁷*Federal State Budgetary Scientific Institution “Institute of Experimental Medicine”, St. Petersburg, Russia*

E-mail: lebedev_dv@pnpi.nrcki.ru

The most important question in the study of chromatin packing is to identify the functional significance of its structural and dynamic characteristics. The integral properties of chromatin packing as a polymer chain are extremely important for understanding the mechanisms of interaction between distant chromatin regions, the formation of loops, and, ultimately, the formation and dynamics of topologically associated chromatin domains - genome regions associated in space and having similar characteristics of transcriptional activity [1,2]. The self-organization and evolution of such domains occurs under the influence of a complex of biochemical (post-translational modification of histone proteins, nucleosome dynamics, interaction of chromatin with specific nuclear proteins [3]), and chemical (charge interactions, macromolecular crowding [4]) factors.

Organization of genetic material in eukaryotes investigated by SANS and USANS has revealed two-phase fractal property of chromatin during interphase, variability in its structure parameters in a number of cell types, and strong effect of macromolecular crowding on both large-scale hierarchy and small-scale nucleosome arrangements, thus providing the experimental basis for the studies chromatin organization throughout its structural hierarchy.

We show that, under certain conditions, the chromatin structure as observed by SANS can be influenced by non-nuclear proteins and protein complexes. Such changes may manifest an important element in epigenetic regulation mechanisms, understanding of which may be important for development of new substances with antitumor and antiviral effects [5].

[1] Roy S.S., et al. (2018) Insights about genome function from spatial organization of the genome. *Hum. Genomics*, 12 (1), 8.

[2] Jost D., et al. (2014) Modeling epigenome folding: formation and dynamics of topologically associated chromatin domains. *Nucleic Acids Res.*, 42 (15), 9553–9561.

[3] Hauer M.H. and Gasser S.M. (2017) Chromatin and nucleosome dynamics in DNA damage and repair. *Genes and Development*, 31 (22), 2204–2221.

[4] Huet S., et al. (2014) Relevance and Limitations of Crowding, Fractal, and Polymer Models to Describe Nuclear Architecture. *International Review of Cell and Molecular Biology*, 307, 443–479.

[5] Lebedev D. V. et al. (2019) Effect of alpha-lactalbumin and lactoferrin oleic acid complexes on chromatin structural organization. *Biochem. Biophys. Res. Commun.*, 520(1), 136-139.

RAGE PEPTIDE (60-76) AND ITS MODIFIED ANALOGUE PROTECT SPATIAL MEMORY IN TRANSGENIC 5XFAD MICE AND INDUCE CALCIUM SIGNALING VIA ACTIVATION OF RAGE

A.V. Kamynina^{1,2}, N. Esteras³, D.O. Korojev², I.S. Okhrimenko¹, N.V. Bobkova⁴,
A.Y. Abramov³, O.M. Volpina²

¹ *Research Center for Molecular Mechanisms of Aging and Age Related Diseases, Moscow Institute of Physics and Technology (National Research University), Dolgoprudny, Russia*

² *Shemyakin-Ovchinnikov Institute of Bioorganic Chemistry RAS, Moscow, Russia*

³ *Department of Clinical and Movement Neurosciences, UCL Institute of Neurology, London, UK*

⁴ *Institute of Cell Biophysics (RAS), Pushchino, Russia*

E-mail: aneskaminina@mail.ru

Receptor for advanced glycation end products (RAGE) is expressed in many cells of the body and involved in Alzheimer's disease. RAGE is associated with the beta-amyloid induced cell death. Previously we have revealed one synthetic peptide corresponding to the amino acid sequence (60-76) of the RAGE which was able to restore the disturbed spatial memory of olfactory bulbectomized mice developing Alzheimer type neurodegeneration, and to inhibit amyloid mediated caspase-3 activation [1,2]. Here we investigate the ability of peptide (60-76) and its analogue Ac-(60-76)-NH₂ to protect spatial memory in transgenic 5xFAD mice. We also study the effect of peptide (60-76) on calcium signal in primary culture of neurons and astrocytes.

Protective activity of the peptides was studied in 5xFAD mice. Animals were intranasally administrated with peptides (60-76) or Ac-(60-76)-NH₂ daily, for 70 days. Then the animals were trained in the Morris water maze and their memory was tested. We have revealed that both peptides protected mouse memory from impairment but the analogue had long-lasting effect.

Application of peptide (60-76) to the primary culture of neurons and astrocytes derived from hippocampus and cortex of rat brain induced peak-like oscillations of calcium in the cells. We found that the presence of FPS-ZM1, a high affinity antagonist of the RAGE, which binds with the V-domain of the receptor, abolished the Ca²⁺ signal in response to the RAGE peptide (60-76).

Thus, both RAGE peptides – (60-76) and its analogue, protect memory of transgenic 5xFAD mice, but the analogue has long-lasting effect. The possible mechanism of the neuroprotective properties of the RAGE peptide involves activation of RAGE leading to calcium signaling. Peptide synthesis and processing of the data were performed with support of RSF grant 20-64-46027. The experiments on animals and cell culture were supported by RFBR grants 19-015-00064 and 20-015-00526.

[1] O.M. Volpina, et al. (2018). Synthetic Fragment of Receptor for Advanced Glycation End Products Prevents Memory Loss and Protects Brain Neurons in Olfactory Bulbectomized Mice. *J. Alzheimers Dis.* 61, 1061–1076.

[2] D.O. Korojev, et al. (2019). A Synthetic Fragment of the Receptor for Glycation End Products and Its Analogue Improve Memory in Transgenic Alzheimer's Disease Mouse Model, *Russian Journal of Bioorganic Chemistry* 45(5), 361-365.

STUDY OF SURFACTANT-POLYMER COMPLEXES STRUCTURE BY SMALL-ANGLE NEUTRON SCATTERING

O.P. Artykulnyi^{1,2}, M.V. Avdeev¹, V.I. Petrenko¹, O.I. Ivankov¹, L.A. Bulavin²

¹Joint Institute for Nuclear Research, Dubna, Moscow Region, Russian Federation

²Taras Shevchenko National University of Kyiv, Kyiv, Ukraine

E-mail: artykulnyi@jinr.ru

The unique behavior of surfactant-polymer interaction driven by self-assembly phenomena gives great variability of possible structures and plentiful phase diagrams that allows manipulating with surfaces and interfaces of nano-scale colloidal systems [1]. In this way, the magnetic nanoparticles initially stabilized by double layer of anionic surfactant such as sodium oleate (SO), dodecylbenzene sulfonate acid (DBSA), can be modified by physicochemical adsorption of poly(ethylene glycol) (PEG) polymer chain in order to create protein-resistive shell that significantly increases the average circulation time of particles in bloodstream.

The influence of PEG addition on the DBSA surfactant micellar systems was studied for the PEG concentration range of 0.5 – 11 vol. % by small-angle neutron scattering (SANS). The experimental curves were analyzed by least squares approximation procedure using the scattering intensity model $I(q)$ of charged ellipsoids (fig.1 left) [2]. The structure of the anionic surfactant DBSA – neutral polymer PEG complexes was studied for a wide range of polymer molecular masses from 1 to 100 kDa (fig 1. right) [3]. The multi-micellar structure formation starts above critical aggregation concentration of surfactant with enough large polymer molecule, at least of 20 kDa, that was found by SANS for weakly concentrated solutions of 0.2 vol. % DBSA with the low concentration of PEG of 0.04 vol. %.

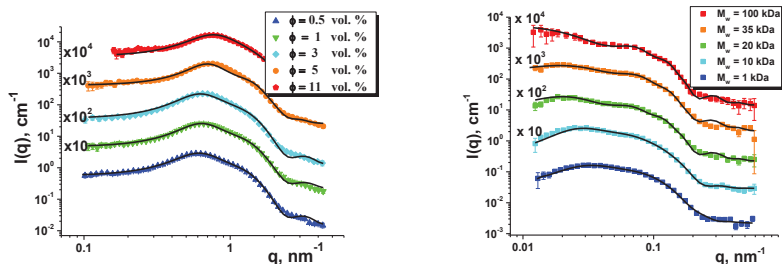


Fig. 1 Experimental SANS curves from mixed DBSA – PEG solutions: with constant DBSA concentration of 3 vol. % and various concentrations of PEG, $M_w = 20$ kDa, (left); with constant concentrations of DBSA (0.2 vol. %) and PEG (0.04 vol. %) and various molecular masses of PEG (right)

[1] B. Kronberg, K. Holmberg, B. Lindman, Surface Chemistry of Surfactants and Polymers, Wiley, 2014.

[2] O.P. Artykulnyi, V.I. Petrenko, L.A. Bulavin, et al. (2019). Impact of poly (ethylene glycol) on the structure and interaction parameters of aqueous micellar solutions of anionic surfactants. J. Mol. Liq. 276, 806-811

[3] O.P. Artykulnyi, A.V. Shibaev, M.M. Avdeev, et al. (2020). Structural investigation of poly(ethylene glycol)-dodecylbenzenesulfonic acid complexes in aqueous solutions. *J. Mol. Liq.* 308, 113045

STRUCTURE OF DIFFUSIVE POLYMER MEMBRANES FOR MOLECULAR AND IONIC TRANSPORT

V.T.Lebedev¹, Yu. V.Kulvelis¹, G. A. Polotskaya², L.V.Vinogradova²,
A.Ya. Vul³, O.N.Primachenko², A.S.Odinokov²

¹*Petersburg Nuclear Physics Institute named by B.P. Konstantinov of NRC "Kurchatov Institute", Gatchina, Leningrad distr., Russia*

²*Institute of Macromolecular Compounds of RAS, St.Petersburg, Russia*

³*Ioffe Institute, St.Petersburg, Russia*

E-mail: lebedev_vt@npi.nrcki.ru

Review of structural studies of diffusive polymer membranes for pervaporation processes and proton transport has been presented. Features of supramolecular ordering and diffusive channels formation were determined in membranes based on polyphenylene oxide matrix with embedded star-shaped macromolecules C₆₀PS₆PVPD₆ (concentration range C = 0 - 5 wt. %) having polystyrene and poly-2-vinylpyridine arms grafted to fullerene center [1]. In basic matrix these slightly segregating macromolecules create the aggregates with tiny regions of free volume joint into the channels providing selective molecular diffusion. For a series of membranes with different content of modifier we determined the structural parameters diffusive channels, their volume fraction in dry and swollen membranes saturated by deuterated methanol for higher channels contrast against polymer matrix. As compared to pervaporation membranes other type of diffusive membranes for proton conductivity was based on perfluorinated copolymers possessing ordered systems of fine channels for water and proton diffusion [2]. In these membranes three structural levels of molecular organization were detected by neutron scattering. At the first level the ionic groups SO₃H attached to side chains of macromolecules are gathered into primary clusters covering the inner surface of diffusive channels. They are grouped into bunches at the second structural level where each channel is coordinated with neighboring ones separated by hydrophobic polymer regions. The third level is attributed to the package of polymer domains and channels' bunches. To improve a conductivity and thermal stability of perfluorinated membranes, we modified them by detonation diamonds (4-5 nm in size) with the surface covered by hydrophilic groups (H, OH, COOH) for better integration into the system of conducting channels and higher protons accumulation on the interfaces with polymer. Neutron scattering experiments allowed comprehend a key role of diamonds making material more strength and stimulating proton conductivity in even at low content (0.25 % et.). Neutron studies confirmed and supplemented by the data of atomic force and electron microscopy promote a development of scientific basement of membrane technologies.

The work was supported by Russian Fund for Basic Researches (grant No 19-03-00249a).

[1] G. Polotskaya, A. Pulyalina, V. Lebedev, Gy. Török, D. Rudakova, L. Vinogradova (2020). Novel view at hybrid membranes containing star macromolecules using neutron scattering and pervaporation dehydration of acetic acid. *Materials and Design*, 186,108352 (1-10).

[2] V. T. Lebedev, Yu. V. Kulvelis, S. S. Ivanchev, A. Ya. Vul, A. I. Kuklin, O. N. Primachenko, A. S. Odinokov (2020). Neutron studies of the structure and dynamics of molecular and polymer self-assembled systems. *Physica Scripta*. 95, 4, 044008.

SMALL-ANGLE NEUTRON SCATTERING STUDY OF POLYMER-CONTAINING (HYBRID) WORMLIKE MICELLES OF IONIC SURFACTANT

A.L. Kwiatkowski¹, V.S. Molchanov¹, A.I. Kuklin² and O.E. Philippova¹

¹*Physics Department of Lomonosov Moscow State University, Moscow, Russia*

²*Joint Institute for Nuclear Research, Dubna, Russia*

E-mail: kvyatkovskij@physics.msu.ru

Wormlike micelles (WLMs) are long flexible aggregates, formed by amphiphilic molecules of the surfactants in aqueous solutions. WLMs consist of central cylindrical part and two hemispheric end-caps. Their length amounts to several microns. Physical networks of entangled WLMs are applied in oil industry, self-care products, cosmetics, etc.

Recently, incorporation of macromolecules of polymer have become widely used by scientists for modification of WLMs of surfactants. Since small-angle neutron scattering (SANS) is an effective experimental technique to obtain the information both about the form and structure of WLMs and conformation and properties of polymer chains, it can be applied to study the polymer-containing (hybrid) WLMs.

Current research was aimed at the SANS study of the form and structure of the hybrid WLMs of anionic surfactant potassium oleate in the presence of potassium chloride embedded with hydrophobic polymer poly(4-vinylpyridine) (P4VP). Contrast variation technique was used to receive scattering curves separately from the WLMs of potassium oleate and from the polymer in the hybrid WLMs. Experiments were carried out with a two-detector system at the YuMO instrument of the high-flux pulsed reactor IBR-2M at the Frank Laboratory of Neutron Physics (Joint Institute for Nuclear Research, Dubna, Russia).

In case of matching the scattering from P4VP such parameters of micelles as radius of gyration R_g and mass of the surfactant per unit length of micelle M_L were attained from the dependence of $\ln(IQ)$ on Q^2 . In case of matching the scattering from molecules of potassium oleate the conformation of macromolecules of P4VP and its persistence length l_p inside the hybrid WLMs were obtained from the scattering curves $I(Q)$ and Kratky IQ^2 on Q , respectively.

According to SANS data incorporation of P4VP by WLMs does not influence nor its' cylindric form nor the value of radius R_g , which remains close to the value of the length of hydrophobic tail of the molecule of potassium oleate. However, injection of P4VP provides the sufficient increase of its persistence length l_p , due to the reduction of the volume, occupied by polymer chain inside the WLMs. P4VP inside the WLMs was shown to be in Gaussian coil conformation.

Acknowledgement: current study was supported by Russian Science Foundation (project № 19-73-20133)

COTTON TEXTILE/IRON OXIDE NANOZYME COMPOSITES WITH PEROXIDASE-LIKE ACTIVITY: PREPARATION AND SANS/SAXS CHARACTERIZATION

I. Safarik^{1,2,3}, J. Prochazkova¹, M. Schroer⁴, V.M. Garamus⁵, P. Kopcansky³, M. Timko³, M. Molcan³, M. Rajnak³, O.I. Ivankov⁶, M.V. Avdeev⁶, V.I. Petrenko⁶ and K. Pospiskova²

¹Biology Centre, Ceske Budejovice, Czech Republic

²Palacky University, Olomouc, Czech Republic

³Institute of Experimental Physics, Kosice, Slovakia

⁴European Molecular Biology Laboratory (EMBL). Hamburg Outstation c/o DESY, Hamburg, Germany

⁵Helmholtz-Zentrum Geesthacht, Geesthacht, Germany

⁶Joint Institute for Nuclear Research, Dubna, Moscow region, Russia

E-mail: ivosaf@yahoo.com

Magnetic iron oxide nano- and microparticles have a great potential in biochemical, biomedical, clinical, biotechnology and environmental applications owing to their many unique properties. These biocompatible nanoparticles exhibit several types of responses to external magnetic fields. In addition, in the year 2007 the new property of magnetic iron oxide nanoparticles (MNPs) was described, namely the presence of intrinsic peroxidase-like activity similar to horseradish peroxidase; this was the first time an inorganic nanoparticle was considered as an enzyme mimetic for potential biomedical applications. The term “nanozyme” was introduced to define nanomaterials with intrinsic enzyme-like activities [1].

Immobilization of (bio)catalysts to an appropriate solid carrier enables their simple separation from the reaction mixture and repeated application. There are many different methods used for (bio)catalyst immobilization, but usually simple and cost-effective methods are preferred. The most used methods are based on physical immobilization (adsorption or physical entrapment) and chemical immobilization (covalent binding and cross linking) [2]. Textile materials represent low-cost carriers applicable for immobilization of wide variety of molecules [3] or particles [4].

Two procedures for the immobilization of iron oxide nanoparticles on cotton textile (2x2 cm) were selected, namely (i) direct application of a mixture of perchloric acid stabilized magnetic fluid and methanol, followed by drying, and (ii) microwave assisted conversion of ferrous sulfate (dried on the textile surface) at 0.01 M NaOH solution. The visual appearance and scanning electron microscopy pictures of the iron oxide nanoparticles modified cotton textile are presented in Figure 1.

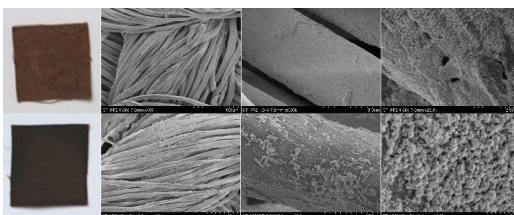


Fig. 1. The visual appearance and scanning electron microscopy pictures of acid magnetic fluid modified cotton textile (2x2 cm, 100 μ L applied, concentration 10 mg/mL; top line) and ferrous sulfate modified textile treated by microwave irradiation (2x2 cm, 100 μ L applied, 20 % FeSO₄·7H₂O solution used; bottom line).

To get structural information and organization at nanoscale averaged from the whole sample volume, cotton textile and cotton textile with MNPs were measured by SANS and SAXS. It is clearly seen different behavior of the experimental SANS curves (Figure 2) for various samples and thus it can be concluded that addition of nanoparticles to textile changes the structural organization at nanoscale. At SANS curves we can see two power laws regions which points out that there are two kinds of scattering objects in the samples. At intermediate q -region power-law behavior of scattering intensity close to -1 corresponds well to cylinder-like objects. In small q -region power exponent is -2.7 or -3.4 depending of the sample. It means that we have transition from mass fractal like organization (Sample 2 and 3) to the surface fractal (Sample 5, 6 and 7). Sample 5 is a precursor of Sample 2, while Samples 6 and 7 represent alternative way of microwave assisted cotton textile modification.

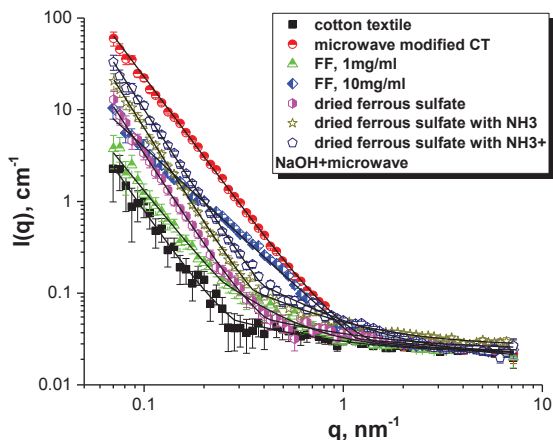


Fig. 2. SANS data for native cotton textile and cotton textile with MNPs.

SANS and SAXS data give us similar and complemented results about structural organization of nanotextile and nanoparticles. Sketch of the different behavior of MNPs was proposed according to the detailed analysis of small-angle scattering curves.

Immobilized iron oxide nanoparticles exhibited peroxidase-like activity using standard peroxidase substrates. Natural enzymes peroxidases have been efficiently used for the decolorization of wide variety of organic dyes. Peroxidase-like activity of textile bound iron oxides also enabled decolorization of selected organic dyes such as crystal violet.

- [1] L.Z. Gao et al. (2017). Iron oxide nanozyme: A multifunctional enzyme mimetic for biomedical applications. *Theranostics* 7, 3207-3227.
- [2] A. Basso, S. Serban (2019). Industrial applications of immobilized enzymes - A review. *Molec. Catal.* 479, 35-54.
- [3] I. Safarik et al. (2018). Magnetically responsive textile for a new preconcentration procedure: Magnetic textile solid phase extraction. *J. Ind. Text.* 48, 761-771.
- [4] E. Baldikova et al. (2018). Non-woven fabric supported manganese dioxide microparticles as a low-cost, easily recoverable catalyst for hydrogen peroxide decomposition. *Mater. Chem. Phys.* 203, 280-283.

CALAMITIC LIQUID CRYSTAL UNDER NANOMETER SPATIAL CONFINEMENT – INVESTIGATION BY SANS AND COMPLEMENTARY METHODS

E. Juszyńska-Gałazka¹, W. Zajac¹

¹*Institute of Nuclear Physics, Polish Academy of Sciences, Kraków, Poland*

E-mail: wojciech.zajac@ifj.edu.pl

The intermolecular arrangement of a liquid crystal (LC) confined in a mesoporous matrix is governed by entropic and energetic effects. The former encompasses ordering phenomena or the contrary: disordering effects, both resulting from spatial conditions. If spatial confinement is tight enough, the final effect might sometimes be treated in terms of negative pressure, although *sensu stricto*, there is no negative pressure under such conditions. The latter include the interactions between soft matter molecules and the pore walls. Much can be learned indirectly from measuring e.g. relaxation dynamics (cf. e.g. [1]).

It is therefore tempting to use a more direct experimental method of studying short-range order of LC molecules under geometric confinement. Small angle neutron scattering (SANS) is an obvious choice here, as it probes fluctuations of scattering length density (SLD), and

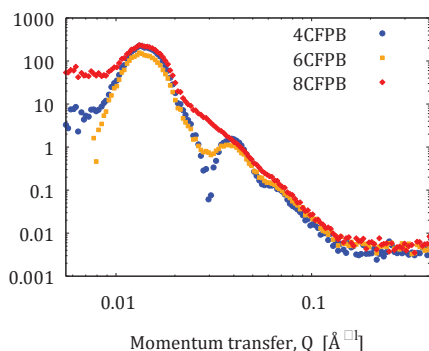


Fig. 1 SANS patterns of three homologues confined in SiO₂ nanoporous (18 nm) membranes.

thus can be sensitive to the variation of SLD with increasing distance from the cavity walls, as well as that resulting from maxima of spatial correlation function [2]. Other small angle scattering methods can also be mentioned in this context, such as SAXS (this work) or grazing incidence angle X-ray scattering [3].

Fig. 1 illustrates recently measured SANS patterns of three homologues with scattering from membrane subtracted. SANS from the same compounds contained within bigger

pores was also measured. The results will be discussed in more detail and compared with SAXS patterns.

[1] T. Rozwadowski. *The influence of pressure on dynamics and polymorphism of 4-cyano-3-fluorophenyl 4-butylbenzoate*, PhD thesis, IFJ PAN, Kraków, 2016 (in Polish), and references therein.

[2] Y.B. Melnichenko, *Small-Angle Scattering from Confined and Interfacial Fluids*, Springer (2016), ISBN 978-3-319-01103-5.

[3] S.H. Ryu, H. Ahn, T. J. Shinc and D. K. Yoona, *Liquid Crystals* **44** 4 713-721 (2017).

VIBRATIONAL DYNAMICS OF MOLECULES PHENYL SUBSTANCES WITH VARYING DEGREES OF MOLECULAR ORDERING

E. Juszyńska-Gałazka¹, W.M. Zając¹, M. Jasiurkowska-Delaporte¹ and D.M.Chudoba^{2,3,4}

¹*Institute of Nuclear Physics, Polish Academy of Sciences, PL-31342 Krakow, Poland*

²*Frank Lab Neutron Phys, Joint Inst Nucl Res, Dubna, Russia*

³*Univ Adam Mickiewicz, Fac Phys, Poznan, Poland*

⁴*St Petersburg State Univ, Fac Phys, St Petersburg, Russia*

E-mail: Ewa.Juszyńska-Gałazka@ifj.edu.pl

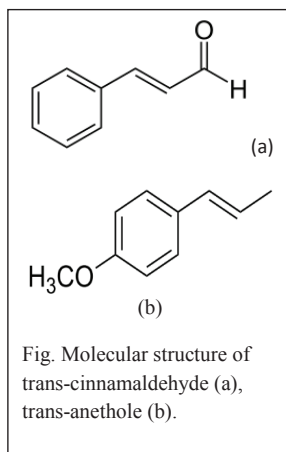
Polar compounds (phenyl alcohols, phenols) tend to form glassy states, the properties of which depend on a cooling rate of supercooled thermodynamic phases. The structure of molecules, inter alia, through the presence or absence of specific atomic groups, or the position of such groups with respect to the molecular skeleton [1], significantly influences the type of thermodynamic phases formed. The latter will often be partially disordered with respect to translational and/or rotational degrees of freedom, thus capable of undergoing glass transitions.

The aim of our research is to determine the physicochemical properties of organic compounds with a single phenyl ring (Fig.), present in various plants.

Such compounds are also of much interest to the food, pharmaceutical or cosmetic industries, what stimulates their studies by complementary methods. In particular, amorphous forms are usually more biocompatible than crystal phases. Along this line, we embarked on the investigation of polymorphism and dynamics in various thermodynamic states that occur in these substances.

Results of calorimetric and spectroscopic studies (spectroscopy: broadband dielectric, infrared absorption and neutron spectroscopy, i.e., inelastic neutron scattering) [2,3] for this type of compounds will be presented. The results of our research will be compared with the literature data for similar molecular systems.

Through Inelastic Neutron Scattering we establish vibrational dynamic of proton group and the nature of hydrogen bond. Moreover, density of states $G(\nu)$, observed in a glass of liquid or plastic crystal phase (Debye vs. non-Debye $G(\nu)$ at small energy transfer and at helium temperature) will give information on the kind of glassy states. A combination of infrared and inelastic neutron scattering spectroscopies with the density functional theory and semi-empirical calculations was applied to propose an assignment of the vibrational spectra of trans-cinnamaldehyde and trans-anethole.



[1] E. Juszyńska, M. Massalska-Arodź, I. Natkaniec, J. Krawczyk, *Physica B* 403 (2008) 109-114.

[2] E. Juszyńska-Gałazka, P.M. Zieliński, M. Massalska-Arodź, J. Krawczyk, *Acta Phys. Pol. A* 124 (2013) 917-925.

[3] E. Juszyńska-Gałazka, W. Zając, Y. Yamamura, K. Saito, N. Juruś, *Phase Transit.*, 91 (2018) 170-185.

NEUTRON TOMOGRAPHY OF ANISOTROPIC ROCKS: ASSESSMENT OF STRUCTURAL, MAGNETIC AND SEISMIC ANISOTROPY

I.Yu. Zel¹, M. Petruzalek², T.I. Ivankina¹, T. Lokajicek², S. E. Kichanov¹, D. P. Kozlenko¹

¹ *Frank Laboratory of Neutron Physics, Joint Institute for Nuclear Research, 141980 Dubna, Russia*

² *Institute of Geology AS CR v.v.i., 165 00 Prague, Czech Republic*

E-mail: ivangreat2009@gmail.com

Physical properties of rock are found to be anisotropic far more often than isotropic. The fundamental difference between anisotropy and isotropy may have a crucial impact to the interpretation of geophysical data and hence should be accounted for. Rock anisotropy itself is structurally dependent and reveals even when constituent phases are isotropic. The sign of anisotropy is usually present as lineation or foliation fabrics that can be visually distinguished. Based on such observations the assumption on anisotropic character of rock properties is often justified.

Generally, anisotropic properties of rock can be controlled by various factors, which can be classified in to two groups of fabrics: crystallographic texture (or lattice preferred orientations, LPOs) and shape texture (spatial alignment of constituents and their grain-scale morphology). The former is successfully studied by diffraction methods, while the later one is still considered in a form of approximations or models.

In our work we present the new methodology for quantitative analysis of anisotropic rock structure using neutron tomography. Two anisotropic rocks, namely biotite gneisses, were tested. The presence of mica minerals provided the contrast on tomographic images due to the large difference in neutron attenuation lengths between mineral components. The virtual 3D model was obtained, from which the distribution of mica minerals within the bulk rock samples was calculated. The novel approach proposed for morphological and spatial analysis reveals the orientation of foliation and lineation, providing also their quantitative measure in terms of shape orientation distribution function, and is shown to be an effective method for description of rock fabrics. The comparison of the obtained results with the pole figures of mica grains (LPOs), magnetic and seismic anisotropy measurements evidenced the direct correlation. The theoretical modeling has shown the high potential of neutron tomography for analyzing the internal structure of anisotropic rock samples and prediction of magnetic and seismic anisotropy.

CRYSTALLOGRAPHIC TEXTURE OF FRESH WATER BIVALVE MOLLUSCS OF THE FAMILY UNIONIDAE

A.V. Pakhnevich^{1,2}, D.I. Nikolaev², T.A. Lychagina²,
M. Balasoiu², I. Orhan³

¹*Borissiak Paleontological Institute of RAS, Moscow, Russia*

²*Joint Institute for Nuclear Research, Dubna, Russia*

³*“Danube Delta” National Institute for Research and Development, Tulcea, Romania*

E-mail: alvpb@mail.ru

Bivalve mollusks of the Family Unionidae are widespread in the fresh waters of Eurasia. Their important role is associated with the natural biofilter of fresh waters. *Unio pictorum* filters up to 550 ml/h, and *Anodonta cygnea* up to 400 ml/h of fresh water [1].

The purpose of our study is to determine the features of the shell crystallographic texture of few representatives of Family Unionidae bivalve mollusks, and to trace the texture changes under different salinity and temperature habitat conditions.

In the present work the shells of the bivalve mollusks *Unio pictorum*, *Anodonta cygnea* collected in the Danube Delta near city Tulcea (Romania) and the shells *Unio pictorum* from the coast of the Gulf of Finland, Baltic Sea in the city St. Petersburg (Peterhof) (Russia) have been used. The measurements were carried out at the FLNP JINR on the SKAT facility in 2019 year. The main pole figures of the crystallographic direction (012) + (121) of aragonite were compared for all above mentioned samples.

The two places where the shells were collected differ in their habitat conditions. Despite the fact that they are located in the temperate climate zone [2], the average annual air temperature in Tulcea is higher than in St. Petersburg. The salinity of fresh water does not exceed 0.5 ‰ [3], whereas it reaches 2 ‰ in the Gulf of Finland [4].

Despite this, the crystallographic texture of aragonite in the shells of *Unio pictorum* was found to be similar. The isolines on the pole figures are elongated in the horizontal direction, repeating the shape of the mollusk valves. The crystallographic texture sharpness of the shells from the Danube delta is 4.17 mrd, while for those from the Gulf of Finland is 3.76 mrd.

The pole figure of the shells of *Anodonta cygnea* has a different shape: it is less elongated and more rounded. The texture sharpness of this mollusk valves is 5.07 mrd. This value is the highest sharpness of the aragonite texture, while for the aragonite nacreous layer of sea mollusks *Mytilus galloprovincialis* it varies within 2.48 –3.05 mrd, in *Mytilus trossulus* is 2.46 mrd, *Mytilus edulis* is 3.36 mrd, and in the fully aragonite shell *Mya arenaria* is 2.63 [5]. The distribution of aragonite crystals in all cases repeats the shape of the studied valves. The pole figures of *Mya arenaria* are very similar to those of *Unio pictorum* but differ in the sharpness.

Thus, it is obtained that the aragonite pole figures of the *Unio pictorum* shells, living at different temperatures and salinity, are very similar in shape, but differ in the sharpness. The sharpest aragonite texture has been revealed for *Anodonta cygnea*.

[1] G.P. Alekhina, I.A. Misetov (2013). Characteristics of filtration capacity of freshwater bivalve molluscs of the Family Unionidae middle reaches of the Ural river. Bulletin of OSU. 10 (159), 34-36.

[2] Physico-geographical atlas of the world (1964), Moscow: Academy of Sciences of the USSR and the Main Directorate of Geodesy and Cartography of the State Geological Committee of the USSR.

- [3] I.I. Dedyu (1989). Ecological encyclopedic dictionary, Chisinau: Ch. ed. Mold. Soviet. Encyclopedia.
- [4] A.D. Dobrovolsky, B.S. Zalagin (1982). Seas of the USSR, Moscow: MSU Publishing House.
- [5] D. Nikolaev, T. Lychagina, A. Pakhnevich (2019). Experimental neutron pole figures of minerals composing the bivalve mollusc shells. Springer Nature Appl. Sci. 1. 344.

NEUTRON DIFFRACTION AND NEUTRON COMPUTED TOMOGRAPHY INVESTIGATION OF SCLERACTINIAN CORALS SKELETON

T.I. Ivankina¹, S.E. Kichanov¹, O.G. Dului^{1,2}, S.Y. Abdo³, M.M. Sherif³

¹Joint Institute for Nuclear Research, Dubna, Russian Federation

²University of Bucharest, Faculty of Physics, Magurele (Ilfov), Romania

³Cairo University, Faculty of Sciences, Giza, Egypt

E-mail: o.dului@upcmail.ro

Two extend the amount of knowledge concerning the architecture and mineral composition of stony (scleractinian) corals, two experimental methods based on the peculiarity of neutron interaction, *i.e.* Neutron Diffraction (ND) and Neutron Computed Tomography (NCT) were used to investigate the skeleton of *Dipastraea pallida* (Dana 1846), an actual hermatypic coral.

The *D. Pallida* coral was chosen due to its almost spherical shape with a diameter of about 14 cm and a uniform distribution on the colony surface of individual polyps. The investigated specimen was manually collected southern of Al Saleef port of Yemen Republic at depth between 5 and 10 m.

ND was used to reconstruct the Orientation Distribution Function (ODF) of the crystalline fibrils which compose coral skeleton as well as to determine its mineralogical composition. All measurements were performed at the SKAT time-of-flight (TOF) neutron diffractometer[1] at the Frank Laboratory of Neutron Physics (FLNPF) pulsed IBR-2 nuclear reactor. The SKAT TOF diffractometer permits the use of Rietveld texture analysis (RTA) for texture evaluation as well as more accurate separation of overlapping pole figures (PF)[2].

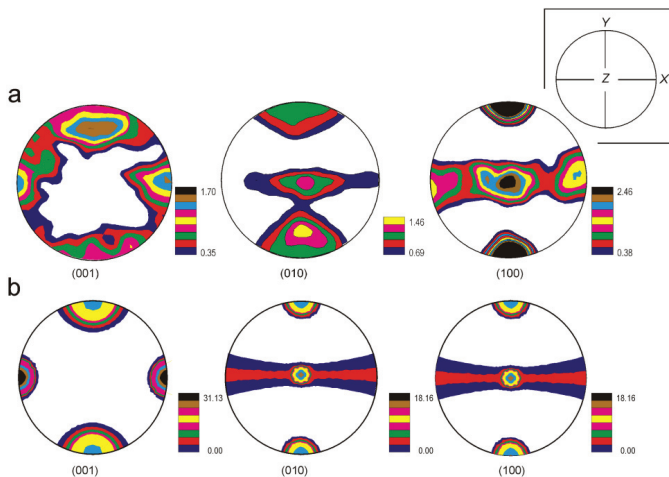


Figure 1 Experimental (a) and simulated (b) PF of *D. pallida* skeleton. The inset illustrates the XYZ coordinate system.

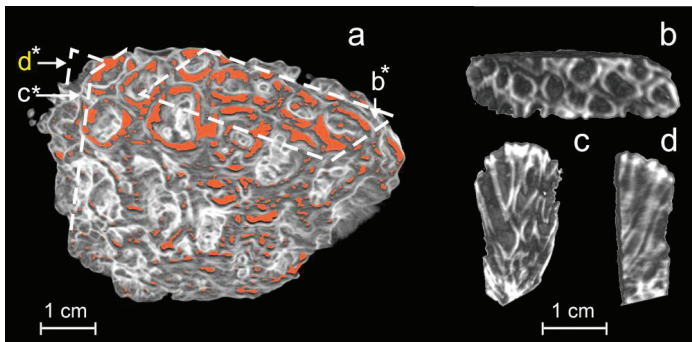


Figure 2 The 3D NCT images of the superior part of the coral slab (a), as well as a transverse (b) and two vertical slices (c) and (d) showing with clarity the reciprocal disposition of polyps cups (calyx). The slices (c) and (d) illustrate the vertical disposition of calyx walls as well as the annual growth sections which appear darker hues. The presence of organic rich matter is evidenced in orange color..

By analyzing 684 ND spectra using the Rietveld method it was possible to prove that the aragonite represents the sole mineral component of coral skeleton. At the same time, this procedure permitted to recalculate the ODF of aragonite fibrils and to represent them by means of (100), (010) and (001) crystallographic planes PF.

Thus recalculated PF showed a remarkable similarity with the simulated ones by considering that aragonite fibrils, which compose coral skeleton, are oriented either along the growth axis of polyp cups or perpendicular to this direction (Fig. 1). This result was in good agreement with the previous observations based on optical microscopy, proving at the same time the availability of ND for such type of investigations [3].

NCT investigations were performed at the FLNP Neutron Radiography and Tomography Facility placed on the 14th neutron beam-line of the IBR-2 reactor with a 150 mm diameter and a $5.5 \cdot 10^6$ neutrons/cm²s flux density. The distance between aperture and neutron detector was of 10 m with a L/D parameter of 200.

NCT determinations permitted evidencing the individual polyp cups, and their interlocked 3D rigid porous structure. At the same time, it was possible to attest the presence of a periodic variation of skeleton density which could be attributed to a seasonal influence of marine environment. The existence of small amount of organic matter were also confirmed (Fig. 3) [4].

[1] K. Ullemeyer, et al. (1998) The SKAT texture diffractometer at the pulsed reactor IBR-2 at Dubna: experimental layout and first measurements, Nucl Instr Meth Phys Res A 412, 80-88.

[2] R. Keppler, et al. (2014) Potential of full pattern fit methods for the texture analysis of geological materials: implications from texture measurements at the recently upgraded neutron time-of-flight diffractometer SKAT, J Appl Cryst 47, 1520-1534.

[3] D.J. Barnes, D.J., and J.M. Lough (1993) On the nature and causes of density banding in massive oral skeletons. J Exp Mar Biol Ecol 167, 91-108.

[4] T.I. Ivankina et al. (2020) The structure of scleractinian coral skeleton analyzed by neutron diffraction and neutron computed tomography, Sci. Rep. 10, Article number: 12869.

DEFORMATION MECHANISMS AND MICROSTRESS EVOLUTION IN POLYCRYSTALLINE MATERIALS STUDIED USING DIFFRACTION AND MODELLING

A. Baczmanski¹, P. Kot¹, S. Wroński¹, M. Wroński¹, E. Gadalińska², M. Wróbel³, Ch. Scheffzuek^{4,5} and G. Bokuchava⁴

¹*AGH University of Science and Technology, Faculty of Physics and Applied Computer Science, al. Mickiewicza 30, 30-059 Krakow, Poland*

²*Institute of Aviation, Materials & Structures Research Center, al. Krakowska 110/114, 02-256 Warszawa, Poland*

³*AGH University of Science and Technology, Faculty of Metals Engineering and Industrial Computer Science, al. Mickiewicza 30, 30-059 Krakow, Poland*

⁴*Frank Laboratory of Neutron Physics, Joint Institute for Nuclear Research, Joliot-Curie 6, 141980 Dubna, Russia*

⁵*Institute of Applied Geosciences, Karlsruhe Institute of Technology, Adenauerring 20b, 76131 Karlsruhe, Germany*

E-mail: Andrzej.Baczmanski@fis.agh.edu.pl

Diffraction methods for lattice strain measurement provide useful information concerning the nature of grains behaviour during elastoplastic deformation. The main advantage of the diffraction methods is the possibility of studying mechanical properties of polycrystalline materials separately in each phase and for groups of grains with a specific orientation. In this work a complete study of the mechanical behaviour of the Al/SiCp composite, pearlitic steel and duplex steel was performed using neutron and synchrotron diffraction, as well as elastic-plastic self-consistent model [1,2,3].

The neutron diffraction study of elastic-plastic deformation was carried out at the TOF (time of flight) diffractometers: FSD and EPSILON in JINR (Dubna, Russia) [1]. An unique advantage of the EPSILON diffractometer is possibility of measurements using nine detector banks determining interplanar spacings simultaneously for 9 different orientations of the scattering vector. The diffraction measurements of lattice strains were performed in situ during compression and tensile tests. The performed analysis of experimental data allowed us to study the evolution of stress tensor and its decomposition into deviatoric and hydrostatic components in both phases of the composite. It was found that the novel Developed Thermo-Mechanical Self-Consistent model correctly predicted stress variation during compressive loading, taking into account the relaxation of thermal origin hydrostatic stresses. The comparisons of model results with experimental data (at the macroscopic level and the level of phases) showed that strengthening of the Al/SiCp composite was caused mostly by stress transfer from the plastically deformed Al2124 matrix to the elastic SiCp reinforcement. It was also found that the thermal stresses relaxed during plastic deformation, but this type of stresses did not significantly affect the overall composite properties.

Synchrotron X-ray diffraction (ESRF, Grenoble, France) was applied to study the evolution of lattice strain and stresses in both phases of pearlitic steel during a tensile test [2]. The advantage of the methodology used in this work is the possibility of experimental study of stress localization. The phase stresses were directly determined from measurements and the experimental results were used to study the process of strain strengthening in lamellar pearlite. It was found that in the elastic range of deformation, both cementite and ferrite are loaded similarly due to the nearly equal elastic properties of both phases, while plastic deformation leads to significant load transfer from ferrite to cementite. The synchrotron

experiment allowed us to determine the critical resolved shear stresses of ferrite phase in the pearlitic steel subjected to different thermal treatments. The role of cementite in material strengthening was evaluated on the basis of von Mises stress evolution, experimentally determined in both phases. It was found that during plastic deformations, the von Mises stress does not change significantly in ferrite compared to an important increase in elastically deformed cementite. Therefore, the partitioning of stresses between phases is mainly responsible for the strain strengthening of the tested pearlitic steel, exhibiting fully lamellar microstructure.

The synchrotron radiation (ESRF, Grenoble, France) was also used to investigate micromechanical behaviour of grains in a duplex steel, which consists of two phases (austenite and ferrite) exhibiting significantly different mechanical properties [3]. The stresses in both phases were experimentally determined in the elastic and plastic range of deformation using synchrotron diffraction. The used methodology enabled to determine the values of initial stresses and to study the evolutions of principal phase stresses and the second order stresses during elastic and plastic deformation. With help of the self-consistent model, the critical resolved shear stresses and the work hardening parameters for slip systems, active in each phase, were also estimated. Comparison of the measured phase stresses and lattice strains evolutions with model results showed a good agreement between prediction and experiment. In calculations the initial stress state in the sample and shape of grains approximated by ellipsoidal inclusions were taken into account.

The overall outcome of the work is a direct determination of stress partitioning between the two phases in the studied polycrystalline materials during deformation. The results of diffraction experiments enabled analyses concerning von Mises, hydrostatic stresses as well as the second order stresses evolutions in both phases during tensile or compression tests. The experimental data were successfully compared with predictions of the self-consistent deformation model. As the result of analysis the critical resolved shear stresses were determined for active slip systems and the mechanisms of materials strengthening were found.

Acknowledgements.

This work was partially supported by grants from the National Science Centre, Poland (NCN) No. UMO-2017/25/B/ST8/00134 and UMO-2015/19/D/ST8/00818.

Przemysław Kot has been partly supported by the EU Project POWR.03.02.00-00-I004/16.

The neutron diffraction experiments were co-financed by the Plenipotentiary Representative of the Government of the Republic of Poland at JINR in Dubna under the Project No. 75/28/2020.

[1] P. Kot, A. Baczański, E. Gadalińska, S. Wroński, M. Wroński, M. Wróbel, G. Bokuchava, Ch. Scheffzük, K. Wierzbowski (2020). Evolution of phase stresses in Al/SiCp composite during thermal cycling and compression test studied using diffraction and self-consistent models. *Journal of Materials Science & Technology*, 36, 176–189

[2] E. Gadalińska, A. Baczański, C. Braham, G. Gonzalez, H. Sidhom, S. Wroński, T. Buslaps, K. Wierzbowski (2020). Stress localisation in lamellar cementite and ferrite during elastoplastic deformation of pearlitic steel studied using diffraction and modelling. *International Journal of Plasticity* 127, 102651

[3] A. Baczański, Y. Zhao, E. Gadalińska, L. Le Joncour, S. Wroński, C. Braham, B. Panicaud, M. François, T. Buslaps, K. Soloducha M. (2016). Elastoplastic deformation and damage process in duplex stainless steels studied using synchrotron and neutron diffractions in comparison with a self-consistent model, *International Journal of Plasticity*. 81, 102–122

NEUTRON DIFFRACTION STUDY OF RESIDUAL STRESSES AT RESEARCH REACTOR IR-8 OF NATIONAL RESEARCH CENTER “KURCHATOV INSTITUTE”

V.T. Em¹, I.D. Karpov¹ and S.A. Rylov¹

¹*National Research Center “Kurchatov Institute”, Moscow, Russian Federation*

E-mail: Em_VT@nrcki.ru; vtem9@mail.ru

Research reactor IR-8 (maximum power 8 MW) at NRC “Kurchatov Institute” has thermal neutrons flux in the reactor core $\sim 2 \cdot 10^{14}$ n·cm⁻²·c⁻¹. There are 12 horizontal channels in reactor for neutron beams. The neutron flux at the outlet of the horizontal channels is $\sim 10^{10}$ n·cm⁻²·sec⁻¹.

The diffractometer STRESS, designed to study internal stresses in various polycrystalline materials, was installed at horizontal experimental channel HEC-3 of reactor IR-8 and put into operation in 2016. Unlike most stress diffractometers the instrument uses a double-crystal monochromator. This allowed creating a compact and high luminosity instrument which is comparable in its characteristics to stress diffractometers at more powerful reactors. The double monochromator (PG002/Si220) provides neutrons with fixed wavelength $\lambda = 1.56\text{\AA}$. At scattering angle $2\theta = 90^\circ$ the resolution ($\Delta d/d$) is $\sim 3 \cdot 10^{-3}$. Maximum available path length in ferritic steel (reflection 112) for strain uncertainty 10^{-4} is 76mm ($GV = 80 \text{ mm}^3$, 1h measurement time).

The main directions of researches are study of residual stresses in thick steel welds and study of residual stresses in metallic materials and components produced by additive manufacturing. The examples of researches of through-thickness stress distribution in thick (~45mm) steel weld with double-V groove and stress distribution in steel low transition temperature (LTT) weld are reported.

The results of stress distribution study in components from various materials (titanium alloy, Inconel, stainless steel) grown by selective laser melting and direct laser metal deposition methods are reported.

INVESTIGATION OF MICROSTRESS EVOLUTION IN Mg-ALLOY USING TOF NEUTRON DIFFRACTION

P. Kot¹, A. Baczyński¹, M. Wroński¹, M. Wróbel², S. Wroński¹ and Ch. Scheffzük^{3,4},
K. Wierzbowski¹

¹AGH- University of Science and Technology, Faculty of Physics and Applied Computer Science, al. Mickiewicza 30, 30-059 Krakow, Poland

²AGH- University of Science and Technology, Faculty of Metals Engineering and Industrial Computer Science, al. Mickiewicza 30, 30-059 Krakow, Poland

³Karlsruhe Institute of Technology, Institute for Applied Geosciences, Kaiserstr. 12, 76131 Karlsruhe, Germany

⁴Frank Laboratory of Neutron Physics, JINR, 141980 Dubna, Russia

E-mail: przemyslaw.kot@fis.agh.edu.pl

The idea of this work is to develop an experimental methodology based on the so-called crystallite group method [1,2] in order to determine the evolution of the stresses localised in polycrystalline grains having different crystallographic orientations. A new methodology based on neutron diffraction experiment was applied to textured Mg alloy and the components of stress tensor were determined directly from measured lattice strains corresponding to chosen orientations of crystallite lattice. Using the experimental data the evolution of von Mises stress was calculated for selected groups of grains, showing a large difference in the hardness of crystallites having different lattice orientations.

The lattice strain evolution was measured in magnesium alloy AZ31 exhibiting basal type of texture. The neutron diffraction time of flight (TOF) method was applied during in-situ compression test along RD (rolling direction) at room temperature. Experiment was performed using EPSILON-MDS instrument (JINR, Dubna) equipped with 9 detectors measuring interplanar spacings d_{hkl} in different directions with respect to the sample. To calculate the strain evolution in twins (created during deformation) the initial values of d_{hkl} -spacings were estimated on the basis of peaks positions measured in different detectors [3].

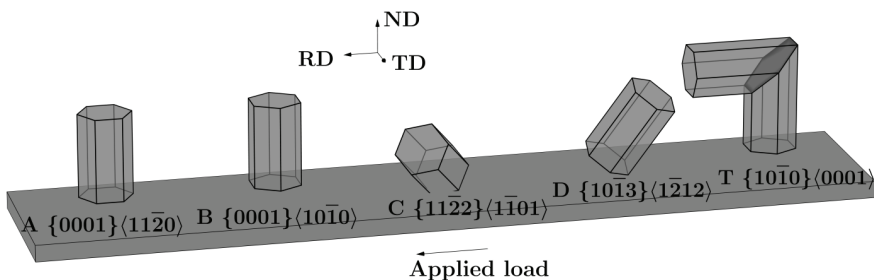


Fig 1. Selected orientations A B, C, D and T – twin. Load is applied in RD direction.

The components of stress tensor were determined directly from measured lattice strains corresponding to chosen orientations of crystallite lattice. Two main hard orientations, named A and B, were selected (Fig. 1). For these orientations the basal slip system cannot be activated because the load is applied in direction parallel to basal plane. Orientation B was completely transformed to twins (having T orientation, cf. Fig. 1) during the compression test.

In the case of the soft orientations C and D, the direction of load is inclined from the basal plane, i.e. the basal system can be activated. The 9 directions of measurements were marked on pole figure of the magnesium alloy and the poles coming from soft orientations detectors were found.

Using the experimental data the evolution of stress tensor and von Mises stress were determined for selected groups of grains. A large difference in the hardness of crystallites having different lattice orientations (Fig. 2) was found. The highest von Mises stress appeared on twins (T – orientation), which was compensated by low stresses localised on soft orientations C and D. The stress localised crystallites having A orientation is close to the macroscopic stress.

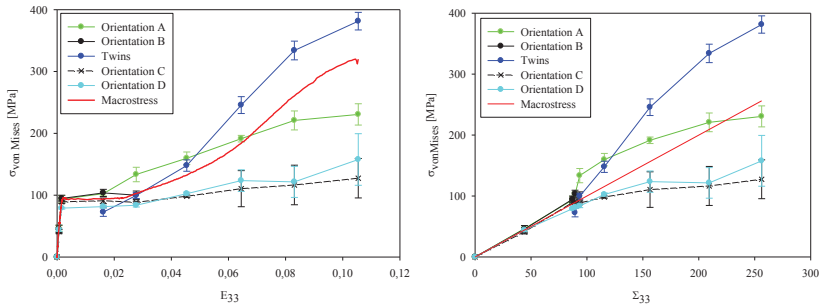


Fig. 2. Evolution of von Mises stress for different orientations presented in function of true strain (a) and true stress (b) applied to the sample. The red line corresponds to the macroscopic stress-strain curve.

Acknowledgements

This work was partially supported by grants from the National Science Centre, Poland (NCN) No. UMO-2017/25/B/ST8/00134 and UMO-2015/19/D/ST8/00818.

Przemysław Kot has been partly supported by the EU Project POWR.03.02.00-00-I004/16.

The neutron diffraction experiments were co-financed by the Plenipotentiary Representative of the Government of the Republic of Poland at JINR in Dubna under the Project No. 75/28/2020.

[1] P.F. Willemse, B.P. Naughton, C.A. Verbraak (1982). X-ray residual stress measurements on cold-drawn steel wire, *Mater. Sci. Eng.* 56 25–37.

[2] V. Hauk (1997) *Structural and Residual Stress Analysis by Nondestructive Methods*.

[3] B. Clausen (2008). Reorientation and stress relaxation due to twinning: Modeling and experimental characterization for Mg, *Acta Materialia* 56 2456-2468.

THE NEUTRON TOMOGRAPHY AND DIFFRACTION AS A ROUTINE RESEARCH METHOD FOR THE NON-FERROUS METAL ARCHAEOLOGICAL OBJECTS

I.A. Saprykina¹, S.E. Kichanov² and A.V. Rutkauskas²

¹*Institute of Archaeology RAS, Moscow, Russia*

²*Joint Institute for Nuclear Research, Dubna, Russia*

E-mail: dolmen200@mail.ru

The method of neutron tomography and diffraction at least now become the one of routine research method in process of studying the cultural heritage [1; 2; 3], especially, the archaeological objects of non-ferrous metal [4; 5]. In this report, we present the main results of studying by means the neutron tomography, radiography and diffraction of some archaeological finds from the last excavations on the territory of Krasnodarsky region and Crimea. This archaeological finds represent the antique and roman periods of the history of the Pontic and Bosphorus kingdom: it is the small silver jar from the sanctuary of Demeter, the silver Bosphoran staters from Phanagoria, the gold amulet from the burial ground of Taurian and Roman times - Frontovoe-3, and others objects.

The neutron tomography experiments were performed at the neutron radiography and tomography facility placed on beamline 14 of the IBR-2 high-flux pulsed reactor. The focus in research of these objects by means neutron tomography, radiography and diffraction was devoted to the reconstruction of theirs manufacturing schemes, defects and identification of internal cavities and their fillings. However, some of these getting results allowed to visualized not only the construction of this rare finds, but some important historical points related to the political, economic and social life in the ancient period of our history.

This research supported by the RSCF: grant № 20-18-00396 «Barbarians and Rome in South-Western Crimea: the interaction of cultures».

[1] Non-Destructive Micro Analysis of Cultural Heritage Materials. Ed. by K. Janssens and R. Van Grieken, Elsevier, Amsterdam, 2005, 828 p.

[2] Teixeira, J.; Magli, R.; Loupiac, C. Neutron Scattering and Imaging: a Tool for Archaeological Studies. *Eur. J. Mineral* 2015, 27, 289–296.

[3] Neutron Methods for Archaeology and Cultural Heritage, Eds: Nikolay Kardjilov and Giulia Festa, Springer International Publishing Switzerland 2016, 350 p.

[4] Saprykina, I.A.; Kichanov, S. E.; Kozlenko, D. P. Possibilities, Limitations, and Prospects of Using Neutron Tomography and Radiography for Preservation of Archaeological Heritage Objects. *Crystallography Reports: Pleiades Publishing, Inc.* 2019, 61(1), 177–180.

[5] Kichanov, S.; Saprykina, I.; Kozlenko, D.; Nazarov, K.; Lukin, E.; Rutkauskas, A.; Savenko, B. Studies of Ancient Russian Cultural Objects Using the Neutron Tomography Method. *Journal of Imaging* 2018, 4, 2

THE STUDY OF ANCIENT ROMANIAN POTTERY FRAGMENTS BY NON-DESTRUCTIVE TECHNIQUES AT THE IBR-2 REACTOR

B.A. Abdurakhimov^{1,2}, S.E. Kichanov¹, C. Talmatchi³, D.P. Kozlenko¹, M. Balasoiu¹, G. Talmatchi³, Marius Belc⁴

¹*Joint Institute for Nuclear Research, 141980, Dubna, Russia*

²*Institute of Nuclear Physics AS RUz, 100214, Tashkent, Uzbekistan*

³*Museum of National History and Archeology, 900745, Constanta, Romania*

⁴*Ovidius University, 900470, Constanta, Romania*

E-mail: bekhzod@jinr.ru

The complex study of fragments of ancient ceramics is the most important task of archeology and other humanities. They give us an insight into the formation of ancestral life and the development of civilization, as well as interesting historical data, including design techniques, stages in the development of trade routes, cultural and social changes, and so on. Non-destructive neutron methods provide valuable structural data such as phase composition, distribution of internal hidden components, presence of cracks and defects, and traces of corrosion propagation in ancient cultural heritage sites.

We present the results of structural studies of the bulk internal organization of several representatives of ancient pottery ceramics found on the territory of the Dobrudja region, Romania. The fragments of medieval ceramics were studied using neutron diffraction, tomography, and Raman spectroscopy. Ceramic fragments from the Museum of national history and archeology of Constanta (Romania) are obtained from archaeological excavations in the historical region of Dobrudja, which occupies the territory between the Danube and the Black sea. The studied ceramic artifacts date back to the IV-VI centuries ad of the Roman and Byzantine periods.

The high penetrating feature and the nature of the interaction of neutrons with matter allowed to non-destructive determine the crystal phase composition of the volume of the pottery fragments, as well as to clarify some structural features of those archeology items. The phase composition of the volume of fragments was tested using the DN-12 neutron diffractometer at the IBR-2 high-flux pulsed reactor (Dubna, Russia). The neutron tomography experiments were performed at the neutron radiography and tomography facility placed on beamline 14 of the IBR-2 high-flux pulsed reactor. Tomography images of investigated objects collected by the detector system based on 6LiF/ZnS scintillator screen with a high-sensitivity camera based on the Hamamatsu CCD chip. The imaging data were corrected by the camera dark current image and normalized to the image of the incident neutron beam using the ImageJ software. Raman spectroscopy experiments were performed using a LabRAM HR spectrometer (Horiba Gr, France) with a wavelength excitation of 633 nm emitted from He-Ne laser, 1800 grating, a confocal hole of 100 μm , and x50 objective.

The rather large grains of presumable silicates were found in the inner volume of the studied fragment using the neutron tomography. The size distribution of those silicate grains was obtained. A near-surface layer with a high neutron attenuation coefficient was detected. It was assumed, the formation of these layers can explain the oxidation processes during the firing of ceramics or chemical processes while preserving archaeological pottery materials.

RESEARCH OF STRUCTURE OF CEMENT MATERIALS FOR STORAGE OF RADIOACTIVE GRAPHITE BY NEUTRON TOMOGRAPHY

M.R. Kenessarin^{1,4}, S.E. Kichanov¹, I.Y. Zel¹, D.P. Kozlenko¹, M.Balasoiu^{1,2},
M.Nicu², L.Ionascu², A.C. Dragolici², F. Dragolici^{2,3}

¹*Frank Laboratory of Neutron Physics, Joint Institute for Nuclear Research, 141980 Dubna, Russia*

²*“Horia Hulubei” National Institute of Physics and Engineering, P.O.BOX MG-6, Bucharest-Magurele, Romania*

³*International Atomic Energy Agency, A-1400, Vienna, Austria*

⁴*Dubna State University, 141980 Dubna, Russia*

E-mail: muratkenessarin@gmail.com

Cement materials are key building elements in the construction of special constructions for the storage of different types of radioactive waste. These building materials are subject to fairly stringent criteria and requirements for mechanical and physico-chemical properties. In particular, to ensure structural stability for about a hundred years, cement materials must have corrosion and radionuclide resistance. This problem is especially especially for cement materials for the long-term disposal or utilization of graphite.

The experimental neutron scattering methods obtained to detailed data on phase analysis or features of the crystal structure, formation of nanoparticles and grains inside the matrix, aging, cracks and pore evolution. They are used to determine the structural characteristics of cement materials and concretes and allow us to understand the nature and origin of the mechanical and chemical properties of cement, predicting the functional properties, presenting ways to optimize the composition of new cement materials.

In this work, we studied the interior structure of some cement materials, perspective for storage of radioactive graphite by neutron tomography method.

The Experiments on neutron radiography and tomography were carried out on the installation of the NRT, on the neutron diffraction on the diffractometers of the DN-6 at the high-flux impulse reactor IBR-2.

The specifics of the interaction of neutrons with different components of the studied fragments of different cements and the use of modern mathematical algorithms for data analysis allowed to get the distribution of graphite in the volume of samples, and also determine the morphological features of graphite inclusions. Based on the conducted structural analysis, the use of the studied cements for the storage of radioactive graphite is discussed.

SYNTHESIS OF NEW MATERIALS AND INVESTIGATIONS USING RAMAN SPECTROSCOPY AND THERMAL ANALYSIS IN FLNP JINR

N.M. Belozerova¹, O.Yu. Ivanshina¹, A.A. Nabiyev¹, A. Pawlukoje¹, I. Zuba¹

¹*Joint Institute for Nuclear Research, Dubna, Russia*

E-mail: ioyu@nf.jinr.ru

Raman spectroscopy, thermogravimetric analysis (TGA) and differential scanning calorimetry (DSC) are developing along with neutron methods for condensed matter research in FLNP JINR. Horiba LabRam HR Evolution spectrometer allows obtaining high-quality Raman spectra in a wide temperature range, as well as at elevated pressure, and can be used in many applications, including characterization of carbon materials, pharmaceuticals, geology and others.

Netzsch TGA 209 F1 Libra gravimeter gives the opportunity to precise the composition of the samples, to determine the content of volatile components in them, and determine the limit of thermal stability of compounds. Recently the effects of gamma irradiation on the structural, morphological and thermal properties of high-density polyethylene with ZrO₂ nanofiller was studied in [1]. The development of polyethylene composites based on metal oxide fillers is important direction in the field of new radiation-resistant materials. The polymer nanocomposites were investigated using small-angle neutron scattering at the IBR-2, and scanning electron microscope, X-ray diffraction, infrared spectroscopy, Raman spectroscopy, DSC and TGA. By means of TGA it was shown that the degradation temperatures of the composites after irradiation were higher than in the pure polymer [1].

Differential thermal analysis is useful addition to the study of phase transformations in materials. For example, the sequence of phase transformations in the process of crystallization of the Sr₂CrMoO₆ by the solid-phase technique from a stoichiometric mixture SrCO₃ + 0.5Cr₂O₃ + MoO has been investigated in [2]. This material is interesting due its magnetic properties (ferrimagnetism with high value of Curie temperature). It was determined that the synthesis of the strontium chrome-molybdate proceeds through a series of stages. By means of the differential thermal analysis and thermogravimetric analysis data, it has been established that five clearly expressed endothermal effects were observed in the temperature range 300–1300 K. Netzsch 204 F1 Phoenix differential scanning calorimeter allows to investigate phase transformations not only during heating, but also at low temperatures (to 93K).

Along with the study of the physicochemical properties of materials, sometimes tasks of the synthesis of new materials arises. The synthesis of the studied materials directly in FLNP can significantly expand the area of our research. And we have this possibility to synthesize materials. Equipment for hydrothermal (solvothermal) synthesis appeared. The main objects of synthesis are inorganic materials, including metal-organic frameworks (MOFs). MOFs are crystalline materials consisting of an infinite network of metal-ions, or metal-ion clusters, bridged by organic ligands through coordination bonds into porous two- or three- dimensional extended structures. They are attracting increasing interest due to their unique adsorption

properties. They are perspective materials for gas storage application, magnetism, luminescence, catalysis and so on. Thermal and diffraction analysis are essential methods for studying these compounds. In addition, MOFs are crystalline substances containing organic fragments, so they are interesting objects of study by Raman spectroscopy. Another important area of use for MOFs is the adsorption of heavy metals. It is important for water purification from harmful ions (Pb^{2+} , Cd^{2+} , Hg^{2+}) and for the extraction of valuable metal ions (Ru^{3+} , Pd^{2+}) from solutions. The use of biomolecules, in particular amino acids, as building blocks for MOFs leads to biocompatibility and various modes of the metal coordination. We investigated several MOFs. Some of the materials described in the literature [3,4,5] were synthesized and studied by X-ray diffraction analysis, Raman spectroscopy, TGA and DSC. Special attention was paid to the stability of materials in an aqueous medium, as well as to the escape of solvent molecules from the pores upon heating (activation process). A new compound $\{[\text{Ni}(\text{L-trp})(\text{bpe})(\text{H}_2\text{O})]\cdot\text{H}_2\text{O}\cdot\text{NO}_3\}_n$ was synthesized based on *L*-tryptophan (L-trp) and 2-bis(4-pyridyl)ethylene (bpe). These materials are stable in an aqueous medium and reversibly lose water molecules during activation. So, they can be interesting for biological applications and for the adsorption of heavy metals from aqueous solutions. The further development of vibrational spectroscopy and hydrothermal synthesis are our nearest plans. We also hope to evolve the synthesis of inorganic materials by other methods.

[1] A.A. Nabyev, A. Olejniczak, A. Pawlukoje, M. Balasoju, M. Bunoju, A.M. Maharramov, M.A. Nuriyev, R.S. Ismayilova, A.K. Azhibekov, A.M. Kabyshev, O.I. Ivankov, T. Vlase, D.S. Linnik, A.A. Shukurova, O.Yu. Ivanshina, V.A. Turchenko, and A.I. Kuklin (2020). Nano-ZrO₂ filled high-density polyethylene composites: structure, thermal properties, and the influence γ -irradiation. *Polymer Degradation and Stability*. 171,109042.

[2] N.A. Kalanda, A.L. Gurskii, M.V. Yarmolich, A.V. Petrov, I.A. Bobrikov, O.Yu. Ivanshina, S.V. Sumnikov, F. Maia, A.L. Zhaludkevich, S.E. Demyanov (2019). Sequence of phase transformations at the formation of the strontium chrome-molybdate compound. *Modern Electronic Materials*. 5(2),69–75.

[3] T. Sakurai and H. Iwasaki (1978). Bis(L-histidinato)nickel(II) Monohydrate. *Acta Cryst.* B34,660-662.

[4] J.A. Gould, J. Bacsá, H. Park, J.B. Claridge, A.M. Fogg, V. Ramanathan, J.E. Warren, and M.J. Rosseinsky (2010). Nanoporous Amino Acid Derived Material Formed via In-Situ Dimerization of Aspartic Acid. *Cryst. Growth Des.* 10,2977-2982.

[5] S. Mendiratta, M. Usman, T. Luo, B. Chang, S. Lee, Y. Lin, and K. Lu (2014). Anion-Controlled Dielectric Behavior of Homochiral Tryptophan-Based Metal–Organic Frameworks. *Cryst. Growth Des.* 14,1572–1579.

NEW EQUIPMENT FOR SAMPLE PREPARATION AND STUDY OF FUNCTIONAL MATERIALS

I.A. Bobrikov¹

¹*Joint Institute for Nuclear Research, Dubna, Russia*

E-mail: bobrikov@nf.jinr.ru

A new chemical lab was created in Frank Laboratory of Neutron Physics (FLNP) and specialized on preparation of electrochemical samples for neutron and X-Ray scattering experiments.

Now the lab is located in the building №42a of FLNP complex. It is equipped with many facilities required for electrochemical cell assembly. Particularly the lab is equipped with devices designed for Li-ion battery electrodes preparation and testing (a tube furnace with controlled atmosphere, precise scales, a planetary mill, various mixers, and dispergators, coating and rolling machines, presses, the Karl-Fischer titrator, a drying vacuum oven, an exhaust system, a glove box with argon atmosphere, polishing machine, electrochemical testers and potentiostats and etc.). There is also a modern X-ray diffractometer PANalytical Emyrean in the configuration with a large number of additional equipment, greatly expanding its capabilities (Co, Cu, Mo radiation; various temperature consoles, positional translators, parallel and focusing mirrors, etc.). The lab resources are successfully used for diffraction, reflectometry, and small-angle experiments with materials for electrochemical issues and with other functional materials. The presentation consists of a brief review of the key facilities in the created lab.

This work was supported by the Russian Foundation for Basic Research (projects no. 17-52-44024 and 18-02-00325) and JINR theme №04-4-1121-2015/2020.

**Abstracts:
Poster
Presentations**

POSTER SESSION 1
FUNCTIONAL AND NANOSTRUCTURED MATERIALS

TRACKING MARTENSITIC TRANSFORMATION IN AISI 321 STAINLESS STEEL USING SCANNING CONTACT POTENTIOMETRY AND THERMAL NEUTRON DIFFRACTION

A.A. Abu Ghazal¹, V.I. Surin², G.D. Bokuchava³, I.V. Papushkin³

¹*Jordan Atomic Energy Commission, Amman, Jordan*

²*National Research Nuclear University, Moscow, Russia*

³*Joint Institute for Nuclear Research, Dubna, Russia*

E-mail: ayman.abughazal@jaec.gov.jo

Joint synchronized experiments, for the first time, carried out to study the destruction processes of AISI 321 stainless steel using scanning contact potentiometry (SCP) and thermal neutron diffraction (TND) methods [1],[2]. Experiment by neutron diffraction performed on the Fourier-stress diffractometer (FSD) in the fast pulsed reactor (IBR-2) at Frank Laboratory of Neutron Physics located in the Joint Institute for Nuclear Research in Dubna city [3]. During the sequence of the experiment, specimens from AISI 321 stainless steel were subjected to external uniaxial tensile load using tensile testing machine LM-29 in-situ where Neutron beams are focused on samples. Thus, the data of scanning contact potentiometry were independently recorded simultaneously with the neutron diffraction spectra. The obtained results confirm that on potentiograms of the SCP method was observed appearance individual small size spots associated with relatively high values of signal amplitude.

Red spots corresponded to the areas with the highest stress values. These values, on the left side of the specimen, are much lower than the right side, where the failure occurred. Probably, in these areas, the martensite phases begin to form (See figure 1).

With increasing the load, the spots size increased, which connected with dynamic processes of the martensite phase formation, its presence of which verified the spectra obtained by the thermal neutron diffraction method. The analysis of intensity diffraction peaks showed noticeable presence of texture in the initial austenitic specimen, also observed high texture in the formed martensite (See figure 2).

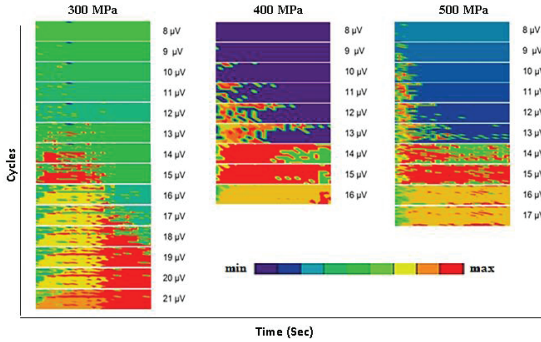


Figure 1 Shows the Linear-time potentiograms of the AISI 321 sample surface obtained by the SCP method during tensile testing. The fracture of the specimen occurs at 700 MPa.

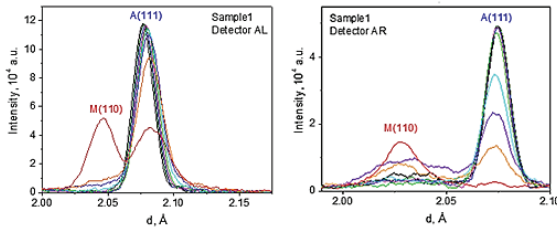


Figure 2 shows part of the neutron diffraction spectrum in the region of austenite peaks (A 111) and martensite (M 110) for the AISI 321 stainless steel specimen, where (AL) is for the left detector and (AR) for the right.

- [1] A.A. Abu Ghazal, P.S. Dzhumayev, A.V. Osintsev, V.I. Polsky, V.I. Surin (2019). Experimental investigation of the failure of steel AISI 316 by the methods of structural analyses. *Letters on Materials*. 9(1), 33-38.
- [2] V.I. Surin (2018). New potential for potentiometry. *Nuclear Engineering International*. 63 (765), 30-32.
- [3] G.D. Bokuchava, V.L. Aksenov, A.M. Balagurov, V.V. Zhuravlev, E.S. Kuzmin, A.P. Bulkin, V.A. Kudryashev, V.A. Trounov (2002). Neutron Fourier diffractometer FSD for internal stress analysis: first results. *Applied Physics A: materials Science and Processing*. 74, 86-88.

NOVEL RESORCINOL-FORMALDEHYDE AEROGELS: SYNTHESIS, STRUCTURE AND FRACTAL PROPERTIES

L.A. Azarova¹, G.P. Kopitsa^{1,2,3}, Yu.E. Gorshkova⁴, S.A. Lermontov⁵, A. N. Malkova⁵, V.V. Volkov⁶, A.E. Baranchikov⁷

¹*Petersburg Nuclear Physics Institute NRC KI, Gatchina, Leningrad district, Russia*

²*National Research Center Kurchatov Institute, Moscow, Russia*

³*Grebenshchikov Institute of Silicate Chemistry of RAS, St. Petersburg, Russia*

⁴*Joint Institute for Nuclear Research, Dubna, Moscow region, Russia*

⁵*Institute of Physiologically Active Compounds of RAS, Chernogolovka, Russia*

⁶*FSRC "Crystallography and Photonics" of RAS, Moscow, Russia*

⁷*Kurnakov Institute of General and Inorganic Chemistry of RAS Moscow, Russia*

E-mail: kopitsa_gp@npni.nrcki.ru

Organic aerogels belong to a very attractive class of aerogel materials possessing the properties inherent to traditional oxide aerogels, and also some unique flexible chemical properties (e.g. the presence of various functional groups). Organic aerogels can be synthesized by polycondensation of resorcinol and formaldehyde under acid or base catalysis producing so called resorcinol-formaldehyde (RF) aerogels. RF aerogels possess high porosity, specific surface area and pore volume, as well as low thermal conductivity (for instance, RF aerogels are better thermal insulators than commercial fiber glass). On the other hand, RF aerogels are stiffer and stronger than inorganic aerogels. Reaction mixture pH, concentration and ratio of monomers (resorcinol/formaldehyde), the catalyst type and resorcinol/catalyst ratio are the key factors determining the final characteristics (density, specific surface area, particle size, pore size distribution) of RF aerogels.

In the present work, the small angle neutron scattering (SANS), the small angle X-ray scattering (SAXS) and low temperature nitrogen adsorption techniques have been used to study the mesostructure and fractal properties of resorcinol-formaldehyde aerogels prepared by the reaction between resorcinol and formaldehyde using different solvents including acetonitrile and perfluoroacetone. The samples of RF-lyogels were aged at temperatures from 20 to 70°C to determine the influence of the aging temperature on the structure and properties of the aerogel materials.

The synthesis of the resorcinol-formaldehyde lyogels was conducted using acetonitrile and hexafluoroacetone hydrate as solvents. Hexafluoroacetone hydrate as a solvent and a gelling agent for the synthesis of RF-lyogels was used for the first time. Using supercritical drying in CO₂ monolithic (including flexible) aerogels of resorcinol-formaldehyde polymers characterized by specific surface area up to 400 m²/g, specific porosity up to 1.3 cm³/g were successfully obtained. All the obtained RF-aerogels were hydrophilic.

It has been established that the volume and composition of the solvent used at the stage of the gel formation allow to vary the texture characteristics of RF-aerogels, and the microstructure of the resulting materials. In particular, the use of acetonitrile as a solvent resulted in aerogels with a highly developed surface; on the contrary, the use of hexafluoroacetone hydrate lead to the formation of macroporous aerogels consisting of submicron dense spherical particles with a virtually smooth surface. It was shown that the rate of gel formation in the resorcinol-formaldehyde system is determined by the composition of the solvent used – in acetonitrile the gel formed in several hours, in hexafluoroacetone hydrate – in few seconds. It was established that the increase in the ageing temperature of RF-lyogels from 20 to 70°C leads to a significant decrease in the fractal dimension D_s of the surface of the corresponding aerogels

(from ~2.5 to 2.0), which indicates a significant smoothing of the surface of the nanoparticle aggregates. This parameter practically does not affect the size of nanoparticle aggregates in the structure of RF-aerogels. It was established that a significant increase in the size of nanoparticle aggregates occurs when the gelling system is diluted (an increase in the volume of solvent in which the gel is formed).

The work was supported by the Russian Science Foundation (grant 19-73-20125).

SPIN-GLASS STATE INFLUENCE ON THE LOW TEMPERATURE TRANSPORT PHENOMENA IN $\text{La}_{0.54}\text{Nd}_{0.11}\text{Sr}_{0.35}\text{Mn}_{1-x}\text{Co}_x\text{O}_3$ MANGANITES

N. Cornei¹, M.-L. Craus^{2,3}, C. Mita^{1,3}

¹"Alexandru Ioan Cuza" University of Iasi, Faculty of Chemistry, 11 Carol I Blvd., 700506 Iasi, Romania

²National Institute of Research and Development for Technical Physics, 700050 Iasi, Romania

³Joint Institute for Nuclear Research, 141980 Dubna, Moscow Region, Russia

E-mail: craus@phys-iasi.ro

The $\text{La}_{0.54}\text{Nd}_{0.11}\text{Sr}_{0.35}\text{Mn}_{1-x}\text{Co}_x\text{O}_3$ (ABO_3) manganites were synthesized by sol-gel. The samples were treated at 800°C and finally treated at 1250°C in air for 10 h. X-ray Diffraction (XRD) was performed with a DRON 2.0 diffractometer, $\text{CoK}\alpha_{12}$ radiation, step 0.01, at room temperature. The lattice constants, positions of cations and anions in unit cell, BO distances, BOB bond angles, average size of mosaic blocks and microstrains being determined by using Fullprof code. Magnetic properties were measured with a VSM type magnetometer, at $H=1\text{T}$, between 77 and 400 K. Transport characteristics were obtained with an installation consisting from a refrigerator, working between 7 and 400 K, an electromagnet which generated a field 1 T, currents through the samples of at the order of microamperes.

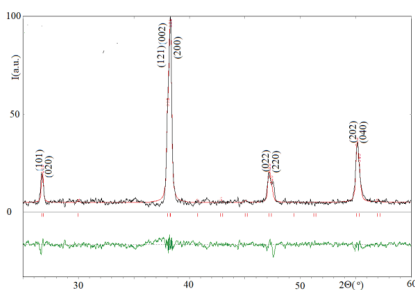


Figure 1 The observed (black), calculated (red) and the difference between the observed and calculated diffractograms (green) for $\text{La}_{0.54}\text{Nd}_{0.11}\text{Sr}_{0.35}\text{Mn}_{0.95}\text{Co}_{0.05}\text{O}_3$

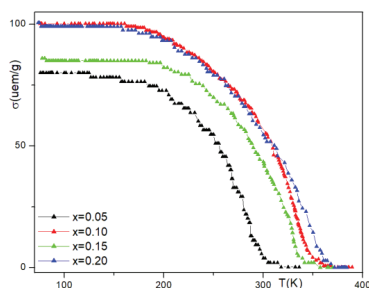


Figure 2 Variation of specific magnetization vs temperature (T) and Co concentration (x) for $\text{La}_{0.54}\text{Nd}_{0.11}\text{Sr}_{0.35}\text{Mn}_{0.95}\text{Co}_{0.05}\text{O}_3$

Table 2. Variation of lattice constants (a, b, c), unit cell volume (V), average size of crystalline blocks (D) and microstrains (ϵ) for $\text{La}_{0.54}\text{Nd}_{0.11}\text{Sr}_{0.35}\text{Mn}_{1-x}\text{Co}_x$ manganites.

x	a(Å)	b(Å)	c(Å)	V(Å ³)	D(Å)	ϵ
0.05	5.4519	7.7095	5.4913	230.81	592	0.00098
0.10	5.4490	7.7192	5.4817	230.57	925	0.00192
0.15	5.4309	7.7117	5.4653	228.90	1114	0.00070
0.20	5.4419	7.7141	5.4756	229.86	572	0.00293

A minimum of unit cell volume with increase Co concentration was observed (s. Table 1). At $x=0.15$ a maximum of size of crystalline blocks and a minimum of microstrains was observed.

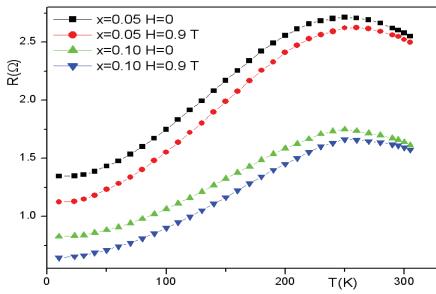


Figure 3 Variation of resistance vsttemperature and magnetic field for $\text{La}_{0.54}\text{Nd}_{0.11}\text{Sr}_{0.35}\text{Mn}_{1-x}\text{Co}_x\text{O}_3$ manganites

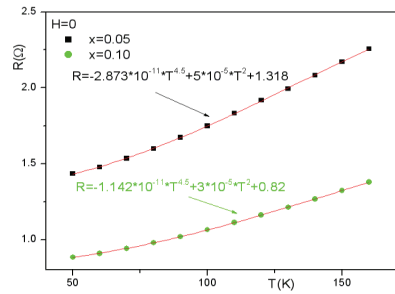


Figure 4 Variation of resistance vsttemperature Co concentration for $\text{La}_{0.54}\text{Nd}_{0.11}\text{Sr}_{0.35}\text{Mn}_{1-x}\text{Co}_x\text{O}_3$ manganites at low temperatures

In the Figure 4, last term of the equations represents the resistance due to the temperature-independent scattering processes, the second term (in T^2) corresponds to the electron–electron scattering processes, and the first term (in $T^{4.5}$) term includes contribution from the electron–magnon scattering or spin wave scattering. All these terms are field dependent.

Increased resistance values at low temperature indicate the presence of an insulator phase into major semiconductor phase, which increase with the increasing Co concentration in the manganites.

The increase of the Mn^{4+} concentration contributes to the enhancement of holes in the e_g band, which should leads to a decrease of resistivity of the samples. It was observed a large difference between the Curie and transition temperature from metallic to insulator state, attributed to the presence of an important amount of defaults, present in the boundaries layers. The present of a boundary layer with a large amount of defaults and characterized by a lower Curie temperature and a high resistivity as the “crystalline core” “masks” the transition temperature of the “crystalline core”. The observed behavior of resistance with temperature at very low temperatures can be attributed to the intergranular spin polarized tunneling mechanism.

Mn with Co ions substitution effects seems to depend strongly on the average radii of ions on A places and chemical disorder degree.

The samples can be described as a mixture of a magnetic region, characterized by the presence of Mn^{3+} -O- Mn^{4+} bonds and a disordered spin-glass region. Mn^{3+} and Mn^{4+} cations interact by double exchange mechanism. A contribution of the cobalt to the magnetic moment could be explained by presence of both Co^{2+} (d^7 , HS) and Co^{3+} (d^6 , HS) cations in the samples.

RESEARCH OF STRUCTURAL TRANSFORMATION MECHANISM IN HIGH STRENGTH STEEL

M.L. Fedoseev¹, S.N. Petrov¹, M.S. Mikhailov¹, A.Kh. Islamov², N.F. Drozdova¹

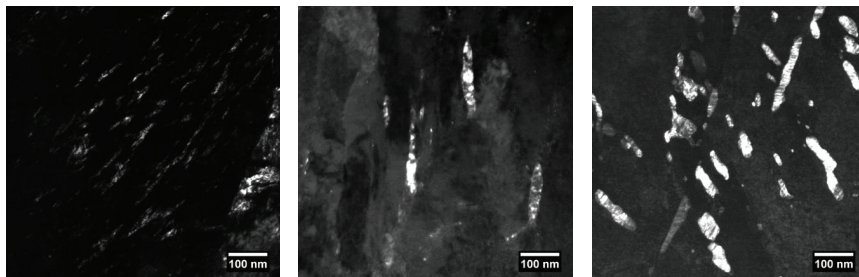
¹NRC "Kurchatov Institute" – CRISM "Prometey", 190015, St. Petersburg, Spalernaya st., 49

²Joint Institute for Nuclear Research, 141980, Dubna, Russia

E-mail: npk3@crism.ru

Because size, shape and chemical composition of carbide phases highly affects to the material properties, carbide quantitative studies are indispensable in the development of new steels. Combined application of different techniques is necessary for deeper insight into the issue. This work includes several methods, namely, small angle neutron scattering (SANS), neutron diffraction (ND) (on research facilities IBR-2 pulsed reactor JINR Dubna [1]) and transmission electron microscopy (TEM). The research goals are determining of dimensions, morphology and volume part of carbide particles in high-strength steel containing 0.42%(wt.) carbon after quenching at different tempering temperatures in the range up to 600 °C. This research continues investigations begun in [2].

The initial structure of the steel after quenching is martensite with retained austenite layers between the martensite laths. Dependence size of dispersed particles versus tempering temperature done on the base of SANS results, taking into account SEM data, see fig. 1-2. Dispersed particles change model proposed. Growth of carbides (Fe_2C) begins immediately after lowest tempering temperature. After 200 °C achieved Fe_2C changes on more stable Fe_3C and it growth within tempering temperature 600 °C [2]. At tempering temperatures ~ 300 - 350 °C: Fe_3C reflexes traces appears, because it size becomes enough to get neutron diffraction on it, also dispersed particles size falling (on SANS), because it average diameter becomes out of the range SANS applicability (~ 100 nm). Quantity of disperse particles decrease, while completely content of Fe_3C increases by neutron diffraction data. The increase in tempering temperature leads to a decrease in the amount of retained austenite.



a) 150 °C

b) 300 °C

c) 500 °C

Fig. 1 TEM microstructures of dispersed phases after tempering temperatures

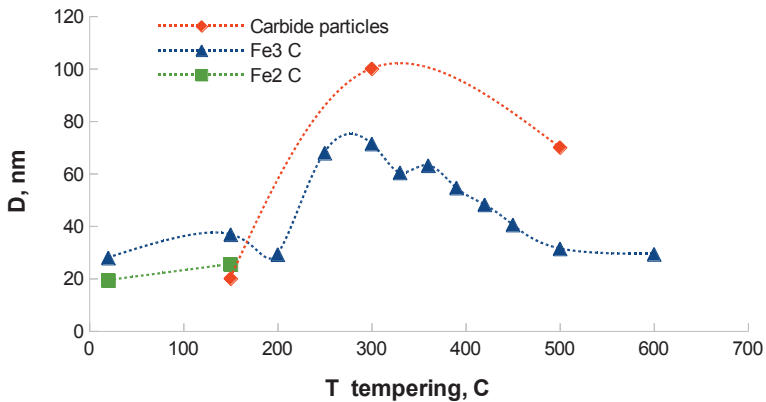


Fig. 2 Dispersed particle size. TEM (◆), SANS approximation on Fe₂C (■), Fe₃C (▲).

Various methods (ND, SANS, TEM) data supplement each other. The result is phase transformation mechanism for tempering steel, but similarly one can study another heat treatments and alloys.

References:

- [1] V.N. Shvetsov (2017). Neutron Sources at the Frank Laboratory of Neutron Physics of the Joint Institute for Nuclear Research. Quantum Beam Science. 6, i1, pp. 1-9.
- [2] M.L. Fedoseev, S.N. Petrov, A.Kh. Islamov, N.F. Drozdova, T.A. Lychagina, D.I. Nikolaev (2018). Research of carbide particle dimensions in high-strength steel by a number of complementary methods. Letters on materials. 8, i3, pp 323-328.

STRUCTURAL CHARACTERIZATION OF YTTRIUM DOPED BARIUM CERATE $\text{BaCe}_{0.85}\text{Y}_{0.15}\text{O}_{3-\alpha}$ FOR APPLICATION IN SOLID OXIDE FUEL CELLS

I.G. Genov^{1,2}, A.V. Rutkauskas¹, E.V. Lukin¹, D.P. Kozlenko¹, S.E. Kichanov¹, G.S. Raykova², D.E. Vladikova², N.M. Belozeroва¹, V.A. Turchenko¹, E.P. Popov^{1,3,4}, K.A. Krezhov⁵

¹*Joint Institute for Nuclear Research, Dubna, Moscow distr., 141980, Russia*

²*Acad. E. Budevski Institute of Electrochemistry and Energy Systems, Bulgarian Academy of Sciences, 10 Acad. G. Bonchev St., Sofia 1113, Bulgaria*

³*Georgi Nadjakov Institute of Solid State Physics, Bulgarian Academy of Sciences, Sofia, 1784, Bulgaria*

⁴*Institute for Nuclear Research and Nuclear Energy, Bulgarian Academy of Sciences, Sofia 1784, Bulgaria*

⁵*Acad. E. Djakov Institute of Electronics, Bulgarian Academy of Sciences, Sofia, 1784, Bulgaria*

E-mail: dedfin45@abv.bg

A cutting-edge trend in the development of solid-fuel fuel cells (SOFC) is the developed Dual membrane fuel cell (dmFC) concept for operation at 600-700°C [1-5]. A major element in dmFC is a central membrane (CM) in which hydrogen and oxygen ions meet and react with each other. The object of these studies is a study of the structural changes at the change of temperature of material $\text{BaCe}_{0.85}\text{Y}_{0.15}\text{O}_{3-\alpha}$ (BCY15) with mixed (proton and oxygen) conductivity, for use as a CM in the new dmFC configuration. Mixed proton and oxide-ion conductivity of ceramic BCY15 is an attractive property for its application in a the new design of a fuel cell which eliminates the formation/evacuation of the water produced during operation from the electrodes.

The phase transitions of powder from BCY15 were studied by neutron diffraction (ND) and X-ray diffraction (XRD) in high temperature range 25 - 800°C. The proton mobility in this material is intimately associated to the crystal phases of the framework host. The results show that in the temperature range from 25°C to 670°C the material BCY15 is in the orthorhombic space group Pnma. Above 670 °C, the space group changes from orthorhombic Pnma to cubic Pm-3m.

An attempt has been made to understand the influence of water on the BCY15 structure. The powder was humidified 50% of D2O before carrying out the measurement of the so-protonated sample. The measurements was made of temperature range 25-400°C. The extensive incoherent scattering of hydrogen from the hydroxyl groups is reflected by the steadily rising contribution to the background with decreasing to zero scattering angles.

The effect of hydration on the BCY15 at ambient temperature has been investigated with optical Raman spectroscopy. The Raman spectra was carried out the region between 50 and 1000 cm⁻¹. Figure 1 exhibits the Raman spectrum of BCY15 samples before and after humidity. The intensity of the peaks after hydration strongly decrease, in comparison with peaks before hydration. It show that even at room temperature in BCY15 occurs the changes after hydration. The ND and Raman spectroscopy of nonhydrated and hydrated powders can shed light on the influence of structural or vibrational properties on the proton transport.

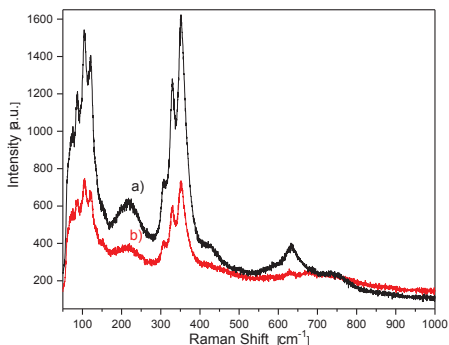


Figure 1. Raman spectra of BCY15 a) dry BCY15; b) wet BCY15

The results obtained from the combined structural studies (XRD, ND and RS) and previous electrochemical studies of BCY15 in addition to its natural property to split water reinforce a new emerging niche for development of other materials with similar structure and mixed conductivity which will further stimulate the development of the dmFC concept for operation in both fuel cell and electrolyzer mode.

- [1] S. Thorel, A. Chesnaud, M. Viviani, A. Barbucci, S. Presto, P. Piccardo, Z. Ilhan, D. E. Vladikova, Z. Stoynov (2009). in *Solid Oxide Fuel Cells 11 (SOFCXI)*, edited by S.C. Singhal, and H. Yokokawa, The Electrochemical Society Proceedings, ECS Transactions. 25, 753-762
- [2] Patent N° 0550696000, March 17th, 2005, Cellule de pile a combustible haute temperature a conduction mixte anionique et protonique ; International extension in 2006, Issue 2, Pennington, NJ (2009) 753.
- [3] D. Vladikova, Z. Stoynov, G. Raikova, A. Thorel, A. Chesnaud, J. Abreu, M. Viviani, A. Barbucci, S. Presto, P. Carpanese (2011). *Electrochim Acta.* 56, 7955- 7962.
- [4] A. Thorel, D. Vladikova, Z. Stoynov, A. Chesnaud, M. Viviani, S. Prest (2012) o. In: *Fuel cell with monolithic electrolytes membrane assembly*, inventors. ARMINES patent #10 20120156573, June 17th.
- [5] Z.B. Stoynov, D.E. Vladikova, E.A. Mladenova (2013). Gigantic enhancement of the dielectric permittivity in wet yttrium-doped barium cerate. *J Solid State Electrochem.* 17, 555-560.

STRUCTURAL ANALYSIS OF THE INGAAS/GAAS HETEROSTRUCTURES BY HIGH-RESOLUTION RECIPROCAL SPACE MAPPING AND NEUTRON SCATTERING

D.V. Iljinov¹, A.D. Shabrin¹ and V.V. Sadilov²

¹Orion R&P Association JSC, Moscow, Russia

²Joint Institute for Nuclear Research, Dubna, Russia

E-mail: dv.iljinov@physics.msu.ru

Improvement of microelectronics, photoelectronics and the creation of new devices based on quantum effects has recently become especially important due to the active development of methods for growing semiconductor epitaxial structures, in particular, molecular beam epitaxy [1, 2]. At present, heteroepitaxial structures and superlattices based on A3B5 semiconductors are greatest interest for optoelectronics [3, 4]. InGaAs/GaAs superlattices and heterostructures were used in different microelectronic devices, for example, in HEMT transistors, photodetectors, as well as in the creation of lasers based on heterostructures. However, the increased demands on the performance of third and fourth generation photodetectors directly depend on the quality of the photosensitive materials used in them. The energy spectrum of charge carriers in quantum wells, and hence some other characteristics in devices based on epitaxial structures made of A3B5 materials, are determined by the features and state of their crystal structure, as well as their compliance with the growth technological parameters. Therefore, it is required to control and characterize the properties and parameters of grown epitaxial structures for nano- and microelectronics, lasers, and other equipment. So this work is devoted to investigation of the crystalline state and characteristics of semiconductor heteroepitaxial systems based on InGaAs/GaAs:

GaAs (sub)/GaAs (800 nm)/GaAs (55 nm)/
({InGaAs (6,2 nm)/GaAs (55 nm)}×30)/GaAs (600 nm) (1)
GaAs (sub) / InGaAs (400nm), (2)
grown by MBE on GaAs (100) substrates by neutron spectroscopy and high-resolution X-ray diffractometry, including reciprocal space mapping [5].

According to the results of the research, the parameters of investigating samples were determined: the value of the fraction of In x in $\text{In}_x\text{Ga}_{1-x}\text{As}$, the thickness of the GaAs and InGaAs layers. The average value of the superlattice period for (1) was calculated. FWHM for the GaAs and InGaAs peaks on the rocking curves for both samples measured without an analyzer crystal was increased compared to theoretical values, not all satellites and thickness oscillations were distinguishable. Therefore the ω -2 θ diffraction scans were recorded using an analyzer crystal to reduce the fraction of incoherent scattering in the spectrum, so parameters of the studied heterosystems were ultimately determined. There was also a noticeable discrepancy between the experimental and theoretical intensities of satellite peaks and zero peaks for a sample containing multiple quantum wells: on the experimental curve, the diffraction maxima were weaker in intensity compared to theoretical ones. This indicates to the possible presence of deformations, which is also evidenced by the absence of some oscillations between satellites and their incomplete coincidence in number and position near the GaAs peak. The reason for the appearance of the diffuse component in the diffracted radiation by the samples can be explained with reciprocal space mapping by various reflexes of the crystal lattice. Symmetric and asymmetric reciprocal space maps were measured in the [110] direction for both researched samples (Fig. 1, 2). The crystal lattice parameters of both samples were calculated based on the obtained reciprocal space maps in the direction of the growth of the structures and in the lateral direction (in the plane of growth) for InGaAs and GaAs.

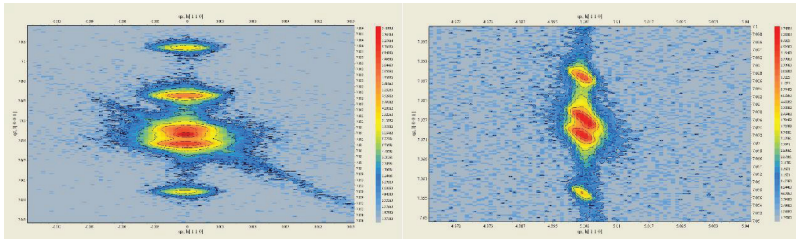


Figure 1 - fragments of reciprocal space maps near Bragg reflections (004) (left) and (224+) (right) for sample (1)

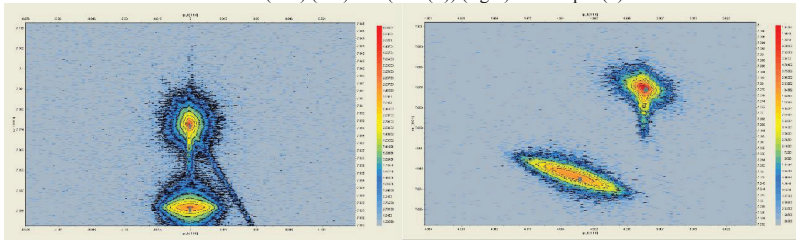


Figure 2 - fragments of reciprocal space maps near Bragg reflections (004) (left) и (224+) (right) for sample (2)

Quantitative and qualitative assessment of parameters for pair of samples based on InGaAs/GaAs heteropair was carried out on the basis of the measured diffraction rocking curves and reciprocal space maps, the neutron spectrum (for sample with multiple quantum wells InGaAs). It was shown that for complete description of the crystalline features of the samples, it was not enough to register only one-dimensional scans in reciprocal space - x-ray diffraction reflection scans (rocking curves), because they didn't explain the reasons for the possible appearance of a diffuse component in diffracted radiation or the discrepancy between the theoretical and experimental diffraction reflection scans. For investigated samples reciprocal space maps were recorded near symmetric and asymmetric Bragg reflections, so the crystal lattice parameters for InGaAs and GaAs were calculated and the elastic stresses and the degree relaxation of layers in heterostructures were determined. The analysis of the correspondence of the calculated parameters by different methods for investigated samples, as well as with technological growth data of MBE, was carried out.

- [1] K.Y. Donald Cheng (2013). Development of molecular beam epitaxy technology for III-V compound semiconductor heterostructure devices. *Journal of Vacuum Science and Technology*. 31. 050814.
- [2] N.V. Rzhetski et al. (2019). Ammonia molecular beam epitaxy of AlGaIn heterostructures on sapphire substrates. *Doklady BGUIR*. 7 (125). 144-151.
- [3] V.M. Ustinov (2018). Molecular beam epitaxial growth of semiconductor heterostructures for THz electronics. TERA-2018. EPJ Web of Conferences. 195.
- [4] P. Gutowski et al. (2017). MBE growth of strain-compensated InGaAs/InAlAs/InP quantum cascade lasers. *Journal of Crystal Growth*. 466. 22-29.
- [5] P. López-Salazar et al. (2016). Characterization of Al_{0.047}Ga_{0.953}Sb layers grown on GaSb using reciprocal space maps. *Materials Letters*. 166. 239-242.

OXYGEN NON-STOICHIOMETRY AND SUPERSTRUCTURAL ORDERING OF Fe/Mo CATIONS IN THE STRONTIUM FERROMOLYBDATE

N.Kalanda¹, M.Yarmolich¹, A.Petrov¹, I.Bobrikov², S.Demyanov¹ and N.Sobolev³

¹Scientific-Practical Materials Research Centre of NAS of Belarus, Minsk, Belarus

²Joint Institute for Nuclear Research, Dubna, Russia

³Universidade de Aveiro, Aveiro, Portugal

E-mail: kalanda@physics.by

The increasing attention of researchers is focused on the study of the strontium ferromolybdate $\text{Sr}_2\text{FeMoO}_{6-\delta}$ (SFMO) ferrimagnetic, which has high values of the negative magnetoresistive effect ($MR \sim 38\%$ in the field of 1.0 T at $T = 50$ K), almost 100% of the spin polarization degree of conduction electrons, and high values of the Curie temperature ($T_C \sim 420$ K) [1, 2]. To obtain the SFMO with optimal magnetic and galvanomagnetic properties, knowledge and control of the anionic composition of materials and the dynamics of Fe/Mo superstructural ordering in the cationic sublattice of the compound are required.

$\text{Sr}_2\text{FeMoO}_{5.99}$ single-phase samples without superstructural ordering of iron and molybdenum cations with a Curie temperature of 407 K were obtained by the solid-phase technique. According to the XRD data the growth dynamics of the degree of Fe/Mo cations superstructural ordering (P) is nonlinear. In this case, the process of reaching the maximum values of the parameter P_{\max} is long and several times lower than the rate of change of the oxygen index $6 - \delta$. It was found that with the increasing temperature of isothermal annealing, the value of P rises and reaches maximum values of 88% at $T = 1320$ K for 120 hours, $P_{\max} = 92\%$ at $T = 1420$ K for $t = 100$ h, while $P_{\max} = 90\%$ at $T = 1470$ K for $t = 45$ hours. It can be assumed that the lower values of P_{\max} at $T = 1470$ K, than at $T = 1420$ K are due to the influence of thermal energy on the destruction of chain ordering of Fe and Mo cations placed in the staggered order. Based on the analysis of the time dependences of the parameter P , it is easy to see two relaxation processes and the dependence $dP/dt = f(t)$ can be conditionally divided into two regions, I and II. It was found that the relaxation time in the region I is shorter than that in the region II. This is due to the fact that the ordering of cations in the $-\text{O} - \text{Fe} - \text{O} - \text{Mo} - \text{O}$ chains in region I requires atomic displacements by approximately one interatomic distance, whereas in region II cation displacements occur over long distances with the formation of long-chain long-range ordering.

This work was supported by the European Union project H2020 –MSCA-RISE-2017-778308-SPINMULTIFILM.

[1] D.Topwal, et al. (2006). Structural and magnetic properties of $\text{Sr}_2\text{Fe}_{1+x}\text{Mo}_{1-x}\text{O}_6$ ($-1 \leq x \leq 0.25$). Physical Review B. 73, 094419 – 1 – 6.

[2] N.A.Kalanda, et al. (2019). Small-angle neutron scattering and magnetically heterogeneous state in $\text{Sr}_2\text{FeMoO}_{6-\delta}$. Physica Status Solidi (b). 256, 1800428-1-7.

THERMODYNAMIC, STRUCTURAL AND MAGNETIC CHARACTERISTICS OF BARIUM FERROMOLYBDATE COMPOUND

N.Kalanda¹, M.Yarmolich¹, A.Petrov¹, M.Kutuzau¹, A.Blokhin², S.Tamulevicius³ and I.Bobrikov⁴

¹*Scientific-Practical Materials Research Centre of NAS of Belarus, Minsk, Belarus*

²*Belarusian State University, Minsk, Belarus*

³*Kaunas University of Technology, Kaunas, Lithuania*

⁴*Joint Institute for Nuclear Research, Dubna, Russia*

E-mail: petrov@physics.by

The $A_2\text{FeMoO}_{6\pm\delta}$ ($A = \text{Ba}, \text{Sr}, \text{etc.}$) double perovskites are highly correlated electronic systems and possess unique physico-chemical properties caused by the formation of zero-dimensional deficiency in the crystal lattice [1, 2]. As the objects of this study, the $\text{Ba}_2\text{FeMoO}_{6-\delta}$ compound was chosen, which shows the low field room temperature magnetoresistance and ferrimagnetic phase transition with $T_C \sim 320 - 340 \text{ K}$.

It was determined according to adiabatic calorimetry data, that the specific heat in the regions at 5–300 K increases monotonically with increasing temperature. In this case, the heat capacity at low temperatures from 5 K to 15 K does not obey the Debye's T-cubes law and has anomalies due to non-cooperative magnetic transformations, which was confirmed by the dependencies of the magnetization on temperature. In the temperature range 300 – 370 K, heat capacity anomalies were discovered due to the transition of the material from the ferrimagnetic to the paramagnetic state. The transitions found are reversible, and the heat capacity values in two independent series of experiments are consistent with each other within 0.1%. The Curie temperature, determined from the maximum of the excess heat capacity in the transition regions for the $\text{Ba}_2\text{FeMoO}_{6-\delta}$ compound, is in a good agreement with the Curie temperature obtained from the results of magnetic measurements ($T_C \sim 320 \text{ K}$).

Based on the polynomial dependences of the smoothed heat capacity values, the thermodynamic functions (reduced enthalpy, entropy, reduced Gibbs energy) were calculated in the temperature range 0 – 370 K. It was found that to extrapolate the heat capacity of compounds to the region $T \rightarrow 0 \text{ K}$, it is necessary to use an equation that takes into account the contributions to the heat capacity of not only lattice vibrations, but also conduction electrons.

This work was supported by the European Union project H2020 –MSCA-RISE-2017-778308-SPINMULTIFILM.

[1] D.Serrate, et al. (2007). Magnetoelastic coupling in $\text{Sr}_2(\text{Fe}_{1-x}\text{Cr}_x)\text{ReO}_6$ double perovskites *J. Phys.: Condens. Matter*, 19, 436226 – 1 – 8.

[2] N.A.Kalanda, et al. (2019). Small-angle neutron scattering and magnetically heterogeneous state in $\text{Sr}_2\text{FeMoO}_{6-\delta}$. *Physica Status Solidi (b)*, 256, 1800428-1-7.

BARIUM TITANATE FROM MULTICOMPONENT GLASS DOPED WITH IRON OXIDE – LOW-TEMPERATURE PHASE TRANSITIONS OF BARIUM TITANATE

K. Krezhov¹, R. Harizanova², E. Lukin³, A. Beskrovny³, E. Popov^{1,3}, D. Kozlenko³, S. Kichanov³, M. Mirzaev⁴

¹*Institute of Electronics and Institute for Nuclear Research and Nuclear Energy, Bulgarian Academy of Sciences, Sofia, Bulgaria*

²*University of Chemical Technology and Metallurgy, Sofia, Bulgaria*

³*Joint Institute for Nuclear Research, Dubna, Russia*

⁴*Institute of Radiation Problems, Azerbaijan National Academy of Sciences, Baku, AZ1143 Azerbaijan*

E-mail: kiril.krezhov@gmail.com

Samples with their concentration, glass-transition temperature and crystallization are presented in Table 1.

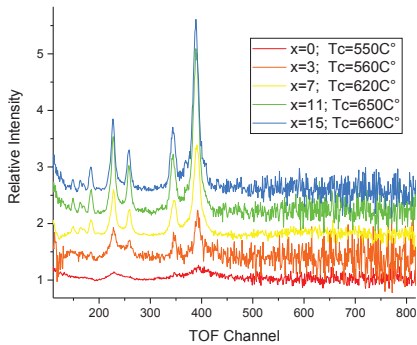
Table 1

System	Sample name	Concentration of Al ₂ O ₃ , mol%	Glass-transition temperature, T _g , °C	Crystallization temperature, T _c , °C
Na ₂ O/BaO/TiO ₂ /B ₂ O ₃ /SiO ₂ / Al ₂ O ₃ /Fe ₂ O ₃	0Al ₂ O ₃ /23.1Na ₂ O – glass F1, x=0	0	420	550
	3Al ₂ O ₃ /20.1Na ₂ O – glass F2, x=3	3	440	560
	7Al ₂ O ₃ /16.1Na ₂ O – glass F3, x=7	7	480	620
	11Al ₂ O ₃ /12.1Na ₂ O – glass F4, x=11	11	530	640, 650
	15Al ₂ O ₃ /8.1Na ₂ O – glass F5, x=15	15	590	660
Na ₂ O/BaO/TiO ₂ /B ₂ O ₃ /SiO ₂ / Al ₂ O ₃	3Al ₂ O ₃ /20.1Na ₂ O – glass NF1, x=3	3	450	650
	7Al ₂ O ₃ /16.1Na ₂ O – glass NF2, x=7	7	490	685
	11Al ₂ O ₃ /12.1Na ₂ O – glass NF3, x=11	11	540	690
	15Al ₂ O ₃ /8.1Na ₂ O – glass NF4, x=15	15	570	695

On the DN-12 neutron diffractometer, samples were created synthesized at various crystallization temperatures T = 550, 560, 620, 650 and 660 ° C from the system (23,1-x)

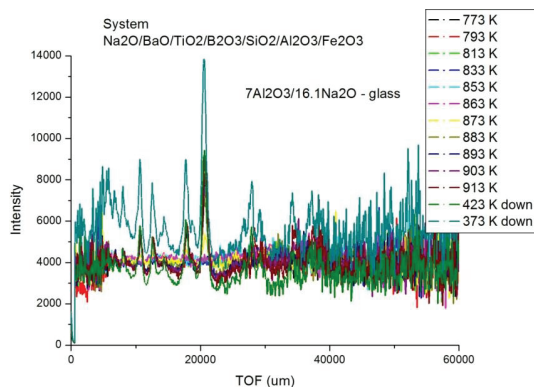
Na₂O / 23,1BaO / 23TiO₂ / 17,4SiO₂ / 7, 6B₂O₃ / xAl₂O₃ / 5.8Fe₂O₃ for x = 0, 3, 7, 11, 15, respectively.

The presented and normalized neutron diffraction spectra for different crystallization temperatures are shown in Figure 1. The different relative intensity of the neutron spectra is the reason for the incomplete transition from the glass state of the system to the crystal structure. The dependence of the intensity of the reflections on the synthesis temperature is clearly observed.



Using a DN-6 neutron diffractometer, we studied samples synthesized at crystallization temperatures $T = 560, 650, 685$ and 690 °C from the system $(16.1) \text{ Na}_2\text{O} / \text{BaO} / \text{TiO}_2 / \text{B}_2\text{O}_3 / \text{SiO}_2 / (7) \text{ Al}_2\text{O}_3 / \text{Fe}_2\text{O}_3$ and $(23.1-x) \text{ Na}_2\text{O} / \text{BaO} / \text{TiO}_2 / \text{B}_2\text{O}_3 / \text{SiO}_2 / (x) \text{ Al}_2\text{O}_3$ for $x = 3, 7, 11$, respectively.

Figure 2 shows the temperature kinetics of the material $(23.1) \text{ Na}_2\text{O} / \text{BaO} / \text{TiO}_2 / \text{B}_2\text{O}_3 / \text{SiO}_2 / (7) \text{ Al}_2\text{O}_3 / \text{Fe}_2\text{O}_3$. It can be seen that crystallization will begin after 863 K (590 C). The picture at 913 K (640 C) shows that crystallization at that temperature has passed completely. Looking at the spectrum of which is manifested in the lowest temperature points, we can say that between 150 C and 100 C there was a phase transition.



ORDERING NANODIAMONDS IN AQUEOUS SYSTEMS WITH ACTIVE MOLECULAR ADDITIVES

V.T.Lebedev¹, Yu.V. Kulvelis¹, A.Ya.Vul², O.A.Kyzyma^{3,4}, T.V.Tropin⁴

¹*Petersburg Nuclear Physics Institute named by B.P. Konstantinov of NRC "Kurchatov Institute", Gatchina, Leningrad distr., Russia*

²*Ioffe Institute, St.Petersburg, Russia*

³*Taras Shevchenko National University, Kyiv, Ukraine*

⁴*Frank Laboratory of Neutron Physics, Joint Institute for Nuclear Research, Dubna, Moscow distr., Russia*

E-mail: lebedev_vt@pnpi.nrcki.ru

Review of neutron studies of dispersions of detonation nanodiamonds (DND, 4-5 nm in size) carrying functional groups interacting in water with dissolved components, fullerenes or macroheterocyclic molecules has been presented. The treatment of diamond surface was developed using annealing in flow of air (hydrogen) to bind the groups (H, OH, COOH) to crystalline facets. In this way the particles self-assembly in aqueous media was regulated finely. The modified crystals form linear chain-like (branched) fractal structures in water at the scales from few diameters of DND up to submicron size. The DNDs' ordering was detected at the levels of primary groups associated into linear and branched chains. Their joining created networks and initiated a transition from dispersions to gels at diamond content exceeded a threshold $C^* \sim 5-7$ wt. % [1]. The neutron small angle scattering (SANS) allowed us determine main features of DNDs' assembly into stable agglutinates remaining bonded in droplets even by five-fold dilution of continuous gel [2]. Here we reported the first prepared complexes of DNDs (positive surface potential) with fullerenes C_{60} dispersed in water by sonication and solvent exchange technique and macroheterocyclic molecules with Europium coordinated between planar ligands (diphthalocyanines). Further the ternary complexes of DNDs with both molecular components were prepared and examined in aqueous solutions by SANS and dynamic light scattering (Fig.1). The developed carbon based and molecular structures carrying magnetic rare earth atoms and possessing high optical catalytic activity will find advanced biomedical applications in photodynamic therapy and Magnetic Resonance Imaging.

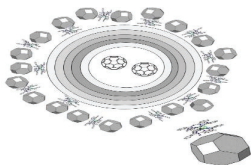


Fig.1. Forming ternary complex C_{60} -DND-diphthalocyanine in aqueous solutions.

The work was supported by the Russian Fund for Basic Researches (gr. No 18-29-19008).

[1] A.Ya. Vul, E.D. Eidelman, A.E. Aleksenskiy, A.V. Shvidchenko, A.T. Dideikin, V.S. Yuferev, V.T. Lebedev, Yu.V. Kulvelis, M.V. Avdeev (2017). Transition sol-gel in nanodiamond hydrosols. // Carbon. 114, 242-249.

[2] V.T. Lebedev, Yu.V. Kulvelis, A.I. Kuklin, A.Ya. Vul (2016). Neutron Study of Multilevel Structures of Diamond Gels. Condensed Matter. 1, 10, 1-9.

NEUTRON DIFFRACTION STUDY OF LOW PH CEMENT-BASED MATERIALS USED FOR ALUMINUM RADIOACTIVE WASTE CONDITIONING: AGING EFFECTS

Tatiana Lychagina¹, Dmitry Nikolayev¹, Cristian Dragolici², Maria Balasoiu^{1,2}, Zakhar Sekretarev¹, Nikolai Lizunov¹, Laura Ionascu², Mihaela Nicu², Felicia Dragolici³

¹*Frank Laboratory of Neutron Physics, Joint Institute for Nuclear Research, Dubna, Russia*

²*Horia Hulubei National Institute of Physics and Nuclear Engineering, Magurele, Romania*

³*International Atomic Energy Agency, A-1400, Vienna, Austria*

E-mail: lychagina@jinr.ru; balas@jinr.ru

Cementitious materials are widely used as repository barriers and for encapsulation of radioactive wastes [1]. The wastes produced as result of nuclear activities are very diverse and it is need to develop special cement matrices to preserve their migration in the environment.

For developing a suitable cement matrix to be used for metallic radioactive aluminum conditioning, the addition of inorganic or organic components into the cement paste were investigated in order to reduce the corrosion rate in alkaline solutions and to obtain a low permeability rate. The developed cementitious materials used for the encapsulation of radioactive waste must resist 300 years, so the monitoring in time of the developed materials structure is very important item.

In order to evaluate the stability of the hardened cement matrix and for taking into consideration the need for long-term durability in disposal conditions, the samples of cement-based materials were measured by means of neutron diffraction each year, in the period from 2016 to 2018, at the SKAT [2] instrument installed at the IBR-2 reactor.

Diffraction patterns were measured for each special direction on a grid of 5° to 5° in the reference coordinate system. Each sample was rotated for 360° around the Z-axis in steps of 5°. By averaging all the diffraction individual patterns measured for 1368 spatial directions, the averaged information over the whole sample is obtained.

In the present work, the results of neutron diffraction experiments on modified CEM III-cement systems highlight aspects of aging processes, depending on the presence in samples of different admixed compounds [3]. The sample with the most stable in time composition was determined.

The obtained studies and results are of high value being a basis for optimizing the cement matrix formulas and further developments, if necessary.

The 2016-2018 JINR – Romania Scientific Program Projects are acknowledged.

[1] Nicu M et al. (2016). Effect of magnesium oxide particle size and the filler content on magnesium potassium phosphate cement properties. *Romanian Journal of Physics* 61(3-4) 543-552.

[2] Keppler R et al. (2014). Potential of full pattern fit methods for the texture analysis of geological materials: implications from texture measurements at the recently upgraded neutron time-of-flight diffractometer SKAT. *Journal of Applied Crystallography* 47, 1520.

[3] T.A. Lychagina et al. (2019). Aging studies of low pH cement-based materials used for aluminum radioactive waste conditioning. *Romanian Journal of Physics* 64, 802(1-8).

FRactal Aggregate Structure of HDPE/SiO₂ Polymer Nanocomposite Films

A.A. Nabiyev^{1,2}, A. Pawlukoje^{2,3}, A.Kh. Islamov², D.V. Soloviov^{2,4,5}, O.I. Ivankov^{2,4,5}, O.Yu. Ivashina² and A.I. Kuklin^{2,5}

¹*ANAS Institute of Radiation Problems, Baku, Azerbaijan*

²*Joint Institute for Nuclear Research, Dubna, Russia*

³*Institute of Nuclear Chemistry and Technology, Warsaw, Poland*

⁴*Institute for Safety Problems of Nuclear Power Plants, Nat. Acad. of Sci. of Ukraine*

⁵*Moscow Institute of Physics and Technology, Moscow, Russia*

E-mail: asifnebi@gmail.com

In recent years, polymer–nanoparticle composite materials have attracted a great deal of attention in the academic and industrial fields, due to their synergistic and hybrid properties derived from several components. These materials offer unique mechanical, electrical, optical and thermal properties. Such enhancements are induced by the physical presence of the nanoparticle and by the interaction of the polymer with the particle and the state of dispersion. One of the advantages of nanoparticles as polymer additives is that compared to traditional additives, the loading requirements are quite low [1]. One of the most frequently used fillers in silicone-based composites is nanometer-sized silica that improves mechanical and electro-physical properties of a polymer. Due to the fact that the nanometer-sized silica has a large specific surface area (high surface-to-volume ratio) insertion of nanoparticle in the polymer matrix leads to changes in the intermolecular interaction at the interfaces of the resulted materials.

The work is devoted to studying the fractal properties of HDPE/SiO₂ nanocomposite films, namely, the study of mechanisms of changing the fractal dimension and the mechanism of transition from a mass fractal to a surface one using small-angle neutron and X-ray scattering. High-density polyethylene (HDPE) composite films with different amounts of SiO₂ nanoparticles (1-20 vol %) were prepared by melt blending using a high-pressure thermal pressing technique. As a filler it has been used the amorphous silica dioxide α -SiO₂ (Sky Spring Nanomaterials, Inc. Houston, USA) with 20~30 nm size of spherical particles, with the specific surface area of $S=160 \text{ m}^2/\text{g}$ and density of $2,65 \text{ g}/\text{cm}^3$.

The results of studying the fractal dimension of different concentrations of nano-silica filled polymer composites by small-angle neutron scattering are consistent with studies using small-angle X-ray scattering. Small-angle neutron scattering (SANS) measurements were performed at the time-of-flight YuMO spectrometer situated at **IBR-2** pulsed reactor (JINR, Dubna, Russia) equipped with a two-detector system [2]. The range of neutron scattering vector Q was $0.006 \text{ \AA}^{-1} < Q < 0.5 \text{ \AA}^{-1}$. The measured neutron scattering spectra were corrected for the transmission and thickness of nanocomposite films, background scattering on the film substrate and on the vanadium (*Vn*) reference sample using SAS software, yielding a neutron scattering intensity in absolute units of cm^{-1} . Small-angle X-ray (SAXS) measurements were carried on the RIGAKU spectrometer (MIPT, Dolgoprudny, Russia).

Here we consider the functional form of the scattering from mass and surface fractals. The mass fractal object of dimension D scales as $M(R) \sim R^D$. For a surface fractal, the surface area scales as $S(R) \sim R^{2-D_s}$, where d_s is between 2 and 3 for a surface fractal in three-dimensional space. It is equal to 2 for a perfectly smooth surface, and approaches 3 for a highly folded/convoluted surface.

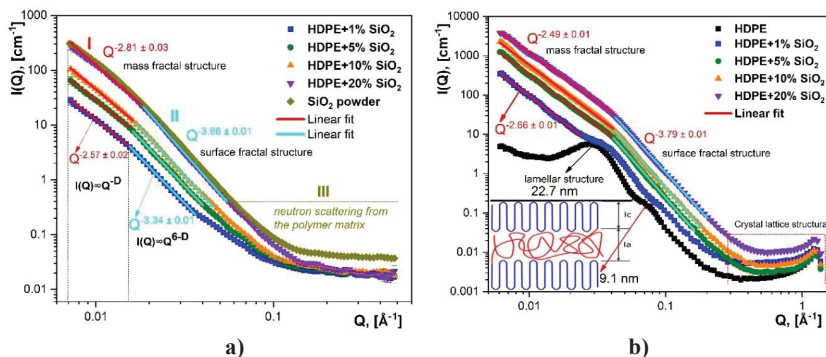


Figure 1. SANS (a) and SAXS (b) scattering curve of HDPE/SiO₂ nanocomposite films

Table 1 shows the different characteristic values derived from the measurement of the slope of the straight line in the relatively I and II region of the SANS curve, and also listed as the possible fractal behavior that associated with the nanocomposite films.

Table 1. Characteristic parameters of the fractal aggregates derived from the SANS data analysis. Here is D_m - mass-fractal dimension, D_s - surface-fractal dimension, Ω_{onset} - size of the aggregate, Ω_{end} - the size of the basic particles (the constituents of the aggregates).

Sample name and linear fit range		Slope (D)		Fractal dimension		Fractal range		Fractal type
		I and II region		D_m	D_s	Ω_{onset}, nm	Ω_{end}, nm	
HDPE+1%SiO ₂	I	2.57 ± 0.02	-	2.57	-	88.5	41.9	mass
	II	3.34 ± 0.02	-	-	2.66	41.9	17.4	surface
HDPE+5%SiO ₂	I	2.59 ± 0.02	-	2.59	-	89.7	41.7	mass
	II	3.42 ± 0.01	-	-	2.58	41.7	15.3	surface
HDPE+10%SiO ₂	I	2.73 ± 0.02	-	2.73	-	89.7	39.3	mass
	II	3.48 ± 0.02	-	-	2.52	39.3	13.7	surface
HDPE+20%SiO ₂	I	2.81 ± 0.03	-	2.81	-	88.5	34.9	mass
	II	3.66 ± 0.01	-	-	2.34	34.9	11.4	surface

SANS and SAXS experiments showed nano-SiO₂ particles mainly distributed in the polymer matrix as fractal aggregates system. All results of SANS and SAXS experiments are very good agreement. The formation of aggregated structures within the nanocomposite was confirmed by studies using SEM [3].

This work was partially supported by the Cooperation Program between Romanian scientific institutions and JINR (project of 04-4-1121-2015/2020, order №. 396/49 and №. 268/48).

[1] G.Schmidt, M. Malwitz (2003). Properties of polymer–nanoparticle composites, Current Opinion in Colloid and Interface Science. 8, 103–108.

[2] A.I. Kuklin, A.I. Ivankov, D.V. Soloviov, A.V. Rogachev, Y.S. Kovalev, A.G. Soloviev, A.K. Islamov, M. Balasoiu, A.V. Vlasov, S.A. Kutuzov, A.P. Sirotnin, A.S. Kirilov, V.V. Skoi, M.I. Rulev, V.I. Gordeliy (2018). High-throughput SANS experiment on two-detector system of YuMO spectrometer. IOP Conf. Series: Journal of Physics: Conf. Series 994 012016

[3] A.A. Nabyev (2020). Influence of nanoparticle weight fraction on morphology and thermal properties of HDPE/SiO₂ composite films, Eurasian Journal of Physics and Functional Materials, 4 (1), 38-49.

EFFECTS OF IRON AND VANADIUM IONS ON LITHIUM-PHOSPHATE GLASSES: MORPHOLOGICAL, STRUCTURAL AND SPECTROSCOPIC PROPERTIES

D. Racolta¹, M. Balasoiu^{2,3}, C. Andronache¹, L. Mihaly-Cosmuta¹, C. Mata^{3,4},
N. Belozeroва³, A. Rogachev^{3,5}, O. Orelovich³, V. Turchenko^{3,6},
A.-M. Balasoiu-Gaina^{3,7,8}, V. Sikolenko²

¹Technical University of Cluj Napoca, North University Center of Baia Mare, Romania

²Joint Institute for Nuclear Research, Dubna, Moscow oblast, Russia

³Horia Hulubei National Institute of Physics and Nuclear Engineering, Magurele, Romania

⁴“Alexandru Ioan Cuza” University of Iasi, Faculty of Chemistry, Iasi, Romania

⁵Moscow Institute of Physics and Technology, Dolgoprudny, Russia

⁶Donetsk Institute for Physics and Engineering named after O.O. Galkin, Kiev, Ukraine

⁷West University of Timisoara, Timisoara, Romania

⁸CMCF, Moscow State University, Moscow, Russia

E-mail: balas@jinr.ru

Glasses containing transition metal ions are important materials for the science, technology, and engineering, for their electrical, optical and magnetic properties that make them suitable for large number of applications in many fields [1-3]. By the addition of transition metal oxides such as Fe₂O₃ and V₂O₅ in phosphate glasses, properties such as low glass transition temperatures, high thermal expansion coefficient, and low melting temperature are acquired by the system. The addition of iron and vanadium ions enriches the characteristics of the lithium phosphate glasses system with magnetic, semiconductor and other properties [4-7]. In the present paper are reported the results of morphological, structural, and spectroscopic investigations of the system $x(\text{Fe}_2\text{O}_3 \cdot \text{V}_2\text{O}_5) \cdot (100-x)[\text{P}_2\text{O}_5 \cdot \text{Li}_2\text{O}]$ with $0 < x < 50$ mol%.

1. It was obtained that the X-ray spectra of the investigated samples are characteristic of vitreous systems. No crystalline phase was observed up to 50 mol% (Fe₂O₃ · V₂O₅).
2. The structural 2D-results from SEM are in good agreement with the 3D-results from SANS. It was found that with the increase of the x concentration the microstructure features of the system are changing from particulate to fractal [8].
3. The Raman and FTIR spectra of studies samples indicate that the (PO₂)⁻ (Q²) characteristic peak of phosphate glass doped with Fe₂O₃ and V₂O₅ are shifted to the lower values and broadened. Its intensity decrease gradually with x. The bands from 900-1100 cm⁻¹ domain pointed out the existence of the Q⁰ (PO₄)⁴⁻ and Q¹ (PO₃)²⁻ phosphate units. The majority of weaker intensity bands from FTIR spectra could be also identified as do to the phosphate blocks and FeO₆ and VO₆ groups. The transition metal ions de-polymerizes phosphate network, formations of Fe-O-P and V-O-P bonds diversifies cross-linking of the phosphate glass network [9]. This alteration turns the phosphate glass into a chemical durable glass.
4. Spectral studies valide that these samples have significant optical transmissions in UV and Visible regions. The positions of observed bands of Fe³⁺ and V⁵⁺ ions are characteristic for octahedral tetragonally distorted symmetry centers. The optical band gap energy values were decreasing slowly with increasing of x values.

The research was partially supported by RO-JINR Projects: No. 268/2020 items 6, 44, 76, and No. 269/2020 items 9, 47, 79.

- [1] W. J. Chung, et al. (2010). Compositional effect on structural and spectroscopic properties of P_2O_5 -SnO-MnO ternary glass system. *Journal of Alloys and Compounds* 505, 661.
- [2] G. Broglia et al. (2014) Lithium vanado-phosphate glasses: Structure and dynamics properties studied by molecular dynamics simulations. *J. of Non-Crystalline Solids*, 403, 53-61.
- [3] I. Ahmed, H. Ren. (2019) Developing Unique Geometries of Phosphate-Based Glasses and their Prospective Biomedical Applications. *Jonathan Booth Johnson Matthey Technol. Rev.*, 63, (1), 34-42.
- [4] C. Andronache. (2012) The local structure and magnetic interactions between Fe^{3+} and V^{4+} ions in lithium-phosphate glasses. *Materials Chemistry and Physics* 136(2-3) 281-285.
- [5] I. Ardelean et al. (2007) Raman study of $xMeO \cdot (100-x)[P_2O_5 \cdot Li_2O]$ ($MeO \Rightarrow Fe_2O_3$ or V_2O_5) glass systems, *Materials Letters* 61, 3301-3304.
- [6] C. Andronache (2010) The Comparative Structural Study of Vitreous Matrices $P_2O_5 \cdot MeO$ [$MeO \equiv Li_2O$ (M1) or CaO (M2)] Systems and $xFe_2O_3(100-x)[P_2O_5 \cdot MeO]$ Glasses by Raman Spectroscopies, *AIP Conference Proceedings* 1203 (1), 352-357
- [7] C. Andronache et al. (2017) Magnetic Properties of $x(Fe_2O_3) \cdot (100-x)[P_2O_5 \cdot Li_2O]$ and $x(Fe_2O_3) \cdot (100-x)[P_2O_5 \cdot CaO]$ Glass Systems. *AIP Conference Proceedings* 1916, 030004(1-4).
- [8] C. Andronache et al. (2019) On the structure of Lithium-Phosphate glasses doped with iron and vanadium ions. *Journal of Optoelectronics and Advanced Materials*. 21(11-12), 726-732.
- [9] A. Gasiorowski, P. Szajerski (2020). Particles size increase assisted enhancement of thermoluminescence emission in gadolinium and dysprosium oxide doped phosphate glasses. *Journal of Alloys and Compounds*, 839, 155479.

ROOM TEMPERATURE CHARGE ORBITAL ORDERING AND ASSOCIATED LOW-TEMPERATURE SPIN ORDERING IN SrMn_{0.85}Mo_{0.15}O₃ PROBED BY NEUTRON DIFFRACTION

Aga Shahee^{1,2}, K. Singh³, Emmanuelle Suard⁴, N. P. Lalla¹ and Charles Simon⁴

¹UGC-DAE Consortium for Scientific Research, University Campus, Indore-452001 (INDIA)

²Center for Novel States of Complex Materials Research, Department of Physics and Astronomy, Seoul National University, Seoul 08826, Republic of Korea

³National Institute of Technology, Jalandhar, Panjab, India

⁴Institut Laue-Langevin, 71 Avenue des Martyrs, 38000 Grenoble, France

E-mail: agashahee@gmail.com, nplallaiuc82@gmail.com

The study of charge-orbital ordering (COO) is of prime importance in the domain of transition metal oxides because it relates to the physics of important phenomena like high- T_C superconductivity, colossal magnetoresistance (CMR) and multiferroicity. Recently electron-doped SrMnO₃ has attracted a great deal of interest for their pronounced COO [1,2], which was rather unexpected due to its wideband nature [3,4]. These wide-band manganite's share a similar pseudocubic network of corner-sharing BO₆ octahedra as that of COO narrow bandwidth La_{1-x}Ca_xMnO₃, but differ in the strength of octahedral tilt. In La_{1-x}Ca_xMnO₃ ($0.3 \leq x \leq 0.9$), the large tilt of these octahedral is stabilized by the Jahn-Teller distortion of the Mn³⁺ associated with $d_{3x^2-r^2}/d_{3y^2-r^2}$ thus favors charge localization [4], while an untitled lattice of electron-doped La_{1-x}Sr_xMnO₃ ($x \geq 0.5$) stabilized by the Jahn-Teller distortion of the Mn³⁺ associated with dx^2-y^2 was expected to favor charge delocalization [5]. But recently we have observed COO in the case of La_{0.33}Sr_{0.67}MnO₃ and SrMn_{0.875}Mo_{0.125}O₃ [1,2] and is interesting owing to the lattice with a compression octahedral distortion, which implies the occupancy of the dx^2-y^2 orbital and thus anisotropic exchange interaction between neighboring Mn(B) ions within the *ab*-plan. According to the Goodenough-Kanamori-Anderson (GKA) rules [6], this type of interaction would not be compatible with the CE type magnetic structure observed in the case of COO La_{1-x}Ca_xMnO₃ and other narrow-bandwidth manganites. Instead, a zigzag $d_{3x^2-r^2}/d_{3y^2-r^2}$ orbital order is observed to be characteristic of the COO in La_{1-x}Ca_xMnO₃ and related compounds. COO associated with a lattice having compressed octahedral distortion around JT ions is a very rare phenomenon and needs further investigation.

Here we report low-temperature neutron diffraction studies on one of the COO composition SrMn_{0.85}Mo_{0.15}O₃ in the temperature range of 1.5 - 400K, to further shed light on this important issue. Utilizing powder neutron diffraction, we have studied the structural changes at the charge order transition (T_{CO}) = 350 K in this B-site doped mixed-valence SrMn_{0.85}Mo_{0.15}O₃ perovskite. Across T_{CO} we find cubic to tetragonal phase transition and a compressed octahedral distortion (i.e. lattice parameter $c < a$) associated with low-temperature tetragonal phase, which indicates the possibility of dx^2-y^2 orbital ordering. Further below this transition, super-lattice peaks are well evident once a pseudo tetragonal structure distortion is stabilized, see Fig (b). The super-lattice peaks have a non-integral modulation vector along [-110] and thus indicates an in-commensurate charge density wave (CDW) type ordering. The COO has been further confirmed through X-ray diffraction and transmission electron microscopy [2]. Thus in the SrMn_{0.85}Mo_{0.15}O₃ case, the nature of the modulated lattice structure gives evidence of a rare case of COO (i.e. charge density wave with dx^2-y^2 orbital order) inconsistent with the Goodenough-Kanamori model [6]. Recently we have reported such type of COO in La_{0.33}Sr_{0.67}MnO₃ too [1]. According to the Goodenough-Kanamori-

Anderson (GKA) rules [6], this type of lattice would not be compatible with the CE spin ordering associated with the COO phase in narrow bandwidth manganites and thus indicate an essential need of another type of spin-lattice association. On further cooling, antiferromagnetic spin ordering takes place below 220K in $\text{SrMn}_{0.85}\text{Mo}_{0.15}\text{O}_3$, as indicated by the development of magnetic peaks in the range $14\text{--}20^\circ$ of 2θ , see Fig.1(a). In this presentation, the observed charge-ordered phase (due to CDW like the behavior of the e_g -electrons of Mn^{3+} ions), the possible orbital-ordering type, and the type of low-temperature spin orders will be discussed.

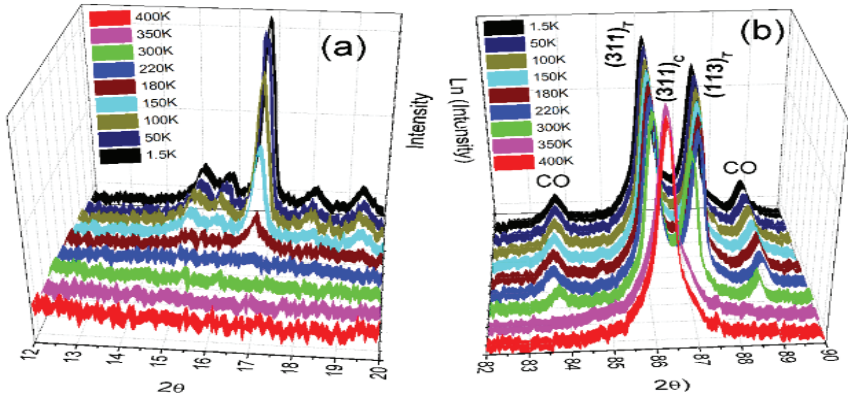


Fig.1: Temperature dependent powder neutron diffraction, evolution of (a) magnetic peaks and (b) CO peaks associated with structure phase

- [1] A. Shahee, S. Kaushik and N. P. Lalla, Charge orbital and spin ordering transitions in $\text{La}_{1-x}\text{Sr}_x\text{MnO}_{3+\delta}$ ($x = 0.67$ & 0.71), *J. Alloy. Compd.*, **782**, 277-287 (2019).
- [2] A. Shahee, and N. P. Lalla, Strong charge ordering above room temperature in B-site disordered electron-doped manganite $\text{SrMn}_{0.875}\text{Mo}_{0.125}\text{O}_3$, *Mater. Res. Express* **2**, 046106 (2015).
- [3] E. Dagotto, Open questions in CMR manganites, relevance of clustered states and analogies with other compounds including the cuprates, *New Journal of Physics* **7**, 67 (2005).
- [4] P. G. Radaelli, D. E. Cox, M. Marezio, & S.-W. Cheong, Charge, orbital, and magnetic ordering in $\text{La}_{0.5}\text{Ca}_{0.5}\text{MnO}_3$. *Phys. Rev. B* **55**, 3015–3023 (1997)
- [5] O. Chmaissem, B. Dabrowski, S. Kolesnik, J. Mais, J. D. Jorgensen, and S. Short, Structural and magnetic phase diagrams of $\text{La}_{1-x}\text{Sr}_x\text{MnO}_3$ and $\text{Pr}_{1-y}\text{Sr}_y\text{MnO}_3$ *Phys. Rev. B* **67**, 094431 (2003).
- [6] J. B. Goodenough, Theory of the Role of Covalence in the Perovskite-Type Manganites $[\text{La}, \text{M}(\text{II})]\text{MnO}_3$, *Phys. Rev.* **100**, 564 (1955).

NEUTRON DIFFRACTION STUDIES OF Ca/Ti DOPED BI FERRITES: HRFD RESULTS

V.V. Sikolenko^{1,2}, D.V. Karpinsky³, M.V. Silibin⁴, D.V. Zhaludkevich³, A.N.Chobot³, V.A. Khomchenko⁵ and I.A. Bobrikov¹

¹Joint Institute for Nuclear Research., Dubna, Russia.

²Karlsruhe Institute of Technology, Karlsruhe, Germany.

³Scientific-Practical Materials Research Centre of NAS of Belarus, Minsk, Belarus.

⁴National Research University of Electronic Technology "MIET", Moscow, Russia.

⁵CFisUC, Department of Physics, University of Coimbra, Coimbra, Portugal.

E-mail: yadim.sikolenko@jinr.ru; dmitry.karpinsky@gmail.com

Magnetolectric multiferroics based on initial compound BiFeO_3 attract persistent attention of scientific society during the last decades due to a fundamental interest and perspectives of practical applications [1, 2]. Most intriguing properties of the bismuth ferrite based oxides were observed for the compounds near the morphotropic phase boundary which can be achieved via co-doping in A- and B- perovskite lattices [3, 4]. The present report is focused on the detailed analysis of the structural phase transitions observed in the $\text{Bi}_{1-x}\text{Ca}_x\text{Fe}_{1-x}\text{Ti}_x\text{O}_3$ ($0.15 \leq x \leq 0.25$) driven by temperature. The temperature evolution of structural parameters of $\text{Bi}_{1-x}\text{Ca}_x\text{Fe}_{1-x}\text{Ti}_x\text{O}_3$ ($0.15 \leq x \leq 0.25$) has been studied by neutron diffraction using High resolution Fourier diffractometer HRFD at the IBR-2 pulsed reactor.

The crystal structure of the compound with $x=0.15$ is characterized by single phase rhombohedral structure (space group $R3c$). Increase in the dopants content up to $x=0.2$ causes a formation of the two-phase structural state, and the diffraction pattern recorded for the compound $\text{Bi}_{0.8}\text{Ca}_{0.2}\text{Fe}_{0.8}\text{Ti}_{0.2}\text{O}_3$ at room temperature was successfully refined assuming a coexistence of three different structural phases, the dominant phase is initial rhombohedral phase (phase fraction 60%), the non-polar orthorhombic phase, specific for the heavily doped compounds (space group $Pbnm$) and the anti-polar orthorhombic phase described by the space group $Pbam$ (phase fraction 30%).

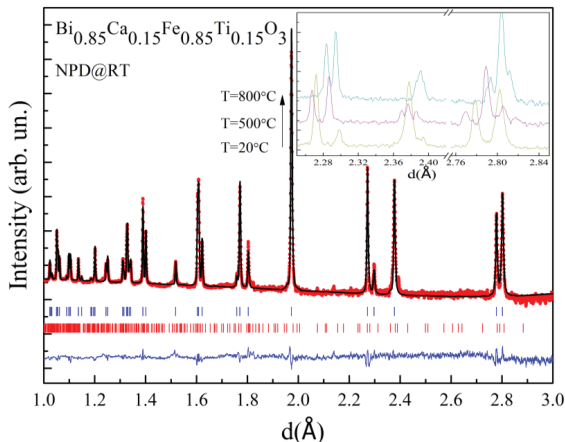


Fig. 1. The NPD pattern of $\text{Bi}_{0.85}\text{Ca}_{0.15}\text{Fe}_{0.85}\text{Ti}_{0.15}\text{O}_3$ obtained at room temperature. An evolution of the diffraction reflections ascribed to different structural phases is noted in the inset.

Further increase in the dopants content leads to a dominance of the non-polar orthorhombic phase. It should be noted that a stabilization of the intermediate anti-polar orthorhombic phase was not declared in the previous studies described the phase transition in the system $\text{Bi}_{1-x}\text{Ca}_x\text{Fe}_{1-x}\text{Ti}_x\text{O}_3$ [5, 6].

The temperature dependent NPD measurements have confirmed metastable character of the anti-polar orthorhombic phase. At temperature $T = 500^\circ\text{C}$ the structural phase of the compound with $x=0.15$ is described by a coexistence of the rhombohedral phase (15%) and a dominance of the anti-polar orthorhombic phase. Increase in temperature leads to a stabilization of non-polar orthorhombic phase (*Pbnm*) which occurs via a formation of the two phases structural state (the non-polar and anti-polar orthorhombic phases). In the compounds with larger content of the dopants ions a temperature range attributed to the anti-polar orthorhombic phase decreases while it is still observed in the compound with $x=0.25$ at elevated temperatures.

The results of the high resolution neutron diffraction measurements have assisted to confirm a formation of the intermediate structural phase described by the space group *Pbam*, which can be considered as the bridge phase in the concentration and temperature driven structural transition in the system $\text{Bi}_{1-x}\text{Ca}_x\text{Fe}_{1-x}\text{Ti}_x\text{O}_3$. Moreover, an observation of the same anti-polar orthorhombic phase in the systems $\text{Bi}_{1-x}\text{RE}_x\text{FeO}_3$ [7, 8] can point at its universal character and can be considered as the bridge phase common for the BiFeO_3 -based compounds in the structural transition from the polar rhombohedral to the non-polar orthorhombic structure.

Acknowledgments

This work has been supported by Russian Foundation for basic research (projects #20-58-00030, 20-52-00023) and Belarusian Republican Foundation for Fundamental Research (projects # F20R-123, T20R-121).

- [1] N. A. Spaldin and R. Ramesh, *Nat. Mater.* **18**, 203 (2019).
- [2] D.V. Karpinsky et al., *Nanomaterials* **10**, 801 (2020).
- [3] D. Wang et al., *J. Adv. Dielect.* **8**, 1830004 (2018).
- [4] A. Singh et al., *Phys. Rev. B* **88**, 024113 (2013).
- [5] V.A. Khomchenko et al., *Mat. Lett.* **254**, 305 (2019).
- [6] V.A. Khomchenko et al., *J. Magn. Magn. Mater.* **491**, 165561 (2019).
- [7] D.V. Karpinsky et al., *J. Am. Ceram. Soc.* **97**, 2631 (2014).
- [8] I.O. Troyanchuk et al., *Phys. Rev. B* **83**, 054109 (2011).

INFLUENCE OF RARE EARTH IN MAGNESIUM CALCIUM ALLOY USED FOR MEDICAL IMPLANTS

R.Steigmann^{1*}, A.Savin¹, F.Novy², M.L.Craus^{1,3*} and V.Turchenko³

¹National Institute of R&D for Technical Physics, Iasi, Romania

²University of Zilina, Zilina, Slovak Republic

³FNLP, JINR, Dubna, Russian Federation

E-mail: asavin@phys-iasi.ro, craus@phys-iasi.ro

Mg and their alloys have attracted many researchers for good damping capacity, low density, good stiffness and satisfactory mechanical resistance [1]. Therefore, the wider application of these alloys is highly dependent on the development of new Mg-based materials with higher corrosion resistance. Mg alloys have low corrosion resistance and therefore degrade rapidly in the human body. Thus, the development of new types of Mg alloys using new alloying elements has emerged as a natural necessity. The main phase in the MgCa_{0.5}Gd_x alloys and x=(0; 0.5; 1.0; 1.5,2.0; 3.0) are a hexagonal structure (GS 194) with the lattice constants close to those of Mg (hexagonal structure). Mg alloys used in medical applications have the selection of alloying elements not only based on their ability to improve mechanical closer to those of natural bone[2] and corrosion rate[3], but also on their biocompatibility.

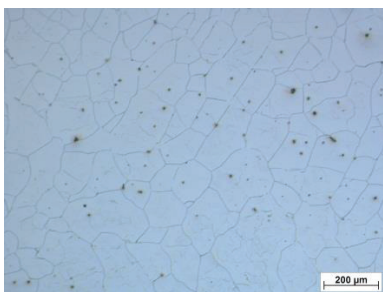


Figure 1. Representative microstructure of grains for MgCa_{0.5}Gd_{0.5}

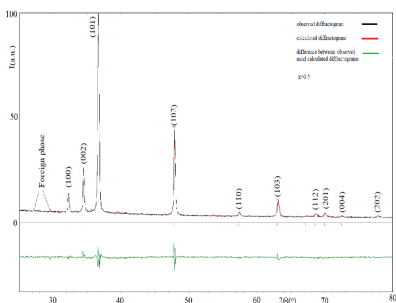


Figure 2. Observed, calculated and the difference between observed and calculated diffractograms for MgCa_{0.5}Gd_{0.5}

In order to study the influence of rare earths in magnesium calcium alloy used for medical implants, MgCa_{0.5}Gd_x alloys were prepared from high purity elements as raw materials (Mg-99.7%, Mg-15Ca and Mg-30Y master alloys), melted in an induction furnace under argon atmosphere in a graphite crucible.

Table 1. Variation of observed lattice constants (a, b, c), volume of unit cell (V), calculated lattice constants (a_{calc}, c_{calc}), average size of crystalline blocks (D) and microstrains (s) with Gd concentration (x) for MgCa_{0.5}Gd_x

x	a=b(Å)	c(Å)	V(Å ³)	a=b _{calc} (Å)	c _{calc} (Å)	D (Å)	ε	Observations
0.5	3.2149	5.2163	46.69	3.2151	5.2205	482	0.00063	Foreign phase
1.0	3.2089	5.2080	46.44	3.2171	5.2237	958	0.00202	-
1.5	3.2124	5.2088	46.55	3.2191	5.2270	799	0.00088	-
2.0	3.2119	5.2108	46.55	3.2211	5.2303	1027	0.00031	Textured ^{*)}
3.0	3.2120	5.2117	46.57	3.2251	5.2368	1027	0.00031	Textured ^{*)}

^{*)}March-Dellase model

The MgCa_{0.5}Gd_x alloys were analyzed by EDX using SEM Quanta 200 3D DUAL BEAM coupled with an EDS-EDAX detector, confirming the nominal composition of the alloy. Microstructure for MgCa_{0.5}Gd_x alloy is presented in Figure 1. Microscopic analysis was obtained using AxioCam MRc5-Zeiss. XRD analysis highlights structures type hexagonal with the formation of some chemical compounds (Figure 2). The calculated lattice constants increase with the Gd concentration (Table 1). It could be observed a maximum of the average size of crystalline blocks (D) and a minimum of microstrains (s) with the Gd concentration. The lattice constants are not dependent on the Mn concentration, despite the difference between the metallic radii of Mg (1.60 Å) and Gd (1.80 Å) (Table 1). If we compare the observed and calculated lattice constants, we can conclude that some large atoms should be observed as separated foreign phases. Because probably its concentration are very small, its cannot be observed by X ray methods. At large concentration of Gd a texture of the alloys appeared. A small concentration of strange phase appears only for alloy corresponding to x=0.05. For x>0.2 no variation of the lattice constants was observed, but the corresponding alloys seem to be textured. The calculated constants increase with the Gd concentration (Table 2). The increasing percentages of Gd introduced into the binary Mg Ca_{0.5} alloy produced a slight increase in elastic modulus and a decrease in hardness, improving corrosion resistance.

Table 2. Sample characteristics

Sample	Gd (%wt)	Density [g/mm ³]	Young modulus [GPa]	Shear modulus [GPa]	Poisson ratio	C ₁ [m/s]	C _t [m/s]
#1	0.5	1567	15.74	41.43	0.315	6105	3170
#2	1.0	1524	16.24	42.43	0.305	6171	3265
#3	1.5	1650	17.03	44.86	0.316	6204	3212
#4	2.0	1772	18.43	48.55	0.316	6227	3225
#5	3.0	1640	17.73	46.26	0.304	6198	3288

We have used the Resonant Ultrasound Spectroscopy (RUS) method for determination of mechanical properties of an elastic object, through the excitation of resonant frequencies (normal modes). The natural frequency depends on the elasticity, size and shape of the object - RUS exploits this solid property to determine the elastic tensor of the material. These frequencies depend on the size, shape, density and elastic properties of the sample. Each frequency corresponds to a particular fascicle of propagating waves and the exchange of modes. These maxims should be repeated at 1/f intervals, where f is the resonance frequency. The presence of density variation and / or microcracks was detected as a change in the shape and amplitude of the signal and as a shift in the resonant frequency of the spectral resonance range. Mechanical parameters of the samples were determined measuring longitudinal C and transversal Ct ultrasound speeds by echo pulse method [2]. Hardness was measured with NOVA 360 instrument.

Numerical simulations (in a wide variation range of G and v) it resulted that always the first maximum corresponds to a torsional mode which, in addition, is the fundamental torsional mode. The paper presents the influence of gadolinium over structure and elastic properties of the Mg Ca_{0.5} alloy in order to choose the best values appropriate with human bones, using complementary methods for test.

[1] A. A. Luo, (2004). Recent magnesium alloy development for elevated temperature applications. International materials reviews, 49(1), 13-30.

[2] A.Savin, N. Iftimie, R. Steigmann, G.S. Dobrescu, B. Istrate, and C. Munteanu, (2019). Ultrasound methods for determining the influence of yttrium in Mg-0.5 Ca-xY. In IOP Conference Series: Materials Science and Engineering, 572, 1, p. 012017.

[3] Y. Li, P.D. Hodgson, C. Wen (2011). The effects of calcium and yttrium additions on the microstructure, mechanical properties and biocompatibility of biodegradable magnesium alloys. Journal of materials science, 46(2), 365-371.

COMPLEX BEHAVIOR OF BaYFeO₄ UNDER MAGNETIC FIELDS

L.T.P. Thao^{1,2}, D.P. Kozlenko³, S.E. Kichanov³, A.V. Rutkaiukas³, N.T. Dang⁴,
L.H. Khiem^{5,6}

¹ *The University of Danang - University of Science and Education, 550000 Danang, Viet Nam*

² *Department of Physics, University of Sciences, Hue University, 530000 Hue, Viet Nam*

³ *Frank Laboratory of Neutron Physics, Joint Institute for Nuclear Research, 141980 Dubna, Russia*

⁴ *Institute of Research and Development, Duy Tan University, 550000 Danang, Viet Nam*

⁵ *Institute of Physics, Vietnam Academy of Science and Technology, 100000 Hanoi, Vietnam*

⁶ *Graduate University of Science and Technology, Vietnam Academy of Science and Technology, 100000 Hanoi, Vietnam*

E-mail: ltpthao@ued.udn.vn

Strong magnetoelectric BaYFeO₄, exhibiting spin-induced ferroelectricity, has drawn great interest in the scientific research community due to potential applications, as well as outstanding physical phenomena. In this work, we have systematically investigated high magnetic field effects on the magnetic properties of BaYFeO₄ using a combination of neutron diffraction, Mossbauer, and magnetization measurements. The sample undergoes a spin density wave (SDW) antiferromagnetic ordering at $T_{N1} \sim 55$ K and then to a cycloidal ordering at $T_{N2} \sim 35$ K, which is the origin of the appearance of ferroelectricity. A reentrant spin glass state was observed below $T^* \sim 17$ K. It has been revealed different behaviors of these magnetic states under the application of magnetic fields, for instance, the SDW and spin glass states are suppressed, whereas the cycloidal one is robust. The stability of the cycloidal order is in contrast to the suppression of ferroelectricity as previously reported. The nature of the observed phenomena has been discussed in detail.

The work was supported by the RFBR and VAST grant No. 20-52-54002. Vietnamese researchers were supported by the Vietnam Academy of Science and Technology under the Program of development in the field of physics by 2020, grant number VAST.CTVL.01/17-20 and the RFBR – VAST cooperation program, grant number QTRU01.02/20-21.

MESOSTRUCTURE OF CALCIUM CARBONATE, OBTAINED IN THE PROCESS OF BIOMINERALIZATION

N.V. Tsvigun¹, D.A. Golovkina², E.V. Zhurishkina², A.D. Yaprntsev³, A.E. Sokolov², A.A.Kulminskaya², L.A. Ivanova², A.E. Baranchikov³, Yu.E. Gorshkova⁴, V.V. Volkov¹, G.P.Kopitsa^{2,5}

¹ FSRC "Crystallography and Photonics" RAS, Moscow, Russia

² Konstantinov Petersburg Nuclear Physics Institute of NRC KI, Gatchina, Russia

³ Kurnakov Institute of General and Inorganic Chemistry of RAS, Moscow, Russia

⁴ Joint Institute for Nuclear Research, Dubna, Russia

⁵ Grebenshchikov Institute of Silicate Chemistry of RAS, St. Petersburg, Russia

E-mail: n_tsvigun@mail.ru

Various environmental factors lead to the formation of cracks in concrete materials. One of the recovery methods is biomineralization, i.e. the formation of minerals by living organisms due to reactions of their metabolism with the environment [1]. In the last decade, the ability of some bacterial strains to precipitate Ca^{2+} ions in the form of CaCO_3 , which can fill the microcracks formed in the walls of buildings, has been revealed. In the process of the vital activity of some bacteria capable of raising the pH of the environment, CO_3^{2-} is formed from CO_2 . If free Ca^{2+} ions are present in the medium near the bacterial cell, CaCO_3 precipitates, due to the fact that the cell wall carries a negative charge, and thus attracts positively charged Ca^{2+} ions. Thus, the surface of bacterial cells plays an important role as a nucleation center [2]. In the present work, the bacterial strain *Bacillus licheniformis* 8782 was cultivated using special liquid media containing urea and calcium chloride in order to obtain CaCO_3 crystals. After 2 weeks of cultivation, the *Bacillus licheniformis* 8782 strain was found to demonstrate the ability to produce significant amounts of CaCO_3 of different morphology and colors. XRD, scanning electron microscopy, low-temperature nitrogen adsorption, small-angle neutron scattering, and small-angle x-ray scattering were used to study the structure of samples of biogenic anhydride CaCO_3 , depending on the environment and the culture conditions of bacterial cells. It has been established that in most cases calcite is formed (trigonal syngony, space group R-3c).

[1] S.Joshi, S.Goyal, A.Mukherjee et al. (2017). J Ind Microbiol Biotechnol. 44(11), 1511-1525.

[2] M.Seifan, A.K.Samani, A.Berenjian. (2016). Appl Microbiol Biotechnol. 100(6), 2591-2602.

EFFECT OF CARBON ADDITIVES ON THE STRUCTURE OF ELECTRODES FOR HIGH ENERGY DENSITY LI-ION BATTERIES BY SMALL-ANGLE NEUTRON SCATTERING

Meir Yerdauletov^{1,2,3}, Philipp Napolsky¹, Mikhail Avdeev^{2,1}, Oleksandr Ivankov², Svetlana Bocharova¹, Serafima Ryzhenkova⁴, Balken Kaparova⁵, Kirill Mironovich⁶, Dmitry Burlyaev⁶, and Victor Krivchenko^{1,7}

¹*Dubna University, Dubna, Moscow Region, 141980 Russia*

²*Frank Laboratory of Neutron Physics, Joint Institute for Nuclear Research, Dubna, Moscow region, 141980 Russia*

³*Institute of Nuclear Physics, Ministry of Energy of the Republic of Kazakhstan, Almaty, 050032 Kazakhstan*

⁴*M.V. Lomonosov Moscow State University, Moscow, 119991 Russia*

⁵*L.N. Gumilev Eurasian National University, Astana, 010000 Kazakhstan*

⁶*NIIEI, JSC, Electrougli, Moscow region, 142455, Russia*

⁷*Institute of Arctic Technology of MIPT, Dolgoprudny, Moscow Region, 141701 Russia*

E-mail: meyr2008@mail.ru

Keywords: high areal capacity electrodes, pouch cell prototype, small-angle neutron scattering, porosity

Energy storage technology based on lithium-ion electrochemical systems makes it possible to manufacture batteries with high specific energy and power densities. Over the past decades, such batteries have been the most widely used ones in applications related to electric vehicles, portable electronics, and robotics. Lithium-ion battery specific parameters can be significantly improved by reducing the mass contribution of inactive components, as well as by controlling the microstructure of the electrode layers.

Using small-angle neutron scattering (SANS), the effect of conducting carbon additives (carbon black, graphene, and carbon nanotubes (CNTs)) on the porous structure of positive electrodes based on lithium iron phosphate (LiFePO₄, or LFP) was studied. To separate scattering by closed pores from scattering by open pores, the electrodes were wetted with a deuterated electrolyte, which made it possible to match the scattering from open pores. The used additives were found to change the electrode porosity to different extents and affect the wettability of the material both through a different efficiency of the incorporation of the initial material into pores and due to a change in the LFP-matrix. Thus, CNT network embedded in the electrode layer provides its greater wettability by an electrolyte compared to widely used carbon black. This results in better electrode C-rate performance.

The structure analysis allowed us to improve and optimize the technology of the fabrication of high areal capacity LFP-based electrodes. It was demonstrated that the use of CNTs as conductive additives opens prospects for producing electrodes with areal capacity of more than 5 mAh cm⁻². The practical applicability of the considered electrode technology was approved on the pouch cell prototype with specific energy density of 150 Wh kg⁻¹/295 Wh l⁻¹. [1] M.V. Avdeev, M.S. Yerdauletov, O.I. Ivankov, S.A. Bocharova, F.S. Napolsky, V.A. Krivchenko, On the Effect of Carbon Additives on the Porosity of Positive Electrodes Based on LiFePO₄ for Lithium-Ion Batteries, *J. Surf. Investigation*. 13(4) (2019) 614–618 [2] F. Napolskiy, M. Avdeev, M. Yerdauletov, O. Ivankov, S. Bocharova, S. Ryzhenkova, B. Kaparova, K. Mironovich, D. Burlyaev, D., V. Krivchenko, On the Use of Carbon Nanotubes in Prototyping the High Energy Density Li-ion Batteries, *Energy Technology* 8 (2020) 2000146

NANODIAMOND-POLY(VINYLPYRROLIDONE) COMPLEX AS PROMISING DRUG CARRIER AND THE AGENT ENHANCING PHOTODYNAMIC THERAPY

Yu.V. Kulvelis¹, V.T. Lebedev¹, A.V. Shvidchenko², E.B. Yudina², A.Ya. Vul², N.P. Yevlampieva³, M.L. Gelfond⁴

¹*Petersburg Nuclear Physics Institute named by B.P. Konstantinov of NRC "Kurchatov Institute", 188300 Gatchina, Leningrad distr., Russia*

²*Ioffe Institute, St. Petersburg, Russia*

³*Saint Petersburg State University, St. Petersburg, Russia*

⁴*NII of Oncology, St. Petersburg, Russia*

E-mail: kulvelis_yv@pnpi.nrcki.ru

Detonation nanodiamonds (DND) having non-toxic and chemical inert core and functionalized surface with positive or negative potential (Z+, Z-) are promising agents for the use in biology and medicine. However, their applications make it necessary a quest of some ways to stabilize diamond ensembles in aqueous media (isotonic solutions). So complexing with water-soluble medical polymers may promote in solving this problem and additionally in appropriate binding the drugs and medical agents with diamonds. Our study was devoted to the search of conditions obtaining stable complexes of DND with poly(vinylpyrrolidone) (PVP) in physiological aqueous solutions (Fig.1). Small angle neutron scattering applied to discover subtle features of PVP association with diamond surface has allowed to establish the influence of polymer on a short-range order in diamond ensembles. As we found, complexing did not violate original mode of DNDs' arrangement mostly to linear or slightly branched fractal aggregates with a correlation length $\sim 30\text{--}40$ nm. Moreover, the PVP provides stronger stabilization of diamond structures. It served as a binding factor for diamonds and eliminated simultaneously some sedimentation trends in dispersions. In structural studies of original DND dispersions and DND-PVP complexes we applied a contrast variation for dissolved components via exchange light water to heavy water to highlight polymer shells around diamonds and observe possible polymer structuring in solutions also. This enabled us to resolve subtle details of the localization of polymer chains around diamonds and contacts with them. This defined finally the thickness (~ 1 nm) and the density ($\sim 40\%$ vol.) of PVP in the shell around diamonds for approximately equal mass proportion of diamond and polymer components in these systems. The experiments confirmed that carboxylated DNDs are able to form complexes with poly(vinylpyrrolidone) (PVP), which are stable in isotonic saline conditions [1]. This biocompatible polymer trend to form complexes with various drugs and in our case the PVP-chains built the shells around DND particles. Therefore, the DND-PVP complex is really prospective for internal use as drug delivery system. The introduction of DND into such systems opens vast additional applications due to unique properties of DND. Particles of DND (diameter 4-5 nm) with the surface grafted by rare-earth elements (Eu, Gd) may obtain luminescent and magnetic properties intensified by defects in diamond lattice. Diamonds having scintillation properties (luminescence under X-ray irradiation) are considered as the converters in the X-ray induced photodynamic therapy (XPDT) of cancer to treat large or deep located tumors, inaccessible for laser irradiation in conventional PDT. We proposed a new approach for XPDT by the use of DND-PVP complexes with Radachlorin[®], currently serving as photosensitizer in clinical practice. Radachlorin[®] introduced into DND-PVP complex has demonstrated good luminescence properties when a high level of singlet oxygen yield was detected by luminescence in IR-range. This makes such system a good candidate for the enhancement of PDT method.

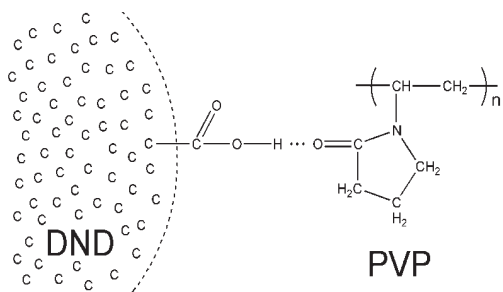


Fig. 1. Formation of hydrogen bonds between polymer and diamond via carboxylic group at the surface of diamond.

The work was supported by Russian Foundation for Basic Research (project 18-29-19008).

[1] Yu.V.Kulvelis, A.V.Shvidchenko, A.E.Aleksenskii, E.B.Yudina, V.T.Lebedev, M.S.Shestakov, A.T.Dideikin, L.O.Khozyaeva, A.I.Kuklin, Gy.Török, M.I.Rulev, A.Ya.Vul (2018). Stabilization of detonation nanodiamonds hydrosol in physiological media with poly(vinylpyrrolidone). *Diamond & Related Materials*. 87, 78–89.

[2] E.B.Yudina, A.E.Aleksenskii, I.G.Fomina, A.V.Shvidchenko, D.P.Danilovich, I.L.Eremenko, A.Ya.Vul (2019). Interaction of Carboxyl Groups with Rare Metal Ions on the Surface of Detonation Nanodiamonds. *Eur. J. Inorg. Chem.* 39-40, 4345–4349.

DYNAMIC LIGHT SCATTERING INVESTIGATIONS OF THE KINETICS OF CLUSTER GROWTH IN FULLERENE C₆₀ SOLUTIONS

N. Jargalan¹, T.V. Tropin², M.V. Avdeev², V.L. Aksenov² and D. Sangaa¹

¹*Institute of Physics and Technology, Mongolian Academy of Sciences, Ulaanbaatar 13330, Mongolia*

²*Frank Laboratory of Neutron Physics, Joint Institute for Nuclear Research, Dubna 141980, Russia*

E-mail: jargalann@mas.ac.mn

Studies of the specific carbon nano-compounds, such as nanotubes, graphite, fullerenes, nano-diamonds, etc., have been intensively conducted in various fields since the early 1990s. Among these studies, the properties of fullerenes in solution have attracted much attention of biologists and medical scientists. Depending on the properties of the solvent, interesting effects such as cluster growth, solvatochromic effects, and nonlinear solubility are observed in fullerene solutions [1-3].

In some previous works, we have studied the kinetics of fullerene dissolution and concomitant processes in low-polar and polar solvents using the UV-Vis light absorption spectroscopy [4,5]. Also, the investigations of cluster growth using small-angle neutron and X-ray scattering have been compared with theoretical works [6,7]. It was shown that donor-acceptor-type bonds form between fullerenes and solvent molecules in the nitrogen-containing solvents. The sizes of clusters and some information on their structure were also obtained within the resolution limits of the methods (1-100 nm).

In the present study, we investigate the kinetics of cluster growth using a dynamic light scattering method (Photocor DLS instrument at the FLNP). Low polar fullerene solutions (C₆₀/Benzene, C₆₀/Toluene, C₆₀/Chlorobenzene), and the polar fullerene solutions (C₆₀/NMP, C₆₀/Pyridine) were prepared in the light and dark environments. In the case of low-polar solutions, the strong effect of light on the cluster growth process was observed during the measurements. However, the polar solvents were not affected by the light. While the clusters with sizes exceeding 100 nm grow in both systems, their populations and distributions are different. We present and discuss the kinetics of growth of the mean hydrodynamic radius for the solutions measured, as well as the cluster-size distribution functions.

[1] R.S. Ruoff, S.T. Doris, R. Malhotra, D.C. Lorents. Solubility of fullerene (C₆₀) in a variety of solvents. *J. Phys. Chem.* 97, 3379 (1993).

[2] R.S. Ruoff, R. Malhotra, D.L. Huestis, D.S. Tse, D.C. Lorents. Anomalous solubility behaviour of C₆₀. *Nature* 362, 140 (1993).

[3] A. Mrzel, A. Mertelj, A. Omerzu, M. Copic, D. Mihailovic. Investigation of encapsulation and solvatochromism of fullerenes in binary solvent mixtures. *J. Phys. Chem. B*, 103, 11256 (1999).

[4] N. Jargalan, T.V. Tropin, M.V. Avdeev, V.L. Aksenov, "Investigation of the dissolution kinetics of fullerene C₆₀ in solvents with different polarities by UV-Vis spectroscopy",

Journal of surface investigation. X-ray, synchrotron and neutron techniques, Vol. 9, Issue 1, pp. 12-16, 2015.

[5] N. Jargalan, T. V. Tropin, M. V. Avdeev, V. L. Aksenov, "Investigation and modeling of evolution of UV-Vis spectra of C60/NMP solution", Journal Nanosystems: physics, chemistry, mathematics, Vol 7, Issue 1, pp. 99-103, 2016.

[6] T.V. Tropin, N. Jargalan, M.V. Avdeev, O.A. Kyzyrna, D. Sangaa, V.L. Aksenov, "The calculation of clustersize distribution functions and SANS data for C60/NMP solution", Journal Physics of the solid state, Vol. 56, Issue 1, pp. 148-151, 2014.

[7] T.V. Tropin, M.V. Avdeev, N. Jargalan, M.O. Kuzmenko, V.L. Aksenov, "Kinetics of cluster growth in fullerene solutions of different polarity", Springer proceedings in physics book series, vol 223 (2019), 249-272.

SMALL ANGLE NEUTRON SCATTERING AND GAMMA RESONANCE SPECTROSCOPY FOR METAL-NANOCARBON CHARACTERIZATION

Yu.V. Kulvelis¹, V.T. Lebedev¹, V.S. Kozlov¹, D.I. Bogmut¹, A.Ya. Vul²

¹Petersburg Nuclear Physics Institute named by B.P. Konstantinov of NRC “Kurchatov Institute”, Gatchina, Leningrad distr., Russia

²Ioffe Institute, St. Petersburg, Russia

E-mail: kulvelis_yv@pnpi.nrcki.ru

Development of advanced technologies for production and modification of metal containing carbon structures based on fullerenes, nanotubes and nanodiamonds makes it necessary a search of new ways of effective incorporation of rare earth and transition metal atoms into hollow carbon frames or covering carbon surfaces by these atoms. Designing various endo- or exostructures of nanocarbon with heavy atoms possessing high magnetic and luminescent properties is relevant for microelectronics, optics and biomedical applications. However, such a precise deposition of metals into carbon cages enclosed or opened (fullerenes, nanotubes) or linking metal atoms to diamond facets can be realized only on the base of knowledge of carbon structures together with metal-carbon mutual coordination. To achieve it we have used a combination of small angle neutron scattering (SANS) with Mössbauer (γ -resonance) spectroscopy developed at PNPI for solving various cross disciplinary tasks.

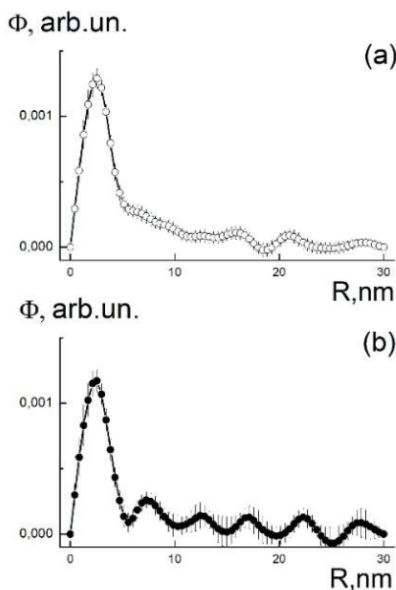


Fig. 1. Volume distribution function of polydisperse spheres vs. their radii in aqueous dispersions of pure DND (a) and with Eu atoms grafted to the surface (b).

Such a combined methodology of the analysis of metal-carbon structures was tested on the samples of detonation nanodiamonds (DND, 4-5 nm in size, negative surface potential ζ - ~ - (40-50) mV) having grafted europium atoms at the surface and dispersed in water [1]. SANS data for pure and metal-doped diamonds demonstrate a short-range order in the ensemble of diamond particles associated into coiled chains [2]. The volume distribution function of polydisperse spheres evaluated from SANS curves with the radii $R = 0-30$ nm are plotted in Fig. 1. The deposition of Eu atoms on the surface of diamonds makes the arrangement of primary DND particles more regular and some preferable dimensions of spherical formations are observed (Fig. 1b). The presence of europium at diamond facets makes their linking stronger due to possible bonds via Eu atoms which are found in the state Eu^{3+} according to the Mössbauer spectroscopy data (Fig. 2). The measurement of the ^{151}Eu Mössbauer spectra was performed on the electrodynamic type spectrometer with $^{151}\text{Sm}_2\text{O}_3$ source. Isomeric shifts are given relative to the spectrum of the Eu_2O_3 compound at 295 K. Calibration of the speed scale was performed relative to generally accepted standard $\alpha\text{-Fe}$. The spectrum of DND-Eu sample (Fig. 2) is a singlet with a line width (2.61 ± 0.10 mm/s) close to Eu_2O_3 (2.76 ± 0.04 mm/s). Comparison of spectra showed only a small negative isomer shift for Europium on diamonds (-0.49 ± 0.07 mm/s).

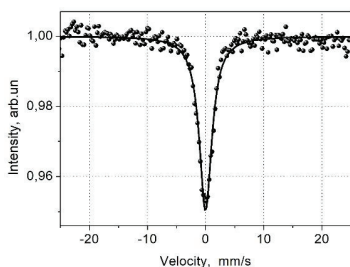


Fig. 2. Mössbauer spectrum for powder sample of DND with grafted Eu atoms. Points – experimental data, solid curve – fitting by Lorentz function.

According to Mössbauer spectrum the state of Eu atoms on diamonds is very close to this one in Eu_2O_3 compound. Diamond nanoparticles are associated stronger due to ions Eu^{3+} bonded with three carboxylic groups or hydroxyls when each atom couples diamond particles. Thus, the integration of neutron methods and gamma resonance spectroscopy has allowed to comprehend clearly the nature of diamonds ordering stimulated by grafting metal atoms to diamond surface.

The work was supported by Russian Foundation for Basic Research (project 18-29-19008).

[1] E.B.Yudina, A.E.Aleksenskii, I.G.Fomina, A.V.Shvidchenko, D.P.Danilovich, I.L.Eremenko, A.Ya.Vul (2019). Interaction of Carboxyl Groups with Rare Metal Ions on the Surface of Detonation Nanodiamonds. *Eur. J. Inorg. Chem.* 39-40, 4345–4349.

[2] Yu.V.Kulvelis, A.V.Shvidchenko, A.E.Aleksenskii, E.B.Yudina, V.T.Lebedev, M.S.Shestakov, A.T.Dideikin, L.O.Khozyaeva, A.I.Kuklin, Gy.Török, M.I.Rulev, A.Ya.Vul (2018). Stabilization of Detonation Nanodiamonds Hydrosol in Physiological Media with Poly(vinylpyrrolidone). *Diamond & Related Materials.* 87, 78–89.

GRAPHENE-NANODIAMOND COMPOSITES FOR BIOSENSOR AND ELECTRONIC APPLICATIONS

Yu.V.Kulvelis¹, M.K.Rabchinskiy², A.T.Dideikin², A.V.Shvidchenko², D.A.Kirilenko², M.V.Gudkov³

¹*Petersburg Nuclear Physics Institute named by B.P. Konstantinov of NRC "Kurchatov Institute", Gatchina, Leningrad distr., Russia*

²*Ioffe Institute, St. Petersburg, Russia*

³*Semenov Institute of Chemical Physics of Russian Academy of Sciences, Moscow, Russia*

E-mail: kulvelis_yv@pnpi.nrcki.ru

The novel complexes based on graphene oxide (GO) and its derivatives with detonation nanodiamonds (DND, particle size 4-5 nm, different sign of surface potential) are reported. Modifications of surface functional groups on reduced GO (rGO) – carboxylated and aminated rGO – make it possible to vary electrical and chemical properties of graphene. As a result, rGO may serve as a unique material prospective to be used as a transducer of electrical signals in electrochemical biosensor systems due to its excellent electrochemical performance and conducting properties. DND particles, being grafted onto graphene surface, can modify the planar graphene structure resulting in its curvature, along with possible enhancing the mechanical and conducting properties depending on the distribution of DND particles on graphene and the type of binding. GO-DND complexes were studied in a form of aqueous suspensions with varying the type and amount of both components. GO-DND aerogels were also prepared from suspensions, making ultra-porous material by removing the solvent.

GO-DND suspensions were studied by small angle neutron scattering (SANS). Additionally, GO-DND suspensions and aerogels were tested by small angle X-ray scattering (SAXS), which allows us to report the structure peculiarities on a scale 1-100 nm.

Fig. 1 shows typical SANS curves on GO and GO-DND aqueous suspensions. While pure GO has planar structure ($\frac{d\Sigma}{d\Omega(q)} \sim q^{-D}$, $D = 2.0$), the slope in GO-DND complexes rises. At few amount of DND in the complex (DND/GO = 1 : 10) $D = 2.1$, demonstrating slightly curved planar surface due to bound DND particles. At large amount of DND added (DND/GO = 1 : 1), the major of DND in the suspension is expected to be free, thus making SANS curve a result of combination of scattering on GO-DND complex and unbound DND. At $q > 1 \text{ nm}^{-1}$ the slope has the value $D \sim -4.0$, characterizing primary DND particles with sharp facets. Scattering at $q < 1 \text{ nm}^{-1}$ has the power-law ~ 2.25 , which is slightly less than 2.3-2.4, typical for DND clusters in hydrosols [1,2] due to the graphene component.

The analysis of differential SANS curves proves that DND particles bound on GO surface lose their rough cluster structure and tend to form dense planar aggregates which generally do not disturb the GO planar structure.

The mechanisms of DND assembly on graphene are discussed.

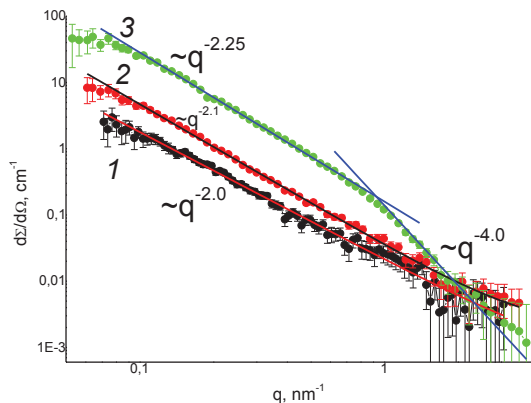


Fig. 1. SANS on GO and GO-DND suspensions with fixed GO concentrations (0.4 % wt). DND concentration = 0 (1), 0.04 % wt. (2) and 0.4 % wt. (3). Points – experimental data, solid curves – power-law approximation.

The work was supported by the Russian Foundation for Basic Research (projects 18-29-19172 and 18-29-19159).

[1] A.Ya.Vul, E.D.Eidelman, A.E.Aleksenskiy, A.V.Shvidchenko, A.T.Dideikin, V.S.Yuferev, V.T.Lebedev, Yu.V.Kulvelis, M.V.Avdeev (2017). Transition Sol-Gel in Nanodiamond Hydrosols. Carbon. 114, 242-249.

[2] V.T.Lebedev, Yu.V.Kulvelis, A.I.Kuklin, A.Ya.Vul (2016). Neutron Study of Multilevel Structures of Diamond Gels. Condensed Matter. 1, 10, 1-9.

SPECIFICS OF FULLERENE C₆₀ AND C₇₀ CLUSTER FORMATION IN TOLUENE / N-METHYL-2-PYRROLIDONE SOLVENT MIXTURE

T.V. Nagorna¹, D. Chudoba^{1,2,3}

¹Joint Institute for Nuclear Research, Dubna, Russia

²Saint Petersburg University, Saint Petersburg, Russia

³Adam Mickiewicz University, Poznan, Poland

E-mail: nagorna@jinr.ru

Special properties of C₆₀ fullerene systems are widely used in optics, radio electronics, chemical industry [1-2], etc. Nowadays fullerenes are the most valuable in medicine [3]. Usage of fullerenes in medical treatment naturally requires synthesis of aqueous fullerene solutions. In recent years several methods of obtaining such dispersions with the fullerene C₆₀ were suggested [4]. However, the particles in them form such big clusters, which disimprove their membranotropic properties. Fullerenes C₇₀ are less explored than fullerenes C₆₀. That is why investigation of properties of fullerenes C₇₀ solutions is as relevant as the exploration of their C₆₀ counterparts. Understanding the processes of transition of fullerenes into liquid medium and discovering means to control formation of clusters is an important step towards improving the methods of obtaining the aqueous solutions with sized-down aggregates of fullerenes.

In the present work, the changes of fullerene C₇₀ dissolved in NMP/toluene mixture was studied. The small-angle X-ray scattering, small-angle neutron scattering, dynamic light scattering methods were used in order to measure the wide range of particle sizes. The purpose was to find out correlation between the cluster size and polarity of system. It was observed that increase of polarity led to further dissolution of existing large agglomerates.

Obtained data were analyzed in comparison with the previous results on the inverse colloidal system, C₇₀/toluene/N-methyl-2-pyrrolidone, with UV-Vis spectroscopy measurements and experimental measurements on similar solutions with fullerene C₆₀.

References:

- [1] L. Wang (2015). Solvated fullerenes, a new class of carbon materials suitable for high-pressure studies: A review. *Journal of Physics and Chemistry of Solids*, 84, 85-95.
- [2] M. Xing, R. Wang, J. Yu (2014). Application of fullerene C₆₀ nano-oil for performance enhancement of domestic refrigerator compressors. *International Journal of Refrigeration*, 40, 398-403.
- [3] S. Afreen, K. Muthoosamy, S. Manickam, U. Hashim (2015), Functionalized fullerene (C₆₀) as a potential nanomediator in the fabrication of highly sensitive biosensors. *Biosensors and Bioelectronics*, 63, 354-364.
- [4] Yu.I. Prylutsky, S.S. Durov, L.A. Bulavin(2001). Structure, vibrational, and calorical properties of fullerene C₆₀ in toluene solution. *Fullerene Science and Technology*, 9 (2), 167-174.

ON THE IMPACT OF CAPILLARY FORCES ON THE MORPHOLOGY OF THIN FILMS OF SINGLE-WALLED CARBON NANOTUBES BY SPECULAR REFLECTOMETRY

O.V. Tomchuk^{1,2}, Ye.N. Kosiachkin^{1,2}, D.V. Krasnikov³, D.A. Ilatovskii³ and A.G. Nasibulin³

¹Joint Institute for Nuclear Research, Dubna, Russia

²Taras Shevchenko National University of Kyiv, Kyiv, Ukraine

³Skolkovo Institute of Science and Technology, Moscow, Russia

E-mail: tomchuk@jinr.ru

Single-walled carbon nanotubes (SWCNTs) are a class of materials with a wide range of properties that depend primarily on the structure of individual SWCNTs, the morphology of their secondary formations, and the content of impurities. The attractive characteristics of idealized SWCNTs make it possible to consider them as a promising component of next-generation products for various fields of science and technology: microelectronics, power engineering, aviation, *etc.* Thereby, for each specific application, SWCNTs with a set of properties specified for a given case are required. Moreover, the final application also determines the optimal approaches to material production: from fluidized bed plants for composites to aerosol chemical vapor deposition (CVD). The latter method favorably differs in the possibility of continuous production of individual carbon nanotubes, which opens up prospects for the creation of products with a predetermined morphology of secondary SWCNT formations, as well as the production of thin, transparent and flexible films [1,2]. Nevertheless, the use of these films as thin transparent electrodes is limited, among other things, by the evolution of the morphology of thin films during their wetting and subsequent drying.

In this work, the latter problem is investigated using the method of specular reflectometry of neutrons (GRAINS [3]) and X-rays (EMPYREAN, PANalytical). Structural transformations of the model system of the film of SWCNTs in its initial state, as well as after wetting with ethanol, were studied. The irreversible compaction effect was observed. The results of reflectometry experiments and complementary methods are discussed in the light of the stabilization mechanism of this nanosystem.

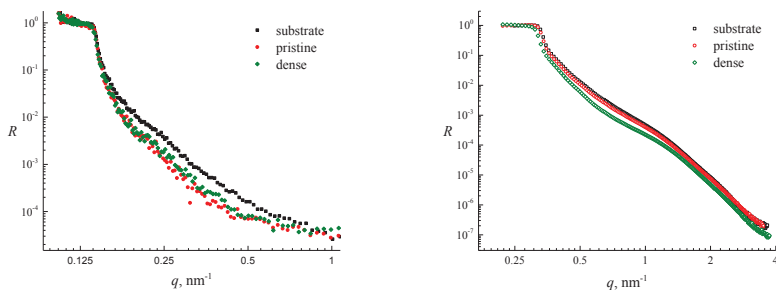


Fig. 1. Neutron (left) and X-ray (right) reflectometry on aerosol SWCNT films.

This work was supported by Russian Science Foundation No. 17-19-01787.

- [1] E.M. Khabushev *et al.* (2020). Structure-dependent performance of single-walled carbon nanotube films in transparent and conductive applications. *Carbon*. 161, 712-717.
- [2] D.S. Kopylova *et al.* (2020). Electrochemical enhancement of optoelectronic performance of transparent and conducting single-walled carbon nanotube films. *Carbon*. 167, 244-248.
- [3] M.V. Avdeev *et al.* (2017). Neutron time-of-flight reflectometer GRAINS with horizontal sample plane at the IBR-2 reactor: Possibilities and prospects. *Crystallography Reports*. 62, 1002-1008.

STRUCTURAL STUDY OF AQUEOUS SOLUTIONS OF C₆₀ AMINO DERIVATIVES FOR BIOMEDICAL APPLICATIONS

A.A. Tomchuk¹, M.V. Avdeev¹, O.I. Ivankov¹, N.N. Shershakova², E.A. Turetskii² and S.M. Andreev²

¹Joint Institute for Nuclear Research, Dubna, Russia

²NRC Institute of Immunology, Moscow, Russia

E-mail: a.a.tomchuk@gmail.com

The development of new efficient methods to obtain stable C₆₀ aqueous solutions is of current interest with respect to practical applications in medicine [1,2]. It was shown [3] that amino acids and aliphatic cyclic amines have a stabilizing effect on aqueous dispersions of C₆₀ and in some cases reduce the particle size, which improves membranotropic properties at acceptable levels of cytotoxicity.

In this study, structural characterization of colloidal aqueous solutions of C₆₀ with lysine, arginine and piperazine as stabilizers were done within a combined approach including small-angle neutron scattering (SANS), small-angle X-ray scattering (SAXS), dynamic light scattering (DLS), UV-Vis absorption spectroscopy and DFT calculations. A stabilization mechanism of the systems at nanolevel is discussed.

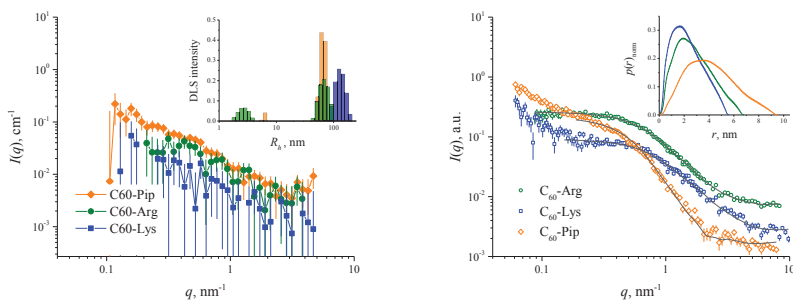


Fig. 1. Small-angle neutron (left) and X-ray (right) scattering by C₆₀-amino derivatives in water. The insets show the results of DLS measurements, as well as the indirect Fourier transform of the SAXS spectra.

The program of cooperation JINR–Czech Republic No.204/25.03.2020/33 is acknowledged.

[1] R. Klimova *et al.* (2020). Aqueous fullerene C₆₀ solution suppresses herpes simplex virus and cytomegalovirus infections. *Fullerenes, Nanotubes and Carbon Nanostructures*. 28, 487-499.

[2] A.A. Tomchuk *et al.* (2020). C₆₀ and C₆₀-arginine aqueous solutions: *In vitro* toxicity and structural study. *Fullerenes, Nanotubes and Carbon Nanostructures*. 28, 245-249.

[3] S. Andreev *et al.* (2015). Study of fullerene aqueous dispersion prepared by novel dialysis method. Simple way to fullerene aqueous solution. *Fullerenes, Nanotubes and Carbon Nanostructures*. 23, 792-800.

SIPM AND ZnS:Li6 BASED NEUTRON SCINTILLATION DETECTOR

M.V. Diachkov¹, E.V. Altynbayev¹, D.N. Trunov^{1,2}, V.N. Marin^{1,2}, V.A. Solovey¹

¹*NRC "Kurchatov Institute" — PNPI, Gatchina, Russia*

²*INR RAS, Moscow, Troitsk, Russia*

E-mail: dyachkov_mv@pnpi.nrcki.ru

The development and study of thermal and cold neutron detectors based on ZnS:Li⁶ and Silicon Photomultiplier (SiPM) is in progress since 2012. The first results were published in 2015 [1].

Tests of the neutron scintillation counter were carried out and amplitude spectra were obtained. We used ZnS(Ag)/LiF as a scintillator, the light is transported by a plexiglass and registered by two SENSL type C silicon photomultipliers (SiPM) [3]. At the edges of the light guide the two focusing "fish eye" lenses are placed in order to increase light collection. The neutron radiation source IBN-8 (²³⁸Pu) was chosen.

In order to determine the amplitude spectra, a two-channel amplitude-digital converter ADC-USB-8K-P2 ASPECT in the mode of pulse amplitude analysis (PAA) was used. In this mode, the amplitudes of input pulse signals are measured by means of analog-to-digital conversion, as well as accumulation of measured codes in the form of spectrum, where each channel accumulates a number corresponding to the number of registered pulses of the corresponding amplitude.

For radiation protection, a casemate consisting of lead bricks was built. The casemate fully covers the volume in which the scintillation counter was located and is at least 10 cm thick. In order to thermalize the neutron flux coming from the source, 10 cm thick polyethylene was used, in addition, the IBN-8 source was also covered with a 15 cm diameter polyethylene cylinder. Two millimeters thick cadmium plates were placed directly between a polyethylene and a lead shielded for neutron collimation. A slit with the width of less than 1 mm from the source to the counter was made in order to register the neutrons coming from the source. As a result, the amplitude spectra from the "fast" and "slow" SiPM signal acquisition channels were measured corresponding to two source positions relative to the photomultiplier tube inside the counter: at a distance of 1 cm to the slit and 10 cm to the slit. Differences in the obtained spectra allow us to consider the possibility to determine the spatial coordinates of neutron registration along the counter.

The work is fulfilled with the financial support of Russian Ministry of Science, agreement №075-15-2019-954 by 31.05.2019, unique identification number of project RFMEFI60718X0200

[1] A New Type of Thermal Neutron Detector Based on ZnS(Ag)/LiF Scintillator and Avalanche Photodiodes Marin, V.N., Sadykov, R.A., Trunov, D.N. et al. Tech. Phys. Lett. (2015) 41: 912. <https://doi.org/10.1134/S1063785015090242>

[2] A Ring Neutron Detector for a Time-of-flight Diffractometer Based on Linear Scintillation Detectors with Silicon Photomultipliers Marin V.N., Sadykov R.A., Trunov D.N., Litvin V.S., Axenov S.N. Instruments and Experimental Techniques. 2018. T. 61. № 1.

[3] <http://sensl.com/products/silicon-photomultipliers/>

[4] <https://www.aspect-dubna.ru/new/page.php%3Fpage=291.html>

DEVELOPMENT OF A TWO-DIMENSIONAL THERMAL-NEUTRON DETECTOR WITH AN ENTRANCE WINDOW OF 600×600 MM

T.I. Glushkova¹, A.G. Krivshich¹, V.A. Solovei¹, M.R. Kolkhidashvili¹

¹*NRC «Kurchatov Institute» - PNPI, Gatchina, Russia*

E-mail: glushkova_ti@pnpi.nrcki.ru

A gas-discharge position-sensitive detector with a sensitive area of 600×600 mm² has been developed by the Petersburg Nuclear Physics Institute (PNPI) based on a multiwire proportional chamber (MWPC). A gas mixture containing ³He is used as a neutron converter.

A detector of this type unites high detection efficiency, a low sensitivity to the γ -ray background from the source, high spatial resolution, a wide range of sensitive areas, stability of its performance characteristics, and a reasonable response speed for most experimental facilities. The uniqueness of the detectors created by the PNPI is based on the use of a special technology for manufacturing electrodes based on ultrapure glass.

A data-acquisition system based on the on-detector electronics and software was developed by the PNPI to collect and process data from the detector with a sensitive area of 600×600 mm². The cathode-strip delay-line readout is used to detect particles in the two-dimensional detector. It allows the coordinates to be determined with a small dead time, which is limited by the length of the delay line (~ 1 μ s), and with a minimum number of readout electronic channels (two channels per cathode).

The following key features have been achieved:

- four time-to-digital converters with a common start;
- the dead time of the module is 3 μ s;
- the differential nonlinearity of the time-to-digital converter is less than 5%;
- the number of channels of the time-to-digital converter is as great as 8192;
- the sensitivity of the time-to-digital converter is 130 ps per channel or higher;
- the rate capability of the system based on a computer running Windows XP 10 OS exceeds 1.5×10^5 cps.

This work was supported by the Ministry of Education and Science of the Russian Federation, contract no. 075-15-2019-954 dated May 31, 2019 (unique project identification no. RFMEFI60718X0200).

MONTE-CARLO SIMULATION OF INELASTIC NEUTRON SCATTERING SPECTROMETER

M.K. Klepacka^{1,2}, D.M. Chudoba^{1,3}

¹*Frank Laboratory of Neutron Physics, Joint Institute for Nuclear Research, Dubna, Russia*

²*Faculty of Chemical Technology, Poznan University of Technology, Poznan, Poland*

³*Faculty of Physics, Adam Mickiewicz University, Poznan, Poland*

E-mail: klepacka.mar@gmail.com

The main goal of work described in *Monte-Carlo simulation of inelastic neutron scattering spectrometer* is to examine the complementarity of virtual and real neutron scattering experiment. Simulation of a virtual experiment was made using McStas software which is based on Monte-Carlo method. The main principle of Monte-Carlo method is repeated random sampling to obtain numerical results in solving multidimensional problems with many variables. Software McStas is a popular tool for designing and modernizing single components or group of components included in the neutron scattering instrument. However, in *Monte-Carlo simulation of inelastic neutron scattering spectrometer* the whole scattering instrument was simulated – from neutron source to detectors, including sample. Simulated sample material was vanadium in a temperature of 300 K.

Real experiment was carried on NERA spectrometer in Frank Laboratory of Neutron Physics (Joint Institute for Nuclear Research, Dubna, Russia). Thanks to cooperation with JINR, thesis *Monte-Carlo simulation of inelastic neutron scattering spectrometer* received substantive support from the leader of Inelastic Neutron Scattering Group (FLNP), Dorota Chudoba PhD.

Comparison of the results obtained in real and virtual neutron scattering experiment showed that McStas software is a very efficient and accurate tool for simulating neutron interactions with elements of neutron scattering instrument. However, the comparison also showed that McStas is not recommended for simulating interactions between neutrons and sample material (simulating atom dynamics).

REACTION CELL FOR *IN SITU* NEUTRON DIFFRACTION STUDIES

A.K. Koryttseva¹, A.N. Tinakov² and A.I. Beskrovnyy³

¹*N.I.Lobachevsky State University of Nizhniy Novgorod, Nizhniy Novgorod, Russia*

²*Algorithm Co, Ltd., Nizhniy Novgorod, Russia*

³*Joint Institute for Nuclear Research, Dubna, Russia*

E-mail: koak@mail.ru

Recently a huge number of compounds with useful properties have been synthesized. These are materials for energy storage, phosphors, catalysts, materials for biomedical applications. The methods of such materials producing are being improved. The number of works on the synthesis of materials is growing faster than works studying their properties. This is due to the fact that optimal synthetic conditions are often found empirically. Knowledge of the mechanisms of nucleation and growth of inorganic compounds allows to avoid the routine selection of conditions and to do a rational design of new compounds.

An analysis of the literature shows that quantitative data that help to understand the processes occurring at the atomic level during a chemical reaction and leading to the formation of the target product are available for a limited range of compounds. As a rule, the products crystallize from heterogeneous mixtures of precursors at elevated temperatures (and often at elevated pressures). *Ex situ* techniques are often used to study such processes: at a certain time, a probe is taken from the reaction media (melt or solution) in the reaction vessel and X-ray diffraction pattern is recorded from the solid after quenching. This method is relatively simple; however, the state of the selected material does not reflect the real situation in the reaction vessel at a given time. For the study of the reaction mechanisms, real-time experiments (*in situ*) are currently relevant [1-2]. They allow establishing: the sequence of the phases formed, to quantitatively characterize the kinetics of the product crystallization. Because the position and intensity of Bragg reflections are used to determine the number of precipitated phases and their ratio, and also to establish the kinetics of growth and enlargement of particles, since the width and shape of the peaks directly depends on the particle size.

Powder diffraction of solids at high temperatures is now a routine technique and design of furnaces, known as high temperature cells, are well known and commercially available. They are used to study phase transitions and thermal stability of solids. But when it comes to chemical reactions, the solvent and / or reactive gas is present in the reaction vessel, the *in situ* reaction cell should meet certain limitations and requirements. To record powder diffraction data from a reaction mixture of chemical reagents at elevated temperatures (and pressures), special equipment is required.

To register data on neutron powder diffraction of synthesis products from precursor solutions on a real-time diffractometer (DRT) (*in situ*) at the IBR-2 pulsed reactor [3], a reaction cell was developed and manufactured taking into account the peculiarities of the neutron experiment and the chemical activity (aggressiveness) of the solution and synthesis products. The inner flask of the cell is made of teflon, a chemically resistant material. The wall thickness of the flask is 0.5 mm. Heat shields of the bottom part of the reaction cell, where reaction products are precipitated and the incident and the scattered neutron beams pass are made of 0.15

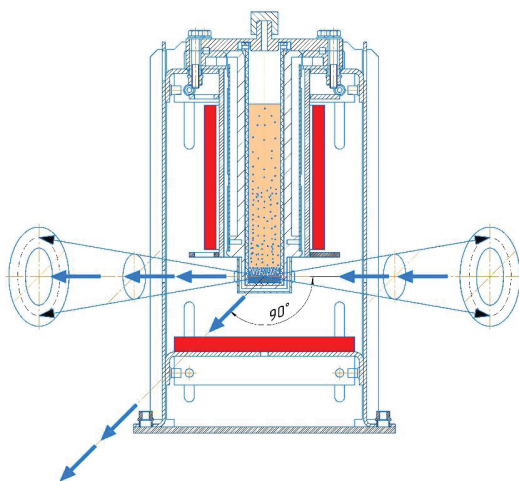


Figure 1. Reaction cell for in situ neutron diffraction studies at the IBR-2 pulsed reactor

mm vanadium. The cylindrical shape of the reaction flask allows simultaneous recording of diffraction spectra in a wide range of angles: at backscattering for maximum interplanar resolution, at intermediate angles $2\theta = 45^\circ - 135^\circ$ and small-angle neutron scattering. Temperature of the solution in the reaction cell is maintained in the range 20-100°C. The setting of the required temperature, the time of its maintenance, as well as the sequence of its change, are set by the program. The figure 1 schematically shows a reaction cell for *in situ* research in real time on a DRT diffractometer at the IBR-2 pulsed reactor.

[1] R.I. Walton, D. O'Hare (2000) Chem. Commun., 2283–2291.

[2] N. Pienack, W. Bensch (2011) Angewandte Chemie, 50, 2014-2034.

[3] A.M. Balagurov, A.I. Beskrovnyy, V.V. Zhuravlev, G.M. Mironova, I.A. Bobrikov, D. Neov, S.G. Sheverev (2016) Journal of Surface Investigation. X-ray, Synchrotron and Neutron Techniques, 10, 467–479.

ELECTROCHEMICAL CELLS FOR NEUTRON REFLECTOMETRY

Ye. Kosiachkin^{1,2}, I.V. Gapon^{2,3}, M.V. Avdeev², V.I. Petrenko^{1,2}, L.A. Bulavin¹

¹ *Physics Department, Kyiv Taras Shevchenko National University, Kyiv, Ukraine*

² *Frank Laboratory of Neutron Physics, Joint Institute for Nuclear Research, Dubna, Moscow Region, Russia*

³ *Institute for Safety Problems of Nuclear Power Plants, NAS Ukraine, Chornobyl, Ukraine*

E-mail: kosiachkin@jinr.ru

At present, the continuous growth of the use of electrochemical energy storage devices requires the development of special approaches for studying the processes taking place inside these devices, including hidden boundaries of charge separation, during their functioning. The application of neutron reflectometry (NR) to planar electrochemical interfaces makes it possible at a new scientific level to monitor the influence on the evolution of the interfaces of the initial characteristics of surfaces and environmental parameters, electrolyte composition, overvoltage, current density and other parameters. The high penetrating power of neutrons makes it possible to study complex systems that are close in conditions to real batteries. For this purpose, electrochemical cells for simultaneous monitoring of voltage/current at the interface under study together with the organization of the neutron beam passing through the interface, followed by the detection and analysis of scattering are designed. The report summarizes the results of the adaptation of NR experiment to study the evolution of the structure of electrochemical interfaces at the GRAINS reflectometer, IBR-2.

The standard scheme of the experiment suggests that incoming neutron beam (incident) is a plane beam and outgoing is reflected from the interface through a massive single-crystal silicon block coated with a thin (about 50 nm thick) electrode film that is in contact with liquid electrolyte. The interface modification, such as the appearance of the so-called solid electrolyte interphase (SEI) layer or lithium deposition during the charge/discharge processes, causes small changes in the depth profiles of the scattering length density (SLD), which are, in their turn, detected by the specular reflectivity curves. The design of the cell in the “beam from bottom” configuration was proposed which provided electrolyte filling with better control and made it possible to significantly reduce the cost of experiments because of less volumes of expensive deuterated electrolytes required in contrast variation. A higher accuracy in respect to the control of the ratio of mixed light and heavy electrolyte components in this type of experiments was achieved.

The problem of optimizing the initial structure of the “solid-liquid” interface was considered in order to maximize weak changes in the specular reflectivity curves caused by small changes of the interface. The interface was modeled as a carrier layer on a substrate, which is in contact with the solution, followed by an adsorption of a new layer from the solution over time (layer thickness up to 200 nm). The study of the specific system (electrochemical interface) made it possible to introduce restrictions on the variation of the initial interface parameters, which significantly simplified the solution of the optimization problem. Possibilities for optimizing the composition of interfaces were also considered experimentally. In particular, for better adhesion of the metal electrode layer during sputtering, an intermediate layer (Ti) is required, which impairs the sensitivity of the reflectometry experiment. Test systems with magnetron sputtering were manufactured (Mirrotron, Hungary) with minimization of the intermediate adhesive Ti-layer. It was found that advanced experimental sputtering capabilities make it possible to obtain a homogeneous

intermediate Ti-film with a thickness of down to 1 nm and less. The most preferred (in terms of sputtering quality) is a structure with a working electrode thickness (Cu) of 50 nm.

Also, to expand the possibilities for contrast variation in NR, it was proposed to use multilayered structures based on ultrathin Ti-Ni sublayers to change the average electrode SLD in a quasihomogeneous approximation. Test sputtering (Mirrotron, Hungary) and analysis of SLD profiles from measurements of neutron and X-ray reflectometry showed the possibility for realizing this idea. The controlled sputtering of such layers with a sublayer thickness of down to 0.5 nm is possible. In this case, the initial regions of the reflectivity curves, which is covered in neutron experiments ($q < 0.1 \text{ nm}^{-1}$), is well described within the quasihomogeneous approximation. Thus, along with a change in electrolyte SLD, the possibility for varying electrode SLD was shown.

Aknowledgments

Work was supported by AYSS 2020 grant № 20-402-05

HIGH-PRESSURE NEUTRON DIFFRACTOMETER DN-6: CURRENT STATE

E.V.Lukin¹, D.P.Kozlenko¹, S.E Kichanov¹, A.V. Rutkauskas¹ and B.N. Savenko¹

¹*Joint Institute for Nuclear Research, Dubna, Russian Federation*

E-mail: lukin@jinr.ru

A powder diffractometer DN-6 for TOF neutron studies in condensed matter at high pressure and low temperatures is described. A parabolic neutron focusing guide provides 5x5 mm² high-flux 3×10^7 n/sec/cm² neutron beam on a sample position allowing experiments with small volume samples about 0.01 mm³. A wide solid angle He³ based detector ring placed on 2 θ scattering angles from 87 to 93 degrees and a new detector ring with the possibility of changing the 2 θ scattering angle from 30 to 60 deg cover d_{hkl} range from 1.5 Å up to 15 Å allowing to obtain information both about crystal structure and long-period type magnetic order simultaneously. The use of closed-cycle cryostat adapted for both a sapphire pressure cells (P up to 10 GPa) and a diamond pressure cells (P up to 50 GPa) makes it possible to obtain temperature down to 4 K. The advantages of this diffractometer, demonstrated by its application to various samples at pressures up to 40GPa are shown.

The work was supported by the Russian Foundation for Basic Research, grant RFBR N19-52-45009 IND_a.

DIFFRACTOMETER MONOPOLY ON COMPACT NEUTRON SOURCE DARIA

A.E. Pavlova^{1,2}, P.I. Konik^{1,2}

¹*Saint Petersburg State University, Saint Petersburg, Russia*

²*Petersburg Institute of Nuclear Physics, Gatchina, Russia*

E-mail: st079699@student.spbu.ru

Currently, wide collaboration of Russian research centers is developing a project for the compact neutron source DARIA, intended for use in universities.

The purpose of this work is to develop a multipurpose time-of-flight diffractometer designed to study both monocrystal and powder samples over a wide range of interplanar distances. The diffractometer concept is characterized by a number of unique features. First, it is assumed to adapt the duration of the proton flash depending on the spectrum used. For nuclear structure studies, wavelengths of about 1-2 AA and a flash duration of about 22-44 μs will be used, while for studies of the magnetic structure, wavelengths of about 5 AA and a flash duration of about 120 μs will be used. Flash durations are selected based on the consideration of matching the deceleration time in the decelerator. It is noteworthy that in this configuration the diffractometer has a constant relative resolution in any operating mode. Second, a mesitylene moderator similar to the one installed on the IBR-2M reactor will be used as a moderator. This moderator is capable of operating over a wide temperature range, which will allow adapting the Maxwell spectrum to a specific study

The work was supported by the RPF grant 19-12-00363 "Development and prototyping of neutron stations for compact neutron sources".

THE INFLUENCE OF THE DELAYED NEUTRONS AT THE IBR-2 REACTOR ON THE INSTRUMENTAL RESOLUTION FUNCTION

V.V. Sadilov^{1,2}, V.I. Bodnarchuk¹ and A. I. Ioffe³

¹*Joint Institute for Nuclear Research, Frank Laboratory of Neutron Physics, Dubna, Russia*

²*Dubna State University, Dubna, Russia*

³*Jülich Centre for Neutron Science at Heinz Maier-Leibnitz Centre, Garching, Germany*

E-mail: sadilov@jinr.ru

The delayed neutrons are emitted by nuclear fission fragments in the time interval from a few milliseconds to several seconds after the fission process and the emission of prompt neutrons. Being a key factor in the stable operation of stationary nuclear reactors, they pose a serious problem for neutron instruments at the IBR-2 pulsed reactor, due to their continuous generation by the core between the primary power pulses (200 ms) [1]. Thermalized in the moderator, they create a continuous background of thermal neutrons, the emission time of which does not correlate with the main reactor pulses. Indeed, their wavelengths as determined by the time-of-flight method do not correspond to wavelengths calculated for neutrons from the main reactor pulse and return erroneously calculated value of the transferred momentum, that in turn reduces the resolution of the instrument.

In this work we estimate the contribution of the delayed neutron background to the resolution function of the time-of-flight instrument and present a method to minimize the influence of this background.

The results have been obtained by numerical calculations and by modeling by the VITESS software package [2].

[1] Anan'ev, et. al., (2004). Startup and investigation of the basic characteristics of the IBR-2 reactor with a new reactivity modulator of heterogeneous type (JINR-R--13-2004-156). Joint Institute for Nuclear Research (JINR)

[2] www.helmholtz-berlin.de/vitess

EPSILON DIFFRACTOMETER: CURRENT STATUS AND PERSPECTIVES

V.V. Sikolenko^{1,2}, B.I.R. Müller¹ and F.R. Schilling¹

¹Karlsruhe Institute of Technology, Karlsruhe, Germany

²Joint Institute for Nuclear Research, Dubna, Russia

E-mail: vadim.sikolenko@kit.edu

The TOF diffractometer Epsilon at the beamline 7a of the IBR-2 reactor dedicated to the high resolution measurements of applied and residual strains of geological samples and functional materials.

A four-axis goniometer permits a rotation around one axis and translation in 3 mutual perpendicular directions. It allows us to measure a strain profile of six independent component of strain tensor. Last years Epsilon had been equipped by variety of dedicated sample environment:

- uniaxial pressure device with possibility of sample rotation under external load with maximal pressure up to 150 MPa for *operando* measurements;
- an acoustic emission system;
- a laser extensometer for macroscopic deformation measurements of the sample with a resolution of 0.5 μm ,
- a triaxial pressure device for operando stress measurements, which allows us in situ determination of Poisson ratio, the bulk modulus and Biot-Willis coefficient.

The whole diffractometer is placed in a cabin to keep the temperature constant for long-lasting experiments, it ensures a high precision of measurements.

In this report we presents the current status of the instrument, possibilities to use it for international scientific community.

PROGRAM PACKAGE “SAS”: STATUS AND NEW FEATURES

A.G.Soloviev¹, O.I.Ivankov², A.V.Rogachev², D.V.Soloviev², A.I.Kuklin²

¹*LIT, Joint Institute for Nuclear Research, Dubna, Moscow region, Russia*

²*FLNP, Joint Institute for Nuclear Research, Dubna, Moscow region, Russia*

E-mail: soloviev@jinr.ru; kuklin@nf.jinr.ru

The methodical specific features of experiment configuration at a small angle neutron scattering spectrometer are essential for the raw data treatment. The YuMO spectrometer located at the 4-th beam-line of the IBR-2 reactor (JINR, Dubna, Russia) has specific features, namely: two-detector system, vanadium standard in front of each detectors, high flux on a sample, a direct view of the reactor core, a central hole of the detectors and special geometry of the beam [1-5]. The methodological specifications of small-angle neutron scattering (SANS) experiments are always beyond the scope of the papers aimed at highlighting the features of measurements. The main feature of YuMO spectrometer is a pulsed reactor. It allows using a wide range of wavelengths (from 0,7 Å to 10 Å) and applying time of flight method [1]. The second feature is two-detector system for small-angle scattered neutrons [3, 4]. Before having been mounted in Dubna in 2000, a similar system did never exist. Now there is at least a couple of known SANS instruments which have two-detector system. The other point is centered detectors without using a neutron guide or bender. Such geometry allows obtaining a high flux on the sample comparable to the flux of ILL in terms of SANS spectrometer, although the power of ILL reactor is much higher. One more point is the usage of a special geometry of scaling rings of gas ³He detectors, i.e. a hole in the center of the detectors. This allows applying a direct-beam detector and decreasing background scattering. Finally, a specific feature of the installation is vanadium standards in front of each detector. They periodically overlap the direct beam of neutrons that have already come through the sample. The changes of the SAS program have been made as an attempt to adapt it to a two-detector system for the YuMO spectrometer [6]. It is shown that applying weight algorithm technique for the raw data averaging procedure allows one to avoid a "sewing" problem resulting from using different detectors in rather wide q-range. The operating scheme and the background details of the experiment are discussed as well. In particular, using the fact the primary spectra are accumulated by a number of short expositions, it is suggested an iterative approach obtaining more smoothed spectra using their averaging with weights. As a result the final spectra in Q-space appears to be extended for small Q.

[1] A.I.Kuklin et al. (2017). Neutronographic investigations of supramolecular structures on upgraded small-angle spectrometer YuMO. *J. Phys. Conf. Ser.* Vol. 848. 2017.

[2] A.I.Kuklin et al. (2011). Analysis of neutron spectra and fluxes obtained with cold and thermal moderators at IBR-2 reactor: Experimental and computer-modeling studies. *Physics of Particles and Nuclear Letters* 8,2 (2011): 119.

[3] A.I.Kuklin, A. Kh. Islamov, and V. I. Gordeliy. (2005). Scientific reviews: Two-detector system for small-angle neutron scattering instrument. *Neutron News* 16.3 (2005): 16-18.

[4] A.I.Kuklin et al. (2006). Optimization two-detector system small-angle neutron spectrometer YuMO for nanoobject investigation. *Journal of Surface Investigation: X-ray, Synchrotron and Neutron Techniques* 6 (2006): 74-83.

[5] A.I.Kuklin et al. (2011). New opportunities provided by modernized small-angle neutron scattering two-detector system instrument (YuMO). *Journal of Physics: Conference Series*. Vol. 291. No. 1. IOP Publishing, 2011.

[6] A.G. Soloviev, et al. (2005). SAS program for two-detector system: seamless curve from both detectors. *J. Phys. Conf. Ser.* Vol. 848. No. 1. 2017.

DESIGN IMPROVEMENTS OF TARGET-MODERATOR-REFLECTOR ASSEMBLY OF COMPACT NEUTRON SOURCE DARIA

V. V. Subbotina^{1,2}, N. A. Kovalenko¹, P. I. Konik^{1,2}, K. A. Pavlov^{1,2}, S. V. Grigoryev^{1,2}, and V. V. Voronin^{1,2}

¹*Petersburg Nuclear Physics Institute Named by B. P. Konstantinov of National Research Centre "Kurchatov Institute", Gatchina, Russia*

²*Saint Petersburg State University, Saint Petersburg, Russia*

E-mail: vsubvgcb@gmail.com

The objective of this work is to simulate target-moderator-reflector assembly (TMR-assembly) of Compact Neutron Source DARIA. Target, moderator, reflector, cold moderator and cooling system are considered. The geometry parameters of TMR-assembly was defined. Also, fast and thermal neutron energy distribution are represented. Thermal calculation of TMR-assembly was performed.

MCNP SIMULATION OF THE BACKGROUND NEUTRON RADIATION IN THE 11B EXPERIMENTAL ROOM OF THE IBR-2 REACTOR

E.S. Teymurov^{1,2,3}, A.Yu. Nezvanov¹ and E.V. Lychagin¹

¹*Joint Institute for Nuclear Research, Dubna, Russia*

²*National Research Nuclear University MEPhI, Moscow, Russia*

³*National Nuclear Research Center, Baku, Azerbaijan*

E-mail: teymurov@jinr.ru

An experimental setup for the prompt gamma-ray thermal neutron activation analysis (PGNAA) is currently under construction for the 11b beamline of the IBR-2 reactor at Frank Laboratory of Neutron Physics [1]. Considered PGNAA technique is significantly sensitive to the background radiation in the experimental room. The neutron background is mostly determined by thermal neutrons transported from a moderator through a curved mirror neutron guide and scattered by the sample. However, there is also a direct beam of fast neutrons with energies up to several MeV, which pass through the vacuum-housings of the neutron guide. As a result, the fast neutron beam is spatially separated from the turned thermal neutron beam by several centimeters.

In this work, we present our results of fast neutron propagation through the boron carbide (3%B₄C) polyethylene composite proposed for the background minimization and the protection from fast neutrons. Monte Carlo N-Particle Transport Code was used to calculate the neutron fluxes through each face of a polyethylene cube as well as neutron angular and energy distributions. Neutrons with discrete energies of 1, 2, and 3 MeV are considered in our simulations. We divided each face of the cube into several segments to see a mesh distribution of the total neutron flux. Recommendations on the optimal size of a protective cube are also given.

[1] Hramco C. et al (2019). Thermal neutron prompt gamma activation facility at IBR-2 reactor. 27th International Seminar on Interaction of Neutrons with Nuclei.

WATER DYNAMICS IN $[\text{Cu}(\text{H}_2\text{O})_4](\text{ReO}_4)_2$ STUDIED BY IR, RS AND NEUTRON SCATTERING METHODSJ. Hetmańczyk¹ and L. Hetmańczyk¹¹ Jagiellonian University, Faculty of Chemistry, Gronostajowa 2, 30-387 Kraków, Poland

E-mail: joanna.hetmanczyk@uj.edu.pl

We report a complementary investigations of phase transition registered in tetraaquacopper(II) rhenate(VII). The polymorphism of the $[\text{Cu}(\text{H}_2\text{O})_4](\text{ReO}_4)_2$ was investigated by us by means of differential scanning calorimetry (DSC). The measurements were performed in the temperature range of 300–120 K on cooling and heating of the sample at different rates (10, 15, 20 K/min). One reversible phase transition of the investigated compounds has been found at $T_c = 232.5$ K on heating and $T_c = 231.3$ K on cooling. The thermal hysteresis of the phase transition temperature T_c equal to ca. 1.2 K and the heat flow anomaly sharpness suggest that the detected phase transition is a first-order one. The entropy change is: $\Delta S \approx 0.4 \text{ J}\cdot\text{mol}^{-1}\cdot\text{K}^{-1}$.

At room temperature tetraaquacopper(II) rhenate(VII) crystallizes in a triclinic crystal system, within the space group No. 2 = P-1, with one molecule in the unit cell [1]. The title compound is isostructural with $\text{Mg}(\text{ReO}_4)_2\cdot 4\text{H}_2\text{O}$ and $\text{Co}(\text{ReO}_4)_2\cdot 4\text{H}_2\text{O}$ [2].

Vibrational-reorientational dynamics of H_2O ligands in the high- and low-temperature phases of $[\text{Cu}(\text{H}_2\text{O})_4](\text{ReO}_4)_2$ was investigated by Fourier transform middle and far-infrared spectroscopy (FT-MIR and FT-FIR), Raman Spectroscopy (RS) and quasielastic and inelastic incoherent Neutron Scattering (QENS and IINS) methods. Vibrational RS and FT-IR spectra for $[\text{Cu}(\text{H}_2\text{O})_4](\text{ReO}_4)_2$ were measured as a function of temperature. Temperature dependent Raman light scattering measurements (RS) (295–95 K range) and Infrared spectroscopy (295–14 K) showed that bands associated with internal H_2O vibrations modes narrow continuously with temperature decreasing. The dynamics of the H_2O molecules in the high (I) and low-temperature (II) phases was investigated by means of band shape analysis performed for IR bands. The temperature dependencies of full width at half maximum (FWHM) of the FT-FIR band at 239 cm^{-1} ($\rho_{\text{r}}(\text{H}_2\text{O})$) suggests that the observed phase transition is not connected with a change of the H_2O reorientational dynamics. The H_2O ligands perform fast ($\tau_{\text{R}} \approx 10^{-12}\text{-}10^{-13} \text{ s}$) stochastic reorientational motions in the both phases (I and II) with a mean values of activation energies: 6.13 kJmol^{-1} . However continuous change of bands connected with hydrogen bonds is observed.

The incoherent inelastic/quasielastic neutron scattering spectra as well as diffraction patterns were measured using the time-of-flight method on a NERA spectrometer [3] at the high flux pulsed reactor IBR-2 in Dubna (Russia) at temperatures: 4, 100, 200 and 295 K.

Comparison of experimental phonon density function $G(\nu)$, Raman scattering and infrared absorption spectra of $[\text{Cu}(\text{H}_2\text{O})_4](\text{ReO}_4)_2$ at the lowest temperature of measurements is presented in Fig. 1. The proton-weighted phonon density functions $G(\nu)$ calculated in one phonon harmonic approximation from the time-of-flight IINS spectra in 4 K show some separate peaks characteristic for ordered phase. The $G(\nu)$ spectra obtained at 295 K are very

diffused, because of a dynamical disorder of H₂O molecules connected with their fast molecular reorientational motions.

Using vibrational spectroscopy methods (IINS, IR and RS) all characteristic wavenumbers of the internal vibrations of H₂O and ReO₄⁻ and external vibrations connected with the stretching of Cu–O and the bending of O–Cu–O bonds in [Cu(H₂O)₄]²⁺ cations were detected. Overall a good agreement between experimental G(ν), IR and RS spectra was achieved.

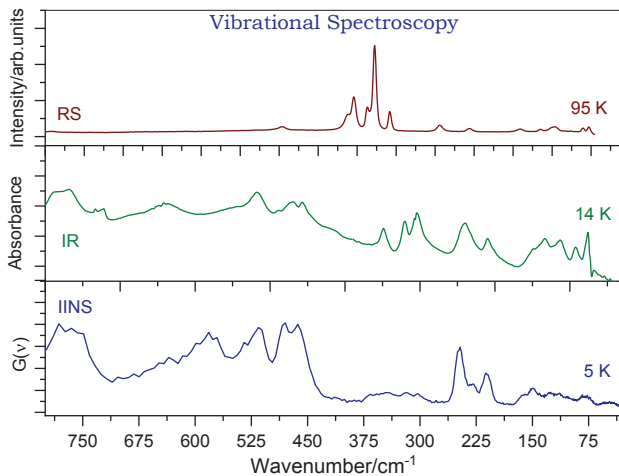


Fig. 1. The experimental phonon density of states spectrum G(ν) of [Cu(H₂O)₄](ReO₄)₂ compared to experimental IR and RS spectra in the low wavenumber range (800–30 cm⁻¹).

The QENS data registered at 4, 100, 200 and 295 K does not show any broadening. This implies, taking into account the resolution of the NERA spectrometer, that the reorientational correlation time τ_R of water ligands is longer than 10^{-12} – 10^{-11} s.

The neutron diffraction patterns (NPD) of [Cu(H₂O)₄](ReO₄)₂ registered at 295 (high temperature phase I) and at 4 K (low temperature phase II) are very similar. However some shifting of particular reflexes was observed.

The density functional theory plane wave calculations of the normal modes within the periodic boundary conditions (CASTEP code [4]) are in progress.

References

- [1] M.B. Varfolomeev, A.N. Zemenkova, V.N. Chrustalev, Ju.T. Struckov, H.J. Lunk, B. Ziemer, *J. Alloys Compd.* 215 (1994) 339–343.
- [2] M.B. Varfolomeev, V.N. Khrustalev, A.P. Pisarevskii, N.B. Shamrai, Yu.V. Syrov, *Zh. Neorg. Khim.* 44, 9 (1999) 1335–1337.
- [3] I. Natkaniec, D. Chudoba, Ł. Hetmańczyk, V.Yu. Kazimirov, J. Krawczyk, I.L. Sashin, S. Zalewski, *Journal of Physics: Conference Series*, 554 (2014) 012002.
- [4] Clark S.J., Segall M.D., Pickard C.J., Hasnip P.J., Probert M.J., Refson K., Payne M.C. (2005), *Zeitschrift fuer Kristallographie*, 220 (5–6), 567–570.

PROTON DYNAMICS IN PHTHALIC ACID ASSOCIATES

Kinga Józwiak¹, E. Goremychkin², Aneta Jezierska¹, Jarosław Panek¹, Aleksander Filarowski¹

¹ *Faculty of Chemistry, University of Wrocław 14 F. Joliot-Curie str., 50-383 Wrocław, Poland.*

² *Frank Laboratory of Neutron Physics, Joint Institute for Nuclear Research 6 F. Joliot-Curie str., 141980 Dubna, Russia.*

The spectroscopic IR, Raman and Incoherent Inelastic Neutron Scattering (IINS) studies of 3-nitrophthalic and 4-nitrophthalic acids have been carried out experimentally and theoretically by Density Functional Theory (DFT) and *Car-Parinello* Molecular Dynamics (CPMD) methods. Strong dynamics of the nitro and carboxyl groups has been investigated on the basis of first-principles CPMD calculations. The fundamental assignments of the hydrogen bond vibrational modes have been accomplished experimentally on the basis of isotopic replacement (OH → OD) and computationally by vibrational Potential Energy Distribution (PED) analysis. The vibrational spectra of nitrophthalic acids were also obtained from molecular dynamics, and compared with experimental results. The dynamics of hydrogen bonds in monomers and dimers of 3- and 4-nitro- isomers of nitrophthalic acid were analyzed on the basis of first-principles CPMD calculations.

POLARIZED NEUTRON AND X-RAY STUDY OF FE/PD/GD MULTILAYERS

N.O. Antropov¹, E.A. Kravtsov¹, M.V. Makarova¹, Yu. Khaidukov^{2,3} and V.V. Ustinov¹

¹*Institute of Metal Physics, Ural Branch of Russian Academy of Sciences, Ekaterinburg, 620990, Russia.*

²*Max-Planck-Institut für Festkörperforschung, D-70569 Stuttgart, Germany.*

³*Max Planck Society Outstation at the Heinz Maier-Leibnitz Zentrum, D-85748 Garching, Germany.*

E-mail: nikoloyantropovekb@gmail.com

Magnetic nanostructures containing thin layers of ferromagnetic and nonmagnetic metals are of considerable interest both for fundamental physics and as potential elements for novel spintronic devices. Exchange coupling of magnetic nanolayers separated by paramagnetic spacers is relatively well studied for purely rare earth (RE) systems or transition metal (TM) ones but little is known about interlayer exchange coupling RM and TM magnetic metals through paramagnets. In particular, complex magnetic order in Fe/Gd multilayers is governed by several competing mechanisms: enhancement and temperature-independence of Gd magnetic moment in the interfacial region near Fe, strong RE-TM antiferromagnetic coupling at interfaces, and Zeeman interaction with external fields.

In this work we report results of neutron/X-ray combined of Fe/Pd/Gd superlattices. Systems were grown with UHV sputtering, good layered structure was confirmed with X-ray reflectometry. By means of neutron reflectometry, we found rich phase diagram of RE/TM heterostructures which arising due to the competition of exchange coupling, magneto crystalline anisotropy and Zeeman energy. The results were obtained in the framework of the fulfillment of the theme “Spin” (grant № AAAA-A18-118020290104-2). The research was partly supported by RFBR Project №. 19-02-00674.

SMALL-ANGLE NEUTRON SCATTERING INVESTIGATION OF SEVERAL FERROFLUIDS FOR MAGNETO-OPTICAL APPLICATIONS

S. Astaf²eva¹, S. Lysenko¹, M. Balasoiu^{2,3,4}, D. Yakusheva¹, E. Kornilicina¹, A. Kuklin^{2,4}, O. Ivankov^{2,4,5}, D. Soloviov^{2,4,5}, V. Turchenko^{2,6,7}, A.-M. Balasoiu-Gaina^{2,8,9}

¹*Institute of Technical Chemistry, Perm Federal Research Center, Ural Branch, Russian Academy of Sciences, Perm, Russia*

²*Joint Institute for Nuclear Research, Dubna, Moscow Region, 141980, Russia*

³*Horia Hulubei National Institute for R&D in Physics and Nuclear Engineering, Bucharest-Magurele, Romania*

⁴*Moscow Institute of Physics and Technology, Dolgoprudny, Moscow Region, Russia*

⁵*Institute for Safety Problems of Nuclear Power Plants of the Ukrainian NAS, Kyiv, Ukraine*

⁶*South Ural State University, 76, Lenin Aven., Chelyabinsk, 454080, Russia*

⁷*Donetsk Institute for Physics and Engineering named after O.O. Galkin, Kiev, Ukraine*

⁸*West University of Timisoara, Timisoara, Romania*

⁹*CMCF, Moscow State University, Moscow, Russia*

E-mail: svetlana-astafeva@yandex.ru

New ferrofluids with improved magneto-optical response are the subject of present work. When a ferrofluid is subjected to an external magnetic field, chain-like aggregates are forming along the field direction. This field-controlled structure acquires excellent optical properties, such as tunable refractive index, magnetochromatics, as well as the thermal lens, magneto-optical, nonlinear optical, and birefringence effects [1].

Hydrothermal synthesis was used to obtain lamellar magnetic particles of barium hexaferrite, and colloidal solutions were prepared on their basis [2]. Coprecipitation method was used for preparation of copper and cobalt ferrites [2, 3]. Magneto-optical effects in colloid solutions of barium hexaferrite, cobalt ferrite and copper ferrite particles were examined. It was found that the aqueous colloidal solution of coarse planar particles of barium hexaferrite is a magneto-optical medium that is nearly two orders of magnitude more effective than the colloid formed from isometric cobalt ferrite particles [2]. Also a considerable magneto-optical response was demonstrated by the copper ferrite ferrofluid [1].

The structure of all these three ferrofluids have been investigated by means small-angle neutron scattering (SANS) at the YuMO facility in function at IBR-2 reactor. The scattering curves have been processed using the SASView software. SANS results on particle sizes are consistent with transmission electron microscopy (TEM) and dynamic light scattering (DLS) data. However, the structure of the stabilizing layer and stabilization mechanism are not still quite clear.

The new ferrofluids with enhanced magneto-optical response are expected to find new application areas [1].

The work was financially supported by the Government of Perm Krai, the research project No. S-26/791 and RO-JINR Project No.268/2020 item 31 (JINR Theme 04-4-1121-15/20).

- [1] S.N. Lysenko et al. (2020) Preparation and magneto-optical behavior of ferrofluids with anisometric particles. *Physica Scripta* 95, 044007(12pp).
- [2] S.N. Lysenko et al. (2018) Magneto-optical effects in colloidal solutions of barium hexaferrite. *Russian Journal of Applied Chemistry* 91 (10), 1574-1580.
- [3] M. Balasoiu et al. (2015) Microstructure investigation of a CoFe_2O_4 /lauric acid/DDS-Na/H₂O ferrofluid. *Journal of Optoelectronics and Advanced Materials* 17(7-8), 1114-1121.

MAGNETIC ORDERING IN Fe/MgO/Cr/MgO/Fe HETEROSTRUCTURES

E.M. Yakunina¹, N.O. Antropov^{1,2}, E.A. Kravtsov^{1,2} and V.V. Proglyado¹

¹Institute of Metal Physics, Yekaterinburg, Russia

²Ural Federal University, Yekaterinburg, Russia

E-mail: eyakuninaart@gmail.com

Fe/MgO/Cr/MgO/Fe is a novel system where the Fe magnetic moments are coupled both across insulating and metallic spacing layers. Magnetic and magnetotransport properties of magnetic multilayer structures with metal/metal and metal/insulator interfaces have been studied in depth, whereas systems including both metal and dielectric spacing layers were much less investigated. In particular, physically interesting Fe/MgO/Cr systems are studied in very limited number of publications ([1], [2]).

In the present study we report on structure and magnetic properties of Fe/MgO/Cr nanoheterostructures. In particular, we focused on the fabrication of samples, their magnetic behavior, including macroscopic properties as well as layer-resolved magnetization reversal.

Fe/MgO/Cr/MgO/Fe nanostructures were grown by UHV sputtering onto (100)MgO monocrystalline substrates without using a buffer layer. A Ta capping layer protects the system from oxidation. We have investigated two samples Fe(10nm)/MgO(1.5nm)/Cr(tnm)/MgO(1.5nm)/Fe(7nm)/Ta(5nm) with $t = 0.9$ nm (sample 1) and $t = 1.8$ nm (sample 2). These Cr thicknesses are known to provide antiferromagnetic and ferromagnetic ordering in Fe/Cr superlattices [3]. Metals were grown by DC magnetron sputtering, the insulating MgO by RF sputtering. X-ray reflectometry (XRR) and diffraction (XRD) for structural characterization of the samples was performed on an Empyrean PANalytical diffractometer using $\text{CoK}\alpha$ radiation in parallel beam geometry. The magnetization was measured by vibrating sample magnetometry (VSM). Representative XRR data and the best-fit model curve for the sample 1 are shown in Fig. 1.

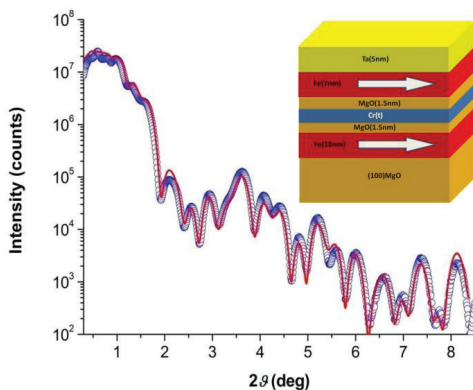


Figure 1: XRR data for sample 1 (points), model structure and resulting fit (line).

The fit of samples shows that layer thicknesses are close to their nominal values, and that there is a well-defined layered structure with sharp interfaces except for Cr with a roughness corresponding to two atomic monolayers.

By using UHV sputtering we have grown high quality Fe/MgO/Cr/MgO/Fe nanoheterostructures, their structural properties were determined with X-ray diffraction and reflectometry. VSM magnetometry shows that magnetization reversal is featured by the presence of intermediate state. This non-collinearity can be controlled by applying small external field of several tens of Oersteds and sample orientation and it is also affected by the thickness of MgO spacer. The performed study may be useful for designing the spintronic devices for operation at room temperature and also at low temperatures, in superconducting spin-valves structures where non-collinearity is required to generate spin triplet condensate.

[1] S.Yuasa, D. Djayaprawira (2007). *Appl. Phys.* 2007, 40, 337-354

[2] A. Koziol-Rachwał, T.V. Nozaki, Zayets, H. Kubota, A. Fukushima, S. Yuasa, Y.J. Suzuki (2016). *Appl. Phys.* 120, 085303.

[3] J.A.C. Bland, B. Heinrich, Edc (1994-2005). *Ultrathin Magnetic Structures*, Vols. I-IV, Springer-Verlag: Berlin

NEUTRON REFLECTOMETRY AND DIELECTRIC SPECTROSCOPY STUDY OF TRANSFORMER OIL-BASED FERROFLUIDS

M. Karpets^{1,2}, M. Rajňák^{1,2}, K. Paulovičová¹, K. Parekh³, R. V. Upadhyay³, I. Gapon⁴, P. Kopčanský¹, M. Timko¹

¹*Institute of Experimental Physics, Slovak Academy of Sciences, Kosice, Slovakia*

²*Faculty of Electrical Engineering and Informatics, Technical University of Kosice, Kosice, Slovakia*

³*K. C. Patel R&D Center, Charotar University of Science & Technology, Changa, India*

⁴*Frank Laboratory of Neutron Physics, Joint Institute for Nuclear Research, Dubna, Russia*

E-mail: karpets@saske.sk

Progress in electrical engineering puts a greater demand on the cooling and insulating properties of liquid media, such as transformer oils. To enhance their performance, researchers develop various nanofluids based on transformer oils [1]. Nanofluids, formed by adding nanoscale particles to insulating oil, are stable and homogeneous suspensions that present advanced performance of electrical insulation and heat dissipation [2].

Transformer oil-based ferrofluids with different concentration of Mn-Zn ferrite and Fe oxide nanoparticles have been characterized at normal conditions. The neutron reflectometer GRAINS with a horizontal sample plane configuration installed at the pulsed IBR-2 reactor at JINR (Dubna, Russia) was employed to study the structure at the ferrofluid/solid interface under external electric fields which are close to the operating values commonly used in high voltage power engineering. The interface structure based on the obtained parameters of the adsorption layers was analyzed, which made it possible to estimate the distribution of magnetic nanoparticles in the layers.

The dielectric-spectroscopy experiments were performed on the LCR meter in the wide frequency range from 20 Hz up to 2 MHz for different AC and DC voltage. We demonstrate changes in the observed relaxation process by applying different electric fields. Dielectric dissipation factor of ferrofluids samples was also compared. The low-frequency relaxation process features observed in experiments was assigned to the electric double layer polarization. If particles are close each to other, then the electrostatic dipole-dipole interactions appear, and together with van der Waals and magnetic dipole-dipole forces contribute to the total particle-particle interaction force.

[1] M. Rajnak et al. (2019). Magnetic Field Effect on Thermal, Dielectric, and Viscous Properties of a Transformer Oil-Based Magnetic Nanofluid. *Energies* 12, 4532.

[2] Z. Huang et al. (2019). Electrical and thermal properties of insulating oil-based nanofluids: a comprehensive overview. *IET Nanodielectrics* 2, 27–40.

PERPENDICULAR MAGNETIC ANISOTROPY OF LAYERED HETEROSTRUCTURE Dy/Co

M.V. Makarova^{1,2}, E.A. Kravtsov^{1,2}, Yu. Khaydukov³ and V.V.Ustinov¹

¹*Institute of Metal Physics, Ural Branch of the Russian Academy of Sciences, Ekaterinburg, Russia*

²*Ural Federal University, Ekaterinburg, Russia*

³*Max Planck Institute for Solid State Physics, Stuttgart, Germany*

E-mail: makarova@im.uran.ru

Rare-earth – transition metals (REM/TM) superlattices and alloys are a large class of magnetic materials allowing us to change their properties in a wide range through a change in the composition, temperatures or application magnetic field. Disordered ferrimagnetic (FI) materials demonstrate some very interesting properties, for example, magnetization compensation point, a point at which there is no magnetization below the Curie temperature [1]. Compared with their crystalline counterparts, the amorphous materials can have differing spin moments, a changed band structure, and strikingly different exchange values. Last years, interest in the Dy/Co system has increased, since it became possible to switch the magnetization of the system without applied magnetic field by means of a femtosecond laser pulses [2]. Important requirements for achieving switchable magnetic films are antiferromagnetic coupling between spins of REM and TM and perpendicular magnetic anisotropy (PMA). Therefore, it is crucial to find the correlation between the microstructure of thinner and thicker multilayers and their magnetic properties. The aim of this investigation was to define the influence of Dy thicknesses on the magnetic properties of Dy/Co multilayers. A series of [Dy (t Å)/Co (30 Å)]₄₀ ($t=4 - 20$ Å) multilayers were fabricated on single-crystal substrates of Si(100) by DC magnetron sputtering. Structural characterization of the samples was performed by X-ray diffraction (XRD) and X-ray reflectometry (XRR). Magnetic properties were investigated by VSM-magnetometry and polarized neutron reflectometry (PNR).

X-ray reflectometry and electron-microscopic studies showed formation of DyCo intermetallic compound and Co nanocrystalline layers during the grown process. Also DyCo intermetallic layers are amorphous [6]. The magnetization DyCo is aligned parallel to normal of sample plane, the Co magnetization is oriented in the direction of applied magnetic field. The superlattices consisting of two layers with uniaxial magnetic anisotropies is considered whose easy axes are oriented perpendicular to each other. By neutron reflectometry we observed strong increase of the intensity of spin-flip scattering which evidences increase of non-collinearity of the system (Fig. 1). We found rich phase diagram of Dy/Co heterostructures which arising due to the competition of exchange coupling, magneto crystalline anisotropy and Zeeman energy.

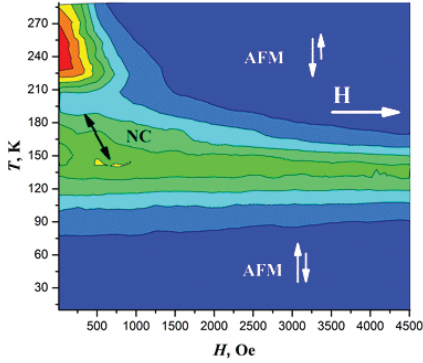


Fig. 1. The H-T phase diagram for $[\text{Dy}(20 \text{ \AA})/\text{Co}(30 \text{ \AA})]_{40}$.

The results were obtained within the state assignment of Ministry of Education and Science of Russia (subject "Spin" no. AAAA-A18-118020290104-2) supported in part by RFBR (projects no. 20-42-660024).

[1] R.C. Taylor and a. Gangulee (1980). Phys.Rev. B. 22,1320.

[2] T. Li, A. Patz, L. Mouchliadis, J. Yan, T.A. Lograsso, I.E. Perakis, J. Wang (2013). Nature. 496, 69-73.

[3] I.A. Subbotin, E.M. Pashaev, A.L. Vasiliev et al. (2019). Physica B. 573, 28.

APPLICATION OF THE GD REFERENCE LAYER APPROACH FOR THE STUDY OF MAGNETIC METALLIC NANOSTRUCTURES

E. S. Nikova^{1,2}, Yu. A. Salamatov¹, E. A. Kravtsov^{1,2}, V. V. Ustinov^{1,2}

¹*M.N.Miheev Institute of Metal Physics UB RAS, 620108, Russia, Ekaterinburg, S. Kovalevskoy str. 18*

²*Ural Federal University, 620002, Russia, Ekaterinburg, Mira str, 19*

E-mail: e.nikova@mail.ru

The polarized neutron reflectometry is one of the most powerful methods for investigation of magnetic nanostructures, and it is able to determine the magnetic moments distribution versus depth. The method is based on the analysis of the specular reflection of polarized thermal neutrons with small incident angle to the sample surface. Previously, Majkrzak et al. [1] and de Haan et al [2] have developed an approach in which the determination of complex amplitude of the reflection coefficient is performed by using a known reference layer. Unfortunately, the technique proposed in [1, 2] cannot be applied for studying magnetic systems because reflection from unknown magnetic structure is magnetic-field dependent.

We describe the model-independent approach to reflectivity analysis [3], which allows to determine the modulus and phase of the reflection coefficient based on the resonant interaction of the neutrons with gadolinium isotopes. This approach was confirmed experimentally [4].

The experiments on the reflection of polarized neutrons from the superlattice Si/Cr(10nm)/[Fe(8nm)/Cr(1.05nm)]₈/Cr(2nm)/Gd(10nm)/V(5nm) with antiferromagnetic Fe layer ordering were carried out. Here the part Gd(10nm)/V(5nm) is the reference layer. The reflectivity experiments were carried out with full polarization analysis at time-of-flight reflectometer REFLEX-P at the pulsed reactor IBR-2 (JINR, Dubna) at room temperature.

In addition, the incidence angles were exactly determined using the resonator type sample Al₂O₃/Nb(50nm)/V(10nm)/Gd(1.2nm)/V(10nm)/Nb(50nm). The experimental reflectometry curves are presented at Figure 1.

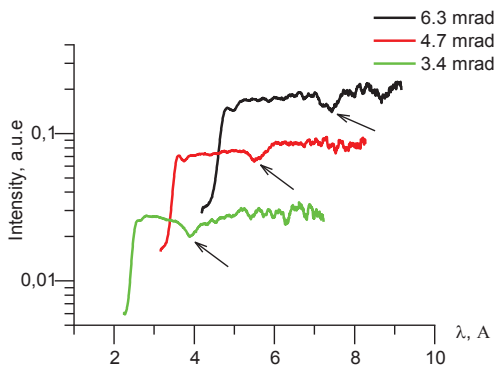


Figure 1 – The reflectometry curves for the resonator type sample. The curves are shifted along y-axis for clarity.

The intensity decrease (marked by arrow) in the region of total external reflection is due to standing wave appearance in the resonator. For different angles it occurs at different wavelength, but with the same q value. This value was calculated for one known angle and then used to determine the two unknown angles of incidence. This procedure is necessary because the reference layer approach requires the most accurate definition of incidence angles.

The research was carried out within the state assignment «Spin» AAAA-A18-118020290104-2, supported in part by RFBR (project 19-02-00674).

- [1] C. F. Majkrzak and N. F. Berk (1995). Exact determination of the phase in neutron reflectometry. *Physical Review B*, 52, 10827.
- [2] V.O. de Haan, A.A. van Well, P.E. Sacks, S. Adenwalla and G.P. Felcher (1996). Toward the solution of the inverse problem in neutron reflectometry. *Physica B*. 221, 524
- [3] Nikova E.S., Salamatov Yu.A., Kravtsov E.A., Ustinov V.V. (2017) Determination of neutron scattering potential of the thin multilayered film with gadolinium reference layer. *Superlattices and Microstructures*. 109, 201.
- [4] Nikova E.S., Salamatov Yu.A., Kravtsov E.A., Makarova M.V., Proglyado V.V., Ustinov V.V., Bodnarchuk V.I., Nagorny A.V. (2019) Experimental approbation of reference layer method in resonant neutron reflectometry. *Physics of metals and metallography*. №9, 120.

STUDY ON THE GRANULARITY OF MAGNETIC NANOPARTICLES IN AQUEOUS SUSPENSIONS. THEORETICAL AND EXPERIMENTAL APPROACH

M. Racuciu¹, L. Barbu-Tudoran², C. Morosanu³, F. Brinza³, D. Creanga³ and M. Balasoiu^{4,5}

¹Lucian Blaga University of Sibiu, Faculty of Sciences, Environmental Sciences and Physics Department, Sibiu, Romania,

²National Institute of Research and Development of Isotopic Technologies, Cluj-Napoca, Romania

³Alexandru Ioan Cuza University, Faculty of Physics, Iasi, Romania

⁴Joint Institute for Nuclear Research, Dubna, Russia

⁵Horia Hulubei Institute of Physics and Nuclear Engineering, Bucharest, Romania

E-mail: mdor@uaic.ro, dorina.emilia.creanga@gmail.com

The biomedical uses of magnetic nanoparticles require their suspension in aqueous media which is accomplished by means of coating molecules. For this reason it is important to study the coating molecule properties that ensure good interactions with magnetic core as well as with surrounding water shell. We focused on the hydrophilic organic molecules with known biocompatibility such as the aspartic acid that is able to cover the iron oxide cores balancing the magnetic dipole attraction and reducing particles agglomeration tendency. Theoretical approach of molecule structure and properties was carried out by using specialized Spartan software that allows the simulation of molecule optimized structure and provides numerical and graphical data on the properties of this structure.

We found the theoretical values of molecule solubility, electrical dipole moment, polarizability, energies of frontier electronic orbitals, electric charge density map and derived other properties.

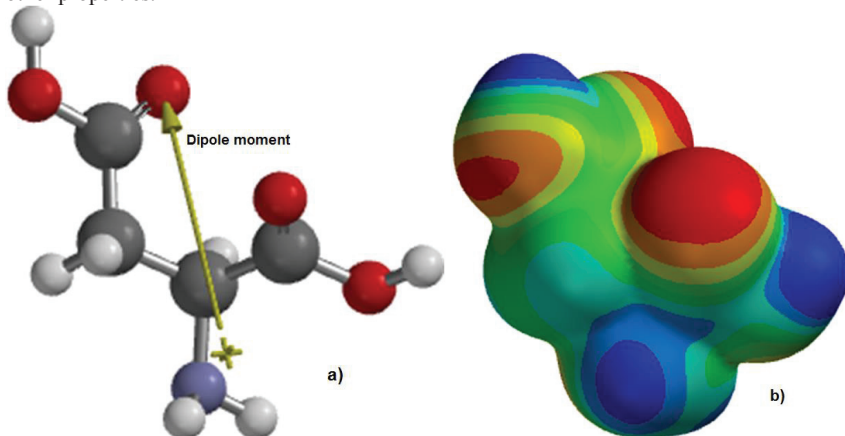


Fig. 1. a) Optimized structure of aspartic acid ($C_4H_7NO_4$) isolated molecule, modeled with Hartree-Fock 6-31G^{*} formalism; b) electrostatic potential map of the studied molecule, in red – negative sites

The dipole moment (Fig. 1 a) of about 1.6 D is close to that of water molecule (1.85 D [1]) suggesting good intermolecular interactions of water and aspartic acid that ensure nanoparticle dispersion in surrounding fluid. The electronic charge accumulation on certain

molecular sites (Fig. 1 b) indicates the availability of aspartic acid to interact with surface ions of magnetic cores, meaning suitable coating and stabilization. Comparative discussion with the properties of other organic structures known for their capacity of electrical stabilization or sterical stabilization was developed emphasizing the promising suitability of aspartic acid for magnetic nanoparticles good granularity in aqueous suspension. Experimental investigation of iron oxide/aspartic acid colloidal suspension was carried out by Transmission Electron Microscopy (TEM) and Nanoparticle Tracking Analysis (NTA). The ferrophase was prepared following a controlled chemical precipitation protocol by alkaline hydrolysis of ferric and ferrous chlorides at room temperature (22 °C) using Berger protocol [2].

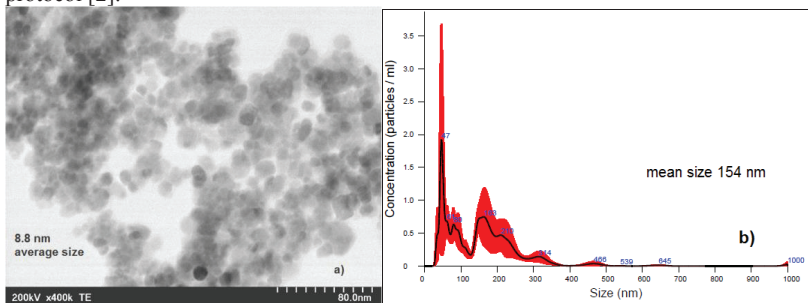


Fig. 2. Granularity data from TEM image; b) Granularity data from NTA

Size statistics carried out on TEM images has led to 8.8 nm average diameter of studied nanoparticles (Fig. 2 a). The suspension investigation by NTA has resulted in hydrodynamic mean diameter of 154 nm which is similar to the values obtained in other studies [3]. The expected results are presented that prove the good choice of this coating shell for biomedical use of magnetic nanoparticles in diluted suspensions. Further investigations are planned based on SANS methods, in order to get detailed insight in the granularity and stability of magnetic nanoparticle suspension.

- [1] M.Drab, E.Gongadze, L.Mesarec, S. Kralj, V.Kralj-Iglic, A.Iglic (2017). The internal and external dipole moment of a water molecule and orientational ordering of water dipoles in an electric double layer. *Elektrotehniski Vestnik*. 84, 221–234.
- [2] P.Berger, N.B. Adelman, K.J. Beckman, D.J. Campbell, A.B. Ellis, G.C. Lisensky (1999). Preparation and properties of an aqueous ferrofluid. *Journal of Chemical Education*. 76, 943-948.
- [3] C.Nadejde, E.Puscasu, F.Brinza, L.Ursu, D.Creanga, C.Stan (2015). Preparation of soft magnetic materials and characterization with investigation methods for fluid samples. *Scientific Bulletin of University Politehnica Bucharest Ser A*, 77, 277-284.

POSTER SESSION 2
SOFT CONDENSED MATTER (BIOLOGICAL NANOSYSTEMS,
LIPID MEMBRANES, POLYMERS)

PECTIN/BETA-LACTOGLOBULIN INTERACTIONS OBSERVED BY SMALL-ANGLE SCATTERING

L. Anghel¹, A.I. Kuklin², V.I. Bodnarchuk², and R.V. Erhan³

¹*Institute of Chemistry, Chisinau, Republic of Moldova*

²*Frank Laboratory of Neutron Physics, Joint Institute for Nuclear Research, Dubna, Russia*

³*Horia Hulubei National Institute for R&D in Physics and Nuclear Engineering, Bucharest - Magurele, Romania*

E-mail: anghel.lilia@gmail.com

The interaction of proteins with polysaccharides has aroused great interest due to their use as starting compounds in various industries including the pharmaceutical, cosmetic, and food industry [1]. Moreover, the physicochemical properties of each compound can be influenced by the presence of each other. For example, the solubility and conformation stability of proteins can be greatly changed through the interaction with polysaccharides [2], whilst the gelation properties of polysaccharides can be altered by the presence of proteins [3]. In the present study, the interactions between a globular protein (beta-lactoglobulin) [4] and an anionic polysaccharide (pectin) were studied using the small-angle scattering technique (Figure 1). The main objective of this work was to identify the main determinants of the formation and properties of pectin/beta-lactoglobulin electrostatic complexes. An understanding of the behavior of these solutions achieved through this study is a key step in optimizing these systems often used in the development of functional products.

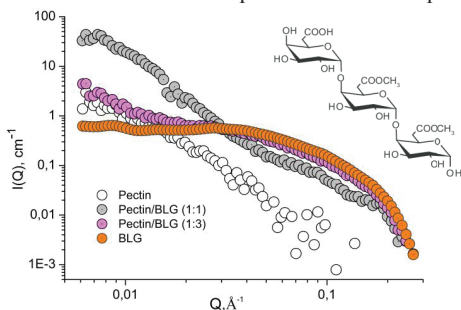


Figure 1. Pectin/beta-lactoglobulin (BLG) interactions seen by small-angle neutron scattering.

[1] C.Costa, B.Medronho, A.Filipe, I.Mira, B.Lindman, H.Edlund, M.Norgren (2019). Emulsion Formation and Stabilization by Biomolecules: The Leading Role of Cellulose. *Polymers*. 11, 1570.

- [2] Z.Cai, M.Zhao, X.Yang (2008) Effect of Polysaccharides on the Functional Properties of Peanut Protein, 2008 International Conference on BioMedical Engineering and Informatics, Sanya, 127-132.
- [3] T.S.C.Harnsilawat, R.Pongsawatmanit, D.J.McClements (2006). Characterization of beta-lactoglobulin-sodium alginate interactions in aqueous solutions: A calorimetry, light scattering, electrophoretic mobility and solubility study. *Food Hydrocolloids*. 20(5), 577-585.
- [4] L.Anghel, A.Rogachev, A.Kuklin, R.V.Erhan (2019). β -Lactoglobulin associative interactions: a small-angle scattering study. *European Biophysics Journal*. 48, 285-295.

STRUCTURAL STUDY OF THE BETA-LACTOGLOBULIN - BETA-GLUCAN SYSTEM USING SMALL-ANGLE NEUTRON SCATTERING

L. Anghel¹, A.I. Kuklin², O. Ivankov², V.I. Bodnarchuk², and R.V. Erhan³

¹*Institute of Chemistry, Chisinau, Republic of Moldova*

²*Frank Laboratory of Neutron Physics, Joint Institute for Nuclear Research, Dubna, Russia*

³*Horia Hulubei National Institute for R&D in Physics and Nuclear Engineering, Bucharest - Magurele, Romania*

E-mail: raul.erhan@gmail.com

β -Lactoglobulin is the major whey protein abundant in cow's milk. β -Lactoglobulin (Figure 1) is a lipocalin whose structure contains β -barrel with eight antiparallel β -strands and one major α -helix at the end of the molecule. This protein has been widely used in the food and pharmaceutical industries due to its rheological and structural characteristics (e.g. unfolding, aggregation and gelation properties) [1].

β -Lactoglobulin is capable of binding various hydrophobic ligands, such as fatty acids and vitamins, carbohydrates, proteins and even inorganic elements [2]. At the present there is a gap with regard to the knowledge of β -lactoglobulin and polysaccharides interactions.

Beta-glucans ($C_{18}H_{30}O_{14}X_2$) are naturally occurring polysaccharides and glucose polymers. Beta-glucans are ubiquitously found in both bacterial or fungal cell walls and have been implicated in the initiation of anti-microbial immune response [3]. One of the active compounds responsible for the immune effects of herbal products is in the form of complex polysaccharides, the beta-glucans.

As immunostimulating agent, beta-glucan can inhibit tumor growth. As example, the beta-Glucan as adjuvant to cancer chemotherapy and radiotherapy injury demonstrated the positive role in the restoration of hematopoiesis following by bone marrow injury [4].

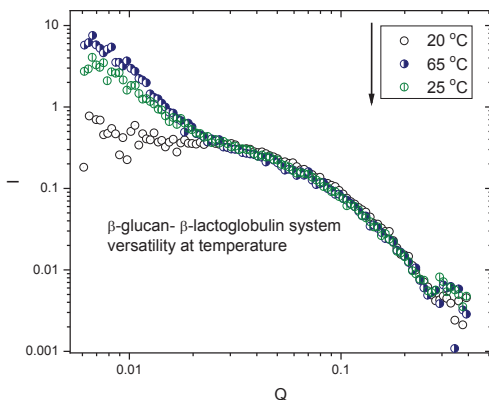


Figure 1. Versatility at temperature study measurement by small-angle neutron scattering at the YuMO SANS spectrometer, IBR-2 pulsed reactor.

A complex SANS study was carried out at the YuMO small-angle neutron spectrometer, IBR-2 pulsed reactor within $0.01 \text{ \AA} \leq q \leq 0.30 \text{ \AA}$ q-range for the β -lactoglobulin / beta-glucan system (see Figure 1).

The general goal of this study is to examine the influence of chemical composition of polysaccharides, effect of molar ratio of β -lactoglobulin:polysaccharide, NaCl presence and temperature on the interactions between β -lactoglobulin molecules and polysaccharides [5]. According to the preliminary interpretation, SANS results indicate that increasing the temperature towards 65°C contributes to formation of stable β -lactoglobulin-polysaccharide rod-like particles of an approx. $R_g=89.45 \text{ \AA}$.

[1] C. Schmitt, S.L. Turgeon (2011), *Advances in Colloid and Interface Science*. 167, 1–2 pp. 63-70.

[2.] S. Le Maux, et al. (2014), *Dairy Science & Technology*. 94, 5 pp 409-426.

[3] G. C.-F. Chan, W. K. Chan & D. M.-Y. Sze (2009), The effects of β -glucan on human immune and cancer cells, *Journal of Hematology & Oncology*, volume 2, Article number: 25.

[4] D. Akramiene, A.Kondrotas, J. Didziapetriene, E. Kevelaitis [2007]. Effects of beta-glucans on the immune system. *Medicina (Kaunas)*.43(8):597-606.

[5] L.Anghel, A.Rogachev, A.Kuklin, R.V.Erhan (2019). β -Lactoglobulin associative interactions: a small-angle scattering study. *European Biophysics Journal*. 48, 285-295.

STUDY OF IMMOBILIZATION OF POLYACRYLAMIDE ON OXIDIZED SILICON SURFACE BY X-RAY REFLECTOMETRY AND ATOMIC FORCE MICROSCOPY

Avdeev M.M.¹, Kosiachkin Ye.N.², Artykulnyi O.P.², Gorshkova Yu.E.², Shibaev A.V.¹, Philippova O.E.¹

¹ Faculty of Physics, M.V.Lomonosov Moscow State University, Moscow, Russia

² Frank Laboratory of Neutron Physics, Joint Institute for Nuclear Research, Dubna, Russia

E-mail: avdeev@polly.phys.msu.ru

Polymer passivation is one of the standard approaches of surface preparation for single-molecule studies (e.g. PALM[1], STORM[2], etc.) including the dynamics of biomolecules (proteins, enzymes[3]) and complex clusters (liposomes[4]). Passivated surface with linked target molecules allows one to observe their evolution and behavior *in situ*.

Poly(ethylene glycol) (PEG) is traditionally used for such kind of procedures, when the coverslip is seeded with a linear polymer brush. In this work, we introduce an alternative method of surface preparation: copolymerization of acrylamide and TMSPMA (3-(Trimethoxysilyl)propyl methacrylate, “anchor”) chemically bonded to the surface. It is supposed that two types of monomers equally involved in the radical polymerization, so, as a result, a nanolayer of an entangled the polymer network (CoPAM) is attached to silica surface. CoPAM is a sufficiently hydrophilic polymer, non-sensitive to salt additives. It is frequently employed in the synthesis and research of surfactant-polymer and copolymer systems. Via variation of concentration and ratio between compounds, one can control the structure of this passivated film. Here, we used fixed component concentrations to achieve reliable results.

The objective of our study is the analysis of the structure and quality of the polymer film. Using the method of X-ray reflectometry, scattering length density profiles of dried polymer films were obtained for a number of samples. Also, the surface of the samples was studied to find out any anomalies with the help of atomic force microscopy (AFM). At the next stage, we plan to investigate the swollen polymer film in water by neutron reflectometry.

Acknowledgement. The work is financially supported by the Russian Science Foundation (project № 18-73-10162).

[1] Betzig E. *et al* (2006). Imaging Intracellular Fluorescent Proteins at Nanometer Resolution. *Science* 313, 1642–1645.

[2] Linde S. *et al* (2011). Direct stochastic optical reconstruction microscopy with standard fluorescent probes. *Nature Protocols* 6, 991–1009.

[3] Rusmini F., Zhong Z. and Feijen J. (2007). Protein Immobilization Strategies for Protein Biochips. *Biomacromolecules* 8, 1775–1789.

[4] Losey E. A., Smith M. D. Meng, M. and Best M. D. (2009). Microplate-Based Analysis of Protein–Membrane Binding Interactions via Immobilization of Whole Liposomes Containing a Biotinylated Anchor. *Bioconjugate Chemistry* 20, 376–383.

CRYSTALLOGRAPHY AND SMALL-ANGLE STUDY OF CYTOCHROME P450 – REDOX PARTNER ELECTRON-TRANSFER COMPLEX

S.S. Bukhdruker¹, A. Kavaleuski², Y.L. Ryzhykau^{1,3}, T. Varaksa², S. Smolskaya⁴, A. Gilep^{2,5,6}, A.I. Kuklin^{1,3}, N. Strushkevich^{2,7} and V.I. Borshchevskiy^{1,8,9}

¹*Research Center for Molecular Mechanisms of Aging and Age-Related Diseases, Moscow Institute of Physics and Technology, Dolgoprudny, Russia*

²*Institute of Bioorganic Chemistry, National Academy of Sciences of Belarus, Minsk, Belarus*

³*Joint Institute for Nuclear Research, Dubna, Russia*

⁴*Sechenov First Moscow State Medical University, Moscow, Russia*

⁵*Institute of Biomedical Chemistry, Moscow, Russia*

⁶*MT-Medicals LLC, Moscow, Russia*

⁷*Skolkovo Institute of Science and Technology, Moscow, Russia*

⁸*Institute of Biological Information Processing (IBI-7: Structural Biochemistry), Forschungszentrum Jülich, Jülich, Germany.*

⁹*JuStruct: Jülich Center for Structural Biology, Research Center Jülich, Jülich, Germany*

E-mail: sergey.bukhdruker@phystech.edu

Cytochromes P450 (P450s or CYPs) are heme proteins, which are involved in the oxidation of numerous endogenous and exogenous compounds, including steroids, bile acids, unsaturated fatty acids and phenolic metabolites. Human CYPs from the families 1-3 are primarily responsible for the Phase I metabolism of the majority of the currently used drugs. P450s are also perspective for biotechnological application, as they catalyze regio- and stereoselective oxidation of diverse substrates. To generate reactive species, most CYPs require two electrons, which are transmitted to the heme from NAD(P)H through the redox partner. Currently, the mechanism of electron transmission from redox partner to P450s is poorly understood, as a limited number of complex structures have been published up to the date [1–4]. One of the main problems is that these complexes tend to be weak and possibly dynamic, which makes a standard protein co-crystallization technique inefficient [5]. To overcome this obstacle, one may stabilize complex via covalent linker [1], but the nativity of the resultant complex is not warranted. Here we report the atomic resolution crystal structure of P450-Cognitive Redox Partner complex. The P450 have been expressed in two ways: with a N and C terminal linker, attached to the Redox Partner, to eliminate the possible contribution of terminal motions. Two complexes share no significant differences, expect small sidechains shifts in the closest vicinity to the terminal residues. Finally, we confirmed the nativity of the resultant complex by applying SAXS. This work contributes to our understanding of electron transport between P450s and Redox Partners as well as confirms viability of the covalent linker strategy for studying metastable protein complexes.

This work was supported by a joint research grant of the Belarusian Republican Foundation for Fundamental Research (B20R-061) and the Russian Foundation for Basic Research (20-54-00005).

[1] I.F. Sevrioukova, H. Li, H. Zhang, J.A. Peterson, T.L. Poulos (1999). Structure of a cytochrome P450-redox partner electron-transfer complex, Proc. Natl. Acad. Sci. U. S. A. 96 1863–1868. <https://doi.org/10.1073/pnas.96.5.1863>.

[2] N. Strushkevich, F. MacKenzie, T. Cherksova, I. Grabovec, S. Usanov, H.W. Park (2011). Structural basis for pregnenolone biosynthesis by the mitochondrial monooxygenase

system, Proc. Natl. Acad. Sci. U. S. A. 108 10139–10143.

<https://doi.org/10.1073/pnas.1019441108>.

[3] S. Tripathi, H. Li, T.L. Poulos (2013). Structural basis for effector control and redox partner recognition in cytochrome P450, *Science* (80-.). 340 1227–1230.

<https://doi.org/10.1126/science.1235797>.

[4] A.H. Follmer, S. Tripathi, T.L. Poulos (2019). Ligand and Redox Partner Binding Generates a New Conformational State in Cytochrome P450cam (CYP101A1), *J. Am. Chem. Soc.* <https://doi.org/10.1021/jacs.8b13079>.

[5] I.F. Sevrioukova, T.L. Poulos (2011). Structural biology of redox partner interactions in P450cam monooxygenase: A fresh look at an old system, *Arch. Biochem. Biophys.* 507 66–74. <https://doi.org/10.1016/j.abb.2010.08.022>.

MOLECULAR MECHANISMS OF BITOPIC PROTEIN FUNCTIONING REVEALED BY STRUCTURAL-DYNAMIC STUDIES OF TRANSMEMBRANE DOMAIN INTERACTIONS

E.V. Bocharov^{1,2}, K.V. Pavlov³, D.M. Lesovoy^{1,2}, O.V. Bocharova^{1,2}, A.S. Urban^{1,2}, Y.V. Bershatsky^{1,2}, P.E. Volynsky², R.G. Efremov^{1,2}, A.S. Arseniev^{1,2}

¹ *Research Center for Molecular Mechanisms of Aging and Age Related Diseases, Moscow Institute of Physics and Technology (National Research University), Dolgoprudny, Russia*

² *Shemyakin-Ovchinnikov Institute of Bioorganic Chemistry RAS, Moscow, Russia*

³ *Federal Clinical Center of Physical-Chemical Medicine of FMBA, Moscow, Russia*

E-mail: edvbon@mail.ru

Bitopic membrane proteins, having only one transmembrane (TM) segment, are directly involved in the development and maintenance of homeostasis of human body tissues, providing a variety of interactions on the cell membrane. Receptor tyrosine kinases (RTK) and related receptors serve as convenient models of bitopic proteins to show how ligand-induced conformational rearrangements of extracellular and TM domains lead to allosteric activation of cytoplasmic domains during signal transmission through the cell membrane [1]. Dysregulated functioning of these receptors has been shown to play significant roles in promotion of number of human diseases, and their inhibitors have been among the most successful examples of targeted therapies to date. At the same time, Alzheimer's disease is an age-related pathology associated with the accumulation of β -amyloid peptides, - products of enzymatic cleavage by membrane sites of bitopic amyloid precursor protein (APP). Over the several years, we experimentally determined alternative conformations and intermolecular interactions of TM segments of APP and RTK-related proteins in membrane-like media. In agreement to the recent biophysical and biochemical data, we shown that the functioning of these bitopic proteins is determined not only by specific protein-protein and protein-lipid interactions, but also by the physical state of the lipid environment, as one of the main components of the self-consistent biological membrane system [1, 2]. This allowed us to propose new principles that underlie signal transmission through the cell membrane and substrate recognition by membrane proteins, as well as the mechanisms of action of a number of TM pathogenic mutations in the TM domains [1, 3].

Bioengineering work and NMR studies were sponsored by the Russian Science Foundation (project 20-64-46027). SAXS studies and MD simulations were supported by the Russian Foundation for Basic Research (projects 18-54-74001 and 18-04-01289).

[1] E.V. Bocharov et al. (2017). Conformational transitions and interactions underlying the function of membrane embedded receptor protein kinases. *BBA - Biomembranes*. 1859, 1417-1429.

[2] E.V. Bocharov et al. (2018). Structural basis of the signal transduction via transmembrane domain of the human growth hormone receptor. *BBA - General Subject*. 1862, 1410-1420.

[3] E.V. Bocharov et al. (2019). Familial L723P mutation can shift the distribution between the alternative APP transmembrane domain cleavage cascades by local unfolding of the ϵ -cleavage site suggesting a straightforward mechanism of Alzheimer's disease pathogenesis. *ACS Chemical Biology*. 14, 1573-1582.

THE PHYSICAL AND CHEMICAL CHARACTERISTICS OF FUSED PROTEIN METHIONINE γ -LYASE FROM *CLOSTRIDIUM SPOROGENES* AND S-3 DOMAIN OF GROWTH FACTOR FROM VACCINIA VIRUS

N.A. Bondarev¹, I.S. Okhrimenko¹, S.V. Bazhenov¹, N.V. Bulushova², A.I. Kuklin^{1,3}, Yu.L. Rizhikov^{1,3}, A.V. Baranova⁴, I.V. Manukhov^{1,2}

¹ *Moscow Institute of Physics and Technology, Dolgoprudny, Moscow Region, Russia*

² *State Research Institute of Genetics and Selection of Industrial Microorganisms of the National Research Centre «Kurchatov Institute», Moscow, Russia*

³ *Joint Institute for Nuclear Research, Dubna, Russia*

⁴ *School of Systems Biology, George Mason University, Fairfax, VA, USA*

E-mail: manukhovi@mail.ru

A chimeric protein MGL-S3 was obtained in which the C-terminus of methionine γ -lyase (MGL) from *Clostridium sporogenes* was fused with the N-terminus of the S-3 domain of growth factor from *Vaccinia virus*. MGL carries out an enzymatic reaction of the decomposition of methionine into ammonium-methylmercaptan and α -ketobutyrate, and it is considered promising for use in anticancer therapy [1, 2]. Methionine gamma lyase from *C. sporogenes* increases the anticancer effect of doxorubicin in A549 cells and human cancer xenografts [3]. The S3 domain of the *V. virus* VGF protein efficiently binds to the epidermal growth factor receptor (EGFR), which is overexpressed on the surface of some types of cancer cells [4]. It is assumed, that the obtained MGL-S3 chimeric protein will bind predominantly with cancer cells and create localized decrease in the methionine concentration in the tumor area, which presumably will allow to reduce the therapeutic dose and to avoid side effects.

In this work, we have determined some of the physicochemical characteristics of the obtained enzyme. In particular: the size of MGL-S3 was determined by SDS-PAAG, its methioninase activity was measured, the solubility in a solution of ammonium sulfate was investigated, and the size of the complex in solution was determined using small-angle scattering (SAXS).

Protein biosynthesis, isolation, purification, and determination of methioninase activity were carried out according to [5].

Protein biosynthesis was carried out in *Escherichia coli* cells using hybrid plasmids containing the target gene under the control of the T7 phage promoter. After cloning MGL-S3 coding genes, the resulting strains were selected according to their growth rate and ability to produce the target protein. The selected strains had the ability to biosynthesize chimeric MGLs with specific methioninase activity comparable to, but still 25% per gram of biomass lower than that of control MGL product (26.3 conventional units against 35). Perhaps the position of S3-domain at the C-terminus decreases the MGL activity, but this effect can also be explained by a decrease in the efficiency of biosynthesis.

The content of the target protein in cell lysates was about 30-40% of the total protein. The sizes of the obtained proteins corresponded to the theoretically predicted: MGL - 400 amino acids, 43.5 kDa.; MGL-S3 - 416 aa., 45.2 kDa.

Protein variants with the addition of the S3 domain differ from the control MGL preparation by SDS-PAAG (Figure 1).

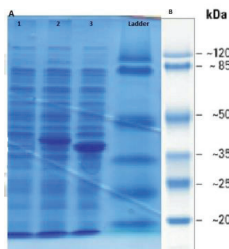


Figure 1. SDS-PAGE. 1 – cell lysate of *E. coli* BL21 pET21 without induction (negative control); 2 – cell lysate of *E. coli* BL21 pMGL-S3, induced with IPTG; 3 – cell lysate of *E. coli* BL21 pMGL, induced with IPTG; Ladder – molecular weight marker.

The solubility of MGL-S3 is slightly reduced compared to MGL. Salting out showed that MGL retains its solubility with an increase in the content of ammonium sulfate in the solution up to 55%, while MGL-S3 begins to precipitate already at 40% ammonium sulfate.

Earlier, using X-ray structural analysis and a number of biochemical methods the MGL from *C. sporogenes* was shown to be predominantly in the form of a tetramer [6]. Determination of the MGL-S3 complex size in solution using small-angle scattering showed that, in contrast to MGL, which is characterized by the tetrameric organization, it is predominantly present in solution in the form of an octamer (dimer of tetramers).

The obtained results allow planning experiments to study the cytotoxicity of a chimeric protein for various cultures of cancer cells and experiments on animals to determine the general toxicity and antiproliferative activity.

- [1] E. Cellarier, X.Durando M.P.Vasson, M.C.Farges, A.Demiden, J.C.Maurizis, J.C.Madelmont, P.Chollet (2003). Methionine dependency and cancer treatment. *Cancer Treat. Rev.*29, 488-489. ;
- [2] Tan Y., Xu M., Hoffman R.M. (2010) Broad selective efficacy of recombinant methioninase and polyethylene glycol-modified recombinant methioninase on cancer cells *In Vitro. Anticancer Res.*, 30, 793-798;
- [3] VS.Pokrovsky, Yu Anisimova N, Zh Davydov D, SV.Bazhenov, NV.Bulushova, GB.Zavilgelsky, VY.Kotova, IV.Manukhov (2019). Methionine- γ -lyase from *Clostridium sporogenes* increases the anticancer effect of doxorubicin in A549 cells and human cancer xenografts. *Invest New Drugs*. Jun 15. doi: 10.1007/s10637-018-0619-4.
- [4] L.T.Nguyen, X-Z.Yang, X.Du, J-W.Wang, R.Zhang, J.Zhao, F-J.Wang, Y.Dong, P.-F.Li (2015). Enhancing tumor-specific intracellular delivering efficiency of cell-penetrating peptide by fusion with a peptide targeting to EGFR. *Amino Acids.* 47(5):997-1006.
- [5] VS.Pokrovsky, Yu Anisimova N, Zh Davydov D, SV.Bazhenov, NV.Bulushova, GB.Zavilgelsky, VY.Kotova, IV.Manukhov (2019). Methionine dependence of cancer and aging: methods and protocols. R.M. Hoffman, Editor. Chapter 18. Methionine gamma lyase from *Clostridium sporogenes* increases the anticancer effect of doxorubicin in A549 cancer cells in vitro and human cancer xenografts. Springer Nature. Springer Science+Business Media, LLC, Humana Press. ISBN 978-1-4939-8795-5].
- [7] S.Revtovich, N.Anufrieva, E.Morozova, V.Kulikova, A.Nikulina, T.Demidkina. Structure of methionine γ -lyase from *Clostridium sporogenes*. *Acta Crystallogr F Struct Biol Commun*. 2016 Jan;72(Pt 1):65-71.

BIOHYBRID COMPLEXES WITH PHYTO-GENERATED ENTITIES FROM NETTLE & GRAPES AND THEIR POTENTIAL APPLICATION IN THE BIOMEDICAL FIELD

Yu.E. Gorshkova¹, M.E. Barbinta-Patrascu², G.D. Bokuchava¹, N. Badea³, C. Ungureanu³, A. Lazea-Stoyanova⁴, A. Vlad⁴, V.A. Turchenko¹, A. Zhigunov⁵, E. Juszynska-Galazka⁶

¹Joint Institute for Nuclear Research, Frank Laboratory of Neutron Physics, Dubna, Russia

²University of Bucharest, Faculty of Physics, Department of Electricity, Solid-State Physics and Biophysics, Bucharest-Magurele, Romania

³University "Politehnica" of Bucharest, Faculty of Applied Chemistry and Materials Science, General Chemistry Department, Bucharest, Romania

⁴National Institute for Lasers, Plasma and Radiation Physics, Bucharest-Magurele, Romania

⁵Institute of Macromolecular Chemistry AS CR, Prague, Czech Republic

⁶Institute of Nuclear Physics, Polish Academy of Sciences, Krakow, Poland

E-mail: Yulia.Gorshkova@jinr.ru

Nowadays, the use of natural resources and, in particular, plants has expanded significantly due to the impressive amount of bioactive ingredients that have a strong beneficial impact on human health. Biohybrid complexes based on silver/silver chloride nanoparticles (Ag/AgCl NPs), chitosan (CTS), bioinspired membranes labelled with chlorophyll α (Lip Chl α) were investigated.

In order to get deep inside about the structure of the Ag/AgCl NP alone, and incorporated into the assemblies with liposomes and chitosan, and about the interaction between the components of the biohybrids, spectral methods have been used: UV-Vis absorption and emission spectroscopy. The internal structural of the hybrid Ag/AgCl NPs in presence of liposomes and chitosan has been studied by Small-angle neutron scattering (SANS), Small-angle X-ray scattering (SAXS), and X-ray diffraction (XRD) at the nanoscale and Infrared spectroscopy (FT-IR) at the molecular scale. The morphology of biohybrid systems has been characterized by Atomic-force microscopy (AFM) and Scanning electron microscopy (SEM). Comprehensive analysis made it possible to study in detail a mechanism of Ag/AgCl NPs fabrication and biohybrids formation. Very stable biohybrid Ag/AgCl NPs with $\zeta = -31.7$ mV were fabricated using eco-friendly "green" approach in synthesis from a mixture of vegetal sources (nettle & grapes). The synthesized hybrid Ag/AgCl NPs are spherical in shape and have a bimodal size distribution of particles with average sizes of 26.1 nm and 86.9 nm. The biohybrid complex I (Ag/AgCl NPs–CTS) is formed from the spherical chitosan-capped Ag/AgCl NPs. The presence of the silver/silver chloride nanoparticles in the biohybrid complexes II (Lip Chl α –Ag/AgCl NPs) and III (Lip Chl α –Ag/AgCl NPs–CTS) causes a change in the morphology of the liposomes. The ellipsoidal shape was determined from SANS and AFM experiments, while the majority of pure liposomes or liposomes surrounded by chitosan appear regularly spherical and not deformed. At the same time, the morphology of the Ag/AgCl NPs does not change. The sizes of hybrid Ag/AgCl NPs associated with liposomes are 64, 69, 77 nm and 97, 122, 172 nm for biohybrid complexes II and III, respectively. These values, as well as the values of "free" (not binded to liposomes) nanoparticles are larger than those found for Ag/AgCl NPs and Ag/AgCl NPs surrounded by CTS.

The bioperformances of the obtained materials are closely related to zeta potential values, size and morphological aspects. Thus, the obtained biohybrid entities exhibited good antioxidant activity ranging from 62 to 75% (in *vitro* tested through chemiluminescence method) and

good antibacterial activity against the pathogenic bacteria: *E. faecalis*, *Escherichia coli* ATCC 8738 and *Staphylococcus aureus* ATCC 2592.

We suppose that chitosan-capped silver/silver chloride nanoparticles will have a practical importance as a highly selective colorimetric probe or SERS substrate. The all obtained biohybrid complexes could be successfully used in biomedical field, as antioxidant and biocide materials.

Acknowledgements

This research was supported by the JINR-Romania (University of Bucharest, Faculty of Physics) Grant № 267 from 20.05.2020 item 17 and Program № 268 from 20.05.2020 items 45, 72.

KNOTTING OF CARBON NANOTUBES IN ISOTACTIC POLYPROPYLENE MATRIX DUE TO THE RESULTS OF SMALL-ANGLE NEUTRON SCATTERING AND LATTICE NUMERICAL MODELING

L.V. Elnikova¹, A.N. Ozerin², V.G. Shevchenko², P.M. Nedorezova³, A. T. Ponomarenko², V.V. Skoi^{4,5} and A.I. Kuklin^{4,5}

¹*NRC “Kurchatov Institute” – Alikhanov Institute for Theoretical and Experimental Physics, Moscow, Russian Federation*

²*Enikolopov Institute of Synthetic Polymeric Materials, RAS, Moscow, Russian Federation*

³*Semenov Institute of Chemical Physics, RAS, Moscow, Russian Federation*

⁴*Joint Institute for Nuclear Research, Dubna, Russian Federation*

⁵*Moscow Institute of Physics and Technology, Dolgoprudny, Russian Federation*

E-mail: elnikova@itep.ru

We present the data obtained by small-angle neutron scattering (SANS) on aggregation of carbon allotrope nanofillers in the matrix of isotactic polypropylene (iPP) [1]. The measurements were performed at the YuMO spectrometer, at the IBR2 reactor in Dubna, Russian Federation. We analyzed the data and determined the fractal shape, dimension, and sizes of nanofiller aggregation in the bulk of isotactic polypropylene over the range of the scattering angles. We estimated the volume distributions and aggregation of different types of carbon nanofillers at different concentrations: single-walled carbon nanotubes (SWCNT) at 1.2, 2.6 and 8 wt%, multi-wall carbon nanotubes (MWCNT) at 3.5 wt% and binary fillers MWCNT/graphene nanoplatelets (GNP) at 0.48 and 3 wt% (the volume ratio for binary fillers MWCNT:GNP is 1:2). To analyze the experimental small-angle scattering curves, we used the procedures of the ATSAS 2.4 software [2]. As the reference scattering, which was subtracted from the experimental curve of small-angle scattering of samples $I(Q)$, scattering from a sample of matrix polymer (iPP) was used. Thus, after taking into account reference scattering, the experimental small-angle scattering curves are characterized by scattering from only heterogeneous regions ("scattering particles") in the system having a scattering length different from the scattering length of the polymer matrix. To calculate regularized scattering curves $I_{reg}(Q)$, optimized over the entire range of scattering angles, the particle distribution function, the integral values of the inertia radii of the particles of the scattering phase and the particle size distribution, we used the GNOM procedure of ATSAS based on the regularization method according to Tikhonov.

We reconstructed the shape of nanoscale aggregates of all nanofillers with DAMMIN and DAMMIF procedures and found that the systems are polydisperse; nanofillers associate in the volume of iPP as fractal dense aggregates with rugged surface, their sizes exceeding original sizes of nanofillers several times (Fig.1). In iPP volume, CNTs twist in coils and knots and become more packaged, the shape of scattering particles (aggregates) can most simply be interpreted as the “entanglements” of neighboring CNTs, by analogy with similar “entanglements” of polymer macromolecules at concentrations higher than the crossover concentration.

To interpret the fractal properties of new aggregates and predict surface geometry for different concentrations of such nanofillers, we adapt the most universal modeling [3], solved with the lattice Monte Carlo algorithm [4] describing topology of aggregation in terms of gauge monopole gas. We show that all the observed with SANS objects with surface fractals (k values at Fig.1) are turned out behaving similarly to the objects in the deconfinement phase for the Dirac strings.

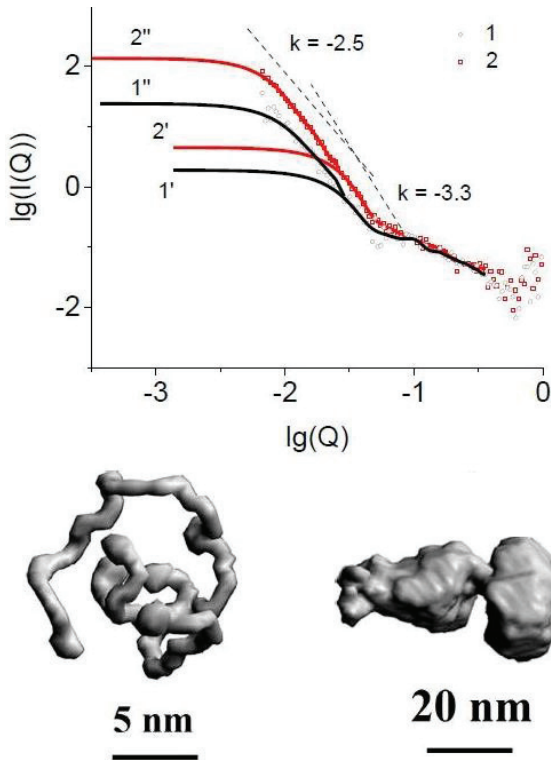


Fig.1. Experimental SANS intensity $I(Q)$ for samples MWCNT/GNP 0.48 wt% (1) and MWCNT/GNP 3 wt% (2) in the coordinates $\lg(I) - \lg(Q)$. The label “1” denotes scattering from particles MWCNT/GNP 0.48 wt%; “1'” is scattering from particle aggregates MWCNT/GNP 0.48 wt%; “2” is scattering from particles MWCNT/GNP 3wt%; “2'” is scattering from MWCNT/GNP 3 wt% particle aggregates. (The top graph). And the shape of scattering particles calculated from the scattering curve of particles (The bottom graph, left) and particle aggregates (The bottom graph, right) of MWCNT/GNP 0.48 wt%.

[1] L.V. Elnikova, A.N. Ozerin, V.G. Shevchenko, P.M. Nedorezova, A.T. Ponomarenko, V.V. Skoi, A.I. Kuklin (2020). Spatial structure and aggregation of carbon allotrope nanofillers in isotactic polypropylene composites studied by small-angle neutron scattering Preprint <https://arxiv.org/abs/2006.07595>.

[2] M.V. Petoukhov, D. Franke, A.V. Shkumatov, G. Tria, A.G. Kikhney, M. Gajda, C. Gorba, H.D.T. Mertens, P.V. Konarev, D.I. Svergun (2012). New developments in the ATSAS program package for small-angle scattering data analysis. *J. Appl. Cryst.* 45,342-350.

[3] A.M. Astakhov, S.K. Nechaev, and K.E. Polovnikov (2018). Statistical Properties of a Polymer Globule Formed during Collapse with the Irreversible Coalescence of Units. *Polymer Science, Series C.* 60,S25–S36.

[4] M.I. Polikarpov (1995). Fractals, topological defects, and confinement in lattice gauge theories. *Physics-Uspekhi.* 38(6),591-609.

MODEL SYSTEM FOR IMMUNOSUPPRESSIVE PEPTIDES INTERACTION STUDY

V.V. Egorov^{1,2,3}, Y.E. Gorshkova⁴, Y.A. Zabdorskaya^{1,2,3,5}

¹ Petersburg Nuclear Physics Institute named by B. P. Konstantinov of the National Research Center “Kurchatov Institute”, Gatchina, Russia

² Smorodintsev Research Institute of Influenza, Russian Ministry of Health, St. Petersburg, Russia

³ National Research Centre Kurchatov Institute, Moscow, Russia

⁴ Joint Institute for Nuclear Research, Frank Laboratory of Neutron Physics, Dubna, Russia

⁵ Peter the Great St. Petersburg Polytechnic University, St. Petersburg, Russia

E-mail: egorov_vv@npni.nrcki.ru

Prevention of immunosuppression caused by influenza virus and other viruses is an important goal in the development of new antiviral drugs. The influenza virus can suppress the T-cell immune response. One of the hypotheses explaining this phenomenon is the interaction of the influenza virus NS1 protein with the intramembrane domain of the T-cell receptor.

The aim of this work was to elucidate the mechanisms of the intramembrane interaction of the T-cell alpha receptor (TCR-alpha) and the influenza NS1 protein on peptide model. Using membrane vesicles, we studied the interaction of peptide CP (Core Peptide, transmembrane fragment of TCR-alpha), known in literature, as the model of TCR-alpha and peptide G51, designed by us, as a potential transmembrane fragment of NS1 protein. We also clarified the role of NS1 protein fragment supramolecular complex formation in TCR-alpha conformational transition during immunosuppression.

We studied the formation these peptides heterooligomers of on membrane vesicles surface. SANS measurements (YuMO@IBR-2, Dubna) indicate the increasing in the radius of phospholipid vesicles when interacting with the CP or G51 (Figure 1).

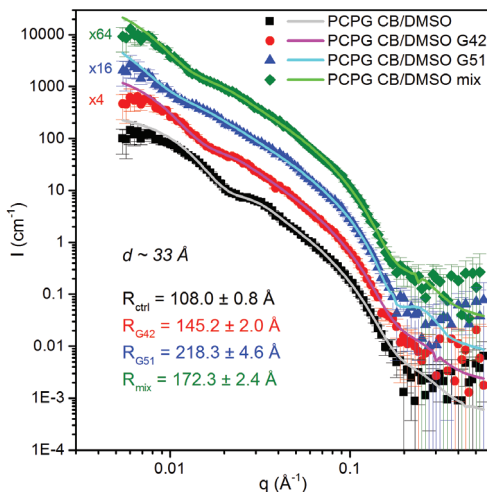


Figure 1 – SANS spectra of membrane vesicles (PCPG – DMPC and PMPG mixture as 70/30) with studied peptides. Vesicles were dissolved in citrate buffer (CB), peptides – in phosphate buffered saline (PBS), containing 1% DMSO-d₆.

Also, it was shown that G51 is able to change the radius of vesicles which were pre-incubated with CP. It indicates that influenza virus NS1 protein fragment can interact with T-cells model membrane containing CP peptide. The transmembrane CP-G51 peptide interaction study will be useful for elucidation of influenza A pathogenicity and antiviral drugs development.

This work was supported by the NRC “Kurchatov Institute” (№ 1363)

MANGANESE OXIDE DOPED LEAD-GERMANATE GLASSES: RAMAN, EPR AND SANS STUDIES

R.V. Erhan^{1,2}, S. Rada^{3,4}, M. Suci³, S. Macavei³, A. Dehelean³ and V. Bodnarchuk¹

¹*Department of Nuclear Physics, Horia Hulubei National Institute for R&D in Physics and Nuclear Engineering, Bucharest-Magurele, Romania*

²*Joint Institute for Nuclear Research, Frank Laboratory of Neutron Physics, 141980, Dubna, Russia*

³*National Institute for Research & Development of Isotopic and Molecular Technologies, Cluj-Napoca, 400293, Romania*

⁴*Department of Physics & Chemistry, Technical University of Cluj-Napoca, 400020, Cluj-Napoca, Romania*

E-mail: raul.erhan@gmail.com

Germanium dioxide is known as glass former and lead dioxide plays a dual role as network modifier and former. In germanate glasses by increasing of modifier oxides contents some physical and thermal properties undergo an inflection at a specific composition. This behavior is known as the germanate anomaly and consists in a growth and then a decline in the number of [GeO₆] octahedral units [1, 2].

The purpose of this work was to justify the induced structural modifications of the increase of MnO content in lead-germanate glasses. The local structure of the obtained glasses in the xMnO·(100-x)[7GeO₂·3PbO₂] composition where x = 0 – 30 mol% MnO was characterized by using data from X-ray diffraction (XRD) analysis, Scanning Electron Microscopy (SEM) micrographs, Raman and Electron Paramagnetic Resonance (EPR) spectra and Small Angle Neutron Scattering (SANS). The structure of the prepared samples was interpreted over a wide range of composition in order to explore the structural role of MnO and PbO in the germanate network.

The Raman analysis shows that manganese-lead-germanate glasses are composed of [GeO₄], [GeO₆], [PbO_n] and [MnO_n] structural units. The number of [GeO₆] octahedral units attains maximum values for the sample with x=20 mol% MnO. With a further increase in MnO content up to 30mol%, the coordination number of germanium atoms change from 6-fold to 4-fold.

The EPR data of the studied glasses consist of two resonance lines centered at g≈4.3 and g≈2.0 values [3]. The resonance line situated at about g≈4.3 corresponds to the rhombic geometry of the Mn⁺² ions. The resonance line located at about g≈2 may be attributed to isolated paramagnetic centers situated in octahedral symmetric sites slightly tetragonal distorted. By increasing of the dopant level in the host matrix some strongly distorted versions of these sites result in the resonance lines located at about g~2 and 4.3.

The predicted coordination number of germanium atoms in the Raman spectra was also compared with SANS data (Figure 1) which show strong evidence in germanate anomaly.

The combining the results provided from Raman, EPR and SANS data we can conclude the apparition of a maximum (or minimum) in the anomaly of the germanate network for the sample with x = 20 % mol MnO.

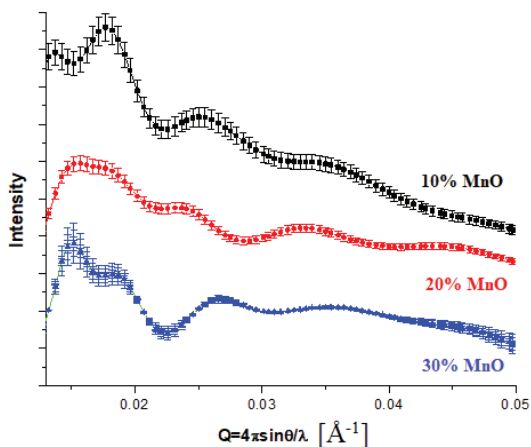


Figure 1. Small Angle Neutron Scattering (SANS) patterns of the studied glasses in the $x\text{MnO} \cdot (100-x)[7\text{GeO}_2 \cdot 3\text{PbO}_2]$ composition where $x = 0 - 30$ mol% MnO.

Acknowledgments: This work was supported by the project financing Romania-JINR-Dubna, Protocol No. 57/2020 with the 04-4-1121-2015/2020 theme code. Some authors are gratefully acknowledged.

- [1] A. A. E. Moneim, H. Y. Alfifi, (2020). *J. Non-Crystalline Solids*. 546, 120275-120285.
- [2] O. N. Koroleva, M. V. Shtenberg, T. N. Ivanova (2019). *J. Non-Crystalline Solids*. 510, 143-150.
- [3] R. Chelcea, S. Rada, E. Culea, I. Coroiu, (2016). *J. Non-Crystalline Solids*. 433, 45-50.

SECONDARY OSTEOPOROSIS IN RATS STUDIED BY SMALL ANGLE NEUTRON SCATTERING

S.E. Erhan^{1,2}, A.I. Kuklin³, R.V. Erhan^{4,5}, K.D. Knudsen^{5,6}, C.L. Roşioru²

¹National Institute for Research and Development of Isotopic and Molecular Technologies, Cluj-Napoca, Romania

²Babeş-Bolyai University, Faculty of Biology and Geology, Cluj-Napoca, Romania

³Joint Institute for Nuclear Research, Dubna, Russia

⁴Horia Hulubei National Institute of Research and Development in Physics and Nuclear Engineering, Bucharest, Romania

⁵Institute for Energy Technology, Kjeller, Norway

⁶Norwegian University of Science and Technology, Trondheim, Norway

E-mail: sabina.erhan@itim-cj.ro

Osteoporosis is a condition resulting in an increased risk of skeletal fractures due to a reduction of bone-mass and micro-architectural deterioration of the tissue. Aside from postmenopausal osteoporosis, the most common secondary cause of this disease is due to the long-term use of oral glucocorticoids, a common cure for many inflammation diseases.

The most significant mechanism of glucocorticoid-induced osteoporosis is enhanced bone resorption and decreased bone formation. [1]

The present study was designed to illustrate the benefit of physical activity, an inexpensive and accessible treatment, in the amelioration of osteoporosis symptoms.

In order to better understand the alterations produced by secondary osteoporosis, in terms of bone density changes and liver modifications, two small-angle neutron scattering (SANS) experiments were performed, using neutron scattering, on the YuMO spectrometer, at IBR-2 pulsed reactor, from Frank Laboratory of Neutron Physics, of Joint Institute for Nuclear Research (JINR), Dubna, Russian Federation and also at the SANS-instrument, JEEP-II reactor, from Institute for Energy Technology (IFE), Kjeller, Norway.

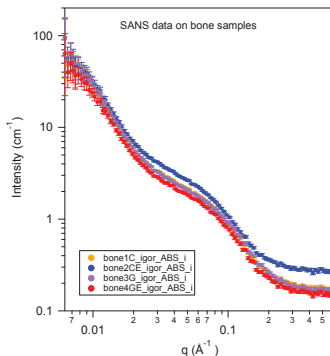


Fig. 1. SANS data obtained from bone samples: bone 1-control animal (C); bone 2- control with effort (CE); bone 3-glucocorticoid animal (G); bone 4-glucocorticoid with effort (GE). (YuMO spectrometer, IBR-2 reactor, Dubna, Russia)

[1] Canalis, E. (2005). Glucocorticoid-induced osteoporosis: pathophysiology, in: Maricic M, Gluck O (eds). Bone disease in rheumatology. New York, Lippincott. 105–110.

CRYSTAL AND SUPRAMOLECULAR STRUCTURE OF BACTERIAL CELLULOSE HYDROLYZED BY CELLOBIOHYDROLASE FROM *SCYTALIDIUM CANDIDUM* 3C: A BASIS FOR DEVELOPMENT OF BIODEGRADABLE WOUND DRESSINGS

L.A. Ivanova¹, Y.E. Gorshkova², N.A. Verlov¹, V.S. Burdakov¹, A. E. Baranchikov³, G. P. Kopitsa¹ and A.A. Kulminskaya¹

¹*Petersburg Nuclear Physics Institute NRC KI, Gatchina, Russia*

²*Joint Institute for Nuclear Research, Dubna, Russia*

³*Kurnakov Institute of General and Inorganic Chemistry of the Russian Academy of Sciences, Moscow, Russia*

E-mail: Ivanova_la@npni.nrcki.ru

The crystal and supramolecular structure of the bacterial cellulose (BC) has been studied at different stages of cellobiohydrolase hydrolysis using various physical and microscopic methods. Enzymatic hydrolysis significantly affected the crystal and supramolecular structure of native BC, in which the 3D polymer network consisted of nanoribbons with a thickness $T \approx 8$ nm and a width $W \approx 50$ nm, and with a developed specific surface $S_{\text{BET}} \approx 260$ m²·g⁻¹. Biodegradation for 24 h led to a ten percent decrease in the mean crystal size D_{hkl} of BC, to two-fold increase in the sizes of nanoribbons, and in the specific surface area S_{BET} up to ≈ 100 m²·g⁻¹. Atomic force and scanning electron microscopy images showed BC microstructure "loosening" after enzymatic treatment, as well as the formation and accumulation of submicron particles in the cells of the 3D polymer network. Experiments in vitro and in vivo did not reveal cytotoxic effect by the enzyme addition to BC dressings and showed a generally positive influence on the treatment of extensive III-degree burns, significantly accelerating wound healing in rats. Thus, in our opinion, the results obtained can serve as a basis for further development of effective biodegradable dressings for wound healing.

INVESTIGATION INTO THE EFFECT OF CHOLESTEROL AND MELATONIN ON THE AMYLOID EMBEDDED MODEL MEMBRANE THROUGH NEUTRON SCATTERING

T. Kondela^{1,5,6}, P. Hrubovčák^{1,2}, E. Dushanov^{3,4}, K. Kholmurodov^{1,7},
O. Ivankov^{1,8,9}, T. Murugova^{1,8}, A. Kuklin^{1,8} and N. Kučerka^{1,5}

¹*Frank Laboratory of Neutron Physics, Joint Institute for Nuclear Research, Joliot-Curie 6, Dubna, Moscow Region, 141980, Russian Federation*

²*Department of Condensed Matter Physics, P. J. Šafárik University, Park Angelinum 9, Košice, 04154, Slovakia*

³*Laboratory of Radiation Biology, Joint Institute for Nuclear Research, Joliot-Curie 6, Dubna, Moscow Region, 141980, Russian Federation*

⁴*Department of Biophysics, Dubna State University, Universitetskaya 19, Dubna, Moscow Region, 141980, Russian Federation*

⁵*Department of Physical Chemistry of Drugs, Faculty of Pharmacy, Comenius University in Bratislava, Odbojárov 10, Bratislava, SK-832 32, Slovakia*

⁶*Department of Nuclear Physics and Biophysics, Faculty of Mathematics, Physics and Informatics, Comenius University in Bratislava, 832 32 Bratislava, Slovakia*

⁷*Department of Chemistry, New Technologies and Materials, Dubna State University, Universitetskaya 19, Dubna, Moscow Region, 141980, Russian Federation*

⁸*Moscow Institute of Physics and Technology, Dolgoprudny, Russia*

⁹*Institute for Safety Problems of Nuclear Power Plants, NAS of Ukraine, Kyiv, Ukraine*

E-mail: tomas.kondela@gmail.com

Alzheimer's disease is a devastating neurodegenerative disease caused by the formation of senile plaques, primarily consisting of amyloid-beta (Ab) peptides. The crucial role in this process is imparted by peptide-membrane interactions, changing the structural properties of membrane. These changes are known to be modulated also by membrane composition. Our previous experiments [1] revealed the counteracting effect of melatonin to that of cholesterol in neat lipid membranes. We have extended our investigations recently by including transmembrane Ab peptide in these model membranes. The structure and dynamics of membranes depend on many external and internal factors that, in turn, determine their biological functions. One of the widely accepted and studied characteristics of biomembranes is their fluidity. We research a simple system with variable fluidity tweakable via its composition. The addition of cholesterol is employed to increase the order of lipid chains, thus decreasing the membrane fluidity, while melatonin is shown to elevate the chain disorder, thus increases the membrane fluidity. The structural changes represented by changes to membrane thickness are evaluated from small angle neutron scattering. Finally, we look at the ability of the two additives to control the interactions between membrane and amyloid-beta peptides. Our results suggest that fluidizing effect of melatonin can promote an insertion of peptide within the membrane interior.

[1]E. Drolle, N. Kucerka, M.I. Hoopes, Y. Choi, J. Katsaras, M. Karttunen, Z. Leonenko (2013). Effect of melatonin and cholesterol on the structure of DOPC and DPPC membranes. *Biochim. Biophys. Acta - Biomembr.* 1828, 2247.

SUPPORT SILICON OXIDE NANOLAYER FOR NEUTRON REFLECTOMETRY SOLID-LIQUID CELL FOR STUDYING BIOLOGICAL SOLUTIONS

M.O. Kuzmenko^{1,2}, I.V. Gapon^{1,3}, M.V. Avdeev¹, Yu.Ye. Gorshkova¹, V.A. Maslova¹, O.P. Dmytrenko²

¹ *Frank Laboratory of Neutron Physics, Joint Institute for Nuclear Research, Dubna, Moscow Region, Russia*

² *Physics Department, Kyiv Taras Shevchenko National University, Kyiv, Ukraine*

³ *Institute for Safety Problems of Nuclear Power Plants, NAS Ukraine, Chornobyl, Ukraine*

E-mail: kuzjamaryna@gmail.com

One of the trends in biorelevant research is the synthesis of new inorganic and organic nanostructures with certain properties for diagnostic or therapeutic purposes. The important aspects to be controlled in this kind of investigations are biocompatibility, the ratio of the toxicity effect, biodistribution, and biodegradation. In some cases, no clear evidence exists for the claimed membranotropic properties of the nanostructures. There is also a problem of predicting their behavior in living organisms (in vivo). It is not surprising that these facts attract much attention and stimulate intensive studies of the interactions of different classes of nano-objects with model membranes using both theoretical and experimental methods. Changes in the properties of particles, the use of nano-objects as drug carriers, as well as the improvement in bioavailability, and the decrease in toxicity – often lead to changes in the structure and interaction of these complexes in the body. In a living cell, the first defensive barrier is its membrane, with which the administered drug initially interacts. Understanding of these processes is a way to improve and develop new drugs.

Development of non-destructive, quickly executable and more accurate research methods in conditions close to real ones – from the point of view of application – is of current interest. Implementation of such methods makes it possible to understand the processes occurring in the system under study and helps in the synthesis of new drugs, as well as in the improvement of the existing ones. Among such methods, neutron reflectometry can be used for diagnostics of multicomponent systems. In recent decades, this method has been expanded to study nanostructures at the interfaces between liquids and liquid colloidal systems with other media. On the one hand, it is a non-destructive technique; and on the other, it allows one to explore hidden interfaces.

To design experiments in structural biology using neutron reflectometry, it became necessary to create a cell with a set of characteristics that would satisfy the requirements both for the subject of research, and for the state of the experimental complex. The problem of the background, as well as the need for measurements in real time, introduce experimental limitations. An additional layer on a silicon crystal in a liquid cell makes it possible to restore the interface structure using specular reflectivity curves measured in a lower dynamic q-range. Simulations of the liquid cell with a change in parameters of an additional support layer show that it is more efficient to use silicon oxide as the main support layer with the thickness of ~100 nm. It provides for both the better experimental sensitivity and the necessary hydrophilic properties. In addition, this layer remains stable in the aquatic environment and especially in chemically aggressive media during the cleansing from organic contaminants after experimentation.

To create thick oxide films on a silicon crystal (working plane 111), the method of dry thermal oxidation was chosen. This method is also used in the commercial production of silicon-based semiconductor components. Because of this, the information about exact

oxidation parameters is restricted. To calculate these parameters, we used 2 models: Deal and Grove (high temperature regime 900-1100 degrees Celsius) [1]; Massoud model (low temperature regime 700-800 degrees Celsius) [2]. Before the oxidation procedure, the surface was chemically cleaned according to INRF standards [3]: solvent clean, RCA01, HF dip, RCA02. As a result, at the last stage of cleaning, a protective oxide film of 1-3 nm was formed on the silicon surface. After oxidation, the resulting layer and surface were evaluated by the following methods: AFM, Raman, diffraction, and X-ray reflectometry. The information was obtained about the phase composition in the silicon layer, as well as about the surface quality and layer thickness. This result meets the requirements of experiments using neutron reflectometry for lipid membranes.

[1] B.E. Deal, A.S. Grove (1965). General Relationship for the Thermal Oxidation of Silicon. *Journal of Applied Physics*. 36 (12): 3770–3778.

[2] H.Z. Massoud, J.D. Plummer, E.A. Irene (1985). Thermal oxidation of silicon in dry oxygen: Growth - rate enhancement in the thin regime II. Physical mechanisms. *Journal of The Electrochemical Society*, 132(11):2693-2700.

[3] <https://www.inrf.uci.edu/facility/sop/wet-dry/>

UNIFIED THEORY OF DYNAMICAL SYSTEMS WITH APPLICATIONS INCLUDING BIOLOGICAL SYSTEMS

Nugzar Makhaldiani¹

¹*Joint Institute for Nuclear Research, Dubna, Russia*

E-mail: mnv@jinr.ru

General theory of linearly extended dynamical systems formulated, applications to the strong coupling problems of standard models from high energy particle physics, condensed state physics and biological structures described, [1-3].

- [1] Nugzar Makhaldiani (2020). Nonperturbative extension of perturbative quantum chromodynamics and fractal dimension of space as a connement phase transition order parameter. *J. Phys.: Conf. Ser.* 1435, 012055.
- [2] N. Makhaldiani (2011). Fractal Calculus (H) and some Applications. *Phys. Part. Nuclei Lett.* 8, 535-544.
- [3] N. Makhaldiani (2011) Regular method of construction of the reversible dynamical systems and their linear extensions - Quanputers. *Atomic Nuclei.* 74, 1040.

STRUCTURAL PARAMETERS OF THYLAKOID MEMBRANE: LIPID AND PROTEIN PARTS

S.D. Osipov¹, A.V. Vlasov^{1,2,3}, Yu.L. Ryzhykau^{1,3}, A.I. Kuklin^{1,4}, V.I. Gordeliy^{1,5,6}

¹*Research Center for Molecular Mechanisms of Aging and Age-Related Diseases, Moscow Institute of Physics and Technology, 141700 Dolgoprudny, Russia*

²*Institute of Crystallography, RWTH Aachen University, 52066 Aachen, Germany*

³*Joint Institute for Nuclear Research, 141980 Dubna, Russia*

⁴*Physikalische Biochemie, Fachbereich Chemie, Technische Universität Darmstadt, Alarich-Weiss-Straße 4, 64287, Darmstadt, Germany*

⁵*JuStruct: Jülich Center for Structural Biology, Forschungszentrum Jülich, 52425 Jülich, Germany*

⁶*Institut de Biologie Structurale Jean-Pierre Ebel, Université Grenoble Alpes—Commissariat à l'Energie Atomique et aux Energies Alternatives—CNRS, 38044 Grenoble, France*

E-mail: kuklin@nf.jinr.ru; valentin.gordeliy@ibs.fr

The protein complex ATP-synthase plays a large role in the life of any organism. It synthesizes ATP (an universal source of energy in many biochemical processes) from ADP and inorganic phosphate. ATP-synthase is a large (from 550 to 1600 kDa) membrane protein complex, which consists of two parts: soluble F₁, called the "head" for its shape, and membrane F_o [1]. Despite the numerous investigations of the complex, today many aspects of its functioning (and also some aspects of its structure) remain unclear [2, 3]. Here presented the result of ATP-synthase study obtained from the spinach chloroplasts.

We used combination of known protocols [4, 5, 6] to isolate and purify the protein. As protein source, we used spinach homogenized with a blender, which was then filtered. In order to isolate the cells from the thylakoid membranes, spinach cells were centrifuged; then subjected to cytolysis. The resulting mixture was centrifuged to precipitate the membranes. Membrane proteins are solubilised with a solutions of different detergents such as oktyl-glykopiranoside, laurilsarcosine and other, then salted out by solution of ammonium sulfate. Then purified proteins were subjected to dialysis.

The proteins were investigated by Western blotting, DLS and SAXS. Thylakoid membranes were measured by small-angle neutron scattering (SANS) using contrast variation method. The parameters separately for protein and lipid structure of thylakoid membrane were obtained.

[1] Kühlbrandt, W. (2019). Structure and mechanisms of F-type ATP synthases. Annual review of biochemistry, 88, 515-549.

[2] Symersky, J., Pagadala, V., Osowski, D., Krah, A., Meier, T., Faraldo-Gómez, J. D., & Mueller, D. M. (2012). Structure of the c 10 ring of the yeast mitochondrial ATP synthase in the open conformation. Nature structural & molecular biology, 19(5), 485.

[3] Vlasov, A. V., Kovalev, K. V., Marx, S. H., Round, E. S., Gushchin, I. Y., Polovinkin, V. A., ... & Ryzhykau, Y. L. (2019). Unusual features of the c-ring of F₁F_o ATP synthases. Scientific reports, 9(1), 1-11.

[4] Hahn, A., Vonck, J., Mills, D. J., Meier, T., & Kühlbrandt, W. (2018). Structure, mechanism, and regulation of the chloroplast ATP synthase. Science, 360(6389).

[5] Varco-Merth, B., Fromme, R., Wang, M., & Fromme, P. (2008). Crystallization of the c14-rotor of the chloroplast ATP synthase reveals that it contains pigments. Biochimica et Biophysica Acta (BBA)-Bioenergetics, 1777(7-8), 605-612.

[6] Kurbatov, N. M., et al. "DDM solubilization-based protocol for isolation and purification of spinach chloroplast ATP synthase." JOURNAL OF BIOENERGETICS AND BIOMEMBRANES. Vol. 50. No. 6. 233 SPRING ST, NEW YORK, NY 10013 USA: SPRINGER/PLENUM PUBLISHERS, 2018.

PREPARATION OF LIPOSOMES FROM NATIVE CELL MEMBRANE FOR SAXS/SANS STUDIES

I.S. Okhrimenko¹, Y.A. Zagryadskaya¹, Y.L. Ryzhykau¹, A.I. Kuklin^{1,2}, N.A. Dencher^{1,3}, Gordeliev V.I.^{1,4,5}

¹ *Research Center for Molecular Mechanisms of Aging and Age-related Diseases, Moscow Institute of Physics and Technology (State University), Dolgoprudny, Russia*

² *Joint Institute for Nuclear Research, 141980 Dubna, Russia*

³ *Physical Biochemistry, Chemistry department, Technical University of Darmstadt, Darmstadt, Germany*

⁴ *Institute of Biological Information Processing (IBI-7: Structural Biochemistry), Forschungszentrum Jülich, Jülich, Germany*

⁵ *IRIC, Institut de Biologie Structurale (IBS), Université Grenoble Alpes, CEA, CNRS, Grenoble, France*

E-mail: ivan.okhrimenko@phystech.edu

To obtain the most native biological membranes derived from human cells suitable for scattering studies we developed the procedure and tested the results by SAXS by means of Rigaku X-Ray HighFlux HomeLab, Rigaku MicroMax 007 HF based at MIPT [1].

The physical properties of biological cell membranes depend not only of the great variety of lipids forming the membranes but also of membrane proteins [2]. Some membranes can consist up to dozens of per cents of proteins, such as mitochondrial membrane [3], membrane of erythrocyte [4] and others. Trans-membrane peptides generally form alpha-helices in lipid bilayer. The extraction procedures with the use of solvents destroy this delicate composition of lipids and membrane proteins making proteins denatured ones. The artificial constructing of lipid bilayers by mixing few number of lipids provides membranes lacking some property features due to the absence of the rest of lipids and transmembrane proteins.

We payed special attention to preserve the native state of the transmembrane parts of the proteins while preparing liposomes (small vesicles) for scattering studies. The absence of the steps dangerous for protein folding is the advantage. We used the human erythrocyte “ghost cells”, resuspended them in experimentally selected PBS-based buffer, than used ultrasonic disintegration on ice taking precautions not to heat the sample. The liposomes after this treatments had characteristic size about 400 nm (Figure 1).

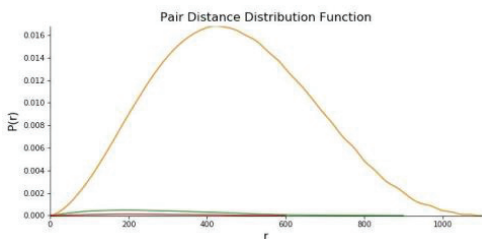


Figure 1. Patterson function graph. The pair distance distribution function of liposomes exposed to ultrasound only obtained by SAXS (red line).

The next step was the further disintegration by means of extruder with MWCO 50 and 100 nm membranes. The resulted characteristic size of liposomes after this step appeared about 400nm (Figure 2, left side). The thickness of liposomes was estimated by Giniér

approximation plot (Figure 2, right side). Radius of gyration (R_g) appeared to be 12.19 ± 1.35 , so thickness according the model was estimated as ~ 4 nm.

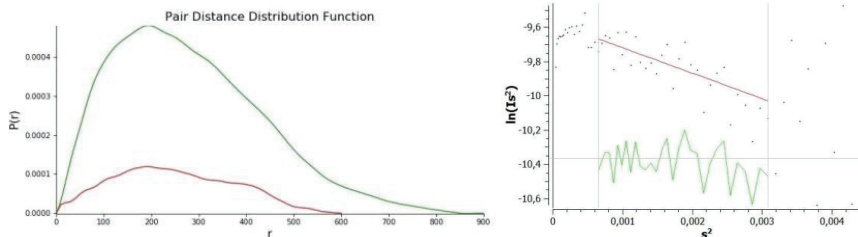


Figure 2. Left side: The pair distance distribution function of liposomes obtained by extrusion using 100 nm (green line) and 50 nm (purple line) MWC membranes. Right side: Guinier plot made for liposomes obtained by extrusion using 100 nm MWC membranes.

We thank the Russian Scientific Foundation (project number 20-64-46027). Prof. Norbert A. Dencher is grateful Russian Foundation for Basic Research (project number 20-015-00526).

[1] Murugova, T. N., et al. (2015). Low resolution structural studies of apoferritin via SANS and SAXS: the effect of concentration. *J. Optoelectron. Adv. Mater*, 17(9-10), 1397-1402.

[2] Reifschneider, N. H., et al. (2006). Defining the mitochondrial proteomes from five rat organs in a physiologically significant context using 2D blue-native/SDS-PAGE. *Journal of proteome research*, 5(5), 1117-1132.

[3] Dencher, N. A., et al. (2007). Proteome alterations in rat mitochondria caused by aging. *Annals of the New York Academy of Sciences*, 1100(1), 291-298.

[4] Pasini, E. M., et al. (2010). Red blood cell (RBC) membrane proteomics—Part I: Proteomics and RBC physiology. *Journal of proteomics*, 73(3), 403-420.

EFFECT OF WATER-SOLUBLE MONOMER ON WORMLIKE MICELLES OF SURFACTANT STUDIED BY SMALL-ANGLE NEUTRON SCATTERING

A.S. Ospennikov¹, O.P. Artykulnyi², A.V. Shibaev¹, A.I. Kuklin² and O.E. Philippova¹

¹*Physics Department, Lomonosov Moscow State University, Moscow, Russia*

²*Frank Laboratory of Neutron Physics, Joint Institute for Nuclear Research, Dubna, Russia*

E-mail: aleks-16-1999@mail.ru

Recently, the study of surfactant wormlike micelles has attracted much attention due to their remarkable rheological properties. Supramolecular chains of surfactants [1] have high responsiveness to external factors due to the nature of non-covalent interactions which bind surfactant molecules together within the micelle. However, mainly the responsiveness of wormlike micelles to non-polar substances (like hydrocarbons), which are not soluble in water, has been studied up to date. The effect of water soluble substances has been studied in much less detail. At the same time, study of the interaction of vinyl monomers with wormlike micelles is as important issue for creating networks of hydrophobically modified polymers by emulsion co-polymerisation.

In this work, the effect of water-soluble monomer – acrylamide - on wormlike surfactant micelles was investigated for the further purpose of subsequent polymerization and obtaining polyacrylamide-surfactant networks. Studying the interaction of acrylamide with micelles, we found that acrylamide has different effects on linear and branched micelles: for linear micelles (at low salt concentrations), the viscosity immediately decreases, and for branched micelles (at high salt concentrations), it first increases, and then decreases. It was shown by small-angle neutron scattering that linear cylindrical micelles transform into spherical micelles, and branched micelles - into short cylindrical ones. This difference in responsiveness of linear and branched micelles is due to different packing of surfactant molecules due to screening of electrostatic interactions upon changing the salt concentration. It was shown by fluorescence spectroscopy that acrylamide molecules incorporate into the micelles, which causes the changes in their structure.

Acknowledgement

The work is financially supported by the Russian Science Foundation (project № 18-73-10162).

[1] A.V. Shibaev, A.S. Ospennikov, A.I. Kuklin, N.A. Arkharova, A.S. Orekhov, O.E. Philippova (2020). Structure, rheological and responsive properties of a new mixed viscoelastic surfactant system. *Coll. Surf. A: Phys. Eng. Asp.* 586, 124284.

INVESTIGATION OF HYDROGELS BASED ON CROSS-LINKED POLYMER AND WORMLIKE SURFACTANT MICELLES BY SMALL-ANGLE NEUTRON SCATTERING

A.S. Ospennikov¹, A.I. Kuklin², A.V. Shibaev¹ and O.E. Philippova¹

¹*Physics Department, Lomonosov Moscow State University, Moscow, Russia*

²*Frank Laboratory of Neutron Physics, Joint Institute for Nuclear Research, Dubna, Russia*

E-mail: aleks-16-1999@mail.ru

Recently, double polymer networks, which consist of two networks with different properties, have attracted great interest, since they have mechanical properties enhanced by orders of magnitude as compared to single polymer network hydrogels. Many double networks based on two crosslinked polymers have been proposed in the literature, but they do not have the ability to quickly restore mechanical properties. Therefore, it is promising to create double networks based on polymer and supramolecular chains (wormlike micelles) of surfactants, since they combine enhanced mechanical strength with the ability to quickly recover the mechanical properties after large deformations. Cylindrical micelles are formed due to the self-organization of surfactant molecules, which are bound together by non-covalent interactions, and they can reversibly break and re-form very quickly (within tens of seconds). Double network gels were obtained containing a crosslinked polymer network and cylindrical surfactant micelles, which have pronounced elastic properties several times higher than the properties of each of the networks taken separately. Based on small-angle neutron scattering data, it was confirmed that surfactant molecules form cylindrical structures in the double network. Microphase separation was found with domains enriched either by polymer or by surfactant, which was manifested at the scattering curves by a strong rise of intensity at low scattering vectors, confirming the formation of larger structures (presumably, with hundreds of nanometers in size).

Acknowledgement

The work is financially supported by the Russian Science Foundation (project № 19-73-20133).

INVESTIGATION OF THE DOMAIN STRUCTURE OF SEGMENTED POLYURETHANE UREAS BY SMALL ANGLE NEUTRON SCATTERING

A.A. Pavlova^{1,2}, A.N. Bugrov^{3,4}, R.Yu. Smyslov^{1,3}, Yu.E. Gorshkova⁵, G.P. Kopitsa^{1,6,7}

¹*Petersburg Nuclear Physics Institute, Gatchina, Russia*

²*Saint Petersburg State University, Saint-Petersburg, Russia*

³*Institute of Macromolecular Compounds, Russian Academy of Sciences, Saint-Petersburg, Russia*

⁴*Saint Petersburg Electrotechnical University "LETI", Saint-Petersburg, Russia*

⁵*Joint Institute for Nuclear Research, Dubna, Moscow region, Russia*

⁶*National Research Center Kurchatov Institute, Moscow, Russia*

⁷*Grebenschchikov Institute of Silicate Chemistry of RAS, Saint-Petersburg, Russia*

E-mail: alina.pavlova.htsc@gmail.com

Polyurethane ureas (PUU) are multiblock copolymers, which consist of alternating soft and hard segments. Since soft and hard segments do not mix, such block copolymers tend to microphase separation.

Interest in the study of microphase separation is since the emerging physical network, the crosslinking nodes of which are aggregates of hard segments (domains), largely determines the mechanical and thermophysical properties of the PUU. Thus, control of the resulting domain structure in PUU makes it possible to purposefully get thermoplastics, elastomers, or thermoplastic elastomers, which are promising for use as adhesives, sealants, packaging, heat-insulating and damping materials [1, 2].

In the present work, in the synthesis of PUU, polycaprolactone diols with molecular weights of 530 and 2000 g/mol were used as soft segments, and hard blocks were formed as a result of the reaction between aromatic diisocyanates (4,4'-methylene diphenyl diisocyanate; 2,4-toluene diisocyanate) and diamines (*m*-phenylenediamine; 4,4'-bis-(4"-aminophenoxy) diphenylsulfone).

This work aimed to study the effect of the length of soft segments and the structure of diisocyanates with chain extender (hard segment) on phase separation and morphology of PUU using small-angle neutron scattering (SANS) method. SANS measurements were performed at the YuMO spectrometer (IBR-2, JINR, Dubna, Russia).

Upon the data obtained, the inclusion of longer aliphatic segments in the structure of the PUU does not affect the size of the hard phase domains (R_c) but increases the distance between them. It has been shown that the R_c value correlates with the length of the hard aromatic segments, while the symmetric diisocyanate in their composition leads to the enlargement of domains as a result of denser packing.

[1] C. Prisacariu (2011). Polyurethane elastomers from morphology to mechanical aspects, Vienna. Springer.

[2] K. Gisselalt, B. Helgee (2003). Effect of soft segment length and chain extender structure on phase separation and morphology in poly(urethane urea)s. *Macromolecular Materials and Engineering*. 288, 265–271.

SANS INVESTIGATION OF MEMBRANE PROTEIN OLIGOMERIZATION: THE CASE OF THE TCS PHOTORECEPTOR COMPLEX *NpSRII/NpHtrII*

Yu.L. Ryzhikau^{1,2}, P.S. Orekhov¹, M.I. Rulev^{4,5,7}, A.V. Vlasov^{1,2,3}, D.V. Zabelskii^{1,4,5,6},
A.V. Rogachev^{1,2}, T.N. Murugova^{1,2}, A.D. Vlasova¹, V.I. Gordeliy^{1,4,5,6} and A.I. Kuklin^{1,2}

¹ *Research Center for Mechanisms of Aging and Age-Related Diseases, Moscow Institute of Physics and Technology, Dolgoprudny, 141700, Russian Federation*

² *Frank Laboratory of Neutron Physics, Joint Institute for Nuclear Research, Dubna, 141980, Russian Federation*

³ *Institute of Crystallography, University of Aachen (RWTH), Aachen, 52056, Germany*

⁴ *Institute of Biological Information Processing (IBI-7: Structural Biochemistry), Forschungszentrum Jülich, Jülich, 52425, Germany*

⁵ *JuStruct: Jülich Center for Structural Biology, Forschungszentrum Jülich, Jülich, 52425, Germany*

⁶ *Institut de Biologie Structurale Jean-Pierre Ebel, Université Grenoble Alpes–Commissariat à l’Energie Atomique et aux Energies Alternatives–CNRS, Grenoble, F-38027, France*

⁷ *Structural biology group, European Synchrotron Radiation Facility, 71 Avenue des Martyrs, Grenoble, 38000, France*

E-mail: valentin.gordeliy@ibs.fr; kuklin@nf.jinr.ru

Two-component systems (TCSs) are responsible for communication of microorganisms with the environment. TCSs are present in almost all domains of life and are the most abundant signaling systems in Nature. The TCS consists of a receptor that senses a specific environmental stimulus, and a response regulator. The first component is usually represented by transmembrane receptors: histidine kinases, chemoreceptors and photoreceptors, which have a similar modulus structure. In the cell membrane, chemo- and photoreceptors form trimers of dimers. Together with kinases CheA and CheW, they form the core unit of the extended signaling arrays [1].

The sensory rhodopsin II/transducer complex from *Natronomonas pharaonis* (*NpSRII/NpHtrII*) is an archaeobacterial photoreceptor, which is widely used for studying how TCSs transfer signals across the membrane [2].

N. pharaonis is a halophilic archaeon, and a salt concentration could significantly affect the shape and oligomerization state of its’ proteins [3]. Reasonable assumption is that *NpSRII/NpHtrII* forms trimers of dimers at salt concentration corresponding to physiological values (~3.5 M NaCl).

We conducted an analysis of how the salt concentration influences on the structure and oligomerization of the full-length *NpSRII/NpHtrII* complex. The *NpSRII/NpHtrII* was prepared in a range of D₂O buffers containing 150 mM, 1.4 M, 2.8 M and 4 M NaCl. Small-angle neutron scattering (SANS) measurements were done on the YuMO spectrometer (IBR-2, Dubna, Russia) [4].

Ab initio structure obtained from SANS data for the *NpSRII/NpHtrII* at 4.0 M NaCl shows a good visual agreement with the “Y”-shaped model of the trimer of dimers [5]. However, attempts to fit the above data with atomic models of the corresponding trimer of dimers have not been successful.

Subsequent analysis shows, that at low salt conditions (150 mM NaCl) *NpSRII/NpHtrII* forms dimers. SANS experiments at NaCl concentrations of 1.4 M and 2.8 M indicated increasing

proportion of trimers of dimers with increasing salt concentration. However, the fraction of trimers of dimers does not reach 100% at 4.0 M NaCl. Resulting weight fractions of trimers of dimers are $21 \pm 3\%$, $29 \pm 3\%$ and $36 \pm 2\%$ for 1.4 M, 2.8 M and 4.0 M, respectively. A discrepancy of this result with *ab initio* structure resembling “Y”-shaped model obtained from the data corresponding to 4.0 M NaCl is explained by the fact that another – “tripod”-shaped – model of trimer of dimers is correct. In contradiction to the “Y”-shaped model, a formation of the “tripod”-shaped trimers of dimers occurs only through the contacts of the cytoplasmic tips of dimers, while their transmembrane parts remain unconnected.

Reported result is of methodological significance, since it shows that SAS data for a protein that is in superposition of different oligomerization states, when it treated at the assumption of monodisperse solution, may give the *ab initio* structure confirming incorrect assumptions about the structure and oligomerization state of the studied protein.

This work was supported by RFBR and DFG in terms of the research project №20-54-12027.

[1] M. Li, G. L. Hazelbauer (2011). Core unit of chemotaxis signaling complexes. Proc. Natl. Acad. Sci. U. S. A. 108, 9390–9395.

[2] V. I. Gordeliy, et al (2002). Molecular basis of transmembrane signalling by sensory rhodopsin II–transducer complex. Nature 419, 484–487.

[3] Budyak I. L. et al (2006). Shape and oligomerization state of the cytoplasmic domain of the phototaxis transducer II from *Natronobacterium pharaonis*. PNAS 103 (42), 15428-15433.

[4] Kuklin A. I. et al (2017). Neutronographic investigations of supramolecular structures on upgraded small-angle spectrometer YuMO. Journal of Physics: Conference Series. 848.

[5] P.S. Orekhov (2016). Signaling and Adaptation in Prokaryotic Receptors as Studied by Means of Molecular Dynamics Simulations. PhD thesis, University of Osnabrück, Germany.

COMPLEX EFFECT OF AgNO_3 AND KNO_3 ON DPPC BILAYER: SANS AND DENSITOMETRY STUDY

V.V. Skoi^{1,2}, D.V. Soloviov^{1,2,3}, A.V. Rogachev^{1,2}, V.V. Chupin², A.I. Kuklin^{1,2},
V.I. Gordeliy^{1,2,4,5}

¹*Joint Institute for Nuclear Research, Dubna, Russia*

²*Moscow Institute of Physics and Technology, Dolgoprudny, Russia*

³*Institute for Safety Problems of Nuclear Power Plants NAS of Ukraine, Kyiv, Ukraine*

⁴*Institut de Biologie Structurale J.-P. Ebel, Université Grenoble Alpes-Commission for Atomic Energy (CEA)-CNRS, Grenoble, France*

⁵*Institute of Biological Information Processing (Institute of Biological Information Processing: Structural Biochemistry), Jülich, Germany*

E-mail: skoi.vv@phystech.edu

The results of the investigation of DPPC lipid suspensions in presence of lapis (AgNO_3 and KNO_3 alloy) by small angle neutron scattering (SANS) and densitometry methods are presented. The combined effect of cosmotropic and chaotropic nitrates on lipid bilayer structure and phase state is discussed.

Medicines containing silver have been actively used since the middle of the XIX century. Despite the widespread application of antibiotics, silver preparations (*e.g.*, lapis) are still used as disinfectant agents. The antiseptic effect of silver preparations is primarily due to the binding of silver ions to bacterial DNA, which leads to blocking of the transcription process. The second possible effect is associated with the violation of electron transport by membrane proteins [1]. At the same time, the influence of silver-based drugs on the lipid components of bacterial and human cell membranes remains not fully studied.

Silver ions are cosmotropic and lead to increasing of the main phase transition temperature (T_m) of phospholipid membranes from gel to liquid phase. Potassium ions are chaotropic and lead to decreasing of T_m . NO_3^- anions are also weakly chaotropic [2].

DPPC lipid with the main phase transition at $\sim 42^\circ\text{C}$ was selected for model lipid membranes preparations, since the influence of AgNO_3 on the phase transition temperature and the repeat distance of multilayer DPPC vesicles is studied in detail [4]. Samples of DPPC/lapis aqueous suspensions with the lipid and lapis mass fractions of 5% and 5% respectively with different storage times were studied by SANS on the YuMO spectrometer [4] at temperature range of $40\text{--}48^\circ\text{C}$. Initial data processing and corrections were performed in SAS package [5]. The presence of peaks on small-angle curves over the entire temperature range indicates the formation of lamellar structures – multilayer lipid vesicles (MLV). The repeat distances vs temperature, calculated from the peaks positions, are shown in Fig. 1.

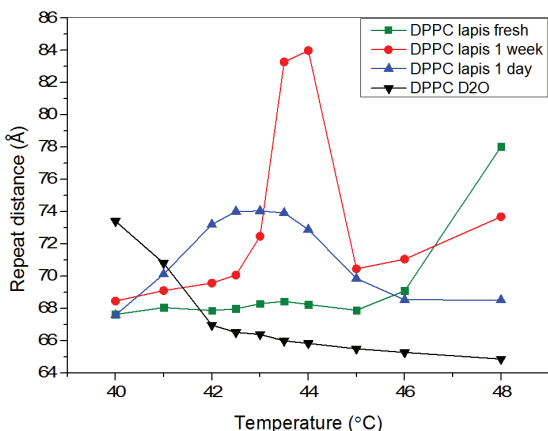


Fig. 1. Temperature dependence of repeat distances for samples of DPPC multilayer vesicle solutions in D₂O in absence and presence of lapis (5%+5% wt/wt) for different times of storage. Black curve – pure DPPC solution, green – fresh DPPC solution with lapis, blue – DPPC with lapis solution stored for 1 day, red – DPPC with lapis solution stored for 1 week.

Temperature dependences of the repeat distances differ significantly for fresh samples and samples stored for 1 day and 1 week. The behavior of repeat distance typical for a phase transition is observed in sample stored for 1 week at a temperature of about 44 °C.

Three samples of DPPC suspensions were prepared in the presence of lapis with mass fractions of DPPC/lapis in solutions of 2% and 2%, 3% and 3%, 5% and 5% in D₂O. The densities of each of the three samples in the temperature range of 38–48 °C were measured using the Anton Paar DMA5000M density meter (FLNP, JINR). Based on the analysis of the densitometric curves, we conclude that the resulting system may undergo significant disordering of the lipid bilayer in the simultaneous presence of AgNO₃ and KNO₃. Remarkably, a significant change in the density is observed in the region of 44–45 °C for all the studied suspension concentrations both during heating and cooling.

The results show that there is a significant change in the structure and phase state of the DPPC lipid bilayer in presence of the lapis preparation. Nevertheless, the lamellar structure of lipid vesicles is preserved. The storage time also dramatically influences the phase state of the DPPC-lapis vesicles and may lead to the reoccurrence of phase transition.

- [1] A.B. Shcherbakov, A.B. Korchac *et al.* (2006). Preparati serebra: vchera, segodnya i zavtra. *Pharmaceuticheskiy jurnal*. 5, 45–57. (in Russian)
- [2] O.V. Vashchenko, Y.L. Ermak & L.N. Lisetski (2013). Univalent ions in phospholipid model membranes: Thermodynamic and hydration aspects. *BIOPHYSICS*. 58, 515–523.
- [3] L.A. Bulavin, D.V. Soloviov *et al.* (2015). Lyotropic model membrane structures of hydrated DPPC: DSC and small-angle X-ray scattering studies of phase transitions in the presence of membranotropic agents. *Phase transitions*. 88(6), 582–592.
- [4] A.I. Kuklin, A.K. Islamov & V.I. Gordeliy (2005). Scientific reviews: Two-detector system for small-angle neutron scattering instrument. *Neutron News*. 16(3), 16–18.
- [5] A.G. Soloviev, T.M. Solovjeva *et al.* (2017). SAS program for two-detector system: seamless curve from both detectors. *J. Phys. Conf. Ser.* 848, No. 1, p. 12020.

PH-TRIGGERED STRUCTURAL TRANSFORMATIONS IN THE MIXTURES OF AN IONIC SURFACTANT AND A HYDROPHILIC POLYMER

A.V. Shibaev¹, A.L. Aleshina¹, A.I. Kuklin^{2,3}, I. Iliopoulos⁴ and O.E. Philippova¹

¹*Physics Department, M.V.Lomonosov Moscow State University, Moscow, Russia*

²*Joint Institute for Nuclear Research, Dubna, Russia*

³*Moscow Institute of Physics and Technology, Dolgoprudny, Russia*

⁴*PIMM, Arts et Metiers, Paris, France*

E-mail: aleshina@polly.phys.msu.ru

Surfactant molecules can self-assemble and form wormlike micelles in aqueous solutions. Under certain conditions, wormlike micelles become rather long, and they form a network of topological entanglements, which imparts special characteristics to the solution: high viscosity and strong viscoelastic properties. Due to these properties, such solutions find applications in various industries, including oil industry, production of consumer products etc. However, their mechanical strength is limited since surfactant molecules are bound together by weak non-covalent interactions. Therefore, different ways of increasing the mechanical properties of wormlike micellar solutions are proposed. One approach is based on mixing wormlike micelles with polymer molecules [1]. In order to increase viscoelasticity, the addition of polymer should not result in the disruption of wormlike micelles, which may happen, for instance, in the case of weakly hydrophobic polymers. Interaction between the components may be tuned by the change of external conditions, e.g. the change of pH, charge of the surfactant, or temperature. The objective of this work is to study the effect of pH on the mixtures of cationic wormlike micelles and nonionic hydrophilic polymer - polyvinyl alcohol (PVA).

It was shown by small-angle neutron scattering (SANS) that, in the absence of polymer, micelles of cylindrical shape are formed in a wide pH range from 5.5 to 11. Rheological measurements confirm that the micelles are very long wormlike objects, which form an entangled network, and their viscoelastic properties are not strongly affected by pH.

The addition of polymer at low pH leads to the disruption of long wormlike micelles and their transformation into very short cylindrical ones. From SANS data, the average length of such micelles was shown to be approximately 100-150 nm. When pH of the mixtures is increased, the micelles grow in length, and the solutions attain high viscosity and elasticity. This effect was explained by changing of the interaction between polymer chains and micelles at the molecular level. As shown by NMR, at low pH macromolecules contain some slightly hydrophobic acetate groups which may interact with the micelles, leading to the wrapping of the polymer chains around the micelles and to the decrease of their length. Upon increase of pH, hydrolysis of the acetate groups takes place, and interaction between the micelles and polymer chains disappears, which is manifested in the increase of viscosity by several orders of magnitude and appearance of strong viscoelasticity.

Acknowledgement. The work is financially supported by the Russian Foundation for Basic Research (project № 19-53-15012 NCNI_a).

[1] A.V.Shibaev, K.A.Abrashitova, A.I.Kuklin, A.S.Orekhov, A.V.Vasiliev, I.Iliopoulos, O.E.Philippova (2017). *Macromolecules*, 50, 339-348.

STABILITY OF FERRITIN PROTEIN COMPLEX AT VARIOUS pH

V.V. Sudarev¹, A.V. Vlasov^{1,2,3}, S.D. Osipov¹, Y.L. Ryzhykau^{1,2}, A.D. Vlasova¹, V.V. Skoy¹, T.N. Murugova^{1,2}, A.V. Rogachev^{1,2}, S.M. Bukhalovich¹, S.M. Dolotova¹, A.S. Kuskov¹, V.I. Gordel'iy^{1,4,5}, A.I. Kuklin^{1,2}

¹Research Center for Molecular Mechanisms of Aging and Age-Related Diseases, Moscow Institute of Physics and Technology, 141700 Dolgoprudny, Russia

²Joint Institute for Nuclear Research, 141980 Dubna, Russia

³Institute of Crystallography, RWTH Aachen University, 52066 Aachen, Germany

⁴Institut de Biologie Structurale Jean-Pierre Ebel, Université Grenoble Alpes—Commissariat à l'Energie Atomique et aux Energies Alternatives—CNRS, 38044 Grenoble, France

⁵JuStruct: Jülich Center for Structural Biology, Forschungszentrum Jülich, 52425 Jülich, Germany

E-mail: Sudarev.VV@phystech.edu, kuklin@nf.jinr.ru

Iron is a trace element which participates in the vital activity of any organism. It is responsible for the supply of oxygen to the tissues of the body and coordination of the active centers of various enzymes. Ferritin is one of the main iron-containing proteins. The main function of this protein is considered to be storage and transport of iron. One ferritin molecule can contain up to 4500 iron ions [1] in the form of ferrihydrite (structurally identical to $5\text{Fe}_2\text{O}_3 \cdot 9\text{H}_2\text{O}$ [2]), enclosed in a protein shell. In solutions this shell forms monomers, dimers and trimers [3]. Concentration of ferritin in the blood increases with age. It indicates the participation of iron and ferritin in the aging processes of the body.

We studied the influence of the pH of an aqueous solution on the protein complex of ferritin. Data were obtained on the state of stability of an aqueous solution of protein (MERCK, ferritin from equine spleen), and the denaturation conditions of the protein. We obtained protein solutions with a concentration of 5.5 mg/ml in a 150 mM NaCl solution with different pH values (1.5, 2, 2.5, 3, 3.5, 4, 7, 10, 11, 12) using dialysis (MWCO = 3.5 kDa, + 4°C, 200 rpm). The concentration of protein and iron ions in solutions was determined by UV spectroscopy on a Shimadzu UV-2450 spectrophotometer with an integrating sphere. The absorption spectra of all protein solutions were measured at wavelengths from 240 to 750 nm. The study of the hydrodynamic radius of ferritin was carried out by the dynamic light scattering (DLS) method on a DynaProNanoStar device (20 series per 5 seconds). DLS data analysis was performed using Dynamics v. 7.1.10 software.

It was found that the prepared samples have the same protein concentration at pH 7; 10 and 3 by the value of absorption at a wavelength of 280 nm. In addition, a consistent decrease in concentration was found in rows 3, 3.5, 4 pH; 10, 11, 12 pH; 3, 2.5, 2, 1.5 pH. Precipitation is observed at 3.5 and 4 pH, as well as 11 and 12 pH.

DLS data for pH = 3; 3.5; 4; 7; 10 show that the hydrodynamic radius of the protein remains 4.5-5 nm. This may be explained by the fact that ferritin does not undergo significant structural changes at the indicated pH. The decrease in the protein concentration at pH 3.5 and 4 can be explained by the proximity of the isoelectric point of the protein ($pI = 4.27$ [4]), which is confirmed by the precipitation. A consistent decrease in protein concentration at high (11, 12) and low (2, 1.5) pH is presumably related to the protein denaturation. This conclusion is also confirmed by DLS data: a decrease in the hydrodynamic radius of the protein from 4.5-5 nm (for solutions with a presumably native protein structure) to 2-3 nm (for solutions with a denatured form) was found.

More detailed information about protein's structure were obtained by small-angle neutron and X-Ray scattering methods. Measurements were performed at YuMO spectrometer [5] and Rigaku [6] correspondingly. It is in agreement with previous conclusions about ferritin complex stability.

[1] Ford G.C. et. al. (1984). Ferritin: design and formation of an iron-storage molecule. Philosophical Transactions of the Royal Society of London B, Biological Sciences. 304(1121), 551-565.

[2] Mann S. et. al. (1986). Structure and composition of ferritin cores isolated from human spleen, limpet (*Patella vulgata*) hemolymph and bacterial (*Pseudomonas aeruginosa*) cells. Journal of molecular biology. 188(2), 225-232.

[3] Zabelskii D.V. et. al. (2018). Ambiguities and completeness of SAS data analysis: investigations of apoferritin by SAXS/SANS EID and SEC-SAXS methods. Journal of Physics: Conf. Series. 994, 012017-1.

[4] Crichton R.R. (1971). Ferritin: structure, synthesis and function. New England Journal of Medicine. 284(25), 1413-1422.

[5] Kuklin A.I. et. al. (2005). Scientific reviews: Two-detector system for small-angle neutron scattering instrument. Neutron News. 16(3), 16-18.

[6] Murugova T.N. et. al. (2015). Low resolution structural studies of apoferritin via SANS and SAXS: the effect of concentration. J. Optoelectron. Adv. Mater. 17(9-10), 1397-14

THE POSSIBILITY OF DIMERIZATION OF ATP SYNTHASE FROM SPINACH CHLOROPLASTS

A.V. Vlasov^{1,2,3}, Yu.L. Ryzhykau^{1,3}, S.D. Osipov¹, Vlasova A.D.¹, N.A. Dencher^{1,4},
A.I. Kuklin*^{1,4}, V.I. Gordeliy*^{1,5,6}

¹Research Center for Molecular Mechanisms of Aging and Age-Related Diseases, Moscow Institute of Physics and Technology, 141700 Dolgoprudny, Russia

²Institute of Crystallography, RWTH Aachen University, 52066 Aachen, Germany

³Joint Institute for Nuclear Research, 141980 Dubna, Russia

⁴Physikalische Biochemie, Fachbereich Chemie, Technische Universität Darmstadt, Alarich-Weiss-Straße 4, 64287, Darmstadt, Germany

⁵JuStruct: Jülich Center for Structural Biology, Forschungszentrum Jülich, 52425 Jülich, Germany

⁶Institut de Biologie Structurale Jean-Pierre Ebel, Université Grenoble Alpes—Commissariat à l'Énergie Atomique et aux Énergies Alternatives—CNRS, 38044 Grenoble, France

E-mail: valentin.gordeliy@ibs.fr, kuklin@nf.jinr.ru

ATP synthase is the key membrane protein in biology. It provides almost all biochemical reactions with adenosine triphosphate molecule (ATP) and establishes metabolic processes in cells. ATP synthase is known to be three types (A-type in archaea, V- and F-type in Eubacteria and eukaryotes). F-type ATP synthases are the most spread among Eubacteria and eukaryotes and are incorporated in cellular and organellar membranes. F-type ATP synthases can be organized as dimers of four different types in mitochondria cristae of eukaryotes and in bacteria and chloroplasts they are monomers [1]. However, the latest publications showed that chloroplast F-type ATP synthases might be present as dimers or higher oligomers in thylakoid membranes [2], [3], [4]. The question of the oligomeric state is open and intensively discussed in literature.

ATP synthase is a large membrane protein complex (~ 600 kDa), therefore, the structural studies of it remain a big challenge. Currently, the perspective crystallization *in meso* technique, which allow obtaining high-resolution structures better than 2.5 Å, have limitations on crystallization of large protein complexes due to small diameters of water channels in lipid cubic phases, and the trials to crystallize *in meso* the intact chloroplast ATP synthase resulted only in a high-resolution structure (2.3 Å) of its' membrane subunit – c-ring [5]. This study revealed striking features of the c-rings of ATP synthases in almost all organisms and showed the necessity of the improvement of protein crystallization techniques (e.g. in lipid mesophases, *in meso*) and imaging of protein crystals towards overcoming limitations on protein size and obtaining a high-resolution crystallographic structure of ATP synthase. For example, the approach of using coherent anti-Stokes Raman scattering for imaging of protein crystals can be used to detect microcrystals of ATP synthase hidden in lipid mesophase as described in [6].

One more possible option for structural studies of large protein complexes is small-angle scattering (SAS). It allows one to investigate the protein in solution without growing crystals. The behavior of proteins is more native than in crystals if using SAS techniques. One should notice that performing SAS experiments with proteins that may form oligomers the influence of structure factors and dependence on protein concentration should be thoroughly analysed as described in [7], [8], [9], [10], [11]. Thus, the investigation of chloroplast ATP synthase by SAS might show the real behavior of the protein.

In this work, we present evidences that F-type ATP synthases from spinach chloroplasts might be organized in dimers. Small-angle X-ray scattering (SAXS) technique was used to recover the 3D *ab initio* low-resolution structure of ATP synthase reconstituted into lipid-protein nanodiscs. The form-factor of the structure is similar to that of ATP synthases incorporated in mitochondria cristae. V-shape form of chloroplast ATP synthases in DMPC/MSP1E3D1 nanodiscs have been shown previously [2]. In addition, we checked POPC/MSP1E3D1 nanodiscs by SAXS and obtained the similar form-factor. The SAXS data were analysed taking into account protein dimerization [9]. Thus, the formation of dimers of ATP synthase might occur in bilayers composed by different lipids and probably it may possibly take place in thylakoid membranes.

- [1] W. Kühlbrandt, "Structure and Mechanisms of F-Type ATP Synthases," *Annu. Rev. Biochem.*, vol. 88, no. 1, pp. 515–549, Jun. 2019.
- [2] A. V. Vlasov, Y. L. Ryzhykau, V. I. Gordeliy, and A. I. Kuklin, "Spinach ATP-synthases form dimers in nanodiscs. Small-angle X-ray and neutron scattering investigations," *FEBS J.*, vol. 284, no. s1, p. 87, 2017.
- [3] H. J. Schwaßmann, S. Rexroth, H. Seelert, and N. A. Dencher, "Metabolism controls dimerization of the chloroplast FoF1 ATP synthase in *Chlamydomonas reinhardtii*," *FEBS Lett.*, vol. 581, no. 7, pp. 1391–1396, Apr. 2007.
- [4] H. Seelert and N. A. Dencher, "ATP synthase superassemblies in animals and plants: Two or more are better," *Biochimica et Biophysica Acta - Bioenergetics*, vol. 1807, no. 9. Elsevier, pp. 1185–1197, 01-Sep-2011.
- [5] A. V. Vlasov *et al.*, "Unusual features of the c-ring of F1FO ATP synthases," *Sci. Rep.*, vol. 9, no. 1, p. 18547, Dec. 2019.
- [6] A. V. Vlasov *et al.*, "Raman Scattering: From Structural Biology to Medical Applications," *Crystals*, vol. 10, no. 1, p. 38, Jan. 2020.
- [7] A. V. Vlasov *et al.*, "Protein structure and structural ordering versus concentration dependence," *FEBS J.*, vol. 281, no. S1 1, pp. 593–594, 2014.
- [8] T. N. Murugova *et al.*, "Low resolution structural studies of apoferritin via SANS and SAXS : the effect of concentration," *J. Optoelectron. Adv. Mater.*, vol. 17, no. 10, pp. 1397–1402, 2015.
- [9] D. V. Zabelskii *et al.*, "Ambiguities and completeness of SAS data analysis: investigations of apoferritin by SAXS/SANS EID and SEC-SAXS methods," *J. Phys. Conf. Ser.*, vol. 994, no. 1, p. 012017, Mar. 2018.
- [10] O. M. Selivanova *et al.*, "To Be Fibrils or To Be Nanofilms? Oligomers Are Building Blocks for Fibril and Nanofilm Formation of Fragments of A β Peptide," *Langmuir*, vol. 34, no. 6, pp. 2332–2343, Feb. 2018.
- [11] Y. L. Ryzhykau, M. Y. Nikolaev, D. V. Zabelskii, A. I. Kuklin, V. I. Gordeliy, and V. I. Gordeliy, "Trimers of dimers of SRII/HtrII full complex. Small angle scattering structural investigation," *FEBS J.*, vol. 284, p. 154, 2017.

STRUCTURAL INVESTIGATION INTERACTION BETWEEN AMYLOID-BETA PEPTIDES AND ASSOCIATED PROTEINS — THE HUMAN SERUM ALBUMIN AND HUMAN CYSTATIN C

A. Żyła^{1,2}, P. Jurczak³, A. Szymańska³, J. Wolak¹, M. Taube¹, I. Zhukov⁴, A.I. Kuklin⁵, M. Kozak^{1,6}

¹*Department of Macromolecular Physics, Faculty of Physics, Adam Mickiewicz University, Poznań, Poland*

²*NanoBioMedical Centre, Adam Mickiewicz University, Poznań, Poland*

³*Department of Biomedical Chemistry, Faculty of Chemistry, Gdańsk University, Gdańsk, Poland*

⁴*Institute of Biochemistry and Biophysics, Polish Academy of Sciences, Warszawa, Poland*

⁵*Frank Laboratory of Neutron Physics, Joint Institute for Nuclear Research, Dubna, Moscow Region, Russia*

⁶*SOLARIS National Synchrotron Radiation Centre, Jagiellonian University, Kraków, Poland*

E-mail: adrzyl@amu.edu.pl

Neurodegenerative disorders (Alzheimer's, Parkinson's diseases) correlates with the extension of the lifetime in our population. These diseases are still a big challenge for science and effective drugs are still not discovered.

The discovery of proteins or peptides associated with aforementioned diseases was a milestone in understanding them at the molecular level and determination of three-dimensional structures of these macromolecules has allowed to discover some of the mechanisms of protein aggregation and the formation of their neurotoxic oligomers or amyloid deposits. Moreover, there are promising studies showing that proteins like human serum albumin (HSA) or human cystatin C (HCC) could be involved in the inhibition of A β peptides aggregation into toxic amyloids.

We have optimized production and purification protocols of HSA and HCC proteins and also the synthesis of selected variants of A β peptides including fluorescent labeling of 3-28 A β peptide. Purified proteins will be used in the biophysical studies of the interaction between those biomolecules and aggregation of amyloid-beta peptides in the presence of HSA and HCC proteins. Currently, we are developing a protocol for the overexpression of deuterated HCC protein for SANS studies of HCC in complexes. Our initial studies include the characterization of amyloid-beta fibrils under atomic force microscopy (AFM) and circular dichroism. Recently, we have initiated the studies of HSA complexes with A β using small angle X-ray and neutron scattering (SAXS/SANS). We studied the interaction between HSA and HCC in solution by using NMR spectroscopy and measurements the SAXS profile of this system. We also proposed a theoretical model of binding the A β peptides to the HCC molecule.

Acknowledgments

P. Czaplewska for MS experiment under her supervision, B. Peplińska for TEM experiment under her supervision. The studies were supported by research grant 2017/27/B/ST4/00485 from National Science Centre, POWR.03.02.00-00- I032/16 from European funds. Development and Joint Institute for Nuclear Research for a beamtime at Dubna Neutron Source.

- [1] Castello MA, Soriano S (2014). *Ageing Res Rev* 13:10-2
- [2] Choi TS et al (2017) *J Am Chem Soc.* 139(43):15437-15445
- [3] Spodzieja M et al (2017) *J Mol Recognit.* 30(2)
- [4] Kurcinski M et al (2015) *NAR.* 1;43(W1):W419-24

THE NEUTRON DIFFRACTION STUDY OF CRYSTAL AND MAGNETIC STRUCTURES OF MULTIFERROIC $\text{Bi}_{2-x}\text{Fe}_x\text{WO}_6$

O.N. Lis^{1,2}, S.E. Kichanov¹, N.M. Belozerova¹, E.V. Lukin¹, B.N. Savenko¹, S. Balakumar³

¹*Frank Laboratory of Neutron Physics, Joint Institute for Nuclear Research, Dubna, Russia*

²*Kazan Federal University, Kazan, Russia*

³*National Centre for Nanoscience and Nanotechnology, University of Madras, Guindy Campus, Chennai, India*

E-mail: lisa_9477@mail.ru

Multiferroic materials have coupled magnetic, electric and even structural order parameters that result in ferromagnetic, ferroelectric, and/or ferroelastic properties at same phase. Therefore, they have attracted the attention of researchers since the discovery of unusual dielectric properties (ferroelectricity) in some perovskite oxides in the 1940s. Also these materials have potential applications in information storage, the emerging field of spintronics and for other applications.

BiFeO_3 Bismuth ferrite (BFO) modified with WO_3 is one of such magnetoelectric material, exhibiting antiferromagnetic and ferroelectric properties in the same crystal structure. As WO_3 has ferroelectric properties at low temperature, it is expected that addition of a small amount of this compound to BFO will result in some interesting multiferroic properties, including a shift of their transition temperature. The Fe^{3+} ions in BFO like multiferroics provide an effective approach in creating a weakly ferromagnetic state in ferroelectric phase. Therefore, for the most complete understanding of the effects occurring in this compound, detailed studies of the structural and magnetic properties of $\text{Bi}_{2-x}\text{Fe}_x\text{WO}_6$ are necessary. Exposure of high pressure is directly method of controlled changing the magnetic interactions by the variation of the interatomic distances and angles, in comparison with other experimental methods.

The present work focuses on detailed studies of the crystal and magnetic structure of $\text{Bi}_{2-x}\text{Fe}_x\text{WO}_6$ by means of neutron diffraction on a DN-6 diffractometer of a pulsed high-flux IBR-2 reactor (FLNP, JINR, Dubna, Russia) using a high-pressure cell with sapphire anvils in the wide pressure and temperature range. The pressure and temperature dependences of the unit cell parameters, the volume and the interatomic bond lengths of the $\text{Bi}_{2-x}\text{Fe}_x\text{WO}_6$ compound were obtained. The calculated compressibility coefficients indicate anomalies in the behavior of interatomic lengths.

The work was supported by the Russian Foundation for Basic Research, grant RFBR N19-52-45009 IND_a.

THE EFFECT OF DOPING OF Sr²⁺ IONS ON THE CRYSTAL AND MAGNETIC STRUCTURE OF BARIUM HEXAFERRITES Ba_{1-x}Sr_xFe₁₂O₁₉

A.V. Rutkauskas¹, D.P. Kozlenko¹, S.E. Kichanov¹, B.N. Savenko¹

¹Frank Laboratory of Neutron Physics, Joint Institute for Nuclear Research, 141980 Dubna, Russia

E-mail: ranton@nf.jinr.ru

Multiferroics have been intensively studied in recent decades. These compounds have a close relationship between magnetic and electrical properties. It makes them promising materials for wide technological application: permanent magnets, microwave devices, spintronics and etc. M-type barium hexaferrites (Ba_{1-x}Sr_xFe₁₂O₁₉) are ones of these compounds. They have remarkable physical properties: high coercive force, large magnetocrystalline anisotropy, high Curie temperature, relatively large magnetization, as well as excellent chemical stability and corrosion resistance.

A significant improvement of the intrinsic magnetic properties of hexaferrites can be obtained by the partial substitution of Sr²⁺ ions. Thus, the concentration of Sr²⁺ ions in Ba_{1-x}Sr_xFe₁₂O₁₉ compounds determines the magnetic properties of the material such as magnetization, Curie temperature and the magnetocrystalline anisotropy.

The neutron diffraction method allows to study simultaneously crystal and magnetic structure of compounds. Also, this method allows to determine light elements or elements with close atomic numbers. The former is especially important when studying complex oxides, where the formation of magnetic ordering is carried out through oxygen ions.

Our work presents the results of study of hexaferrites Ba_{1-x}Sr_xFe₁₂O₁₉ (x = 0, 0.25, 0.5, 0.75) by means of neutron diffraction method at room temperature. The structural parameters and magnetic moments of Fe ions were calculated. Their dependences on concentration of Sr²⁺ ions were also obtained. The lattice parameters and bond distances have an anisotropic behavior with increasing of Sr²⁺ concentration. Doping of Sr²⁺ ions have not changed the type of the magnetic structure among the studied samples.

This work was supported by the Russian Foundation for Basic Research (project no. 20-02-00550-«a»)

HIGH PRESSURE INDUCED STRUCTURAL AND MAGNETIC PHASE TRANSFORMATIONS IN BaYFeO₄

D.P. Kozlenko¹, I.Yu. Zel¹, T.N. Dang^{2,3}, T.P.T. Le^{4,5}

¹ Frank Laboratory of Neutron Physics, Joint Institute for Nuclear Research, 141980 Dubna, Russia

² Institute of Research and Development, Duy Tan University, 550000 Da Nang, Viet Nam

³ Faculty of Natural Sciences, Duy Tan University, 550000 Da Nang, Viet Nam

⁴ University of Education, The University of Da Nang, 550000 Da Nang, Viet Nam

⁵ Department of Physics, University of Sciences, Hue University, 530000 Hue, Viet Nam

E-mail: ivangreat2009@gmail.com

Multiferroic materials exhibiting the magnetism-driven ferroelectricity, where ferroelectricity is induced by magnetic ordering, have been attracting continuous attentions in scientific research due to their application potential as well as from the fundamental science angle. It is worth to note that the magnetism-induced ferroelectricity is commonly observed in magnetically frustrated systems such as BaYFeO₄, since spin frustration induces spatial variation in magnetization, which leads to the loss of the lattice inversion symmetry, thereby resulting in the occurrence of ferroelectricity. The geometric magnetic frustration due to its structural complexity gives rise to their peculiar physical properties, raising from the complex interplay among magnetic frustration due to competing superexchange interactions and spin, lattice, charge and orbital degrees of freedom. To better understanding the nature of magnetoelectric phenomena in the sample, we have performed high pressure effect on the crystal and magnetic structure of BaYFeO₄ by using a combination of neutron diffraction and Raman spectroscopy up to 5.2 and 18 GPa, respectively. It has been established that BaYFeO₄ possess two long-range magnetic transitions: one at 55 K corresponding to a formation of the spin density wave antiferromagnetic (AFM) order (SDW), which then transforms to the cycloid AFM order at 36 K. The latter one is supposed to be the origin of ferroelectricity of the sample. It has been observed that application of pressure, $P > 2$ GPa, tends to convert the lower-temperature cycloid order to the SPW one, pointing a pressure-induced suppression of ferroelectricity. The Neel temperature T_N of the SPW order almost linearly decreases upon compression with pressure coefficient of -1.4 K/GPa. Moreover, at $P \sim 5$ GPa a structural phase transformation accompanied by anomalies in pressure behavior of vibrational modes was observed. The observed phenomena have been discussed using by the DFT calculations.

The work has been supported by the Russian Foundation for Basic Research, grant 20-52-54002 Вьет_a

TENSIONAL RESIDUAL STRAIN INVESTIGATION BY FORCE DIRECTION OF THE REBAR STEEL SAMPLE USING TIME-OF-FLIGHT NEUTRON DIFFRACTION AT THE STRAIN/STRESS DIFFRACTOMETER EPSILON

A.Badmaarag^{1,2}, D.Sangaa¹, V. Sikolenko², Ch.Scheffzük^{2,3}, L.EnkhTUR⁴, Y.Duinkherjav⁵, P.Otgobayar⁵

¹*Institute of Physics and Technology, Ulaanbaatar, Mongolia*

²*Frank Laboratory of Neutron Physics, Joint Institute for Nuclear Research, Dubna, Russia*

³*Karlsruhe Institute of Technology, Institute of Applied Geosciences, Karlsruhe, Germany*

⁴*National University of Mongolia, Ulaanbaatar, Mongolia*

⁵*The Mongolian University of Science and Technology, Ulaanbaatar, Mongolia*

E-mail: badmaarag@jinr.ru

Here, we presented in-situ residual strain and stress measurements for the rebar steel sample using the time-of-flight neutron diffraction technique EPSILON. It was demonstrated in this study that the three-dimensional deformation behavior of the rebar steel, can be accurately scanning measured residual strain. In this aim, the measurements of lattice strains by neutron diffraction were performed in-situ during the tensile test up to sample fracture. A residual strain scan has been carried out along the axis of a sample ($d = 10$ mm, $l = 100$ mm). Residual strain values of rebar steel samples have been detected with a minimum of 2.5×10^{-3} , and maximum strain values of 12.6×10^{-3} .

References

- [1] Taran Y.V., Balagurov A. M., Sabirov B., Davydov V. and Venter A. (2014), *Materials Science Forum*. **768-769**, 697-704
- [2] Scheffzük Ch., Müller B.I.R., Breuer S., Altangerel B. and Schilling F.R. (2016), *Mongolian Journal of Physics*. **2**, 433-441.
- [3] Scheffzük Ch., Hempel H., Frischbutter A., Walther K., and Schilling F. R. (2012) *J. Phys. Conf. Ser.* **340** 012038 [doi:10.1088/1742-6596/340/1/012038]. Rietveld H.M., (1967), *Acta Cryst.***22**. 151.
- [4] Scheffzük Ch., Walther K. and Frischbutter A. (2014) *Materials Science Forum*. **777**, 136-141.
- [5] Badmaarag A., Scheffzük Ch., Sangaa D. (2016), *Mongolian Journal of Physics*. **2**, 442-448.

RESIDUAL STRESS DISTRIBUTION AFTER A QUENCHING TREATMENT OBTAINED BY NEUTRON DIFFRACTION EXPERIMENTS AND FEM SIMULATION

G. Carro-Sevillano¹, R. Fernández Serrano¹, G. Bokuchava², L. Millán¹ and G. González-Doncel¹

¹ *CENIM-CSIC, Madrid, Spain*

² *FLNP, Dubna, Russia*

E-mail: gabriel.carro@cenim.csic.es

In a quenching treatment, metallic materials undergo a rapid cooling from high temperatures, around 800K in aluminium alloys, to room temperature. This process generates a rapid contraction of the material that generates an inhomogeneous distribution of macroscopic residual stresses.

The aim of this work is to compare the macroscopic residual stresses determined experimentally and those obtained by finite element simulation, FEM. The use of FEM simulation allows to describe the stress distribution from the thermal, mechanical (elastic and plastic) properties of the alloys and the sample size and geometry. In this work, results of macroscopic residual stress distribution simulated by FEM are presented considering the evolution of thermal and mechanical properties with temperature during the cooling process. Stress distribution in axial, radial and hoop directions has been determined experimentally by neutron diffraction at the FSD instrument of the FLNP institute in Dubna, Russia, for the AA2014 and AA5083 alloys after cooling from 813 K to room temperature. The FEM simulations have been carried out by COMSOL multiphysics. The effect of the elastic limit and its evolution with temperature, elastic modulus and sample size on macroscopic residual stresses calculated has been determined from FEM simulations. It will be shown how it is possible to find equivalent macroscopic residual stress states by combining the parameters described above.

FEATURES OF THE STRUCTURE OF THE CHELYABINSK METEORITE ACCORDING TO NEUTRON SAS

A.K. Kirillov¹, T.A. Vasilenko³, A. Kh. Islamov²

¹*Institute for Physics of Mining Processes, NAS Ukraine, Dnipro, Ukraine*

²*Joint Institute for Nuclear Research, Dubna, Russian Federation*

³*Saint-Petersburg Mining University, St.-Petersburg, Russian Federation*

E-mail: kirillov_ak@ukr.net

Our study is another demonstration of the abilities of neutron physics in the study of natural and industrial materials. The object of the study is a fragment of the Chelyabinsk meteorite, which was investigated in [1].

The studied fragment of the Chelyabinsk meteorite was found on February 23, 2013 close to the enrichment plant of Deputatsky settlement near Yemanzhelinsk, Chelyabinsk region, Russian Federation. The meteorite is referred to the LL5 chondrite.

Experimental: Small-angle neutron scattering (SANS) experiments were performed on YuMO time-of-flight spectrometer [2]. The diameter of the sample in the beam was 14 mm and the exposure time was 20 min. The measured neutron scattering spectra were corrected for the transmission and thickness of the sample, background scattering and on the vanadium reference sample with using SAS software [3], yielding a neutron scattering intensity in absolute units of cm^{-1} . Scattering length density was calculated using the actual elemental composition of the meteorite.

Results: The specific pore surface and porosity of the material of the meteorite fragment for the power-law dependence of the neutron scattering intensity with an exponent $\alpha = 3.69$ are calculated in the approximation of the fractal model and those by Porod and Guinier. We obtained the size distribution of scattering centers using the GNOM software package, which have the form of an exponential function with parameter $c = 11.4$ nm.

The best approximation of the scattering curve is achieved by solving the inverse problem for voids of flat geometry, which are the most likely formed during collision processes of the parent meteorite body and the passage of the meteorite through the Earth's atmosphere. The characteristic sizes of the heterogeneities are shown in Table 1. The variants designated as R , R_p , $\langle R \rangle$, l_{cor} , are calculated in various ways in the Porod approximation.

Table 1. Variants of the size of inhomogeneities of scattering centers (nm)

R_f Fractal model	R_g Guinier	R_∞	R_p	$\langle R \rangle$	l_{cor}	c Gnom	$R_{p(f)}$ Gnom
240	26.5±1.1	30	113	25	11.7	11.4	7.8

Conclusions: The presented results demonstrate the advantages of neutron physics in the study of heterogeneous samples of natural origin, since in this case the quantum and wave properties of neutrons are fully realized.

[1] S. E. Kichanov et al. (2019). A structural insight into the Chelyabinsk meteorite: neutron diffraction, tomography and Raman spectroscopy study. *SN Applied Sciences*. 1, 1563.

[2] A.I. Kuklin et al. (2005). Scientific Reviews: Two-detector System for Small-Angle Neutron Scattering Instrument. *Neutron News*. 16(3), 16-18.

[3] A.G. Soloviev et al. (2003). SAS The Package for Small Angle Neutron Scattering Data treatment. Version 2.4. Long write-Up and User's Guide (Russian). JINR Communication P10-2003-86. Dubna.

TEXTURE STUDY OF SINANODONTA WOODIANA SHELLS BY X-RAY DIFFRACTION

M. Kucerakova¹, J. Rohlicek¹, D. Nikoayev² and T. Lychagina²

¹*Institute of Physics, Czech Academy of Sciences, Prague, Czech Republic*

²*Frank Laboratory of Neutron Physics, Joint Institute for Nuclear Research, Dubna, Russia*

E-mail: kucerakova@fzu.cz

Study of the preferred orientation of biological materials (bones, shells, etc.) represents the use of crystallographic methods in biophysics to search for new possibilities in material science. Much attention is paid to texture of bivalve mollusc shells. However, for quality systematic investigation of crystallographic preferred orientation of these shells, it is necessary to examine many representatives from different parts of the world [1].

In our study X-ray diffraction was used to examine the crystal preferential orientation of adult shell of the species *Sinanodonta woodiana* collected from Czech freshwater streams. The texture of artificially grown young shells was also measured. Pole figure measurements of Aragonite phase (planes 111, 102, 200, 121, 022 and 122) were provided by using high-resolution X-ray diffractometer SmartLab Rigaku with Cu rotating anode X-ray source (Institute of Physics, Prague, Czech Republic).

[1] D. Nikolayev, T. Lychagina and A. Pakhnevich (2019). Experimental neutron pole figures of minerals composing the bivalve mollusc shells, SN Applied Sciences, DOI: 10.1007/s42452-019-0355-1.

STUDY OF RESIDUAL STRESSES IN AN EXTRUDED ALUMINIUM ALLOY AFTER THERMAL TREATMENTS

L. Millán¹, G. Bokuchava², J.I. Hidalgo³, R. Fernández¹, G. Kronberger⁴, P. Haldova⁵, A. Sáez⁶, I. Papushkin², O. Garnica³, J. Lanchares³, and G. González-Doncel¹.

¹*Department of Physical Metallurgy. Centro Nacional de Investigaciones Metalúrgicas (CENIM) C.S.I.C. Av. de Gregorio del Amo, 8, Madrid E-28040, Spain*

²*Frank Laboratory of Neutron Physics. Joint Institute for Nuclear Research, Joliot-Curie Str. 6, Dubna 141980, Russia*

³*Adaptive and Bioinspired System Group. Universidad Complutense de Madrid, C. del Profesor José García Santesmases, 9, Madrid E-28040, Spain*

⁴*Heuristic and Evolutionary Algorithms Laboratory, University of Applied Sciences Upper Austria, Softwarepark 11, 4232, Hagenberg, Austria*

⁵*Structural and System Diagnostic. Research Centre Rez, Husinec-Rez, 130, Prague 25068, Czech Republic*

⁶*Department of Technology. Centro de Investigaciones Energéticas, Medioambientales y Tecnológicas (CIEMAT) Av. Complutense, 40, Madrid E-28040, Spain*

E-mail: mglauri@cenim.csic.es, gizo@nf.jinr.ru, hidalgo@ucm.es, ric@cenim.csic.es, Gabriel.Kronberger@fh-hagenberd.at, patricehaldova@evrez.cz, alberto.sae@ciemat.es, piv@nf.jinr.ru, ogarnica@ucm.es, julandan@ucm.es, ggd@cenim.csic.es

This paper aims to calculate the macroscopic and microscopic residual stresses (M-RS and m-RS) in extruded cylindrical samples of non-ageing aluminium alloy 5083 (Al-Mg) generated with a treatment at 530°C followed by quenching in water. It was also planned to study the RS state when slow (furnace) cooling is carried out. We start from the premise that the alloy is single-phased and not isotropic at the microscopic scale; it consists of a multitude of grains that present different mechanical response depending on their crystallographic orientation and their neighboring grains. The study of RSs has been carried out using data obtained by neutron diffraction on the high-resolution FSD instrument of the IBR-2 pulsed reactor (fast pulsed reactor) at the FLNP-JINR Institute, in Dubna, Russia. The plastic anisotropy of the individual grains gives rise to non-homogeneous plastic deformation in the axial direction during the extrusion process, which results in the development of a crystallographic texture (fibre texture). Due to the inhomogeneity of the extrusion process (friction with the die), a texture gradient is generated across the diameter of the bar. With the quenching process, a parabolic M-RS is developed. With slow cooling, however, this M-RS profile should not appear. In this first analysis, the profile of the M-RS produced with both treatments is studied. It is observed that, indeed, a parabolic profile (which obeys the equilibrium conditions of Mechanics) in the quenched sample is generated, and a flat profile (indicating the absence of a M-RS) in the slow cooled one. Results with the Rietveld method confirmed this affirmation. It is shown the absence of an effect of the texture gradient on the parabolic M-RS profile. Furthermore, it is also seen that a m-RS is still present after slow cooling. This suggests high stability of the original m-RS field arising from the extrusion process. A more detailed study of this observation is ongoing.

The m-RS depends on the treatment imposed, the microstructure, and the mechanical strength of the alloy grains. The microstructure was analyzed in the axial, radial and hoop sections of cubes taken from different positions along the diameter of the original cylindrical samples. The microstructural parameters of each grain were obtained employing EBSD technique: orientation, area, number of first neighbours, aspect ratio, and inclination. Genetic

programming was used to calculate m-RS considering that each diffraction peak describes the stress distribution of a group of grains having a certain orientation and stress. The Genetic Programming algorithm assigns to each grain a stress value according to the peak distribution and the microstructural parameters of these grains. (423)

References

- [1] P. Fernández-Castrillo (2006). Macro and micro-residual stress distribution in 6061 Al-15 vol.% SiCw under different heat treatment conditions. *Compos. Sci. Technol.* 66, 11–12, 1738–1748.
- [2] Cioffi, F. (2014). Analysis of the unstressed lattice spacing, d_0 , for the determination of the residual stress in a friction stir welded plate of an age-hardenable aluminum alloy - Use of equilibrium conditions and a genetic algorithm. *Acta Mater.* 74, 189–199.
- [3] Hidalgo, J. (2016). Using Evolutionary Algorithms to determine the residual stress profile across welds of age-hardenable aluminum alloys. *Applied Soft Computing.* 40, 429–438.
- [4] R. Fernández (2018) A multi-scale analysis of the residual stresses developed in a single-phase alloy cylinder after quenching. *Mater. Des.* 137, 117–127.
- [5] G. Bokuchava(2018). Neutron Fourier Stress Diffractometer FSD at the IBR-2 pulsed reactor. *Crystals.* 8, 318.
- [6] G. Bokuchava (2019). Characterization of precipitation in 2000 series aluminium alloys using neutron diffraction, SANS and SEM methods. *Romanian Reports in Physics.* 71, 502, 1-12.

SYNCHROTRON ENERGY DISPERSIVE METHOD AND GRAZING INCIDENT X-RAY DIFFRACTION USED TO MEASURE STRESSES IN SURFACE LAYERS OF POLYCRYSTALLINE MATERIALS

A. Oponowicz¹, M. Marciszko-Wiąckowska², A. Baczmanski¹, M. Klaus³, Ch. Genzel³, S. Wronski¹, M. Wróbel⁴

¹AGH-University of Science and Technology, WFIS, al. Mickiewicza 30, 30-059 Kraków, Poland

²AGH-University of Science and Technology, ACPIN, al. Mickiewicza 30, 30-059 Kraków, Poland

³Abteilung für Mikrostruktur- und Eigenspannungsanalyse, Helmholtz-Zentrum Berlin für Materialien und Energie, Albert-Einstein-Str. 15, Berlin 12489, Germany

⁴AGH-University of Science and Technology, WIMiP, al. Mickiewicza 30, 30-059 Kraków, Poland

E-mail: Adrian.Oponowicz@fis.agh.edu.pl

Residual stresses together with microstructure are one of the most important parameters for materials characterization. The stress state and material properties are usually heterogeneous in the near-surface volume of the machined samples. This is why, designing and determination of these properties, by appropriate experimental methods, is of great importance. The X-ray diffraction stress analysis (XSA) in reflection mode, due to its many advantages, is a commonly used non-destructive technique. Especially important and useful are these XSA methods which allow for residual stress determination in well-defined layers under the surface of the sample or within the sample volume.

In this study a new way for analysis of the ED (energy dispersive) synchrotron data was proposed and tested on the examples of mechanically treated Ti surfaces [1]. This analysis (called MMXD - multireflexion and multiwavelength X-ray diffraction) allowed to determine depth-dependent stress profile vs. penetration depth with a step of 2 μm . The applicability of the MMXD method for samples exhibiting strong stress gradient is evident due to fact that the data are grouped for much smaller ranges in comparison with the standard ED. Special care should be taken when analysing MMXD data for samples consisting of near-perfect crystals, when the extinction effect should be taken into account in calculation of the information depth for which experimental points are grouped.

For the mechanically treated surfaces of Ti-alloy samples, a good convergence was obtained between the stresses measured using synchrotron radiation (MMXD and standard ED methods) and those determined with Cu $K\alpha$ radiation on laboratory diffractometer (MGIXD multireflexion grazing incidence X-ray diffraction) Fig.1 a. Certainly, synchrotron radiation with higher energies allowed measurements for larger depths in comparison with laboratory X-rays. The indisputable advantage of the MGIXD and MMXD methods is the possibility of determination of both a_0 (Fig. 1 b) and c_0/a_0 (Fig. 1 c) strain free lattice parameters in the well-defined surface region of the sample.

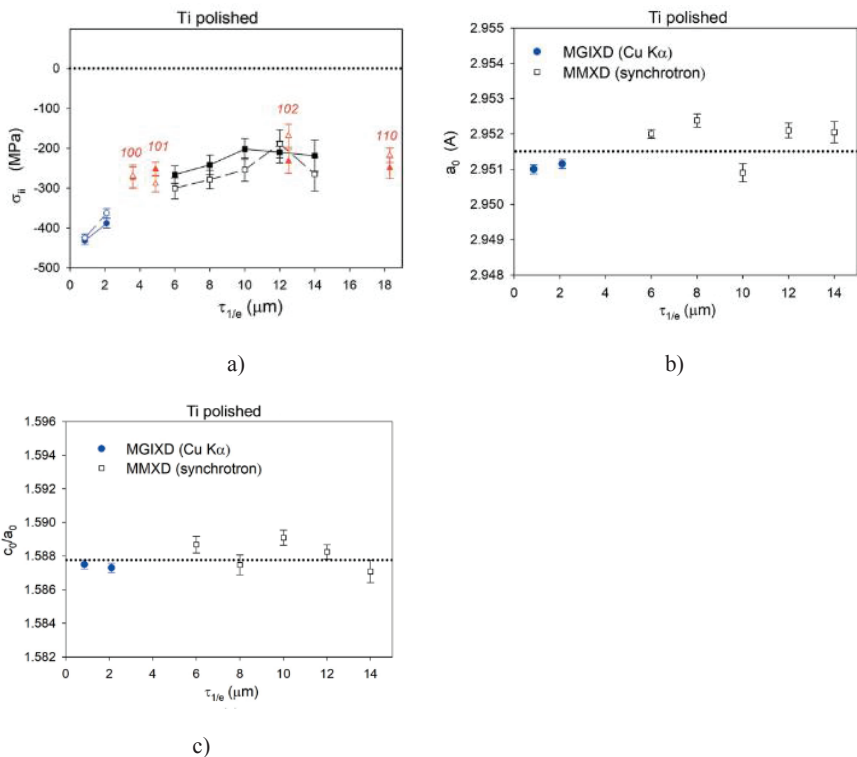


Figure 1. The in-depth profiles of stresses (a), a_0 (b) and c_0/a_0 (c) parameters for mechanically polished (bi-directional polishing) and ground (where σ_{11} is parallel to grinding direction) Ti- grade 2 samples, as well as the reference powder sample, obtained by MGIXD method. The Cu $K\alpha$ radiation and pseudo-Voigt profile were used for fitting.

Acknowledgements

This work was partially supported by grants from the National Science Centre, Poland (NCN), No. UMO-2017/25/B/ST8/00134. Oponowicz A. has been partly supported by the EU Project POWR.03.02.00-00-1004/16

[1] M. Marciszko, A. Baczmanski, M. Klaus, C. Genzel, A. Oponowicz, S. Wronski, M. Wróbel, C. Braham, H. Sidhom and R. Wawszczak, J. Appl. Cryst. (2018). 51, 732-745

PRELIMINARY STUDY OF RESIDUAL STRESS DISTRIBUTION IN HIGH STRENGTH STEEL WIRES AT EPSILON NEUTRON DIFFRACTOMETER

P.N. Silva¹, R.V. Erhan^{2,3}, C. Scheefzuk⁴ and J.A.C.P. Gomes¹

¹*COPPE - Federal University of Rio de Janeiro (UFRJ), Rio de Janeiro, Brazil;*

²*Institute for Energy Technology (IFE), Kjeller, Norway;*

³*Horia Hulubei National Institute for R&D in Physics and Nuclear Engineering (IFIN-HH), Bucharest - Magurele, Romania*

⁴*Frank Laboratory of Neutron Physics - Joint Institute for Nuclear Research (FLNP/JINR), Dubna, Russia*

E-mail: pedronetto@metalmat.ufrj.br

Unbonded flexible pipes used for transporting process fluids in offshore oil and gas production systems consist of concentric polymer and metallic layers. Typically, tensile armours are the outermost metallic layers, which are constructed of high strength carbon steel wires helically or circumferentially wound around inner pressure layers [1]. These wires provide axial strength and torsion resistance to the pipes, allowing them to sustain its own weight and resist to stresses associated to environmental conditions and vessel motion.

The tensile wires are confined in the region of the pipe commonly referred to as annulus, between inner and outer polymer sheaths. During operation, carbon dioxide and seawater are often found in the annulus, generating a corrosive environment which, associated with high stress levels, may lead the high strength steel wires to fail as a result of stress corrosion cracking. This is a complex degradation mechanism in which the combination of tensile stresses, a susceptible microstructure and a corrosive environment can cause the material to crack.

Due to their structural role, degradation of the tensile wires can compromise the integrity of the entire pipe, shortening its service life. Early shutdowns may follow as soon as a potential problem is identified, or, in worse cases, premature failure may not be avoided [2] and result in serious repercussions, including large scale damage to marine ecosystems.

The tensile wires are subject to heavy plastic deformation during the manufacturing process of the pipe [3], thus one hypothesis is that residual stresses play an important role in the cracking mechanisms. In the present work, preliminary neutron studies at the EPSILON stress/strain diffractometer, IBR-2 pulsed neutron source, was performed to verify the effect of plastic deformation on the microstructure of the wire in order to validate the method for further and more detailed analyses, such as quantification of residual stress levels.

Two wire samples were used in the experiments: as received (unstrained) and bent to a certain deflection (strained). Neutron measurements were performed in two different positions. Experiment A was carried out with the neutrons beam arriving at the wire surface perpendicular to the XZ plane (where the X-axis corresponds to width and the Z-axis corresponds to length), and experiment B was performed with the neutrons beam reaching the wire perpendicular to the YZ plane (where the Y-axis corresponds to thickness).

Results from experiment A are shown in Figure 1, where the peak relative to the strained sample is slightly shifted to the left compared to that of the unstrained sample. Because the neutron beam arrived at the tensioned surface of the strained wire perpendicular to the XZ plane, data obtained from this reading was qualitative, as due to considerable penetration of the beam in the sample through its thickness, readings included inner and less deformed layers of the wire. Penetration of the beam could be reduced by decreasing beam intensity, but that would result in experiments with much longer duration.

In experiment B, to focus mostly on the surface of the samples, the thickness of the beam was reduced to a minimum to avoid reaching inner layers of the wire. However, due to the much smaller area reached by the incident beam, quality of acquired data decreased significantly, especially for the strained sample. One alternative to reduce noise and improve quality of the data would be to increase exposure time dramatically.

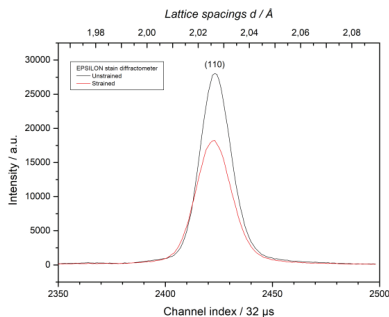


Figure 1. Preliminary neutron evaluation and measurement on the studied specimens obtained at the EPSILON strain diffractometer, IBR-2 pulsed reactor. Effect of plastic deformation on the lattice spacing of (110) planes.

Results have shown that for these bent wire samples neutron measurements would require very long exposure times, which is often unpractical and usually very costly. Changing the deformation process for uniaxial straining instead of bending could be a valid alternative. Other techniques, such as synchrotron X-ray diffraction and the contour method, have been suggested as reasonable alternatives for the study of such materials [3] and should also be considered.

- [1] D.Fergestad and S.A.Løvteit, editors (2017). Handbook on Design and Operation of Flexible Pipes. NTNU, 4Subsea and SINTEF Ocean.
- [2] Un-bonded Flexible Risers – Recent Field Experience and Actions for Increased Robustness (2013), Rev. 5, For PSA Norway. 4Subsea.
- [3] U.S.Fernando, M.Davidson, K.Yan, M.J.Roy, T.Pirling, P.J.Withers and J.A.Francis (2017). Evolution of Residual Stress in Tensile Armour Wires of Flexible Pipes During Pipe Manufacture. Proceedings of the ASME 36th International Conference on Ocean, Offshore and Arctic Engineering.

COMPARISON OF LOCAL AND GLOBAL TEXTURE IN FRICTION STIR PROCESSED ALUMINUM ALLOYS

M. Wróbel¹, D. Nikolayev², T. Lychagina², M. Kopyściański¹,
S. Dymek¹, M.S. Węglowski³, Z. Sekretarev², A. Baczmański¹

¹AGH University of Science and Technology, 30 Av. Mickiewicza, 30-059 Kraków, Poland

²Joint Institute for Nuclear Research, Joliot-Curie, 6, 141980, Dubna, Russia

³Lukasiewicz Research Network –Welding Institute, 16 Błogosławionego Czesława, 44-100 Gliwice, Poland

E-mail: mwrobel@agh.edu.pl, dmitry@nf.jinr.ru, lychagina@jinr.ru, mkopys@agh.edu.pl,
gmdymek@cyfronet.pl, marek.weglowski@is.gliwice.pl, sekretarev@jinr.ru,
andrzej.baczmański@fiz.agh.edu.pl

The Friction Stir Processing (FSP) is a solid state process designed to modification of microstructure and properties of the metal surface and subsurface layers (e.g. to improve resistance to corrosion, fatigue etc.). The basic concept of FSP is shown in Fig. 1. Thus, a non-consumable, rotating tool with a cylindrical shoulder and a specially profiled pin, plunged into the processed work piece, scan the material along the predefined line. During this process the hot plastic deformation can change the microstructure, crystallographic texture and consequently some properties of the worked material.

This paper deals with the global and local texture (GT and LT, respectively) development due to the friction stir processing (FSP) of the AlSi9Mg alloy. This type alloys are commonly used in mechanical constructions, car and motor industry, electrical appliances etc. [1]. The AlSi9Mg alloy is composed of two phases: Al solid solution and Si crystals.

A multiple-pass FSP with 50 % overlap between the successive passes has been applied in two configurations: in the first configuration the material retreating side of consecutive passes cover the advancing sides of the former pass while in the second configuration the situation is reversed, i.e. the advancing side covers the retreating one (sample labeled K and K1).

The GT of both phases was measured on the SKAT diffractometer operating at the beam line 7 in the Joint Institute for Nuclear Research, Dubna, Russia. The LT and the microstructure studies were performed in the AGH University in Kraków, Poland. The LT was measured both by the X-ray diffraction and by the Electron Backscatter Diffraction (EBSD) in a Scanning Electron Microscope. The dislocation structure was determined by the Transmission Electron Microscopy (TEM) JEM-2010 ARP.

It has been found that the typical dendrite solidification microstructure with a network of large (in size of several hundred μm) plate or needle shaped Si particles together with a non-uniform distribution of eutectic phases containing Mg and Fe was significantly refined due to

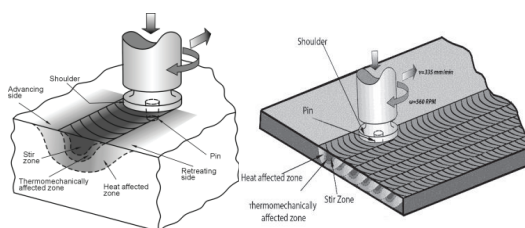


Fig. 1 Schematic representation of the FSP process.

FSP [2]. Firstly, the material porosity was nearly completely eliminated. Secondly, the microstructure has been reinforced by second phase particles (i.e., breakup of large Si particles has been fragmented and uniformly distributed within the matrix with the significantly reduced grain size). Thirdly, surprisingly, the processed material was not completely recrystallized, as was shown by TEM studies. Also, the crystallographic texture of the matrix and the Si particles were developed during the FSP. The textures for applied processing methods are mutually symmetrical and slightly different in intensity (Tab. 1). Finally, it was shown that overall GT and LT are compatible with each other. That is why, some large volumes of the material can be well characterized by the GT and can be directly related to the material macroscopic properties. On the other hand, the LT can be rather used for the analysis of physical processes occurring during the FSP.

Tab. 1 GT, 111 pole figures

Sample	K	K1
Matrix		
Silicon		

Acknowledgement

The JINR – Poland Scientific Program 2019-2020 is acknowledged.

[1] Silafont, Rheinfelden, <https://rheinfelden-alloys.eu/en/alloys/silafont/>

[2] M.S. Węglowski, S. Dymek, Archives of Metallurgy and Materials, **57**, 2012, 71-78

Научное издание

Condensed Matter Research at the IBR-2

Programme and Abstracts of the International Conference

Исследования конденсированных сред на реакторе ИБР-2

Программа и аннотации докладов международной конференции

E3-2020-19

Сборник отпечатан методом прямого репродуцирования
с оригиналов, предоставленных оргкомитетом.

Ответственная за подготовку сборника к печати *Т. И. Иванкина*.

Подписано в печать 29.09.2020.

Формат 60 × 90/16. Бумага офсетная. Печать офсетная.
Усл. печ. л. 15,25. Уч.-изд. л. 23,85. Тираж 70. Заказ 59982.

Издательский отдел Объединенного института ядерных исследований
141980, г. Дубна, Московская обл., ул. Жолио-Кюри, 6.

E-mail: publish@jinr.ru

www.jinr.ru/publish/